

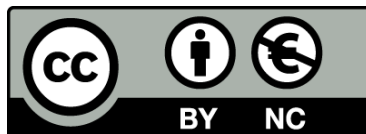


UNIVERSITAT DE
BARCELONA

Effects of flow discontinuities on carbon gas fluxes in a Mediterranean fluvial network

Efecte de les discontinuïtats hidrològiques sobre
els fluxes gasosos de carboni en una xarxa fluvial Mediterrània

Lluís Gómez Gener



Aquesta tesi doctoral està subjecta a la llicència **Reconeixement- NoComercial 3.0. Espanya de Creative Commons.**

Esta tesis doctoral está sujeta a la licencia **Reconocimiento - NoComercial 3.0. España de Creative Commons.**

This doctoral thesis is licensed under the **Creative Commons Attribution-NonCommercial 3.0. Spain License.**

TESI DOCTORAL



**UNIVERSITAT DE
BARCELONA**

Universitat de Barcelona

Departament d'Ecologia

Programa de Doctorat en Ecologia Fonamental i Aplicada

**Effects of flow discontinuities on carbon gas fluxes in a
Mediterranean fluvial network**

**Efecte de les discontinuïtats hidrològiques sobre els fluxes gasosos de
carboni en una xarxa fluvial Mediterrània**

Memòria presentada per Lluís Gómez Gener
per optar al grau de Doctor per la Universitat de Barcelona

Lluís Gómez Gener

Barcelona, Desembre de 2016

Vist-i-plau dels directors de tesi:

Dr. Biel Obrador Sala
Professor Agregat Interí
Universitat de Barcelona

Dr. Daniel von Schiller Calle
Investigador
Universidad del País Vasco

A ma mare.

Contents

Agraïments.....	vii
Informe dels directors.....	xi
Abstract.....	xv
Resum.....	xvii
List of figures.....	xix
List of tables.....	xxi
List of abbreviations.....	xxiii
1 GENERAL INTRODUCTION AND OBJECTIVES.....	25
1.1 THE ROLE OF INLAND WATERS IN THE GLOBAL CARBON CYCLE.....	27
1.2 CARBON EMISSIONS FROM INLAND WATERS.....	29
1.3 THE STUDY OF BIOGEOCHEMICAL PROCESSES AT A FLUVIAL NETWORK SCALE.....	36
1.4 MEDITERRANEAN FLUVIAL NETWORKS AS IDEAL SETTINGS TO TEST THE EFFECTS OF FLOW DISCONTINUITIES ON CARBON GAS FLUXES.....	38
1.5 DISSERTATION OBJECTIVES.....	44
2 STUDY SITE AND SAMPLING DESIGN.....	45
2.1 THE FLUVIÀ RIVER CATCHMENT.....	47
2.2 DISCONTINUITIES ALONG THE FLUVIÀ RIVER NETWORK.....	48
2.3 SAMPLING DESIGN.....	51
3 HOT SPOTS FOR CARBON EMISSIONS FROM MEDITERRANEAN FLUVIAL NETWORKS DURING SUMMER DROUGHT.....	53
3.1 INTRODUCTION.....	57
3.2 MATERIALS AND METHODS.....	59
3.3 RESULTS.....	67
3.4 DISCUSSION.....	72
3.5 CONCLUSIONS AND IMPLICATIONS.....	78
4 WHEN WATER VANISHES: MAGNITUDE AND REGULATION OF CARBON DIOXIDE EMISSIONS FROM DRY TEMPORARY RIVERS.....	81
4.1 INTRODUCTION.....	835
4.2 MATERIALS AND METHODS.....	86
4.3 RESULTS.....	94
4.4 DISCUSSION.....	99
4.5 CONCLUSIONS AND IMPLICATIONS.....	102

5	EFFECT OF SMALL WATER RETENTION STRUCTURES ON DIFFUSIVE CARBON EMISSIONS ALONG A HIGHLY REGULATED RIVER.....	103
5.1	INTRODUCTION	107
5.2	MATERIALS AND METHODS	109
5.3	RESULTS.....	114
5.4	DISCUSSION.....	120
5.5	CONCLUSIONS AND IMPLICATIONS.....	123
6	LOW CONTRIBUTION OF INTERNAL METABOLISM TO CARBON DIOXIDE EMISSIONS ALONG LOTIC AND LENTIC ENVIRONMENTS OF A MEDITERRANEAN FLUVIAL NETWORK	125
6.1	INTRODUCTION	129
6.2	MATERIALS AND METHODS	131
6.3	RESULTS.....	138
6.4	DISCUSSION.....	146
6.5	CONCLUSIONS AND IMPLICATIONS.....	151
7	GENERAL DISCUSSION.....	153
	THE RIVER DISCONTINUUM.....	155
7.1	THE INFLUENCE OF SMALL WATER RETENTION STRUCTURES ON SHAPING CARBON GAS FLUXES ALONG A MEDITERRANEAN FLUVIAL NETWORK.....	157
7.2	DRY RIVERBEDS AS HOT SPOTS FOR CARBON DIOXIDE EMISSIONS	164
7.3	THE ROLE OF PHYSICS AS A VALVE REGULATING CARBON GAS EXCHANGE BETWEEN FLUVIAL NETWORKS AND THE ATMOSPHERE	170
7.4	INTEGRATING FLUVIAL NETWORK DISCONTINUITIES IN A MEDITERRANEAN RIVER: IMPLICATIONS FOR CARBON GAS EMISSIONS UNDER PRESENT AND FUTURE HYDROLOGICAL SCENARIOS	171
8	GENERAL CONCLUSIONS..	177
	References.....	181
	Supporting Information.....	207
	Appendix A. Supporting information for Chapters 3, 4, 5 and 6.....	207
	Appendix B. Supporting information for Chapter 7	220
	Appendix C. Publications of the present dissertation.....	224

Agraïments

Suposo que el fet d'arribar en aquest punt i estar redactant aquestes línies és un indicatiu de que aquesta Tesi és una realitat. Mare meva, com passa el temps... Com si fos ara, recordo aquell moment en que en Biel em trucava per avisar-me de que tenia bastantes opcions de ser el candidat seleccionat d'una beca FPI que em permetria realitzar la Tesi Doctoral a la Universitat de Barcelona. Òbviament, el meu habitual "cagadubtisme" va fer acte de presència: Un Químic a la facu de Biologia? Al departament d'Ecologia? Aquest d'en Biel ho té clar? I ara em toca anar a viure a Barcelona si jo sóc més de poble que les "bajoques"? Ai mare....

I si, com si es tractés d'una d'aquelles ascensions "clàssiques" a una gran paret m'hi vaig embarcar:

Normalment, els primers passos que es fan una vegada tens clar el projecte muntanyenc que vols dur a terme consisteixen en demanar o buscar referències de la via on vols anar (ressenyas) o bé experiències d'altres cordades que han repetit la línia. És, en aquest moment quan els teus companys et donen consell i t'animen (o no...) a tirar endavant el projecte que et corre pel cap... En el cas d'aquesta Tesi, aquests heu estat la gent del Departament. Els del "Galliner" (Anna, Sílvia, Núria C., Txell, Alba, Myrto, Astrid, Bet, Eusebi, Dani DdQ i totes les noves incorporacions...), els de la peixera de FEM (Polilla, Pablo, Pau, Núria, Daniel), les noies del 5è (Núria DC, Esther, Isis, Lúdia, Mari, Rebeca) i els "marinos" que els poso a tots al mateix sac... (Eneko, Aurora, Pol2, Max). Tots vosaltres us heu encarregat en més o menys mesura d'explicar-me les vostres experiències, donar-me consell, ajudar-me, fer-me riure i sobretot fer més fàcil aquesta estada de 4 anys a la gran urbe. Entre d'altres, m'heu portat al Cangrejo a aguantar la barra, my god que lokes que estan l'Anna i la Silvia (però com molen!), a fumar shisha (o com es digui) al local de la Carmen de Mairena (Pol, deixa ja la Catximba!), a veure Absenta al Marsella (clar exemple de que els límits del terme droga no són del tot clars...) o simplement a fer unes birres pel Raval o al Bar del Jaime.

Una vegada et plantes al peu de la paret (moment de la veritat), es quan comencen els dubtes: és aquesta via massa difícil per mi? Vaig poc preparat mentalment per assumir aquesta fita? I físicament? He agafat el material adient? Pot ser em falten un parell més

d'enquestadors? Hauria d'haver agafat un segon estrep per passar la fissura en A1? És aquí on rau la importància de tenir un o uns bons companys de cordada. En aquest cas, en Dani i en Biel han estat els millors companys de cordada. Han confiat en mi, sense dubtar (no ho tinc clar... heheheh) i animant-me en aquells passos "clau" de la via. En tot moment lligat a ells però sempre deixant-me la corda justa per poder progressar més àgilment en aquelles seccions fàcils de l'aventura. Moltes gràcies nois, m'heu format com a investigador (en la mesura que sigui...) però també com a persona. Sou un exemple (com a mínim per mi) de supervisor i de científics. Sense vosaltres no estaria escrivint aquestes línies, PAM! (ja veieu que amb això dels agraïments em deixo anar i tot eh... que pilota!!)

Al CARBONET- Team. Com en la muntanya ho fan els companys i les "velles glòries", vosaltres també m'heu nodrit d'experiències i coneixements que m'han permès progressar durant aquest 4 anys de Tesi. Rafa, moltes gràcies per la teva ajuda desinteressada al llarg de la tesi. Ah, i per les bones recomanacions literàries durant els viatges a Bilbo (quina manera de descollonar-nos, eh Marina (que tu i jo també hem passat moltes estones al camp!!!)). Isabel i Sergi, d'alguna manera heu sigut els pares de tot això. Moltes gràcies pels bons consells i per fer les coses fàcils! Margarita i Pili, moltes gràcies també a vosaltres. Vicenç, tot i que no vas voler ser el meu supervisor (en plan conya eh hehehe), moltes gràcies pels teus cops de ma i ànims continus (algun d'ells des de Washington). Lorenzo, ets la bomba, gràcies a tu també! Carmen, tot i que penses que jo i el JP som uns "persons" (i m'ho has dit a la cara...) també t'agreixo la teva paciència durant el primer any de mostrejos per Girona. JP, de tu també he après molt, sobretot de música!! hehe. Ah, quina sort van tenir els nostres "jefes" de que cuallés aquest bon rotlo entre els dos eh?? Mira que tot un any vivint una setmana al mes a casa teva... Quines "risses" !! I quins entrepans de llom amb formatge a les russes... Hi tornarem un dia? Si, oi? Txell, com a líder del Palitos-Team et mereixes l'honor de ser la última en mencionar. A tu, moltes gràcies per ser tant dolça i agraïda. Ets un sol!! I molts ànims que ja ho tens!

Durant el transcurs de la tesi, he tingut la sort de fer dues estades, ambdues per Escandinàvia. A Dinamarca, tot i el mal temps, el "Brazilian-team" em va ajudar a fer les estones lliures molt més amenes. Peter, gràcies a tu per fer-me un lloc al teu equip i pel teu bon sentit de l'humor! I a Suècia vaig anar amb en Ryan. Encara ara estic dubtant de com un Yankee (amb tot els ets i uts) i un Català (una mica de poble) van congeniar tant. A Umeå vaig aprendre un altre manera de veure i (pot ser entendre) la ciència. Gràcies per tot Ryan, no puc demanar més del tracte que vas tenir amb mi durant l'estada. També vull

donar les gràcies al climbing-team d'Umeå (Gerard, Dagmar, Maria, Cameron...). Gerard, a veure si ens veiem aviat per l'Aran!

També vull agrair a tots aquells i aquelles que malgrat mai heu sabut massa bé que estava fent per Barcelona, sempre us heu interessat per mi. Un agraïment a les meves germanetes (o de vegades 2nes mares), a l'Ernest i al Joan, i a tots els nebotets. Als meus tiets i cosins (sobretot al Tiet Joan i l'Adela que em van acollir a Menorca durant un dels mostrejos a les basses temporals i el Joanet que sempre m'ha vingut a veure!). A la gent de la Colla del poble (Matas, Blay, Sus, Guillem, Oscar i Sandra, David i Maria (artistes!), Yeti, Antrax, Merino...), companys de l'Associació excursionista, al Pipo i al Roger per les sortides aquests últims dies a la Mola i la Serra de l'Argentera i al grup d'amics de la Uni de Tarragona (Lau, Anna, Marta, Emma, Racio, Mulet, Cerra, JC i Gloria) perquè son part de la família.

Per últim, els agraïments més especials van dirigits a la Mamà i a l'Alba. Vosaltres heu estat el pilar que ha mantingut l'estabilitat i les ganes necessàries per afrontar aquest capítol de la meva vida. Sense vosaltres cap cim com el que avui assoleixo podria haver estat possible (intens eh?). Mamà, gràcies per ensenyar-me a valorar el que és realment important. Alba, gràcies pel teu somriure i la força que m'has donat! Ah, i per aguantar-me...

Riudecanyes, 25 de Novembre de 2016

He tingut el suport econòmic d'una Beca FPI (BES-2012-059743) del Ministerio de Economía, Industria y Competitividad associada al projecte CARBONET (CGL2011-30474-C02-01) del Plan Nacional del Ministerio de Economía, Industria y Competitividad . A més, part de la meva recerca també ha estat financada pel projecte FUNSTREAM (CGL2014-58760-C3-1-R) del Plan Nacional del Ministerio de Economía, Industria y Competitividad: i per la beca Oriol de Bolòs de Ciències Naturals 2015 obtinguda de l'Ajuntament d'Olot. Per altra banda, també he disposat de dues beques de mobilitat de la Facultat de Biologia per assistir a un congrés i a una curs, dues ajudes per estades breus associades a la beca FPI, dues beques de l'acció EU-COST NETLAKE (Networking Lake Observatories in Europe) per assistir a cursos de formació i una beca de l'Associació Ibèrica de Limnologia (AIL) per assistir a un congrés.

Informe dels directors

El Dr. Biel Obrador Sala, de la Universitat de Barcelona, i el Dr. Daniel von Schiller Calle, de la Universidad del País Vasco, directors de la Tesi Doctoral elaborada pel Sr. Lluís Gómez Gener, i que porta per títol “Effects of flow discontinuities on carbon gas fluxes in a Mediterranean fluvial network”,

INFORMEN

Que els treballs de recerca portats a terme per Lluís Gómez Gener com a part de la seva formació predoctoral i inclosos en la seva Tesi Doctoral han donat lloc a tres articles publicats, i un manuscrit que properament serà enviat a una revista internacional. A continuació es detalla la llista d'articles així com els índexs d'impacte del Journal Citation Reports de Thomson Reuters per a les revistes on han estat publicats o està previst que es publiquin els treballs.

Gómez-Gener, L.; Obrador, B.; von Schiller, D.; Marcé, R.; Casas-Ruiz, J.; Proia, L.; Acuña, V.; Catalán, N.; Muñoz, I.; Koschorreck, M. 2015. Hot spots of carbon emissions from Mediterranean fluvial networks during summer drought. *Biogeochemistry* 125: 409-426.

L'índex d'impacte de la revista *Biogeochemistry* l'any 2015 va ser de 3.407. Aquesta revista està situada en el **primer quartil** de la categoria “Environmental Sciences”, que té una mediana d'índex d'impacte de 1.737. La revista *Biogeochemistry* ocupa el lloc 44è de les 225 revistes considerades en aquesta categoria.

Gómez-Gener, L.; Obrador, B.; Marcé, R.; Acuña, V.; Catalan, N.; Casas-Ruiz, J.P.; Sabater, S.; Muñoz, I.; von Schiller, D. 2016. When water vanishes: magnitude and regulation of carbon dioxide emissions from dry temporary streams. *Ecosystems* 19: 710-723

L'índex d'impacte de la revista *Ecosystems* l'any 2015 va ser de 3.751. Aquesta revista està situada en el **primer quartil** de la categoria "Ecology", que té una mediana d'índex d'impacte de 1.832. La revista *Ecosystems* ocupa el lloc 30è de les 150 revistes considerades en aquesta categoria.

Gómez-Gener, L.; von Schiller, D.; Marcé, R.; Aroitia, M.; Casas-Ruiz, J.P.; Staehr, P.A.; Acuña, V.; Sabater, S.; Obrador, B. 2016. Low contribution of internal metabolism to carbon dioxide emissions along lotic and lentic environments of a Mediterranean fluvial network. *Journal of Geophysical Research - Biogeosciences* (doi 10.1002/2016JG003549)

L'índex d'impacte de la revista *Journal of Geophysical Research - Biogeosciences* l'any 2015 va ser de 3.318. Aquesta revista està situada en el **primer quartil** de la categoria "Geosciences/Multidisciplinary", que té una mediana d'índex d'impacte de 1.659. La revista *Journal of Geophysical Research - Biogeosciences* ocupa el lloc 27è de les 184 revistes considerades en aquesta categoria.

Gómez-Gener, L.; Gubau, M.; von Schiller, D.; Marcé, R.; Casas-Ruiz, J.P.; Obrador, B. Effect of small water retention structures on diffusive carbon emissions along a highly regulated river (*to be submitted to Aquatic Sciences*)

Es preveu enviar aquest manuscrit a la revista *Aquatic Sciences*. L'índex d'impacte de la revista *Aquatic Sciences* l'any 2015 va ser de 2.398. Aquesta revista està situada en el **primer quartil** de la categoria "Marine & Freshwater Biology", que té una mediana d'índex d'impacte de 1.498. La revista *Aquatic Sciences* ocupa el lloc 20è de les 104 revistes considerades en aquesta categoria.

Alhora CERTIFIQUEN

Que el Sr. Lluís Gómez Gener ha participat activament en el desenvolupament del treball de recerca associat a cadascun d'aquests articles així com en la seva elaboració. En concret, la seva participació en cadascun dels articles ha estat la següent:

- Participació en el plantejament inicial dels objectius de cadascun dels treballs.
- Disseny de la part de mostreig de camp i posada a punt de les metodologies de camp i de laboratori associades a cadascun dels capítols.
- Mostrejos de camp, processat i anàlisi de totes les mostres obtingudes (exceptuant el quart capítol en què va col·laborar activament en les tasques de laboratori, sense liderar-les).
- Càlcul de resultats i anàlisi de dades, incloent modelització de metabolisme aquàtic en el tercer capítol.
- Redacció dels articles i seguiment del procés de revisió dels mateixos.

Part d'aquestes tasques es van realitzar durant dues estades de recerca al *Department of Bioscience* de la *Aarhus University*, Dinamarca (equip del Dr. Peter A. Staehr), i al *Department of Ecology and Environmental Sciences* de la *University of Umeå*, Suècia (equip del Dr. Ryan Sponseller).

Finalment, certifiquem que cap dels coautors dels articles abans esmentats i que formen part de la Tesi Doctoral del Sr. Lluís Gómez Gener ha utilitzat ni té previst utilitzar implícita o explícitament aquests treballs per a l'elaboració d'una altra Tesi Doctoral.

Barcelona, 25 de novembre de 2016

Dr. Biel Obrador Sala
Professor Agregat Interí
Universitat de Barcelona

Dr. Daniel von Schiller Calle
Investigador
Universidad del País Vasco

Abstract

Inland waters are active components of the global carbon (C) cycle that transform, store and outgas more than half of the C they receive from adjacent terrestrial ecosystems. In particular, C emissions from fluvial networks to the atmosphere represent a substantial flux in the global C cycle. However, fundamental uncertainties regarding the spatiotemporal patterns, controls and sources of C gas fluxes in fluvial networks still exist. For instance, current biogeochemical models addressing C transport and processing in fluvial networks from a continuous perspective, do not integrate the effects of local discontinuities such as river impoundment or stream flow intermittency on the dynamics of C gas fluxes.

The present dissertation aims to examine how flow discontinuities (i.e., river impoundment, flow fragmentation and drying) shape the spatiotemporal patterns, the controls and the sources of C gas fluxes in a Mediterranean fluvial network. The study was performed from December 2012 to March 2015 in the Fluvià River (NE Iberian Peninsula). This river is characterized by a high density of impounded waters associated to small water retention structures (SWRS; i.e., weirs and small to very small impoundments with a surface area $< 0.1 \text{ km}^2$ and a volume $< 0.2 \text{ hm}^3$) as well as fragmented river sections dominated by isolated water pools and dry riverbeds coinciding with dry periods.

Results of this dissertation show that river discontinuities associated to SWRS and flow intermittency modulate the spatiotemporal patterns, controls and sources of C gas fluxes in the studied fluvial network. However, the magnitude of these effects varied depending on the nature of the discontinuity (i.e., river impoundment or flow intermittency), the type of C gas (i.e., carbon dioxide (CO_2) or methane (CH_4)) and the hydrological condition (i.e., high or low flow).

The presence of SWRS, despite their relatively small water capacity, attenuated the turbulent conditions occurring in free-flowing river sections. As a consequence, the diffusive CO_2 emissions from impounded waters were significantly lower than from free-flowing river sections. Contrarily, no reduction in CH_4 emissions from impounded river sections

associated to the presence of SWRS was detected. This result suggests that the higher internal CH₄ production at the impounded river sections, which remained very stable over time, compensated the attenuated physical effect on CH₄ emissions. Despite potential inaccuracies in capturing the temporal and spatial heterogeneity, ebullition was the predominant pathway of CH₄ emissions in impounded river sections. Moreover, sources other than internal metabolism (i.e., external inputs, internal geochemical reactions or photochemical mineralization) sustained most of the fluvial network CO₂ emissions. Specifically, the magnitude and sources of CO₂ emissions depended on flow conditions in the free-flowing sections, whereas they remained relatively stable and independent of hydrological variation in the impounded river sections.

The channels of temporary rivers remain as active biogeochemical habitats, degassing significant amounts of CO₂ to the atmosphere after flow cessation. In contrast, the CH₄ efflux from dry beds was undetectable in almost all cases, most likely due to the high aeration limiting the redox requirements for microbial CH₄ production. Our results also suggest that the source of CO₂ emitted from dry riverbeds remains unclear, although CO₂ produced from biological mineralization of fresh and labile organic matter fractions could be an important source.

Future hydrological scenarios considering the combined effects of climate change and human pressures on water resources in the Mediterranean region show the rather low sensitivity of the annual CO₂, CH₄ and total C emissions to shifts in river discharge. In contrast, they stress the high sensitivity of annual CH₄ and total C emissions to shifts in the surface area of lentic waterbodies associated to SWRS.

Overall, the main findings of this dissertation point to the need for a shift away from a continuous and system-centric view to a more inclusive approach that incorporates spatiotemporal discontinuities (i.e., SWRS and flow fragmentation and drying) as a suitable framework to understand the dynamics of C gas fluxes in fluvial networks. We acknowledge that our results represent a first approximation to better understand the role of flow discontinuities on C gas fluxes from fluvial networks. Further work on the temporal and spatial patterns of the C gas fluxes is needed to provide a more conclusive understanding.

Resum

Les aigües continentals o ecosistemes d'aigua dolça són uns components molt actius en el cicle del carboni (C). Aquests, transformen, emmagatzemen i emeten la meitat de C que reben dels ecosistemes terrestres adjacents. En concret, les emissions de C des de les xarxes fluvials a l'atmosfera representen un dels fluxos més significatius de tot el cicle del C. No obstant, encara existeix una elevada incertesa pel que fa als patrons espaciotemporals, factors de control i principals fonts dels fluxos gasosos de C en xarxes fluvials. Per exemple, els models biogeoquímics actuals que avaluen tant el transport com el processat de C en xarxes fluvials, no inclouen els efectes de discontinuïtats locals com el represament de rius o la intermitència del règim hidrològic sobre les dinàmiques de fluxos gasosos de C.

Aquesta Tesi Doctoral té com a objectiu examinar com les discontinuïtats en el règim hidrològic (això és, represament del riu, fragmentació del canal o assecament del riu) modulen els patrons espaciotemporals, factors de control i origen de les principals fonts dels fluxos gasosos de C en xarxes fluvials. Aquest estudi es va dur a terme al Riu Fluvià (NE de la Península Ibèrica) des del Desembre de 2012 al Març de 2015. Aquest riu es caracteritza per una elevada densitat d'aigües represades en estructures de retenció d'aigua de mida petita (ERMP) així com d'una elevada cobertura de seccions fluvials que tendeixen a fragmentar-se duran els moments més secs de l'any (això és, seccions dominades per basses d'aigua aïllades i lleres de riu seques).

Els resultats d'aquesta Tesi Doctoral mostren que les discontinuïtats en el règim hidrològic associades al represament de rius o la intermitència tenen un paper fonamental en la modulació dels patrons espaciotemporals, factors de control i fonts dels fluxos gasosos de C en xarxes fluvials. La magnitud d'aquests efectes varia, però, en funció de la naturalesa de la discontinuïtat (això és, represament del riu o intermitència del règim hidrològic), el tipus de gas (això és, diòxid de carboni (CO₂) o metà (CH₄)) i la condició hidrològica (això és, cabals alts o baixos).

Tot i la seva capacitat relativament petita d'emmagatzemar aigua, la presència de ERMP va atenuar les condicions turbulents que caracteritzen les seccions del riu amb aigües corrents. Com a conseqüència, les emissions difusives de CO₂ des de les aigües represades

van ser significativament inferiors a aquells des d'aigües corrents. Contràriament, la presència de ERMP no va suposar un efecte negatiu sobre les emissions de CH₄. Aquest fet suggereix que l'elevada producció interna de CH₄ a les seccions de riu represades, la qual és manté força estable al llarg del temps, pot compensar l'efecte físic d'atenuació sobre les emissions de CH₄. Tanmateix, fonts diferents al metabolisme intern (això és, inputs externs i reaccions geoquímiques o fotoquímiques internes) van sostenir, en gairebé la totalitat, les emissions de CO₂ de la xarxa fluvial. La magnitud i fonts d'aquestes van dependre de les condicions hidrològiques en el cas dels trams d'aigües corrents, mentre que es van mantenir relativament estables i independents de la hidrologia en aquelles seccions de riu represades.

Les lleres dels rius intermitents romanen actives pel que fa a la emissió de CO₂ a l'atmosfera una vegada el flux superficial d'aigua cessa. Per contra, el flux d'emissió de CH₄ des de les lleres seques va ser indetectable en gairebé tots els casos, probablement degut a les condicions d'alta aeració que limiten els requisits redox per a la producció microbiana de CH₄. El flux d'emissió de CO₂ des de les lleres seques va doblar a l'emès des de les lleres amb aigües corrents i va ser comparable a l'emès des dels sòls terrestres adjacents. No obstant, les lleres seques i els sòls terrestres adjacents van resultar ser molt diferents des d'un punt de vista fisicoquímic, mostrant així diferències en els principals factors i fonts que en regulen les emissions de CO₂.

Els escenaris de futur que consideren els efectes combinats del canvi climàtic i les pressions antropogèniques sobre els recursos d'aigua a la regió Mediterrània van mostrar una baixa sensibilitat de les emissions de CO₂, CH₄ i emissions totals de C sobre canvis de cabal. En contra, les mateixes prediccions postulen una elevada sensibilitat de les emissions de CH₄ i C total emès a canvis en la superfície d'aigua represada associada a un increment de ERMP.

En resum, les principals troballes fetes en aquesta tesi apunten cap a una necessitat clara de substituir els models continus i limitats espacialment per aquells models que incorporen discontinuïtats espaciotemporals (això és, represament del riu o intermitència del règim hidrològic) per tal d'entendre en millor mesura les dinàmiques dels fluxos gasosos de C en xarxes fluvials.

List of Figures

1.1	Simplified scheme of the global C cycle and its anthropogenic perturbation.....	28
1.2	Conceptual model showing the primary and the less known sources and pathways involved in the production and removal of CO ₂ and CH ₄ in lentic freshwater ecosystems.....	34
1.3	Conceptual model showing the primary and the less known sources and pathways involved in the production and removal of CO ₂ and CH ₄ in lotic freshwater ecosystems.....	35
1.4	Spatial configuration of a fluvial network from both the continuum and the discontinuum point of view	37
1.5	Schematic figure illustrating two contrasted hydrological situations in Mediterranean fluvial networks: hydrological expansion and hydrological contraction.	39
1.6	Location of the arid and semiarid regions in the world.....	40
1.7	Map of the global location and distribution of large- and medium-size dams.....	42
2.1	Location of the Fluvià River catchment, with the corresponding position of all the study sites sampled from December 2012 to March 2015.....	47
2.2	Climatic regime of the Fluvià River catchment	48
2.3	Examples of some representative study sites grouped by environment type.....	50
3.1	Location of the Fluvià River with the corresponding position of the study sites sampled in Chapter 3	60
3.2	Efflux of CO ₂ and CH ₄ measured from running waters, impounded waters, isolated pools and dry river and impoundment beds.....	68
3.3	Basal respiration as a function of dry bed water content and dry bed organic matter. Efflux of CO ₂ as a function of dry bed water content and dry bed organic matter.	70
3.4	Efflux of CO ₂ as a function of k_{600} and $p_{\text{CO}_2, \text{w}}$ for all the aquatic study sites.....	71
3.5	Contour plots simulating the effect of a broad spectrum of potential hydrological scenarios on C emission fluxes.....	78
4.1	Location of the Fluvià River with the corresponding position of the study sites sampled in Chapter 4	87

4.2	Mean CO ₂ efflux from dry riverbeds, flowing riverbeds and adjacent upland soils of the studied streams	94
4.3	Multivariate ordination (PCA) plot of dry riverbed sediments and upland soils based on physical and chemical descriptors.....	95
4.4	Multivariate regression analysis (PLS) plot for the CO ₂ emissions from dry riverbeds and adjacent upland soils	98
5.1	Location of the Fluvia River catchment, with the position of the study sites sampled in Chapter 5.....	110
5.2	Mean CO ₂ efflux, CH ₄ efflux, $p_{\text{CO}_2, \text{w}}$, $p_{\text{CH}_4, \text{w}}$, k_{CO_2} and k_{CH_4} of the 11 SWRS grouped by sampling units during the 3 sampled seasons.....	116
5.3	Longitudinal patterns of $p_{\text{CO}_2, \text{w}}$ and $p_{\text{CH}_4, \text{w}}$ in spring, summer and winter for the 3 different SWRS units.....	117
5.4	Multivariate regression analysis (PLS) for $p_{\text{CO}_2, \text{w}}$ and $p_{\text{CH}_4, \text{w}}$	119
6.1	Location of the Fluvia River catchment with the corresponding position of the study sites sampled in Chapter 6	132
6.2	Temporal variation (from December 2012 to November 2013) of water residence time, CO ₂ efflux, $p_{\text{CO}_2, \text{w}}$ and k_{CO_2}	140
6.3	Relationship between $F_{\text{CO}_2 \text{ metabolism}}$ and $F_{\text{CO}_2 \text{ emission}}$ and $p_{\text{CO}_2, \text{w}}$ for both lotic and lentic segments.....	142
6.4	$F_{\text{CO}_2 \text{ metabolism}}$ as a function of water residence time for both lotic and lentic segments	143
6.5	Source apportionment of $F_{\text{CO}_2 \text{ emission}}$ for lotic and lentic segments	144
6.6	Relative contribution of internal metabolism, upstream inflow and other non-measured sources to CO ₂ emissions as a function of the water residence time for lotic and lentic segments	145
6.7	Summary of the CO ₂ fluxes determining CO ₂ variations within the studied lotic and lentic segments.....	150
7.1	Conceptualization of the general downstream longitudinal patterns in concentration of dissolved CO ₂ in water, concentration of dissolved CH ₄ in water, CO ₂ efflux and CH ₄ efflux along a fluvial network integrating SWRS	163
7.2	Comparison of CO ₂ effluxes measured in the dry beds of 4 aquatic ecosystem types: streams and rivers, reservoirs, wetlands and temporary ponds.	165
7.3	Estimated percentage contribution of the CO ₂ efflux from dry watercourses to the total fluvial network CO ₂ efflux divided by COSCAT regions.....	168

List of Tables

1.1	Compilation of the global surface area and the annual C fluxes between freshwater ecosystems and the atmosphere.....	30
2.1	Temporal and spatial extent, measured C gas fluxes and specific objectives addressed in each chapter of this dissertation.....	52
3.1	Summary of $p_{\text{CO}_2, \text{w}}$ and $p_{\text{CH}_4, \text{w}}$, the direct and the indirect k_{600} , the total efflux of CO ₂ and CH ₄ and the percentage molar ratio between CH ₄ and CO ₂ flux (CH ₄ flux : CO ₂ flux) along the different studied environments.....	69
3.2	Hydromorphological descriptors, and sediment physical and chemical properties of the different impounded waters	71
4.1	Physiographic and land use characteristics of the study sites and their corresponding subcatchments	88
4.2	Overview of X and Y variables included in the PCA and PLS models.....	93
4.3	Physical and chemical properties of the dry streambed sediments and upland soils at each study site.....	97
6.1	Summary of the CO ₂ fluxes determining CO ₂ variations within the studied lotic and lentic segments	148
7.1	Summary of the areal CO ₂ , CH ₄ and total C fluxes from the three types of environments studied along the Fluvia River network.	172
7.2	Summary of upscaled surface areas and CO ₂ , CH ₄ and total C fluxes for the entire Fluvia River network.....	172
7.3	Summary of expected changes in surface areas and annual CO ₂ , CH ₄ and total C fluxes for the entire Fluvia River network under 3 future hydrological scenarios.....	174

List of Abbreviations

Alk	Alkalinity
ANOVA	Analysis of variance
BIX	Biological index derived from fluorescence spectra
C	Carbon
CH ₄	Methane
Chl <i>a</i>	Chlorophyll a
CO ₂	Carbon dioxide
CO ₂ efflux	Flux of carbon dioxide across the air-water interface
CO ₂ emission	Flux of carbon dioxide across the air-water interface
DIC	Dissolved inorganic carbon
DO	Dissolved oxygen
DOC	Dissolved organic carbon
DOM	Dissolved organic matter
dp/dt	Slope of gas accumulation in the chamber
EC	Electrical conductivity
EEM	Excitation–emission matrix
ER	Ecosystem respiration
<i>f</i>	F-statistic value
F_{CO_2}	Flux of carbon dioxide across the air-water interface
$F_{\text{CO}_2 \text{ emission}}$	Flux of carbon dioxide across the air-water interface
$F_{\text{CO}_2 \text{ inflow}}$	Flux of CO ₂ imported from upstream surface waters
$F_{\text{CO}_2 \text{ metabolism}}$	Flux of CO ₂ derived from aerobic metabolic processes
$F_{\text{CO}_2 \text{ others}}$	Flux of CO ₂ associated to these unmeasured sources
$F_{\text{CO}_2 \text{ outflow}}$	Flux of CO ₂ exported to downstream surface water
FI	Fluorescence index derived from fluorescence spectra
GPP	Gross primary production
HIX	Humification index derived from fluorescence spectra
HCl	Hydrogen chloride.
IPCC	Intergovernmental Panel on Climate Change
k_{600}	Standardized gas transfer velocity or piston velocity. Corresponds to the gas transfer velocity of CO ₂ at 20°C in freshwater
k_{CH_4}	Gas transfer velocity of CH ₄
k_{CO_2}	Gas transfer velocity of CO ₂

k_h	Henry's constant
l	Lotic or lentic segment length
NEP	Net ecosystem production
OC	Organic carbon
OM	Organic matter
p	Statistical significance
PAR	Photosynthetically active radiation
PCA	Principal components analysis
$p_{\text{CH}_4,\text{a}}$	Atmospheric partial pressure of CH_4
$p_{\text{CH}_4,\text{w}}$	Surface water partial pressure of CH_4
$p_{\text{CO}_2,\text{a}}$	Atmospheric partial pressure of CO_2
$p_{\text{CO}_2,\text{w}}$	Surface water partial pressure of CO_2
PLS	Partial least squares analysis
POC	Particulate organic carbon
R	Ideal gas constant
r^2	Coefficient of determination of a statistical model
s	River or stream slope
S	Chamber surface area
Sc	Schmidt number
SUVA ₂₅₄	Specific UV absorbance at 254 nm
SWRS	Small water retention structures (i.e., weirs and small to very small impoundments with a surface impounded area < 0.1 km ² and a volume < 0.2 hm ³)
t	Time
T	Air temperature
TDN	Total dissolved nitrogen
Temp	Surface water temperature
TN	Total nitrogen
TP	Total phosphorus
v	Water velocity
V	Chamber volume
VIP	Variable influence on projection (PLS model)
w	Lotic or lentic segment width
WC	Water content
WEOM	Water extracted organic matter
WRT	Water residence time
z	Lotic or lentic segment depth



General introduction and objectives

1.1 The role of inland waters in the global carbon cycle

Carbon (C) in the Earth is unevenly distributed among three major reservoirs: the continents, the oceans and the atmosphere. The global C cycle is the biogeochemical cycle by which C is exchanged among these three reservoirs (Figure 1.1). Atmospheric C gases contribute to the regulation of the energy balance of the Earth-climate system. Since pre-industrial times (~1750), the concentration of carbon dioxide (CO₂) has increased by 40% from 278 ppm to 390 ppm [IPCC, 2013]. During the same period, atmospheric methane (CH₄) has raised by 150% from 722 ppb to 1803 ppb [IPCC, 2013], a highly significant increase considering the ~30-fold higher global warming potential of CH₄ compared to that of CO₂ over a 100-year time horizon [IPCC, 2013]. These increases of CO₂ and CH₄ reflect only about half of the C emissions; the other half is assumed to be sequestered in the oceans and the continents before reaching the atmosphere (IPCC [2013]; Figure 1.1).

The location and magnitude of these climate-critical C sinks (i.e., oceans and continents) remains uncertain [Heimann, 2009]. Therefore, depictions of the global C cycle generally consisted of two active boxes (i.e., oceans and continents) connected through gas exchanges with a third box, the atmosphere [Siegenthaler and Sarmiento 1993; IPCC, 2001]. However, this rather simplistic approach has also led to the identification of major knowledge gaps, such as apparent imbalances in the continental C budget or the uncertain response of these reservoirs to large-scale phenomena such as global change [Cole *et al.*, 2007; Battin *et al.*, 2009a; Tranvik *et al.*, 2009].

As models developed further, more sub-components and processes were added to unravel the link between the continental ecosystems and the oceans [Foley *et al.*, 1996; Canadell *et al.*, 2000; Cramer *et al.*, 2001]. Among them, the integration of inland waters (i.e., streams, rivers, lakes, reservoirs and wetlands), which have a significant role in the transport, mineralization, sequestration and emission of C, has been identified as crucial for an appropriate understanding of the global C cycle [Cole *et al.*, 2007; Battin *et al.*, 2009a; Tranvik *et al.*, 2009]. The most updated estimates that include inland waters indicate that the C discharged to the oceans (0.7- 0.9 Pg C y⁻¹) is only a fraction (<50%) of that entering rivers from terrestrial ecosystems (1.7 - 2.8 Pg C y⁻¹) via soil respiration, leaching, chemical weathering, and physical erosion. Most of this C influx is returned to the atmosphere from

inland waters as CO_2 or CH_4 ($0.8 - 1.2 \text{ Pg C yr}^{-1}$; $\sim 50\%$), whereas another fraction ($0.2 - 0.6 \text{ Pg C yr}^{-1}$; $\sim 20\%$) is buried in sedimentary deposits within freshwater ecosystems (*Battin et al.*, [2009a]; *Aufdenkampe et al.*, [2011]; *Regnier et al.*, 2013; *IPCC* [2013]; Figure 1.1).

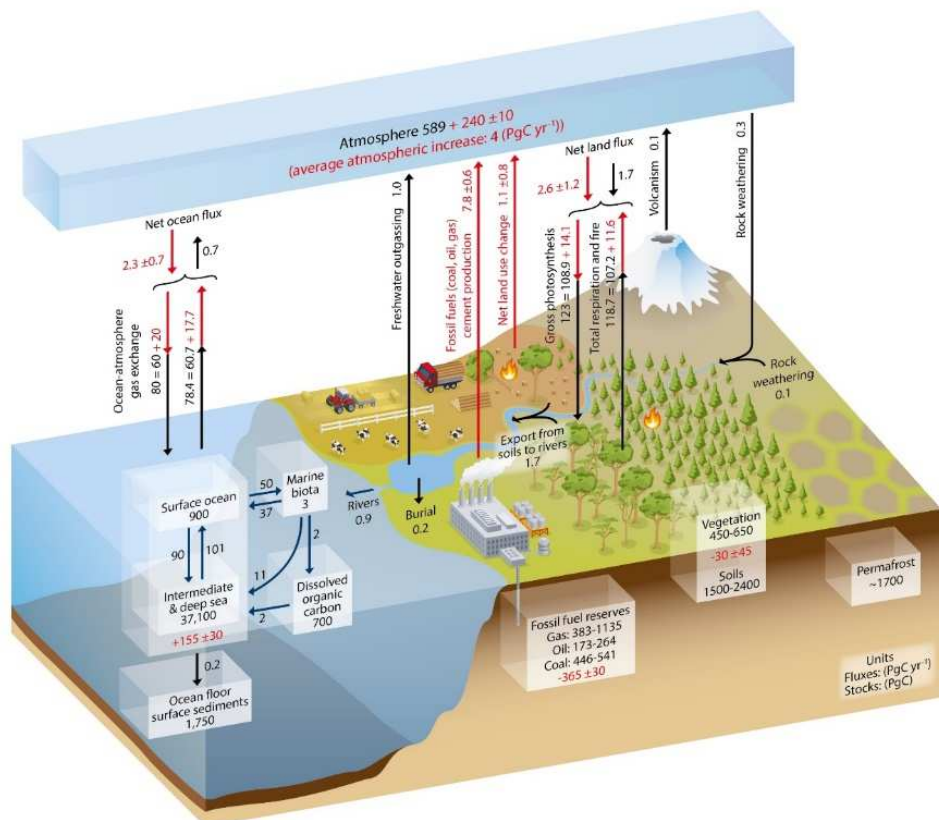


Figure 1.1 Simplified scheme of the global C cycle and its anthropogenic perturbation. Numbers represent reservoir mass or ‘C stocks’ in Pg C ($1 \text{ Pg C} = 10^{15} \text{ g C}$) and annual C exchange fluxes (in Pg C yr^{-1}). Black numbers and arrows indicate reservoir mass and exchange fluxes estimated for the time prior to the Industrial Era, about 1750. Red numbers in the reservoirs denote cumulative changes of anthropogenic C over the Industrial Period 1750–2011. By convention, a positive cumulative change means that a reservoir has gained C since 1750. *Figure source:* [IPCC, 2013].

1.2 Carbon emissions from inland waters

Over the past years, several studies have demonstrated that CO₂ emissions from inland waters show a similar magnitude to the C export from land to sea (*Aufdenkampe et al.*, [2011]; *Striegl et al.*, [2012]; *IPCC*, [2013]; Figure 1.1) as well as to the net ecosystem productivity of the terrestrial biosphere (*Cole et al.*, [2007]; *Jonsson et al.*, [2007]; *IPCC*, [2013]; Figure 1.1). The most updated global estimate, places the efflux of CO₂ emitted from streams and rivers at 1.8 Pg C y⁻¹ and from lakes and reservoirs at 0.32 Pg C y⁻¹, resulting in a global estimate of CO₂ emissions from inland waters of 2.1 Pg C y⁻¹ [*Raymond et al.*, 2013]. Conversely, our understanding of the magnitude of CH₄ emissions from freshwater ecosystems has lagged well behind that of CO₂. The few global estimates, which are based on meta-analyses of existing data of CH₄ emissions concluded that lakes, rivers and reservoirs emit 0.09 Pg C y⁻¹ (3.25 Pg C-CO_{2e} y⁻¹; CO_{2e}= CO₂-equivalents; 1g CH₄ = 28 g CO_{2e} [*IPCC*, 2013]) in the form of CH₄ of which 0.02 Pg C y⁻¹ (0.75 Pg C-CO_{2e} y⁻¹) is emitted from streams and rivers [*Stanley et al.*, 2016] and 0.07 Pg C y⁻¹ (2.5 Pg C-CO_{2e} y⁻¹) from lakes and reservoirs [*Bastviken et al.*, 2011; *Deemer et al.*, 2016].

Adding CO₂ and CH₄ emissions results in a global total C emission from freshwater ecosystems of approximately 2.2 Pg C y⁻¹ (5.1 Pg C-CO_{2e} y⁻¹) [*Bastviken et al.*, 2011; *Raymond et al.*, 2013; *Borges et al.*, 2015; *Stanley et al.*, 2016]. According to the most recent global C budget (*IPCC* [2013]; *Le Quéré et al.*, [2016]; Figure 1.1), these values are highly significant when compared to other C fluxes at global scale such as C emission from fossil fuels and industry (7.8 ± 0.6 Pg C y⁻¹), emissions derived from land use change (1.1 ± 0.8 Pg C y⁻¹), the ocean C sink (2.3 ± 0.7 Pg C y⁻¹) and the continental C sink (2.6 ± 0.9 Pg C y⁻¹).

Although the growing interest in aquatic C studies, and for C gases in particular, has brought to relatively robust estimates of C emissions from inland waters (Table 1.1), large critical uncertainties still remain. Among these, we may include the underrepresentation of some geographical regions [*Borges et al.*, 2015], the exclusion of potentially active environments for C emissions such as wetlands [*Kirschke et al.*, 2013; *Melton et al.*, 2013], temporary freshwater ecosystems [*Fenner and Freeman*, 2011; *Catalán et al.*, 2014] and small freshwater ecosystems [*Laurion et al.*, 2010; *Holgerson and Raymond*, 2016], or the

poor understanding of the mechanisms underlying C emissions [Borges *et al.*, 2015; Hotchkiss *et al.*, 2015; Stanley *et al.*, 2016]. These uncertainties preclude evaluating potential changes in C fluxes in response to human pressures, including land use and climate change.

Table 1.1 Compilation of the global surface area and annual C fluxes between freshwater ecosystems and the atmosphere.

System type	Surface Area ($\times 10^6 \text{ km}^2$)	Annual C Mass Flux (Tg C y^{-1})		Annual CO_2e Mass Flux ($\text{Tg CO}_2\text{e y}^{-1}$)	
		CO_2	CH_4	CO_2	CH_4
Lakes	3.7 - 4.5 ^{a,b}	70 - 860 ^{c,f,g,h}	31.7 - 71.6 ^{i,k*}	257 - 3153	1183 - 2673
Small ponds	0.15 - 0.86 ^c	26 - 132 ^c	0.0 - 8.3 ^{c,**}	95 - 484	0 - 310
Reservoirs	0.31 - 1.5 ^{b,d}	32 - 43 ⁱ	8.9 - 22.2 ^{i,*}	117 - 157	332 - 828
Wetlands	8.6 - 26.9 ^a	-1280 ^j	106.4 - 198.9 ^{a,*}	-4693	3957 - 7392
Streams and rivers	0.36 - 0.65 ^f	1550 - 2050 ^f	1.1 - 20.1 ^{l,**}	5683 - 7517	41 - 750

The annual CO_2e was calculated by multiplying the mass-based flux (in units of Tg of CO_2 or CH_4 per year) by the 100-year global warming potential (i.e., radiative forcing) of each gas (1 for CO_2 , 28 for CH_4) obtained from IPCC [2013]. Lakes defined as natural non-running (and non-impounded) water bodies with a surface area higher than 0.001 km^2 . Small (and very small) ponds defined as natural non-running water bodies (i.e., lakes) with a surface area lower than 0.001 km^2 . Negative values indicate atmospheric carbon sequestration by the system.

^a Downing *et al.*, [2006]; ^b Verpoorter *et al.* [2014]; ^c Hølgerson and Raymond [2016]; ^d Lehner *et al.* [2011]; ^e Melton *et al.* [2013]; ^f Raymond *et al.*, [2013];

^g Aufdenkampe *et al.*, [2011]; ^h Tranvik *et al.*, [2009]; ⁱ Deemer *et al.* [2016]; ^j Mitch *et al.*, [2012]; ^k Bastviken *et al.*, [2011]; ^l Stanley *et al.*, [2016]

* Diffusive and ebullitive CH_4 efflux

** Only diffusive CH_4 efflux pathway

1.2.1 Mechanisms of C gas exchange across the air-water interface

Biogeochemical C gases are emitted from freshwater ecosystems by two major mechanisms. The first and most frequently studied is the diffusive pathway [Fick, 1855; Bade, 2009; Baulch *et al.*, 2011]. The second, which is particularly important for CH_4 because of its specific low solubility [Weiss, 1974; Yamamoto *et al.*, 1976], is the bubble-mediated (ebullitive) pathway [Bastviken *et al.*, 2004; Baulch *et al.*, 2011; Crawford *et al.*, 2014a; DelSontro *et al.*, 2016],

The diffusive flux of a given gas across the air-water interface requires a concentration difference between both phases [Fick, 1855]. Accordingly, a higher concentration of the gas in the water compared to the air phase results in a concentration gradient that drives the diffusion of the gas from the water to the atmosphere. Conversely, a higher concentration

of the gas in the air compared to the water results in a concentration gradient that drives the diffusion of the gas from the atmosphere to the water. The rate or intensity of this diffusive flux is ultimately modulated by the gas exchange ability or gas transfer velocity (k_{600}) at the water-atmosphere layer [Fick, 1855], a physical component that mostly depends on the turbulence at the air-water interface [Bade, 2009; Vachon et al., 2010]. Consequently, in lentic freshwater ecosystems such as lakes [Wanninkhof, 1992; Cole and Caraco, 1998; Crusius and Wanninkhof, 2003; Vachon et al., 2013], reservoirs [Guérin et al., 2006, 2007a] and large rivers [Alin et al., 2011; Beaulieu et al., 2012], the k_{600} is often concluded to be determined by the water turbulence created by wind speed over the water surface. Although other physical processes such as penetrative convection due to heat loss [MacIntyre et al., 2002; Rutgersson and Smedman, 2010] or rain [Ho et al., 1997, 2007] may affect k_{600} at low wind-speeds, most empirical models used to parameterize k_{600} in lentic ecosystems are based on wind speed. In contrast, the main driver of k_{600} in lotic ecosystems (i.e. rivers and streams) is suggested to be water turbulence created by variations in stream hydromorphology [Tsvoglou and Neal, 1976; Hope et al., 2001; Raymond et al., 2012; Long et al., 2015]. Because turbulence conditions are often very variable in space, C emissions can vary greatly within fluvial networks [Wallin et al., 2011; Wehrli, 2013]. Hence, a good understanding of the spatial variability in k_{600} is required to accurately scale up C gas emissions to fluvial networks, whole regions or even larger scales [Benstead and Leigh, 2012; Raymond et al., 2013; Borges et al., 2015].

The ebullitive emission pathway has so far received much less attention than the diffusive pathway [Bastviken et al., 2011]. CH_4 production and subsequent ebullition is especially important in stagnant waters that typically experience high depositional rates and high storage of fresh organic stocks in the sediments. For instance, CH_4 ebullition can be an important pathway of CH_4 efflux in wetlands [Stamp et al., 2013] and lakes [Bastviken, 2004] as well as the primary source of CH_4 emissions in large reservoirs [Delsontro et al., 2010; Fearnside and Pueyo, 2012; Beaulieu et al., 2016] and smaller impounded systems [Maeck et al., 2013] worldwide. Similarly to the diffusive flux, recent studies have shown that the CH_4 ebullitive flux is also very dependent on physical factors such as decreases in hydrostatic pressure as a consequence of water level drawdowns or atmospheric pressure changes [Maeck et al., 2014; Deshmukh et al., 2015]. Moreover, other physical properties of

the sediment such as its bulk density or its temperature can also play an important role on driving the ebullitive CH₄ flux, at least over short time scales [Crawford *et al.*, 2014].

In addition to the Fickian diffusive emissions and the ebullitive emissions, other less studied pathways of CH₄ emissions, such as CH₄ microbubble-mediated pathway [Beaulieu *et al.*, 2012; Prairie and Giorgio, 2013; Tang *et al.*, 2014; McGinnis *et al.*, 2015] or plant-mediated transport [Yavitt and Knapp, 1995; Bergström *et al.*, 2007; Liang *et al.*, 2016] may also potentially contribute to CH₄ emissions from fluvial networks.

1.2.2 Sources and sinks of CO₂ and CH₄ in inland waters

In fluvial networks, there are two major processes that determine the concentration gradient of CO₂ (by adding CO₂ to or removing CO₂ from the water) between lentic (solid arrows in Figures 1.2a) or lotic (solid arrows in Figures 1.3a) waterbodies and the atmosphere: i) internal aquatic mineralization of organic matter (OM) [Cole *et al.*, 2000; Duarte and Prairie, 2005]), and ii) external surface and subsurface hydrological inputs of water with high dissolved inorganic carbon (DIC) content derive from either soil respiration [Humborg *et al.*, 2010a; Maberly *et al.*, 2012] or mineral weathering within the catchment [Marcé *et al.*, 2015; Nöges *et al.*, 2016]. Likewise, the role of geochemical reactions such as precipitation and dissolution of carbonate minerals [Otsuki and Wetzel, 1974; Stets *et al.*, 2009; Nöges *et al.*, 2016] or photochemical mineralization of organic solutes [Amon and Benner, 1996; Cory *et al.*, 2014; Vachon *et al.*, 2016] on the concentration gradient of CO₂ remains largely undefined both in lentic (dashed arrows in Figure 1.2a) and lotic (dashed arrows in Figure 1.3a) freshwater ecosystems.

Among the best-known processes, internal aquatic mineralization of OM (i.e., internal metabolism) has typically been considered the main process driving the concentration of CO₂ in lakes and rivers [Cole *et al.*, 2000; Duarte and Prairie, 2005]. Therefore, when no other processes are adding or removing CO₂ besides internal metabolism, the concentration of CO₂ should be in line with the degree of net autotrophy (i.e., gross primary production exceeding respiration) or net heterotrophy (i.e., respiration exceeding gross primary production) in the corresponding aquatic ecosystems. However, recent studies have shown a persistent disagreement between the CO₂ produced by internal metabolism

and the CO₂ present in both lentic and lotic ecosystem [Stets *et al.*, 2009; McDonald *et al.*, 2013; Winterdahl *et al.*, 2016]. These findings indicate that sources other than internal metabolism sustain CO₂ supersaturation and thus CO₂ emissions in both lotic and lentic freshwater ecosystems within fluvial networks.

For CH₄, the air-water concentration gradient mostly depends on the activity of methanogens in the sediments of either lentic (solid arrows in Figures 1.2b) or lotic (solid arrows in Figures 1.3b) ecosystems [Stanley *et al.*, 2016]. The presence and activity of methanogens is typically limited by their strict redox-dependent requirements: specific C substrates such as acetate or other small organic molecules as well as the presence of terminal electron acceptors such as oxygen, nitrate and oxidized forms of manganese, iron or sulphur [Reeburgh, 2007; Likens *et al.*, 2009]. These strict conditions probably explain why the conventional wisdom among aquatic scientists has been that CH₄ should be scarce in streams and rivers. Consequently, the understanding of the magnitude and sources of CH₄ emissions from lotic ecosystems has lagged well behind that of lentic systems such as lakes, reservoirs and wetlands [Zaiss *et al.*, 1982; Trimmer *et al.*, 2012].

Other processes that may add to or remove CH₄ from lentic (dashed arrows in Figure 1.2b) and lotic (dashed arrows in Figure 1.3b) ecosystems include the import of CH₄ via different hydrological flow paths (i.e., surface discharge, hyporheic exchange, groundwater discharge), export from the system mainly via surface discharge and gas movement/dissolution into the system [Bastviken *et al.*, 2004; Stanley *et al.*, 2016]. Examples of hydrological linkages that deliver CH₄ include shallow groundwater flows that travel from saturated soils or peat deposits to the channel [Jones and Mulholland, 1998; Hope *et al.*, 2001; Crawford *et al.*, 2014a], water passing through hyporheic sediments [Schindler and Krabbenhoft, 1998; Anthony *et al.*, 2012], and connection to inundated floodplains [Richey, 1988; Pullman, 1992; Teodoru *et al.*, 2015] or adjacent wetlands [Crawford *et al.*, 2013; Bresney *et al.* 2015].

Finally, oxidation of CH₄, which is an advantageous process from an energetic point of view, can be an important sink of CH₄ under aerobic [Guérin and Abril, 2007b; Stanley *et al.*, 2016], and even under anaerobic conditions [Deutzmann *et al.*, 2011; Magonigal *et al.*, 2013; Segarra *et al.*, 2015].

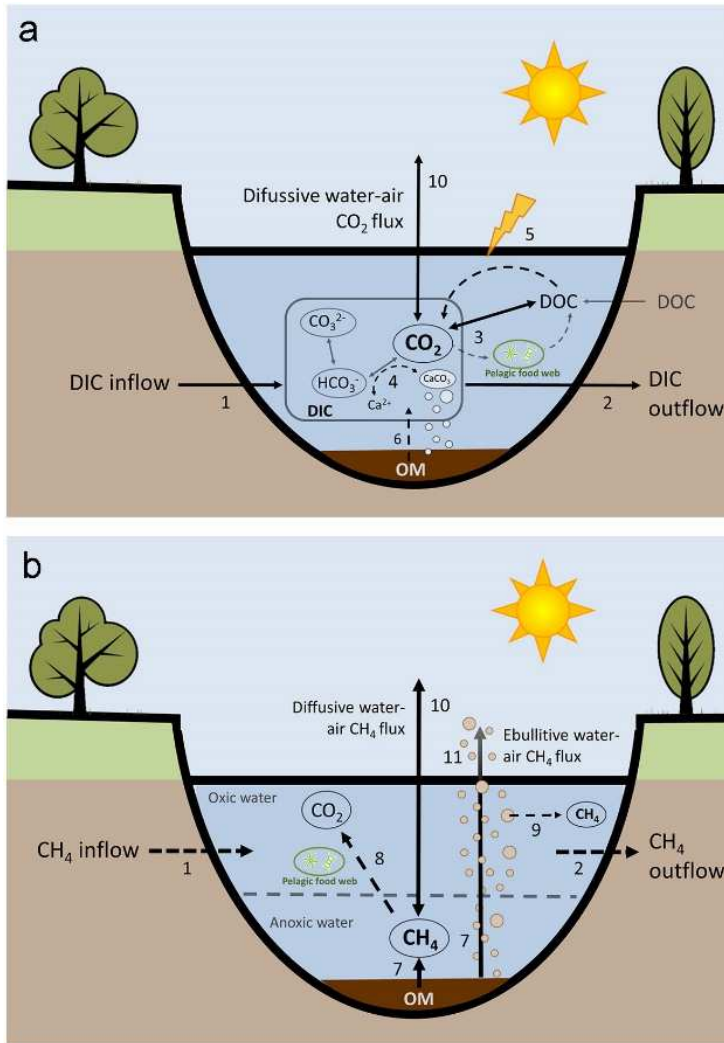


Figure 1.2 Conceptual model showing the primary (solid arrows) and the less known (dashed arrows) sources and pathways involved in the production and removal of (a) CO₂ and (b) CH₄ in lentic freshwater ecosystems. DIC and CH₄ are imported to (1) or exported from (2) the system following different hydrological flow paths (i.e., surface discharge, hyporheic exchange, groundwater discharge). Internal metabolism (3) and calcite dissolution and precipitation (4) can consume or release CO₂ within the systems. Photochemical mineralization of OM in the water column (5) and biological mineralization of OM in the sediment (6) releases CO₂ into the system. Water column, benthic, and hyporheic methanogenesis incorporate CH₄ either dissolved or in the form of bubbles into the water column (7) while CH₄ oxidation (i.e., methanotrophy) consumes CH₄ (8). Bubble dissolution (9) also takes place in the water column and alters the cycling of CH₄. Finally, gas exchange, which can occur via diffusion for both CO₂ and CH₄ (10) and via ebullition only for CH₄ (11), either dissolve the gas into- or evade the gas out from- the system.

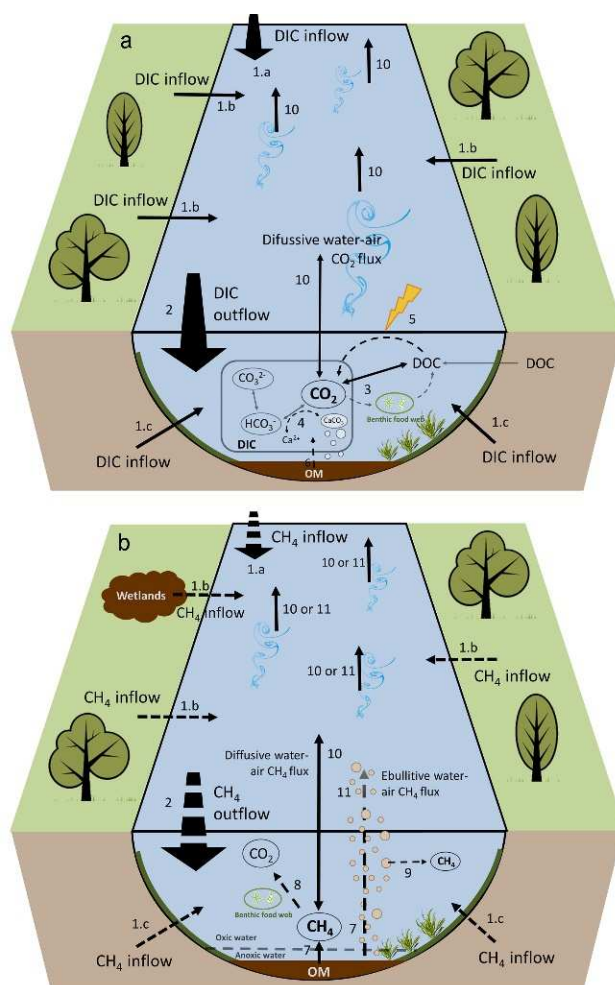


Figure 1.3 Conceptual model showing the main (solid arrows) as well as the less known (dashed arrows) sources and pathways involved in the production and removal of (a) CO₂ and (b) CH₄ in lotic freshwater ecosystems. DIC and CH₄ are imported to the system (1) following different hydrological flow paths (i.e., surface discharge (1.1), lateral discharge (1.2) and groundwater and hypothetical discharge (1.3)). In lotic waterbodies, DIC and CH₄ are exported from the system primarily via surface discharge (2). Internal metabolism (3) and calcite dissolution and precipitation (4) can consume or release CO₂ within the systems. Photochemical mineralization of OM in the water column (5) and biological mineralization of OM in the sediment (6) release CO₂ into the system. Benthic, and hyporheic methanogenesis can incorporate CH₄ either dissolved or in the form of bubbles into the system (7) while CH₄ oxidation (i.e., methanotrophy (8)) consumes CH₄. Bubble dissolution (9) also takes place in the water and alters the cycling of CH₄. Bubble dissolution may be enhanced in lotic waterbodies as a combined effect of oxygenic conditions and high turbulence. Finally, gas exchange, which can occur via diffusion for both CO₂ and CH₄ (10) and via ebullition only for CH₄ (11), either dissolve the gas into- or evade the gas out from- the system.

1.3 The study of biogeochemical processes at a fluvial network scale

Fluvial networks are hieratically organized systems, composed of a set of subsystems that are linked and interact with each other as well as with other components of the landscape (i.e., soils, groundwater, atmosphere and oceans) from large to small spatial scales [Frissell *et al.*, 1986; Lowe *et al.*, 2006].

Due to their inherent characteristic of unidirectional flow, most models assume that the physical and chemical properties of a stream segment within a fluvial network will always be more similar to those of neighbouring segments. This gradient should elicit a series of responses within the constituent populations resulting in a continuum of biotic adjustments and consistent patterns of loading, transport, utilization, and storage of OM along the length of a river [Vannote *et al.*, 1980]. However, no river is a continuum, but, on the contrary, at any spatial scale, rivers are regularly divided into discrete parts based on non-arbitrary distinctions [Frissell *et al.*, 1986; Poole, 2002]. Therefore, the sequential ability of a fluvial network to transport and process organic and inorganic materials rather depends on the presence or absence of flow paths between persistent fluvial patches [Fisher *et al.*, 2004; Freeman *et al.*, 2007; Larned *et al.*, 2010]. Framed within this idea, the discontinuum view assumes that the flow paths between persistent fluvial patches might be laterally, vertically or longitudinally constrained over time [Ward and Stanford, 1983; Stanley *et al.*, 1997; Stanford and Ward, 2001; Fisher *et al.*, 2004; Larned *et al.*, 2010].

The “serial discontinuity concept of lotic ecosystems” was perhaps the first conceptual framework describing the spatial complexity of biogeochemical patterns in fluvial networks considering the effect of flow discontinuities [Ward and Stanford, 1983; Stanford and Ward, 2001]. More recent conceptual models [Fisher *et al.*, 2004; Battin *et al.*, 2009b; Larned *et al.*, 2010], empirical studies [Tank *et al.*, 2010; McGuire *et al.*, 2014; Dent and Grimm, 2016] or even simulation exercises [Acuña and Tockner, 2010a] have also attempted to provide a framework that facilitates the transition from classical fluvial network biogeochemical models assuming system homogeneity (Figure 1.4a) to those ones that consider the natural heterogeneity inherent to fluvial networks (Figure 1.4b).

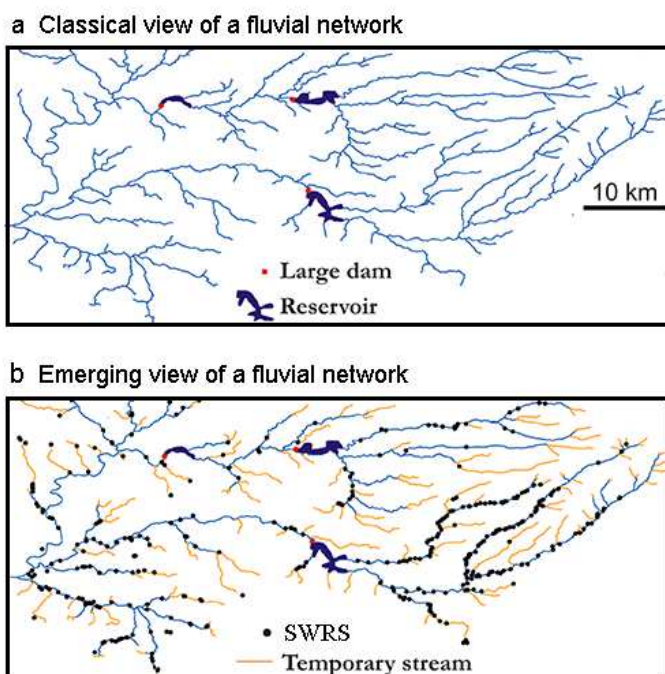


Figure 1.4 Maps exemplifying the spatial configuration of a fluvial network from two contrasted points of view: (a) the classical continuous point of view, where flow discontinuities such as temporary streams and small man-made water retention structures (SWRS) are not considered and, (b) the emergent discontinuum point of view, where SWRS and temporary streams that run dry at some point in space and time are integrated within the complexity of fluvial networks. Figure by courtesy of Rafael Marcé.

Some studies (mostly conceptual) dealing with fluvial C biogeochemistry have emphasized the potential influence of network discontinuities (in time and in space) on modulating C cycling within fluvial networks [Ward and Stanford, 1983; Battin *et al.*, 2009b; Larned *et al.*, 2010; Acuña and Tockner, 2010]. Specifically, these studies highlight i) the importance of flow discontinuities associated to the presence of dams on enhancing heterotrophic processes along fluvial networks, or ii) the effect of flow fragmentation and the associated repeated cycles of transport and retention of organic materials occurring in temporary rivers on leading recurrent fluvial network heterogeneities in C processing. Nevertheless, the vast number of empirical studies focused on C gas flux dynamics in fluvial networks [Wallin *et al.*, 2010; Striegl *et al.*, 2012; Crawford *et al.*, 2013; Peter *et al.*, 2014] rarely

address the effect of local discontinuities such as the presence of impoundments or the effect of flow intermittency in temporary rivers. Therefore, these studies may be potentially missing the true spatial complexity of biogeochemical patterns and processes that is inherent to fluvial networks.

1.4 Mediterranean fluvial networks as ideal settings to test the effects of flow discontinuities on carbon gas fluxes

1.4.1 Climate setting and hydrological regime

The Mediterranean climate is characterized by a pronounced seasonality with warm temperatures in summer and moderate temperatures in winter [Gasith and Resh, 1999a]. The total annual precipitation varies substantially among different Mediterranean regions (from 275 to 900 mm; [Lulla, 1987]); however, precipitation shows in general a highly predictable pattern, with most of it often falling in few major storm events during the cool wet season [Lulla, 1987]. The discharge regime of Mediterranean streams and rivers generally follows that of the rainfall pattern; thus, discharge also exhibits a predictable seasonal pattern with high flow in the wet period (late autumn to early spring) and low flow in the dry period (from late spring to early autumn) [Gasith and Resh, 1999a; Bonada and Resh, 2013]. During the wet period, both the hydrological connectivity within the fluvial network and between the fluvial network and the catchment is maximized and most of the fluvial network area is covered with surface water (i.e., hydrological expansion; Figure 1.5a). In this situation, the mobilization of solutes such as nutrients [von Schiller et al., 2011; Bernal et al., 2013] and C gases [Hope et al., 2001; Öquist et al., 2009b; Leith et al., 2015] is enhanced by promoting the longitudinal and lateral supply pathways across the fluvial network. At the same time, reduced water residence time during high flows limits the capacity of the biota to interact with organic substrates [Battin et al., 2009b], thereby constraining the processing and retention of nutrients and C [Bernal et al., 2013] and homogenizing the sources of DIC [Hotchkiss et al., 2015] and DOC [Raymond et al., 2015].

In contrast, during the dry period, the hydrological connectivity decreases across all the spatial dimensions and the area of the fluvial network covered with surface water is drastically reduced (i.e., hydrological contraction; Figure 1.5b). Consequently, the fluvial network is often converted into a fragmented heterogeneous riverscape characterized by slow-moving waters, isolated river pools and dry beds (*Stanley et al.*, [1997]; *von Schiller et al.*, [2011]; *Bernal et al.*, [2013]; Figure 1.5b). In this situations, the reduced hydrological connectivity also hampers the lateral and longitudinal supply of nutrients and C [*von Schiller et al.*, 2011; *Bernal et al.*, 2013] and favours, in turn, in-stream processes through the easier interaction with biological actors [*Battin et al.*, 2009b]. Similarly, flow intermittency in temporary rivers also creates discontinuities in the source and degradation of OM [*Casas-Ruiz et al.*, 2015; *von Schiller et al.*, 2015; *Abril et al.*, 2016]. However, little is known about how flow intermittency can affect C gas flux dynamics in Mediterranean fluvial networks.

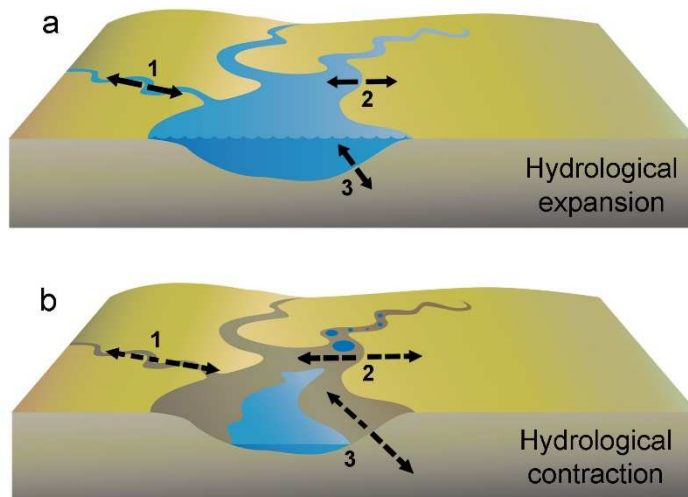


Figure 1.5 Schematic figure illustrating two contrasted hydrological situations in Mediterranean fluvial networks: (a) hydrological expansion and (b) hydrological contraction. Solid and dashed arrows indicate respectively high and low hydrological connectivity within longitudinal (1), lateral (2) and vertical (3) spatial dimensions of fluvial networks.

Temporary rivers that recurrently run dry mainly occur in arid and semiarid regions such as the Mediterranean, although they can also be found in many other areas of the world (Tooth, [2000]; Acuña *et al.*, [2014]; Datry *et al.*, [2014]; Figure 1.6). Due to their temporal and spatial dynamism, estimates of the total length, surface area and discharge of temporary rivers are still very rough [Acuña *et al.*, 2014; Datry *et al.*, 2014]. Low-order streams deserve special attention, since they account for more than 70% of the area of fluvial networks and are particularly prone to flow intermittency [Lowe *et al.*, 2006]. These low-order temporary streams are very dynamic systems in time and space, and analysing their spatial coverage is particularly difficult to detect by traditional mapping techniques [Benstead and Leigh, 2012]. We can therefore suspect that the surface area of temporary watercourses in the global fluvial network can be higher than 50% [Datry *et al.*, 2014], while their importance is increasing as a result of the combined effects of climate and land use changes [Palmer *et al.*, 2008; Larned *et al.*, 2010; Hoerling *et al.*, 2012].

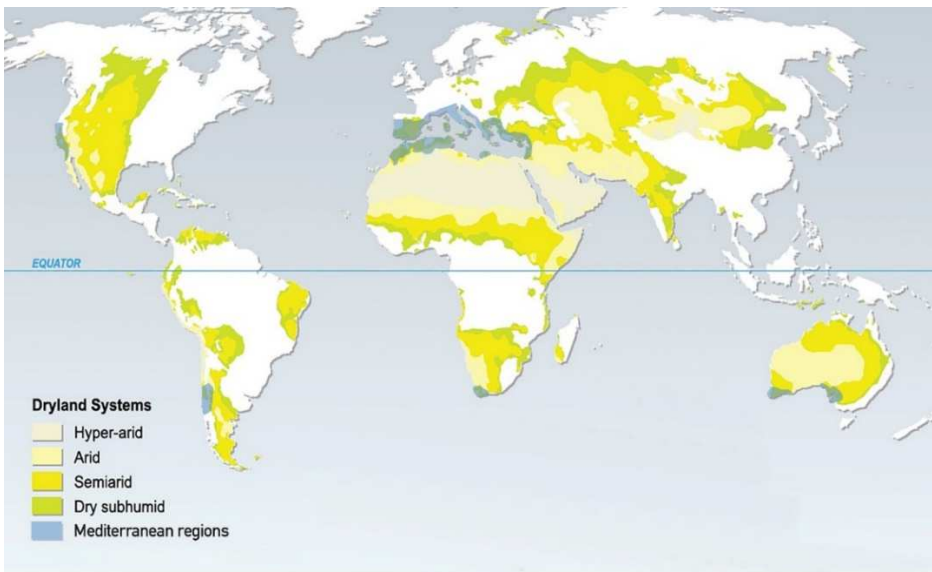


Figure 1.6 Location of the arid and semi-arid regions (i.e., dryland systems) in the world. The area of Mediterranean regions is specifically highlighted (in blue). Figure by courtesy of Xisca Timoner.

Our understanding of the biogeochemical processes that occur in temporary rivers lags well behind that of perennial watercourses [Acuña *et al.*, 2014; Datry *et al.*, 2014; Leigh *et al.*, 2016]. By extension, far less is known about the biogeochemical processes that occur in the dry beds of these temporary streams and rivers (hereinafter referred to as dry riverbeds) [Steward *et al.*, 2012]. These unexplored habitats have been largely overlooked by aquatic and terrestrial ecologists and biogeochemists [Steward *et al.*, 2012]. However, dry riverbeds are dynamic habitats [Stanley *et al.*, 1997; Boulton, 2003], representing spatial (i.e., transitional zones between dissimilar habitats) and temporal (i.e., transitional periods between persistent and dissimilar states) ecotones [Naiman and Decamps, 1997]. Thus, against the traditional view of being “biogeochemically inactive”, dry riverbeds are likely to be potential active sites for materials transformations [McClain *et al.*, 2003]. In general, there is little knowledge on the biogeochemistry of dry riverbeds [Larned *et al.*, 2010; Steward *et al.*, 2012; Leigh *et al.*, 2016]; although recent studies advanced that microbial activity [Pohlen *et al.*, 2013; Febria *et al.*, 2015] and associated C and nitrogen processing in dry riverbed sediments can be maintained to some degree during stream desiccation by the activity of well-adapted biofilms [Zoppini and Marxsen, 2011; Timoner *et al.*, 2012, 2014; Merbt *et al.*, 2016]. Nevertheless, our understanding of the effects of flow intermittency and associated river fragmentation and drying on C gas fluxes across Mediterranean fluvial networks remains limited.

1.4.2 Intense damming

Due to the high human demand for energy and water, most fluvial networks worldwide are already or in the process of being regulated (Nilsson *et al.*, [2005]; Döll *et al.*, [2009]; Lehner *et al.*, [2011]; Zarfl *et al.*, [2014]; Figure 1.7). Regulation is achieved through a variety of hydraulic structures, ranging from very large dams to smaller reservoirs, impoundments and weirs (Figure 1.7). Mediterranean fluvial networks are no exception, having mainly been modified by small man-made water retention structures (SWRS; i.e., weirs and small to very small impoundments with surface area $< 0.1 \text{ km}^2$ and a volume $< 0.2 \text{ hm}^3$) for centuries [García-Ruiz *et al.*, 2011].

Disruption of water flow by dams enhances the loss of longitudinal connectivity [Stanford and Ward, 2001] and modifies hydrological dynamics [Kondolf and Batalla, 2005; Grill *et al.*, 2015] of fluvial networks by prolonging the residence time in waters associated to dams. Moreover, dams alter water physicochemistry [Ward and Stanford, 1983] and the transport dynamics of suspended materials [Syvitski *et al.*, 2005; Maeck *et al.*, 2013], with severe impacts on biological communities [Ward and Stanford, 1983; Stanford and Ward, 2001; Haxton and Findlay, 2008] and biogeochemical cycles at the different scales of organization [Ward and Stanford, 1983; Stanford and Ward, 2001; Friedl and Wüest, 2002].

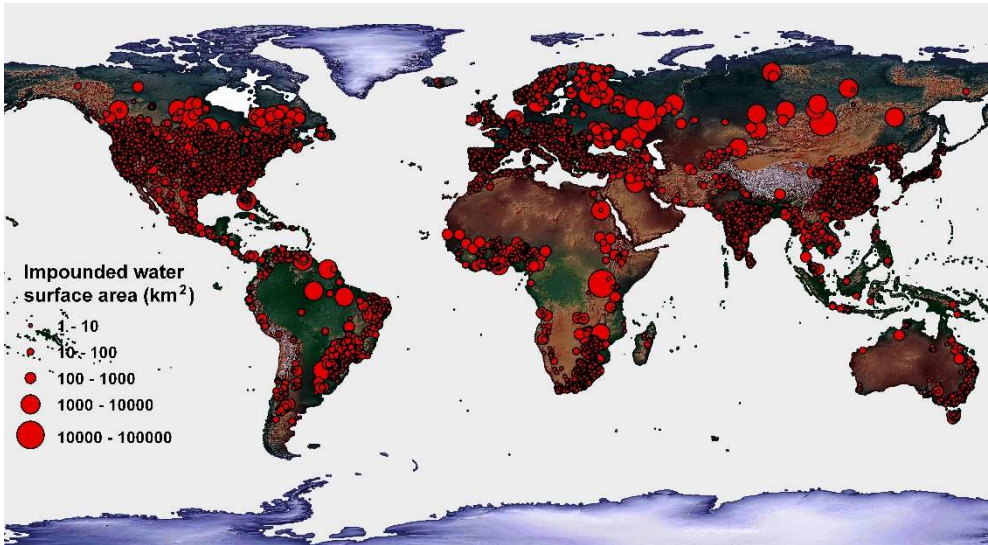


Figure 1.7 Map of the global location and distribution of large- and medium-size reservoirs ($1-10^5$ km² of impounded water surface area). Figure constructed with data from the Global Reservoir and Dam Database (GRand) [Lehner *et al.*, 2011].

Most quantitative estimates of C emissions from impounded waters have mainly been obtained for very large ($> 10^4$ km²), large ($10^4 - 10^2$ km²) and medium ($100 - 1$ km²) size reservoirs [St. Louis *et al.*, 2000; Barros *et al.*, 2011; Deemer *et al.*, 2016]. These estimates point out that the depositional zones close to the river inflow, where freshly allochthonous materials enter the reservoir (i.e., riverine-lacustrine transition zone, *sensu* Wetzel [2001]),

are very active compartments in terms of CO₂ and CH₄ production and emission despite their relatively small areal coverage [Beaulieu *et al.*, 2016]. The sedimentation of fresh OM in the riverine-lacustrine transition zone, which in the case of smaller systems (< 1 km²) can cover a major fraction of the impounded water surface area, fuels intense CO₂ and CH₄ production, making these systems potential biogeochemical hotspots for C emission to the atmosphere [Maeck *et al.*, 2013]. However, the effects of SWRS on C gas flux dynamics have so far remained poorly examined, despite they represent the most common water retention structure causing river fragmentation worldwide [Downing *et al.*, 2006; Lehner *et al.*, 2011; Verpoorter *et al.*, 2014].

1.5 Dissertation Objectives

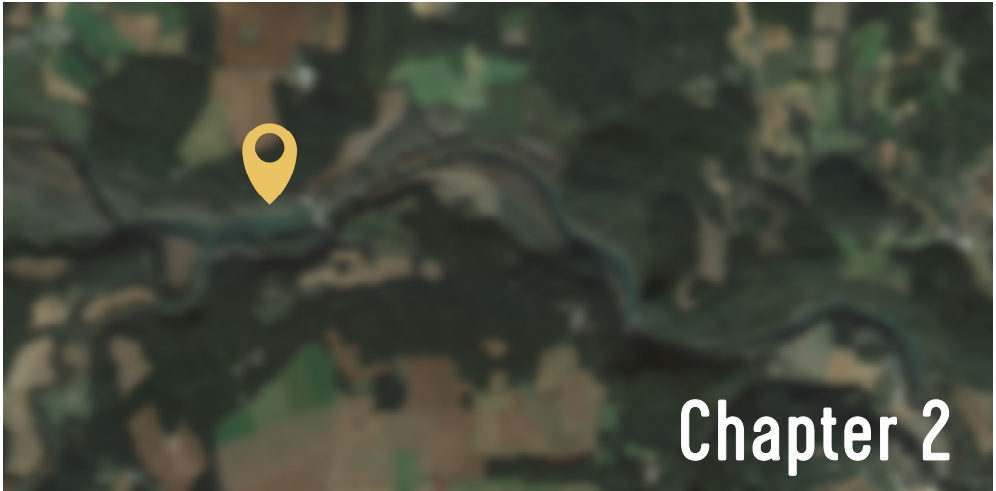
The overarching goal of this dissertation is to investigate how flow discontinuities (i.e., river impoundment, flow fragmentation and drying) shape the spatiotemporal patterns, controls and sources of carbon (C) gas fluxes in a Mediterranean fluvial network. This goal is addressed along four chapters, each one corresponding to an independent publication. The first two chapters focus on the effect of flow fragmentation and drying, whereas the other two chapters focus on understanding the effect of small and very small water retention structures (SWRS).

Chapter 3 of this dissertation explores and compares the magnitude, spatial patterns and potential drivers of carbon dioxide (CO₂) and methane (CH₄) emissions in a variety of environments (i.e., running waters, slow-moving waters impounded in SWRS, isolated river pools and dry riverbeds) typically observed in the fragmented heterogeneous riverscape characteristic of Mediterranean fluvial networks during summer.

Chapter 4, focuses on those parts of the fluvial network that recurrently cease to flow and run dry. Specifically, it aims to quantify CO₂ emissions from dry riverbeds, comparing them to those during the flowing period and to those from adjacent upland soils. Differences and similarities in the controls and sources of CO₂ emissions between dry riverbeds and upland soils are also explored.

Chapter 5 investigates how and to what extent the presence of SWRS influence i) the longitudinal patterns of the concentrations and diffusive CO₂ and CH₄ emissions along the river, and ii) the interplay between patches of distinct aquatic habitats (i.e., lotic and lentic) in terms of concentrations and diffusive CO₂ and CH₄ emissions.

Finally, **Chapter 6** of this dissertation evaluates and compares the magnitude, controls and sources of CO₂ emissions from lotic (i.e., free-flowing) and lentic (i.e., impounded waters stored in SWRS) river sections within the fluvial network, with special focus on their response to different hydrological conditions.



Study site and sampling design

2.1 The Fluvià River catchment

Field work was conducted in the Fluvià River catchment, located in the North-East of the Iberian Peninsula (Figure 2.1), from December 2012 to March 2015. The Fluvià River main stem is 97-km long and drains a 990-km² catchment covered with mixed forests (78%), agricultural (19%) and urban (3%) areas (Land Cover Map of Catalonia 2009, Centre of Ecology and Forestry Research of Catalonia, <http://www.creaf.uab.es/mcsc/>). The catchment is mostly calcareous, with some areas (<15%) of siliceous materials (Cartographic and Geological Institute of Catalonia, 2006, <http://www.icc.cat/>).

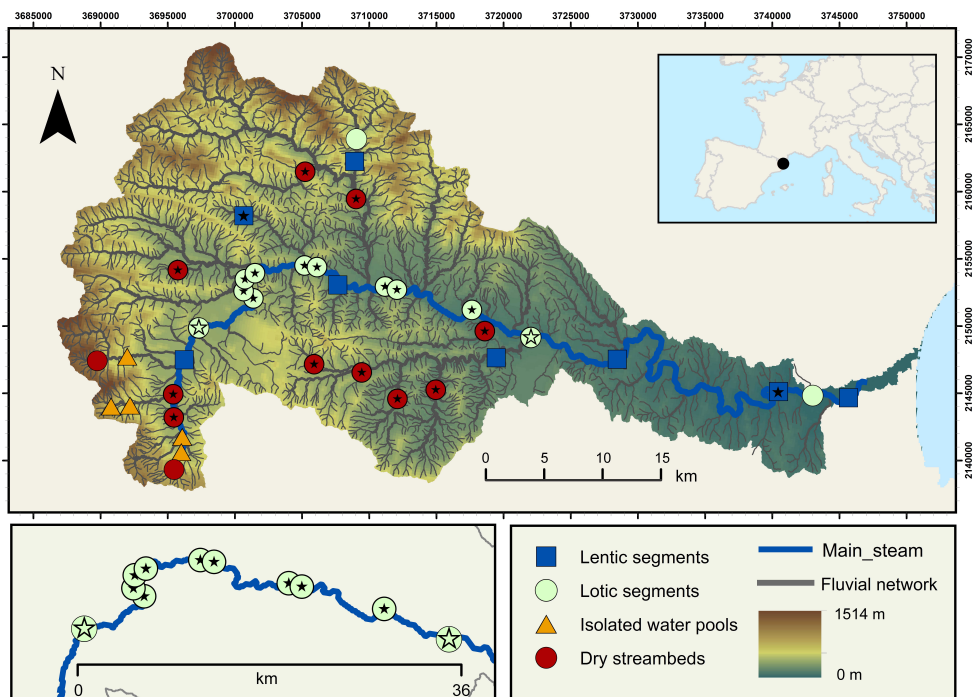


Figure 2.1 Location of the Fluvià River catchment (NE Iberian Peninsula), with the corresponding position of the study sites ($n=38$) sampled from December 2012 to March 2015. The considered study sites included 8 lotic segments (also called running waters or free-flowing river sections along the dissertation), 13 lentic segments associated to a SWRS (also called impounded waters or impounded water sections along the dissertation), 5 isolated water pools and 12 dry stream or river beds (dry riverbeds throughout the dissertation). Stars inside the symbols are used to differentiate the sites sampled in the different chapters of this dissertation (see section 2.3 and Table 2.1 for a detailed description of the sampling strategy).

The climate in the area is typically Mediterranean (Figure 2.2); the mean monthly air temperature ranges from 6 °C in January to 26 °C in July and the mean annual precipitation is 660 mm, with rainfall primarily occurring in autumn and spring, with occasional storms in summer (Data from 2004 to 2014, Catalan Water Agency, <http://aca-web.gencat.cat>).

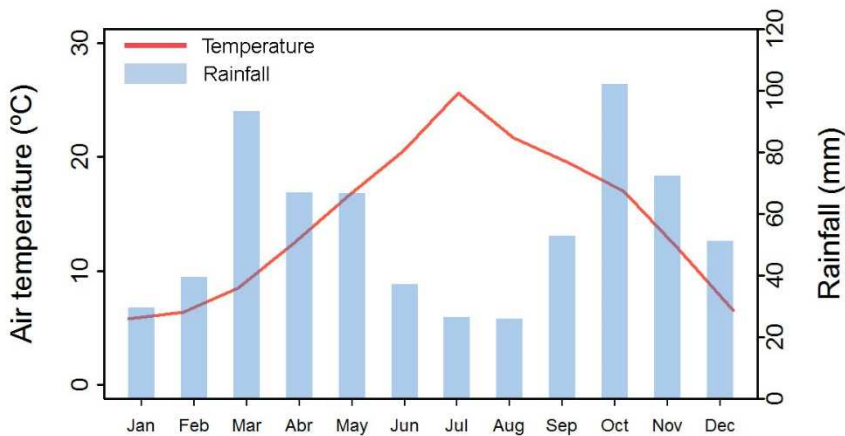


Figure 2.2 Climatic regime of the Fluvià River catchment (NE Iberian Peninsula) exemplified by the temporal variation of the mean monthly temperature (solid line) and rainfall (solid bars) registered between 2004 and 2014. Data from 2004 to 2014 obtained from the Banyoles Meteorological station situated in the central part of the studied catchment (Catalan Water Agency).

2.2 Discontinuities along the Fluvià River network

Similarly to that of other rivers situated in the Mediterranean region [*Gasith and Resh*, 1999; *Bonada and Resh*, 2013], the flow regime of the Fluvià River shows a wide seasonal variation driven by changes in rainfall. Consequently, from late summer to early autumn, its fluvial network is transformed into highly heterogeneous fragmented riverscape characterized by discontinuous sections dominated by dry riverbeds and isolated water pools (Figure 2.3). These intermittent river sections are mainly located in the headwaters of the Fluvià River network, and result from a combination of natural water scarcity and human water abstraction for irrigation.

The flow of the Fluvià River has been highly regulated since the early 20th century due to the high human demand for energy and water in the area [García-Ruiz *et al.*, 2011]. Nowadays, the Fluvià River network presents up to 61 small man-made water retention structures (SWRS; i.e., weirs and small to very small impoundments with surface area < 0.1 km² and a volume < 0.2 hm³; Figure 2.3) that cause recurrent flow discontinuities from its headwaters to the river mouth [Pavón, 2010]. The spatial distribution of these structures along the fluvial network is not homogeneous. Around 98% (60 of 61) of the SWRS are situated within the Fluvià River main stem, from which 60% (2.24 structures km⁻¹) are situated in the upper part of the catchment, 22% (0.73 structures km⁻¹) in the middle part and 18% (0.58 structures km⁻¹) in the lower part [Ferrer *et al.*, 2009].

Overall, the abundance of impounded waters associated to SWRS as well as fragmented sections dominated by isolated water pools and dry riverbeds makes the Fluvià River network an ideal setting to test hypotheses about the effects of flow discontinuities on C gas fluxes in fluvial networks.



Figure 2.3 Examples of some representative study sites grouped by environment type (i.e., running waters, impounded waters associated to SWRS, isolated water pools and dry river and reservoir beds). Photographs by courtesy of Matthias Koschorreck, Daniel von Schiller and Vicenç Acuña.

2.3 Sampling design

To address the objectives of the present dissertation, we combined field sampling surveys of different frequency and spatiotemporal extent from December 2012 to March 2015 (Table 2.1).

In **Chapter 3**, one sampling campaign was conducted at the end of summer (from 26 August to 6 September 2013) in order to measure the CO₂ and CH₄ fluxes and their potential drivers in a variety of environments typically observed in Mediterranean fluvial networks during summer. The considered environments included 6 running water reaches (empty blue squares in Figure 2.1 and Table 2.1; visual examples in Figure 2.3), 4 impounded waters stored in SWRS (2 empty green circles + 2 green circles with open stars in Figure 2.1 and Table 2.1; visual examples in Figure 2.3), 5 isolated water pools formed during the fragmentation of the fluvial network (orange triangles in Figure 2.1 and Table 2.1; visual examples in Figure 2.3) and 2 dry beds (empty red circles in Figure 2.1 and Table 2.1; visual examples in Figure 2.3). Two additional sites (i.e., 1 impounded water and 1 dry reservoir belt) from a nearby catchment (i.e., Muga River, NE of Iberian Peninsula) were also sampled in order to expand the dataset.












In **Chapter 4**, the focus was placed on 10 temporary tributaries of the Fluvità River that recurrently cease to flow and run dry (red circles with stars in Figure 2.1 and Table 2.1; visual examples in Figure 2.3). At each sampling site, we measured CO₂ fluxes and took samples for physicochemical characterization of the dry riverbeds sediments and the adjacent upland soils during the dry (August 2014) and the wet period (March 2015).

In **Chapter 5**, the sampling focused on an intensively regulated 36-km stretch in the upper part of the river main stem (lower left corner in Figure 2.1 and Table 2.1) to investigate the direct interplay between lotic and lentic waterbodies in terms of C gas fluxes. To address this, we measured the dissolved concentrations and fluxes of CO₂ and CH₄ in a selection of 11 impounded waters associated to SWRS (green open circles with stars in Figure 2.1 and Table 2.1; visual examples in Figure 2.3) and their adjacent free-flowing sections. To characterize the potential temporal variations, 11 impounded river sections and their

adjacent free-flowing sections were sampled three times in 2014: in spring (28 to 30 April), summer (2 to 4 September) and winter (9 to 11 December).

In **Chapter 6**, we measured CO₂ emissions and the underlying fluxes that drive variation in CO₂ concentration within a set of 12 segments situated throughout the fluvial network (from headwaters to lowlands; Figure 2.1) along 12 monthly samplings (December 2012 to November 2013), in order to cover the wide spectrum of hydrological conditions occurring in the fluvial network. The segments included 8 lotic sections (i.e., running water reaches; blue solid squares in Figure 2.1 and Table 2.1; visual examples in Figure 2.3) and 4 lentic sections (i.e., stagnant waters associated to a dam or weir; 2 green open circles + 2 green open circles with open stars in Figure 2.1 and Table 2.1; visual examples in Figure 2.3).

Table 2.1 Temporal and spatial extent, measured C gas fluxes and specific objectives addressed in each chapter of this dissertation.

Chapter	Temporal extent		Spatial extent		Measured C gas	Specific objectives			
	Frequency	Duration	Environment	N		Symbol	Magnitude and spatio-temporal patterns	Controls	Sources
3	1 sampling (summer)	2 weeks	Lot	6		CO ₂ & CH ₄	✓	✓	
			Len	4		CO ₂ & CH ₄	✓	✓	
			Iso	5		CO ₂ & CH ₄	✓	✓	
			Dry	2		CO ₂ & CH ₄	✓	✓	
4	2 samplings (summer & spring)	1 week	Dry	10		CO ₂	✓	✓	✓
5	Seasonal	1 year	Len	11	 + 	CO ₂ & CH ₄	✓	✓	✓
6	Monthly	1 year	Len	4	 + 	CO ₂	✓	✓	✓
			Lot	8	 + 	CO ₂	✓	✓	✓

Lot = lotic segment (also called running water or free-flowing river section along the dissertation), *Len* = lentic segment associated to a SWRS (also called impounded water or impounded water section along the dissertation), *Iso* = isolated water pool, *Dry* = dry bed

Symbols are described in the legend of Figure 2.1

Grey font indicates objectives that were not directly addressed



**Hot spots for carbon emissions from Mediterranean
fluvial networks during summer drought**

Abstract

During summer drought, Mediterranean fluvial networks are transformed into highly heterogeneous riverscapes characterized by different environments (i.e., running and impounded waters, isolated river pools and dry beds). This hydrological setting defines novel biogeochemically active areas that could potentially increase the rates of carbon (C) emissions from the fluvial network to the atmosphere. Using chamber methods, we aimed to identify hot spots for carbon dioxide (CO₂) and methane (CH₄) emissions from two typical Mediterranean fluvial networks during summer drought. The CO₂ efflux from dry beds (mean ± SE = 209 ± 10 mmol CO₂ m⁻² d⁻¹) was comparable to that from running waters (120 ± 33 mmol m⁻² d⁻¹) and significantly higher than from impounded waters (36.6 ± 8.5 mmol m⁻² d⁻¹) and isolated pools (17.2 ± 0.9 mmol m⁻² d⁻¹). In contrast, the CH₄ efflux did not significantly differ among environments, although the CH₄ efflux was notable in some impounded waters (13.9 ± 10.1 mmol CH₄ m⁻² d⁻¹) and almost negligible in the remaining environments (mean < 0.3 mmol m⁻² d⁻¹). Diffusion was the only mechanism driving CO₂ efflux in all environments and was most likely responsible for CH₄ efflux in running waters, isolated pools and dry beds. In contrast, the CH₄ efflux in impounded waters was primarily ebullition-based. Using a simple heuristic approach to simulate potential changes in C emissions from Mediterranean fluvial networks under future hydrological scenarios, we show that an extreme drying out (i.e., a 4-fold increase of the surface area of dry beds) would double the CO₂ efflux from the fluvial network. Correspondingly, an extreme transformation of running waters into impounded waters (i.e., a 2-fold increase of the surface area of impounded waters) would triple the CH₄ efflux. Thus, C emissions from dry beds and impounded waters should be explicitly considered in C assessments of fluvial networks, particularly under predicted global change scenarios, which are expected to increase the spatial and temporal extent of these environments.

Original publication (*Appendix C in the Supporting information section*):

Gómez-Gener, L., B. Obrador, D. von Schiller, R. Marcé, J. P. Casas-Ruiz, L. Proia, V. Acuña, N. Catalán, I. Muñoz, and M. Koschorreck (2015), Hot spots for carbon emissions from Mediterranean fluvial networks during summer drought, *Biogeochemistry*, 125(3), 409–426, doi:10.1007/s10533-015-0139-7

3.1 Introduction

Increasing evidence has demonstrated the active role of inland waters in the global carbon (C) cycle and the capacity of these water bodies to emit significant amounts of carbon dioxide (CO₂) and methane (CH₄) to the atmosphere [Cole *et al.*, 2007; Battin *et al.*, 2009a]. Recent global estimates of C emissions have shown that inland waters, including both running and impounded waters, emit approximately 2.1 Pg C y⁻¹ in the form of CO₂ [Raymond *et al.*, 2013a] and 0.09 Pg C y⁻¹ in the form of CH₄ [Bastviken *et al.*, 2011a]. Expressed as CO₂ equivalents, these emissions correspond to 3.25 PgC-CO₂e y⁻¹, assuming that 1 kg of CH₄ corresponds to 28 kg of CO₂ over a 100-year period [IPCC, 2013]. In this context, regional and local studies conducted in arctic and subarctic [Kling *et al.*, 1991; Lundin *et al.*, 2013], boreal [Jonsson *et al.*, 2007; Campeau and Lapierre, 2014], temperate [Hope *et al.*, 2001; Halbedel and Koschorreck, 2013] and tropical biomes [Abril, 2005; Guérin *et al.*, 2007; Fearnside and Pueyo, 2012] have confirmed the role of streams, lakes and reservoirs as net emitters of CO₂ and CH₄ to the atmosphere. Nonetheless, there is limited information concerning the relevance of C release from inland waters to the atmosphere in arid and semiarid regions, such as the Mediterranean [López *et al.*, 2011; Obrador and Pretus, 2013; Morales-Pineda, 2014].

Because of the climatic conditions of Mediterranean regions, with warm, dry summers and mild, humid winters, Mediterranean fluvial networks are characterized by a highly seasonal and intermittent hydrological regime [Gasith and Resh, 1999a]. During the wet period (late autumn to early spring), the hydrological longitudinal connectivity increases, and most of the fluvial network area is covered with surface water. In contrast, during the dry period (from late spring to early autumn), the hydrological longitudinal connectivity decreases, and the area of the fluvial network covered with surface water is drastically reduced. Consequently, during summer drought, the fluvial network is converted into a fragmented heterogeneous riverscape characterized by slow-moving waters, isolated river pools and dry streams and river beds (hereinafter referred to as dry riverbeds). Temporary rivers experiencing these patterns are not restricted to arid and semiarid regions, but they can be found in many areas of the world [Tooth, 2000; Acuña *et al.*, 2014; Datry *et al.*, 2014]. Moreover, as a consequence of climate change and water abstraction for socio-economic

uses, their global surface area is expected to increase in the Mediterranean and other regions where a negative water flow trend has been predicted [Milliman *et al.*, 2008; Tockner *et al.*, 2009; Larned *et al.*, 2010].

Dry beds are defined as the parts of the fluvial network exposed to air during dry periods [Steward *et al.*, 2012]. They are habitats in their own right and differ from adjacent riparian and other terrestrial habitats in their substrate composition, topography, microclimate, vegetation cover, inundation frequency, and biota [Steward *et al.*, 2012]. Dry river beds play an important role as dispersal corridors and contain a unique diversity of aquatic, amphibious, and terrestrial biota [Williams 2006; Lake 2011]. Moreover, recent studies have reported that the energy flow, nutrient cycling and other biogeochemical processes also continue when the river runs dry. For example, Zoppini and Marxsen [2011], Timoner *et al.*, [2012] and Pohlen *et al.*, [2013] showed that extracellular enzymatic activities and C processing through sediment biofilms could be maintained to some degree during desiccation. Similarly, Gallo *et al.*, [2013] and von Schiller *et al.* [2014] showed that temporary streams can release significant amounts of CO₂ when they are dry. Nevertheless, our understanding of the biogeochemical processes that occur in dry beds and the role of these environments as emitters of CO₂ and CH₄ to the atmosphere remains limited [Steward *et al.*, 2012].

The hydrological contraction of the fluvial network also affects impounded waters stored in dams, weirs and small impoundments. These aquatic environments are abundant in Mediterranean regions because of the growing human demand for water and electricity [García-Ruiz *et al.*, 2011]. The reduction of the river flow as a consequence of seasonal drought prolongs the residence times of the water in impoundments, which favour C processing through the promotion of the interaction between OM and biological actors [Battin *et al.*, 2009b; Acuña and Tockner, 2010]. As a result, C emissions from impounded waters might increase during hydrological contraction. Furthermore, the reduction of the volume and surface area during summer drought also increases the areal extent of exposed dry sediments along the shore of impounded waters, which together to those from dry stream and riverbeds may be potentially active, but frequently neglected, sites for C emissions [Mitchell and Baldwin, 1999; Forzieri *et al.*, 2014].

Knowledge on the biogeochemistry of isolated river pools is also limited despite they are abundantly observed along temporary rivers during hydrological contraction (Bernal et al. 2013; Datry et al. 2014). Isolated pools show high residence times and potentially suitable conditions for methanogenesis (i.e., organic matter (OM) accumulation and low dissolved oxygen concentration) [Vazquez et al., 2010; von Schiller et al., 2011]. Nevertheless, the hydrological isolation in these pools creates individual systems that are highly influenced through particular local conditions [Dahm et al., 2003; Bonada et al., 2006].

In the present study, we aimed to quantify C emissions and to identify C emission hot spots from Mediterranean fluvial networks during summer drought. To this end, we measured the CO₂ and CH₄ effluxes and their potential drivers in a variety of environments (i.e., running waters, impounded waters stored in reservoirs, weirs and small dams, isolated river pools and dry river and impoundment beds) typically observed in Mediterranean rivers during summer drought. We hypothesized that the reduction of flow during summer drought would promote the spatial heterogeneity of C fluxes along the fluvial network and enhance the contribution of dry beds, isolated pools and impounded waters to these fluxes. Moreover, we use a simple heuristic approach to explore the potential future implications of increasing river desiccation and impoundment of running waters on the total C emissions from Mediterranean fluvial networks.

3.2 Materials and Methods

3.2.1 Study sites and sampling design

The Fluvià River (NE Iberian Peninsula; Figure 3.1) is a 97-km long river that drains a 990-km² catchment covered with mixed forests (78%), agricultural (19%) and urban (3%) areas (Land Cover Map of Catalonia, Centre of Ecology and Forestry Research of Catalonia, 2009). The catchment is mostly calcareous, with some areas (< 15%) of siliceous materials (Cartographic and Geological Institute of Catalonia, 2006).

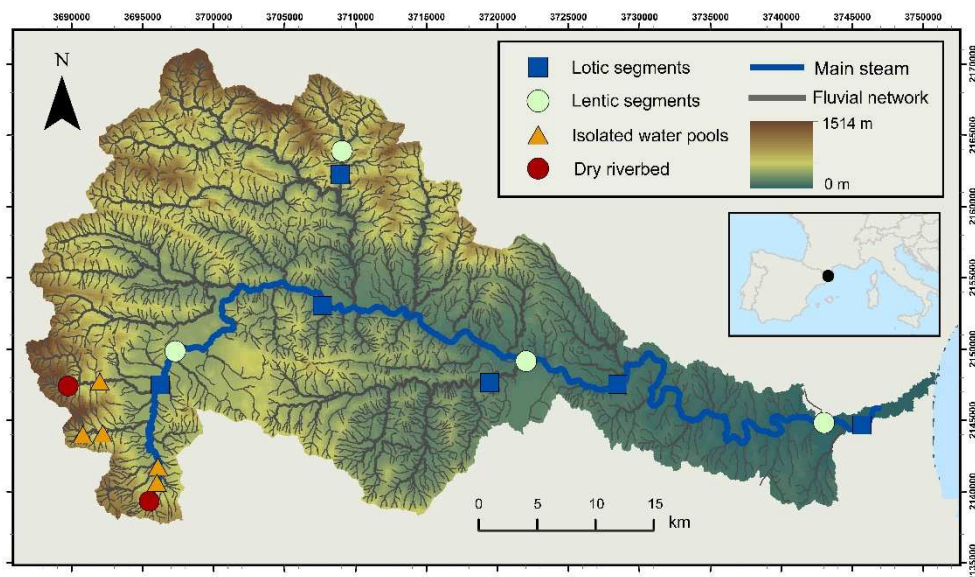


Figure 3.1 Location of the Fluvià River in Catalonia (NE Iberian Peninsula), with the corresponding position of the study sites ($n = 17$). Blue squares indicate lotic segments (i.e., running waters ($n = 6$)), green circles lentic segments (i.e., impounded waters stored in small water retention structures ($n = 4$)), orange triangles isolated river pools ($n = 5$) and red circles dry river beds ($n = 2$).

The climate in this area is typically Mediterranean. The mean monthly air temperature ranges from 6 °C in January to 26 °C in July. The mean annual precipitation is 660 mm, with rainfall primarily occurring in autumn and spring, with occasional storms in summer (Data from 2004 to 2014, Catalan Water Agency).

The water flow of Fluvià River has been deeply modified due to the high human demand for energy and water [García-Ruiz *et al.*, 2011]. Its fluvial network presents up to 61 small to very small water retention structures (SWRS) such as weirs and small impoundments that cause flow interruptions from its headwaters to the river mouth [Pavón, 2010].

We conducted the sampling campaign at the end of summer (from 26 August to 6 September 2013), prior to the first post-summer rainfall events that typically occur in the region during autumn [Bernal *et al.*, 2013]. We sampled a total of 17 sites along the Fluvià River network to cover a wide spectrum of environments typically observed during summer drought (Figure 3.1; Table A.3.1 in the Supporting information section). The considered

environments included running water reaches (n=6), impounded waters stored in SWRS (n=4), isolated river pools formed during the fragmentation of the fluvial network (n=5) and dry river beds (n=2). Two additional sites (i.e., 1 impounded water and 1 dry reservoir belt) from a nearby catchment (i.e., Muga River, NE of the Iberian Peninsula) were also sampled in order to expand the dataset. The dry beds in rivers had been dry for less than 4 weeks and the dry bed in the reservoir for approximately 2-3 months.

3.2.2 Determination of CO₂ and CH₄ fluxes

To guarantee the comparability of the flux measurements, we used the same approach (chamber method, *Frankignoulle* [1988]) to directly measure the CO₂ and CH₄ fluxes in all environments. We monitored the gas concentrations in the chamber every 30 s for a total of 10 min using a Fourier-Transform-Infrared (FTIR) Spectrometer (GASMET DX4000, Temet Instruments, Finland) after passing through an in-line moisture trap (Drierite, USA) at a rate of 2.9 L min⁻¹. Measurement accuracy of the GASMET DX4000 FTIR was within 2% of the calibrated range. We calculated the total fluxes of both gases (F , mmol m⁻² d⁻¹) from the rate of change of CO₂ and CH₄ inside the chamber:

$$F = \left(\frac{dp}{dt} \right) \left(\frac{V}{RTS} \right) \quad (1)$$

where dp/dt is the slope of the gas accumulation in the chamber ($\mu\text{atm s}^{-1}$), V is the volume of the chamber (dm^3 ; aquatic chamber = 14.6 dm^3 , soil chamber = 2.2 dm^3), S is the surface area of the chamber (dm^2 ; aquatic chamber = 9.8 dm^2 , soil chamber = 2.0 dm^2), and T is the air temperature (K) and R is the ideal gas constant ($\text{L atm K}^{-1} \text{mol}^{-1}$). Positive F values represent gas evasion to the atmosphere, and negative F values indicate gas invasion from the atmosphere. We calculated the diffusive flux of CO₂ and CH₄ from the linear concentration change of both gases in the chamber. We identified ebullitive episodes (bubbling), only in the case of CH₄, as notorious non-linear increases in the concentration of CH₄ during the course of chamber measurements. We estimated the ebullitive flux of CH₄ as the difference between the total and the diffusive flux [*Campeau and Lapierre*, 2014].

The artificial enhancement of the gas transfer velocity through disturbance of the surface boundary layer during the chamber deployment and subsequent measurement could be a critical aspect [Guérin *et al.*, 2007; Vachon *et al.*, 2010]. To minimize this, we carried out specific chamber deployment procedures in each environment. In running waters, we used a rope to deploy the chamber at a fixed position onto the water column. In impounded waters, we cautiously deployed the chamber from an anchored boat onto the water surface in the centre of the system. In isolated river pools, we slowly lowered the chamber onto the water surface in the central part of the pool using a rope. In the case of dry beds, we inserted the chamber into the exposed sediments. A total of 3 replicate measurements were obtained at every aquatic site. The number of replicate measurements was increased at each dry site (5-10) to cover the maximum spatial variability in terms of dry bed OM and water content. In both the aquatic and the dry environments, we flushed the chamber with ambient air between consecutive measurements.

3.2.3 Determination of $p_{\text{CO}_2, \text{w}}$, $p_{\text{CH}_4, \text{w}}$ and k_{600}

At every aquatic site, we determined the partial pressure of CO₂ ($p_{\text{CO}_2, \text{w}}$) and CH₄ ($p_{\text{CH}_4, \text{w}}$) in water at the same location as flux measurements. We measured the $p_{\text{CO}_2, \text{w}}$ using an infrared gas analyser (EGM-4, PP-Systems, USA) coupled to a membrane contactor (MiniModule, Liqui-Cel, USA). The water was circulated via gravity through the contactor at 300 mL min⁻¹, and the equilibrated gas was continuously recirculated into the infrared gas analyser for instantaneous p_{CO_2} measurements [Teodoru *et al.*, 2010]. The accuracy of the infrared gas analyser was estimated to be within 1% over the calibrated range. We determined the $p_{\text{CH}_4, \text{w}}$ using the headspace equilibrium technique and gas chromatography according to Striegl *et al.*, [2012]. Briefly, we collected 30 ml of water with a 60 ml polypropylene syringe, creating a headspace with ambient air of 1:1 ratio (sampled water:ambient air). To facilitate the kinetics of equilibration between the liquid and the gas phase, we shook the syringe for 1 min and submerged it in water at each sampling site for 30 min to maintain constant equilibrium temperature. The water temperature was recorded using a portable sensor, and no changes were observed during equilibration. Subsequently, we transferred the 30 mL of the equilibrated gas to a pre-evacuated gas-

tight glass tube (2-RV, Chromacol, USA). The CH₄ samples were analysed in the laboratory using a gas chromatograph coupled to a Flame Ionization Detector (Trace GC Ultra, Thermo Fisher Scientific, USA). The measurement accuracy of the gas chromatograph was estimated to be within 4% over the calibrated range. The water temperature during equilibration was used to calculate Henry's coefficient between the liquid and the gas phase (Stumm and Morgan 1996).

The CO₂ flux measured with the chamber was used to calculate the direct gas transfer velocity of CO₂ (k_{CO_2}) from Fick's law of gas diffusion:

$$F_{\text{CO}_2} = k_{\text{CO}_2} K_h \left(p_{\text{CO}_2, \text{w}} - p_{\text{CO}_2, \text{a}} \right) \quad (2)$$

where k_{CO_2} is the specific gas transfer velocity for CO₂ (m d⁻¹), F_{CO_2} is the chamber-measured CO₂ flux between the surface water and the atmosphere (mmol m⁻² d⁻¹), K_h is Henry's constant (mmol μatm^{-1} m⁻³) adjusted for salinity and temperature [Weiss, 1974; Millero, 1995], and $p_{\text{CO}_2, \text{w}}$ and $p_{\text{CO}_2, \text{a}}$ are the surface water and the atmosphere partial pressures of CO₂ (μatm), respectively. Because the gas transfer velocity is temperature- and gas-dependent, we standardized k_{CO_2} to a Schmidt number of 600 (k_{600} ; m d⁻¹), which corresponds to CO₂ at 20°C in freshwater, following Jähne and Münnich [1987]:

$$\text{Direct } k_{600} \text{ (m d}^{-1}\text{)} = k_{\text{CO}_2} \left(\frac{600}{Sc} \right)^{-n} \quad (3)$$

where Sc is the Schmidt number of a given gas at a given water temperature [Wanninkhof, 1992]. In accordance with Bade [2009], the exponent n was set to 2/3 at sites with a smooth water surface (sheltered impounded waters and isolated pools) and 1/2 in the more turbulent environments (open impounded waters and running waters).

The k_{600} was also indirectly determined after applying different methods depending on the specific type of aquatic environment. In running waters, we obtained the indirect k_{600} from the night time drop in the oxygen concentration [Hornberger and Kelly 1975]. Briefly, photosynthesis ceases from sunset to sunrise, thus night time dynamics are dependent on the respiration rate and reaeration coefficient. During the night, respiration reduces the oxygen levels until the atmosphere equilibrium is reached. In parallel, reaeration

approaches the oxygen concentration to saturation. Thus, when we plot the night time oxygen concentration per unit of time versus the oxygen saturation deficit, a linear trend is obtained. The intercept of the regression corresponds to the respiration ($\text{g O}_2 \text{ m}^{-2} \text{ h}^{-1}$) and the slope to the mean gas transfer velocity of oxygen (k_{O_2} ; m d^{-1}). The k_{O_2} was transformed to indirect k_{600} using equation (3). The dissolved oxygen concentration and temperature used in the night time reduction in oxygen method, were obtained at the running water sites at a frequency of 10 minutes with a multiparameter probe (YSI 600 OMS V2, Yellow Springs, USA).

In impounded waters, we estimated the value of indirect k_{600} from the wind speed based equation (4) of *Crusius and Wanninkhof* [2003]:

$$\text{Indirect } k_{600} \text{ (m d}^{-1}\text{)} = 0.17 U_{10} \quad (4)$$

where U_{10} is the wind speed at 10 m above the surface (m s^{-1}). The wind speed at a given height (U_x ; m s^{-1}) was converted to that at 10 m (U_{10} ; m s^{-1}) from the equation described by *Donelan* [1990]. The wind speed for these calculations was obtained from measurements during the chamber deployments using a portable anemometer (Kestrel 4000, Kestrel Meters, UK) fixed to a tripod at 2 m above the water surface.

In the case of isolated pools, we estimated the indirect k_{600} from a wind speed based model previously applied in small, shallow and low turbulence ponds [*Laurion et al.*, 2010b]:

$$\text{Indirect } k_{600} \text{ (m d}^{-1}\text{)} = 0.19 + 0.26 U_{10} + 0.02 U_{10}^2 \quad (5)$$

Due to the sheltered location, there was no noticeable wind in any of the isolated pools sites, resulting in a constant indirect k_{600} of 0.19 m d^{-1} (intercept of equation 5), a parameter reflecting the effect of the other physical processes occurring in addition to wind that cause turbulence at the air-water interface.

We acknowledge that the floating chamber approach could be problematic in some of our environments, particularly in running waters where the employed method might not capture the complex turbulence regime that characterizes this environment. To assess these potential biases, we compared the site-specific CO_2 and CH_4 fluxes obtained from the chamber method (direct) versus the system-integrated fluxes of CO_2 and CH_4 derived from

the Fick's law of gas diffusion (indirect) using equation (2). We detected a good agreement between direct and indirect CO₂ fluxes ($\log(\text{indirect CO}_2 \text{ efflux}) = 1.096(\log \text{ direct CO}_2 \text{ efflux}) - 0.28$, $r^2 = 0.81$, $p < 0.001$, $n = 16$) and between direct and indirect CH₄ fluxes ($\log(\text{indirect CH}_4 \text{ efflux}) = 0.322 \log(\text{direct CH}_4 \text{ efflux}) - 0.647$, $r^2 = 0.33$, $p = 0.019$, $n = 6$). These significant relationships support the reliability of the chamber method for quantifying C emissions in our study. However, the slope < 1 for the CH₄ equation indicates the overestimation of the direct CH₄ efflux with respect to the indirect CH₄ efflux. Therefore, it is likely that, in addition to Fickian and ebullitive transport, other pathways of CH₄ efflux, such as microbubble release, were also involved in CH₄ emission [Beaulieu *et al.*, 2012; Prairie and Giorgio, 2013; McGinnis *et al.*, 2015].

3.2.4 Physicochemical characteristics of sediments and dry beds

To characterize the inundated sediments of the impounded waters, we collected three replicates of sediment cores (diameter = 6 cm) from the deepest part of the impounded waters with a gravity corer (UWITEC, Austria). We sub-sampled the upper 5 cm of the sediment cores and determined the water content (%), dry bulk density (g cm⁻³) and porosity [Sobek *et al.*, 2011]. We also determined its OM content (mg cm⁻³) by sample combustion following the loss on ignition method [Dean 1974].

To characterize the dry river and impoundment beds, we first measured *in-situ* the dry bed water content and temperature at the dry bed surface of every chamber location (upper 5 cm) along two dry sites (1 dry river bed and 1 dry impoundment bed) using a portable soil probe (Decagon ECH₂O 10HS, Pullman, USA). We then collected sediment samples (upper 5 cm) to determine the dry bed OM content using the loss on ignition method. We estimated the basal microbial respiration rate ($\mu\text{g CO}_2 \text{ g}^{-1} \text{ h}^{-1}$) of the dry bed samples using a microrespirometry system (MicroResp, Macaulay Scientific Consulting Ltd, UK) according to Campbell and Chapman [2003]. Briefly, four replicates of 0.5 g of the sample taken at the dry bed surface of every chamber location (upper 5 cm) were added to a deep well microplate. The samples were incubated for 6 h at 20°C, and a colorimetric method was used to measure the evolution of CO₂ immediately before and after the incubation. The % change of CO₂ was converted to basal respiration ($\mu\text{g CO}_2 \text{ g}^{-1} \text{ h}^{-1}$) considering the

incubation time and temperature, the gas constant, the headspace volume and the soil dry weight as indicated in the MicroResp technical manual.

3.2.5 Hydromorphological characteristics

We measured the mean cross-sectional depth (m) and width (m) of the running water sites at the same location where the gas fluxes were measured. We measured the mean cross-sectional water velocity (m s^{-1}) with an acoustic-Doppler velocity metre (Sontek, YSI, USA), and we combined it with the measured section to derive the water discharge ($\text{m}^3 \text{s}^{-1}$). The discharge data were used to obtain averages of water velocity and stream depth along a 1-km segment using the hydraulic modelling software HecRas 2.2 (US Army Corps of Engineers) and hydromorphological data from the Catalan Water Agency.

We estimated the surface area, volume, and mean and maximum depths of the impounded waters sites from digitized bathymetric maps using a geospatial-processing software (ArcMap 10, ArcGis, USA). We calculated the residence time combining the volume obtained from the bathymetric map and the measured inflow at each impounded water site.

3.2.6 Data analysis

We grouped the 19 studied sites into 4 major environments (i.e., running waters ($n = 6$), impounded waters ($n = 5$), isolated pools ($n = 5$) and dry river beds ($n = 3$)). We tested the effect of the factor environment on the CO_2 and CH_4 fluxes, $p_{\text{CO}_2, \text{w}}$ and $p_{\text{CH}_4, \text{w}}$, direct and indirect k_{600} and percentage molar ratio between CH_4 and CO_2 efflux ($(\text{CH}_4 \text{ efflux} / \text{CO}_2 \text{ efflux}) * 100$) using one-way analysis of variance (ANOVA) and subsequent post hoc comparisons (Tukey's Honest Significant Differences test).

For the dry beds, we assessed the effect of dry bed basal respiration, water content and OM content on the CO_2 efflux using linear and non-linear regressions. For aquatic environments, we assessed the relative contributions of $p_{\text{CO}_2, \text{w}}$ and indirect k_{600} on the CO_2 efflux using simple and multiple linear regressions. When the statistical techniques required it, we log-transformed the variables to meet the conditions of homogeneity of

variance, normality and to avoid the deleterious effect of extreme large values. All statistical analyses were conducted in the R statistical environment [R Core Team 2013] using the Vegan package [Oksanen *et al.*, 2013].

3.3 Results

3.3.1 CO₂ and CH₄ effluxes along the fluvial network

The studied environments were net emitters of CO₂ (mean \pm SE = 95.7 ± 43.9 mmol m⁻² d⁻¹, range = 17 – 219 mmol m⁻² d⁻¹) and CH₄ (3.6 ± 3.4 mmol m⁻² d⁻¹, 0.1 – 13.8 mmol m⁻² d⁻¹) to the atmosphere (Figure 3.2, Table 3.1). However, significant differences among these environments, in terms of CO₂ efflux (ANOVA, $f = 23.2$, $p < 0.001$, $n = 19$; Figure 3.2a), were observed. The CO₂ efflux from dry beds (mean \pm SE = 209 ± 10 mmol m⁻² d⁻¹) was statistically comparable to that from running waters (120 ± 33 mmol m⁻² d⁻¹) and significantly higher than the CO₂ efflux from impounded waters (36.6 ± 8.5 mmol m⁻² d⁻¹) and isolated pools (17.2 ± 0.9 mmol m⁻² d⁻¹). The intra-environment variability of the CO₂ efflux was highest in running waters and lowest in isolated pools (Figure 3.2a, Table 3.1).

In contrast to CO₂, no significant differences in the CH₄ efflux were observed among the studied environments (ANOVA, $f = 2.62$, $p > 0.05$, $n = 19$; Figure 3.2b). The CH₄ efflux from impounded waters (14 ± 10 mmol m⁻² d⁻¹) was the highest among the studied environments, but also showed the highest intra-environment variability (Figure 3.2b, Table 3.1) and was thus, not significantly different from that of running waters (0.2 ± 0.1 mmol m⁻² d⁻¹), isolated pools (0.10 ± 0.05 mmol m⁻² d⁻¹) and dry beds (0.2 ± 0.2 mmol m⁻² d⁻¹).

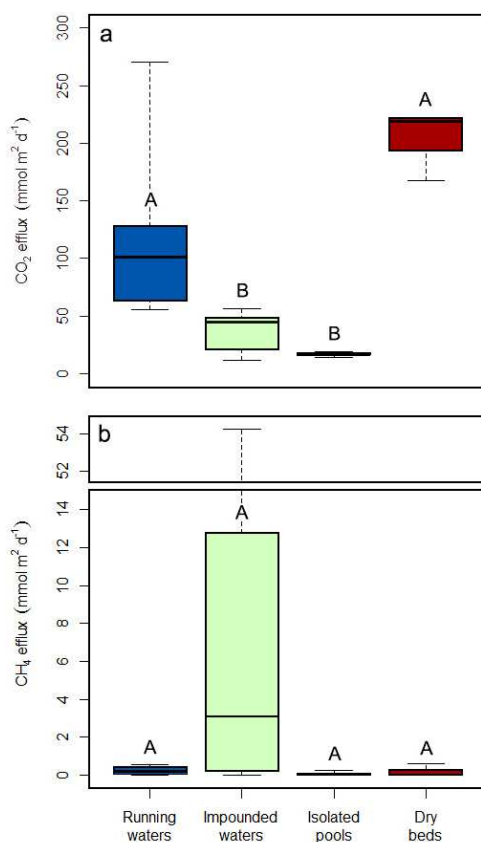


Figure 3.2 Efflux of (a) CO₂ and (b) CH₄ measured from running waters (blue box; n = 6), impounded waters (green box; n = 5), isolated pools (orange box; n = 5) and dry river and impoundment beds (red box; n = 3). Box plots display the 25th, 50th and 75th percentiles; whiskers display minimum and maximum values. Significant differences of CO₂ and CH₄ efflux between environments ($p < 0.05$, Tukey's post hoc test) are marked with different capital letters above the box plots.

Diffusion was the only mechanism driving CO₂ efflux in all studied environments (Table 3.1). Similarly, diffusion was most likely the only efflux mechanism for CH₄ in running waters, isolated pools and dry beds, while the predominant mechanism of CH₄ efflux in impounded waters was ebullition (> 85%; Table 3.1). Moreover, the percentage molar ratio between CH₄ and CO₂ efflux was significantly higher in impounded waters ($37.8 \pm 53.4\%$) than in running waters ($0.2 \pm 0.1\%$), isolated pools ($0.4 \pm 2.4\%$) and dry beds ($0.2 \pm 2.7\%$), where this ratio was nearly negligible (ANOVA, $f = 4.64$, $p < 0.001$, $n = 19$; Table 3.1).

Table 3.1 Summary table showing the mean, the standard error (SE) and the total number of studied sites per environment (n) of the surface water partial pressures of CO₂ and CH₄ in water ($p_{\text{CO}_2, \text{w}}$ and $p_{\text{CH}_4, \text{w}}$), the direct and the indirect gas exchange coefficients (k_{600}), the total efflux of CO₂ and CH₄ and the percentage molar ratio between CH₄ and CO₂ flux (CH₄ flux : CO₂ flux) along the different studied environments. In brackets the percentages of ebullitive CO₂ and CH₄ effluxes in relation to the total CO₂ and CH₄ effluxes.

Parameter	Running waters			Impounded waters			Isolated pools			Dry beds			ANOVA test
	Mean	SE	n	Mean	SE	n	Mean	SE	n	Mean	SE	n	p-value
$p_{\text{CO}_2, \text{w}}$ (μatm)	1841 ^A	242	6	1295 ^A	228	5	2553 ^B	224	5	NA	NA	NA	0.009
$p_{\text{CH}_4, \text{w}}$ (μatm)	123	33	6	669	380	5	345	4.2	5	NA	NA	NA	0.12
Direct k_{600} (m d^{-1})	2.2 ^A	0.4	6	1.1 ^A	0.3	5	0.2 ^B	0.0	5	NA	NA	NA	< 0.001
Indirect k_{600} (m d^{-1})	2.0 ^A	0.4	6	0.7 ^B	0.4	5	0.2 ^B	0.0	5	NA	NA	NA	< 0.001
CO ₂ efflux ($\text{mmol m}^{-2} \text{d}^{-1}$)	120 ^A (0)	32	6	36.6 ^B (0)	8.5	5	17.2 ^B (0)	0.9	5	209 ^A (0)	10	3	< 0.001
CH ₄ efflux ($\text{mmol m}^{-2} \text{d}^{-1}$)	0.2 (0)	0.1	6	13.8 (87)	10.1	5	0.1 (0)	0.0	5	0.2 (0)	0.5	3	0.089
CH ₄ efflux : CO ₂ efflux (%)	0.2 ^A	0.1	6	37.8 ^B	53.4	5	0.4 ^{AB}	2.4	5	0.2 ^{AB}	2.7	3	< 0.001

Significant differences between environment types for each parameter were determined with a one-way ANOVA followed by Tukey's post hoc test and are displayed as different capital letters above the mean values. NA: Not available

3.3.2 Drivers of CO₂ and CH₄ effluxes

In dry beds, the basal respiration showed a significant positive linear relationship with both the dry bed water content ($r^2 = 0.72$, $p < 0.001$, $n = 10$; Figure 3.3a) and the dry bed OM content ($r^2 = 0.71$, $p < 0.001$, $n = 10$; Figure 3.3b). In contrast, the CO₂ efflux was inversely related to the dry bed water content ($r^2 = 0.75$, $p < 0.001$, $n = 10$; Figure 3.3c) and showed no significant relationship with the dry bed OM content ($r^2 = 0.21$, $p > 0.05$, $n = 10$; Figure 3.3d). This resulted in a significant negative exponential relationship between the basal respiration and CO₂ efflux in dry beds ($r^2 = 0.53$, $p < 0.001$, $n = 10$).

In aquatic environments, the two main parameters directly involved in the diffusion of CO₂ across the water-atmosphere boundary (i.e., surface water $p_{\text{CO}_2, \text{w}}$ and k_{600} ; equation (2)) were directly related to the CO₂ efflux. When all aquatic environments were pooled together, the k_{600} and CO₂ efflux exhibited a significant positive relationship ($r^2 = 0.79$, $p < 0.001$, $n = 16$; Figure 3.4a), while no dependency between surface water $p_{\text{CO}_2, \text{w}}$ and the CO₂ efflux was detected ($p > 0.05$, $n = 16$; Figure 3.4b). However, the CO₂ efflux and $p_{\text{CO}_2, \text{w}}$ were positively related when the isolated pools were excluded from the model ($r^2 = 0.49$, $p = 0.015$, $n = 11$; Figure 3.4b). The multiple regression analysis revealed that

$p_{\text{CO}_2, \text{w}}$ and k_{600} explained 0.1% and 86% of the total variation in the CO_2 efflux, respectively, when all aquatic environments were included in the model. In contrast, when isolated pools were excluded from the multiple regression analysis, $p_{\text{CO}_2, \text{w}}$ and k_{600} explained 49% and 38% of the total variation in the CO_2 efflux, respectively ($r^2 = 0.87$, $p = 0.003$, $n = 11$).

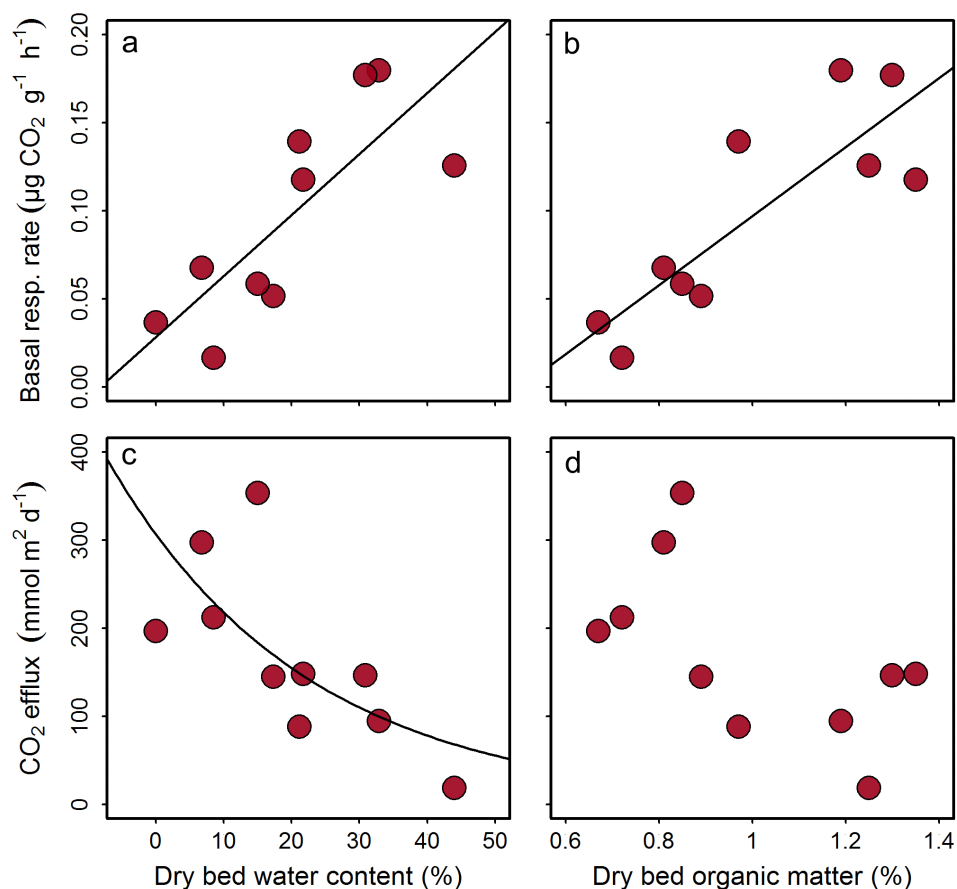


Figure 3.3 Basal respiration as a function of (a) dry bed water content and (b) dry bed organic matter. Efflux of CO_2 as a function of (c) dry bed water content and (d) dry bed organic matter. The continuous line in a ($r^2 = 0.72$, $p < 0.001$, $n = 10$) and b ($r^2 = 0.71$, $p < 0.001$, $n = 10$) represent the linear regression model fitting line between predictor and response variables. The continuous line in c ($r^2 = 0.65$, $p < 0.001$, $n = 10$) represents the exponential regression model fitting line between predictor and response variables. Absence of continuous line in (d) represents that no significant regression model fitted with the observed values.

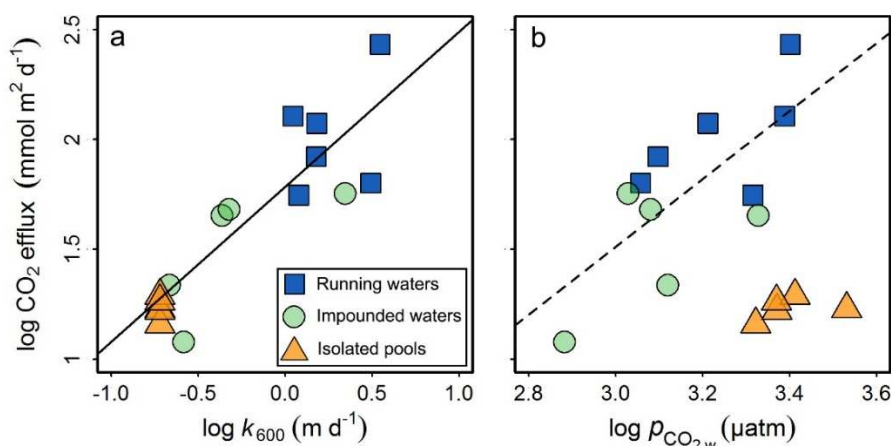


Figure 3.4 Efflux of CO₂ as a function of (a) k_{600} and (b) surface water $p_{\text{CO}_2, \text{w}}$ for all the aquatic study sites. Blue squares: running waters; green circles: impounded waters; Orange triangles: isolated river pools. The continuous line in (a) represents the linear regression model fitting line incorporating all the environments ($r^2 = 0.79$, $p < 0.001$, $n = 16$). The dashed line in (b) represents the linear regression model fitting line excluding isolated river pools ($r^2 = 0.49$, $p = 0.015$, $n = 11$).

A high contribution of ebullition to the CH₄ efflux was detected in the impounded waters, with increased residence time, higher sediment OM content and porosity and lower dry bulk density (Table 3.2). However, both the low number of study sites where ebullition of CH₄ was detected and the narrow range of ebullitive efflux values prevented a robust statistical analysis of the potential drivers that control the ebullitive CH₄ efflux.

Table 3.2 Hydromorphological descriptors, and sediment physical and chemical properties of the different impounded waters.

Site	Ebullition of CH ₄		Hydromorphological characteristics			Sediment properties			
	Detection (yes/no)	Flux (%)	Residence time (hours)	Mean depth (m)	Max. depth (m)	Water content (%)	Dry bulk density (g cm ⁻³)	Porosity	Organic matter (mg cm ⁻³)
1	Yes	82	4247.6	16.5	45.5	0.69	0.41	0.84	26.2
2	Yes	87	49.7	1.8	5.7	0.63	0.51	0.77	35.5
3	Yes	90	39.8	2.5	5.4	0.58	0.62	0.69	29.8
4	No	0	5.1	1.5	3.6	0.41	1.00	0.41	18.7
5	No	0	3.7	1.1	2.6	NA	NA	NA	NA

Flux indicates the percentage of ebullitive efflux to the total CH₄ efflux. NA: Not available

The surface water physicochemical or hydromorphological variables (Table A.3.1 in the Supporting information section) were not significantly related to the CO₂ and CH₄ effluxes or the $p_{\text{CO}_2, \text{w}}$, $p_{\text{CH}_4, \text{w}}$ and k_{600} in these aquatic environments.

3.4 Discussion

3.4.1 Hot spots for CO₂ and CH₄ effluxes

Among the different environments investigated in the present study, running waters and dry beds emitted significantly higher amounts of CO₂ than the other environments. Several studies have highlighted the importance of running waters as hot spots for CO₂ efflux [Cole *et al.*, 2007; Battin *et al.*, 2009a; Raymond *et al.*, 2013]. The results of the present study also show that the dry beds associated with the dry phase of Mediterranean temporary rivers are not only inert but also active sites in terms of CO₂ emissions to the atmosphere. The CO₂ efflux from dry beds (mean = 209 mmol m⁻² d⁻¹, range = 189 to 220 mmol m⁻² d⁻¹) was higher than that from dry desert streams in Arizona (43.5 mmol m⁻² d⁻¹, range = 19.6 to 65 mmol m⁻² d⁻¹; Gallo *et al.*, [2013]), to our knowledge the only study reporting CO₂ emissions from dry beds in different catchments. The CO₂ efflux from dry beds was also higher than the global mean CO₂ efflux from soils (123 mmol m⁻² d⁻¹, range = 121 to 125 mmol m⁻² d⁻¹; Raich *et al.*, [2002]) and the regional mean CO₂ efflux from desert soils (104 mmol m⁻² d⁻¹, range = 95 to 110 mmol m⁻² d⁻¹; Raich and Schlesinger [1992]), and it was in the upper range of values for the regional mean CO₂ efflux from Mediterranean soils (188 mmol m⁻² d⁻¹, range = 44 to 371 mmol m⁻² d⁻¹; Bond-Lamberty and Thomson [2012]). Although the magnitude of CO₂ efflux from dry beds was within the range of reported soil emissions, the CO₂ from this environment should not be considered terrestrial because the C processed in dry beds has either already left from the terrestrial ecosystems and entered into the fluvial network or has been produced within the fluvial network. In addition, the sediments from dry rivers and terrestrial soils are different environments in terms of physical structure and biogeochemical dynamics [McIntyre *et al.*, 2009; Larned *et al.*, 2010; Steward *et al.*, 2012]. Thus, we emphasize that dry beds should be included in CO₂ balances from fluvial networks, particularly in arid and semiarid regions, such as the Mediterranean.

Despite the high variability of CH₄ efflux detected for impounded waters, this environment likely represents a hot spot for CH₄ efflux to the atmosphere. This result is consistent with the notion that impounded waters stored in dams and smaller impoundments play a prominent role in the CH₄ efflux from fluvial networks [Maeck *et al.*, 2013; Xiao *et al.*, 2013]. Furthermore, the other three environments studied (running waters, isolated pools and dry beds) were net emitters of CH₄. Although previous studies have detected CH₄ efflux from rivers [Striegl *et al.*, 2012; Crawford *et al.*, [2013]; Campeau and Lapierre, 2014; Crawford *et al.*, 2014b] and dry beds [Gallo *et al.*, 2013], this study provides to our knowledge the first evaluation of the CH₄ efflux from isolated river pools.

Ebullition was the primary pathway for CH₄ efflux from impounded waters. This finding is consistent with previous studies [Delsontro *et al.*, 2010; Maeck *et al.*, 2013] and contrary to the efflux pathway of CO₂ which is a more soluble gas that primarily follows a strictly diffusive pathway of emission to the atmosphere [Belger *et al.*, 2010]. The ebullitive CH₄ efflux from impounded waters, as the only environment experiencing ebullition in the present study, contributed to more than 85% of the total CH₄ efflux when the evasion of CH₄ was detected.

The CH₄ efflux was estimated using a floating chamber, reported as the most appropriate method for water-atmosphere diffusion flux measurements [Cole *et al.*, 2010]. Nonetheless, the floating chamber approach can be problematic in the case of ebullition measurements from aquatic systems [Bastviken *et al.*, 2004; Delontro *et al.*, 2010; Crawford *et al.*, 2013]. The vast spatial and temporal heterogeneity of CH₄ ebullitive fluxes is generally not captured through short-term floating chamber experiments (10 min in our study). An inverted funnel survey designed to cover the maximum surface area of the impounded waters would likely have reduced potential sampling bias and increased the accuracy of the spatially and temporally integrated final dataset for CH₄ ebullitive fluxes [Bastien and Demarty, 2013; Maeck *et al.*, 2013]. Although we did not observe ebullition in running waters and isolated pools (i.e., we never observed non-linearity in $d\text{CH}_4/dt$ during the chamber deployments or bubbles emerging from the stream or isolated pool sediments), a sampling design with inverted funnel-style bubble traps would have improved the characterization of CH₄ ebullitive fluxes from these environments [Baulch *et al.*, 2011; Crawford *et al.*, 2014a]. Despite the potential inaccuracies in capturing the temporal and

spatial heterogeneity, the results indicate that the contribution of ebullitive efflux of CH₄ to the total CH₄ efflux is substantial in Mediterranean impounded waters during summer drought, and that they should be taken into account in CH₄ flux assessments.

3.4.2 Physical and biogeochemical regulation of CO₂ and CH₄ effluxes

The unexpected negative relationship between the basal respiration and CO₂ efflux indicates potential decoupling between CO₂ production and CO₂ emission from dry river and impoundment beds. This decoupling between processes suggests the existence of a physical factor restricting the evasion of the biologically produced CO₂. Based on the results obtained in the present study, the dry bed water content might play a dual role in the CO₂ generation-emission mechanism. On the one hand, higher water content enhances C respiration by facilitating the contact between microorganisms and available substrates [Koschorreck and Darwich, 2003; Xu *et al.*, 2004; Luo and Zhou, 2010]. On the other hand, higher water content diminishes the CO₂ efflux through the restriction of the gas diffusivity through the dry media, consistent with the results from Howard and Howard [1993] and Fujikawa and Miyazaki [2005] showing that the diffusivity of CO₂ and other gases in soils is strongly reduced when the air-filled porosity decreases with increasing water content. Taken together, these results suggest that the water content might modulate the uncoupling between CO₂ production and CO₂ emission from dry beds. However, it has to be noted that dry bed water content is highly dynamic in both space and time, and other non-biotic CO₂-generating processes (e.g., interactions with the groundwater system [Rey, 2015], reactions with the carbonate system [Angert *et al.*, 2014] or photochemical degradation reactions [Austin and Vivanco, 2006] could potentially contribute to the observed uncoupling between the respiratory process and the emission of CO₂. Hence, further studies are required to understand the relative importance of environmental variables (e.g., air temperature, precipitation, vegetation) with respect to the role of local conditions (e.g., water content, temperature, OM content and type, grain size distribution of the substrate, light regime, and carbonate content) in driving the CO₂ efflux from dry beds.

In aquatic environments, the diffusive CO₂ efflux depends on both the surface water $p_{\text{CO}_2, \text{w}}$, which is primarily regulated through biogeochemical processes [Sobek and Algesten, 2003; Campeau and del Giorgio, 2013], and the k_{600} , which is a physical factor including the turbulent and molecular diffusion of CO₂ [Bade, 2009]. However, the extent to which these two factors regulate the aquatic CO₂ efflux from Mediterranean fluvial networks during summer drought and whether there are shifts in the relative importance of these two parameters across the different aquatic environments remain unknown. The results of the present study show that k_{600} acts as the primary control for the CO₂ efflux along the studied aquatic environments. Although the three types of aquatic environments were supersaturated in terms of $p_{\text{CO}_2, \text{w}}$, strong evidence for the active role of the physical turbulence (measured here as k_{600}) as a factor enhancing the exchange process between generated CO₂ and emitted CO₂ was observed [Halbedel and Koschorreck, 2013]. In running waters, the aquatic environment experiencing the highest CO₂ efflux, the CO₂ gas is immediately emitted because the high turbulence disrupts the surface boundary layer [Alin et al., 2011; Demars and Manson, 2013]. With values of $p_{\text{CO}_2, \text{w}}$ similar to those from running waters, impounded waters showed a lower efflux of CO₂, suggesting a partial physical limitation of CO₂ gas. An extreme effect of the physical limitation of CO₂ efflux occurred in the isolated river pools, where CO₂ efflux was lowest despite showing the highest $p_{\text{CO}_2, \text{w}}$.

Because of the unbalanced contribution of diffusion and ebullition to the total CH₄ efflux in the different environments, any statistical assessment of the factors controlling the CH₄ efflux could not be performed. In any case, the total CH₄ efflux was detectable, but low, from all environments, except impounded waters, where the dominant efflux pathway was the ebullitive one (see above). Nonetheless, our results are consistent with those of previous studies showing that both the residence time and the sediment physical and chemical composition also play a crucial role in controlling the biological activity involved in the generation of CH₄ in the sediment layer [Sobek et al., 2012; Maeck et al., 2013]. The amount and composition of stored OM are key factors affecting the biological activity in sediments and, therefore, the CH₄ efflux [Mulholland and Elwood, 1982; Downing et al., 2008; Sobek et al., 2012]. Moreover, the porosity of the sediment plays an important role by limiting or

favouring the diffusion of CH₄, the shape of CH₄ bubbles and the capacity for CH₄ to escape from or be retained in the sediment media [Delsontro *et al.*, 2010; Meier *et al.*, 2011]

Unexpectedly, the CH₄ efflux in isolated pools was low, despite the high water residence time and optimum redox conditions for methanogenic activity, suggesting that these systems contain much less stored OM compared with impounded waters which are more active OM traps. Thus, we speculate that the amount of OM could be a limiting factor for the CH₄ generation in the sediments of isolated pools. Nevertheless, the hydrological isolation in the pools generates individual systems highly influenced through particular local conditions [Bonada *et al.*, 2006; von Schiller *et al.*, 2011]. For example, these observations would likely differ under contrasting situations, such as increased canopy cover and higher leaf input. Thus, further investigation of the hydrological and biogeochemical processes in isolated pools over time and across contrasting systems is needed to better understand the dynamics of C emissions from these systems.

3.4.3 Potential changes in C emissions from Mediterranean fluvial networks under future hydrological scenarios

River desiccation and impoundment of running waters through the construction of dams or small weirs have been recognized as some of the most important environmental pressures on fluvial networks worldwide [Nilsson *et al.*, 2005a; Sabater, 2008; Vörösmarty *et al.*, 2010; Steward *et al.*, 2012]. The influence and interplay between these two processes largely determines the relative surface area of the different environments comprising the fluvial network. Estimation of the areal extent and distribution of different environments along the fluvial network is key aspect when upscaling specific biogeochemical processes to the entire fluvial network [Benstead and Leigh, 2012]. However, the high temporal and spatial dynamism of Mediterranean rivers makes these estimations extremely difficult and subject to high inaccuracies [Benstead and Leigh, 2012; Datry *et al.*, 2014].

Herein, we applied a simple heuristic approach using different potential scenarios to evaluate how river desiccation and running water impoundment might affect the C emissions from fluvial networks. We combined the mean CO₂ and CH₄ effluxes measured

for each environment with the relative surface area (%) of each environment in each scenario to obtain a mean fluvial network efflux of CO₂, CH₄, and total C (i.e., sum of CO₂ and CH₄), and the total C considering the global warming potential (i.e., C_{GWP}; expressed as CO₂ Eq)(Figure 3.5). We then combined the annual mean relative area per environment from the COastal Segmentation analysis and the related CATchments regions for the study region (*Meybeck et al.*, [2006], COSCAT Region 418) with the data from the dry and total river effective areas from the same region [*Raymond et al.*, 2013] to situate an idealized Western Mediterranean fluvial network in the scenarios contour map (Figure 3.5). The idealized fluvial network (with an annual mean relative surface area of running waters, impounded waters and dry river and impoundment beds of 54.8, 30.7 and 14.5%, respectively) emits 107 mmol m⁻²d⁻¹ of CO₂, 4.4 mmol m⁻² d⁻¹ of CH₄, 112 mmol m⁻² d⁻¹ of total C and 217 mmol m⁻² d⁻¹ of total C_{GWP}.

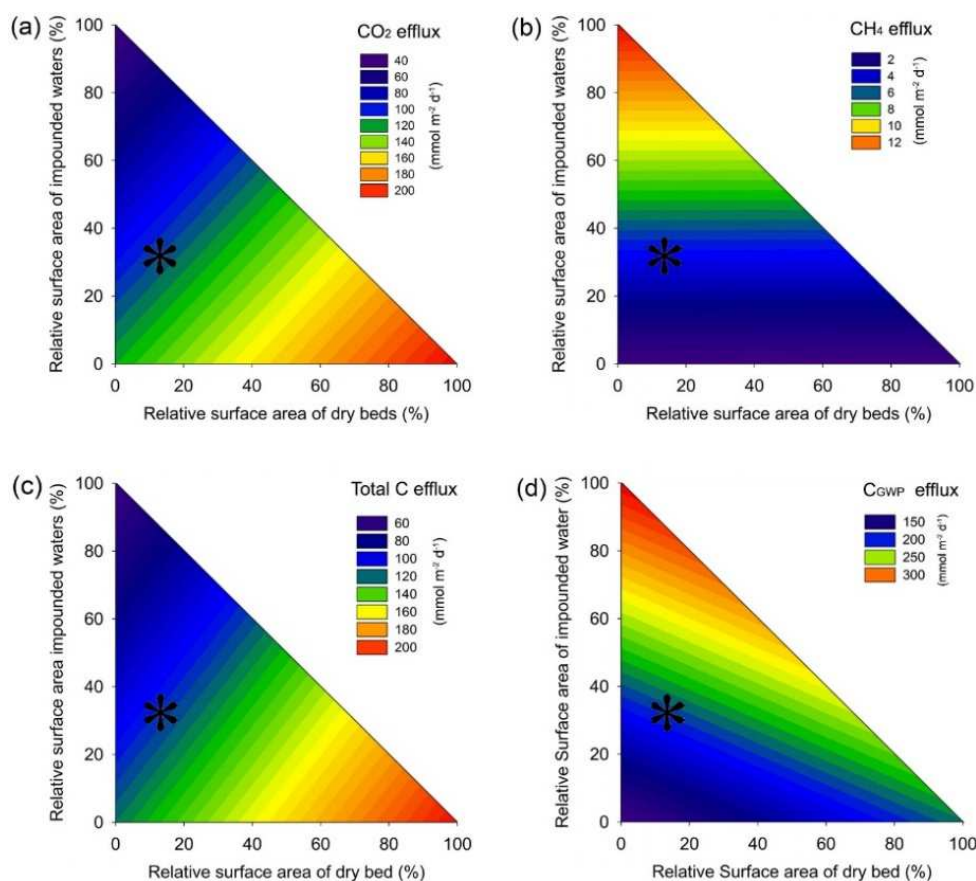


Figure 3.5 Contour plots simulating the effect of a broad spectrum of potential hydrological scenarios of river desiccation and transformation of running waters into impounded waters of an hypothetical Mediterranean fluvial network during summer drought (expressed in terms of relative surface area of dry bed (x-axis) and relative surface area of impounded waters (y-axis)) on (a) the mean fluvial network CO_2 efflux, (b) the mean fluvial network CH_4 efflux, (c) the mean total fluvial network C efflux and (d) the mean total C efflux considering the global warming potential of CH_4 (expressed as CO_2 Eq). The marked asterisks represent an idealized Western Mediterranean fluvial network. Details of calculations are provided in the text.

3.5 Conclusions and implications

The results of the present study show that dry beds and running waters (for CO_2) and impounded waters (for CH_4) are hot spots for C efflux from Mediterranean fluvial networks during summer drought. These results suggest dry beds as active sites in terms of C

emissions, which should be considered in C balances from fluvial networks in arid and semiarid areas. The CO₂ efflux, which was only mediated via diffusion, is mostly physically limited in both dry and aquatic environments. In contrast, the CH₄ efflux, which is predominantly mediated through ebullition, is primarily controlled through the biological activity in the sediments. The duration, spatial extent and severity of flow intermittency and the degree of river impoundment will play a decisive role in shaping the C efflux from fluvial networks in response to global change.



When water vanishes: magnitude and regulation of carbon dioxide emissions from dry temporary rivers

Abstract

Most fluvial networks worldwide include watercourses that recurrently cease to flow and run dry. The spatial and temporal extent of the dry phase of these temporary watercourses is increasing as a result of global change. Yet, current estimates of carbon (C) emissions from fluvial networks do not consider temporary watercourses when they are dry. We characterized the magnitude and variability of C emissions from dry watercourses by measuring the carbon dioxide (CO₂) flux from 10 dry riverbeds of a temporary fluvial network during the dry period and comparing it to the CO₂ flux from the same riverbeds during the flowing period and to the CO₂ flux from their adjacent upland soils. We also looked for potential drivers regulating the CO₂ emissions by examining the main physical and chemical properties of dry riverbed sediments and adjacent upland soils. The CO₂ efflux from dry riverbeds (mean \pm sd = 781.4 \pm 390.2 mmol m⁻² d⁻¹) doubled the CO₂ efflux from flowing riverbeds (305.6 \pm 206.1 mmol m⁻² d⁻¹) and was comparable to the CO₂ efflux from upland soils (896.1 \pm 263.2 mmol m⁻² d⁻¹). However, dry riverbed sediments and upland soils were physicochemically distinct and differed in the variables regulating their CO₂ efflux. Overall, our results indicate that dry riverbeds constitute a unique and biogeochemically active habitat that can emit significant amounts of CO₂ to the atmosphere. Thus, omitting CO₂ emissions from temporary streams and rivers when they are dry may overlook the role of a key component of the C balance of fluvial networks.

Original publication (*Appendix C in the Supporting information section*):

Gómez-Gener, L., B. Obrador, R. Marcé, V. Acuña, N. Catalán, J. P. Casas-Ruiz, S. Sabater, I. Muñoz, and D. von Schiller (2016), When water vanishes: magnitude and regulation of carbon dioxide emissions from dry temporary streams, *Ecosystems*, 19(4), 710–723, doi:10.1007/s10021-016-9963-4.

4.1 Introduction

Fluvial networks emit significant amounts of carbon dioxide (CO₂) to the atmosphere [Raymond *et al.*, 2013a; Lauerwald *et al.*, 2015]. However, considerable uncertainties regarding the magnitude and controls of CO₂ emitted from fluvial networks still exist [Wehrli, 2013]. For instance, current global estimates do not accurately consider the CO₂ emitted from expanded areas of rivers and streams during floods, which can increase the areal extent of fluvial networks by several orders of magnitude [Richey *et al.*, 2002]. Also, these estimates, based on continuous models, do not include the CO₂ emitted from local discontinuities along the fluvial network, such as weirs, rapids, waterfalls or turbine releases in hydropower plants [Wehrli, 2013]. Finally, current estimates do not consider the CO₂ emitted from the areas of temporary watercourses that recurrently run dry [Raymond *et al.*, 2013a].

Temporary watercourses can be found in many areas of the world [Acuña *et al.*, 2014]. In Australia, roughly 70% of the 3.5 million kilometres of watercourses are considered temporary [Sheldon *et al.*, 2010], and more than half of the total length of watercourses in the United States, Greece, and South Africa are also temporary [Larned *et al.*, 2010]. Low-order streams deserve special attention, since they account for more than 70% of fluvial networks surface area and are particularly prone to flow intermittency [Lowe *et al.*, 2006]. These are very dynamic systems in time and space, and analysing their spatial coverage is particularly difficult to detect by traditional mapping techniques [Benstead and Leigh, 2012]. We can therefore suspect that the surface area of temporary watercourses in the global fluvial network can be higher than 50% [Datry *et al.*, 2014a], while their importance is increasing as a result of the combined effects of climate and land use changes [Palmer *et al.*, 2008; Larned *et al.*, 2010; Hoerling *et al.*, 2012].

The dry beds of temporary streams and rivers hereinafter referred to as dry riverbeds [Steward *et al.*, 2012], are dynamic habitats [Stanley *et al.*, 1997; Boulton, 2003], representing spatial (i.e., transitional zones between dissimilar habitats), and temporal (i.e., transitional periods between persistent and dissimilar states), ecotones [Naiman and Decamps, 1997]. These systems are constrained by the strength of interactions with their adjacent ecosystems. Thus, against the traditional view of being “biogeochemically

inactive”, dry riverbeds are likely to be potential active sites for materials transformations [McLain and Martens, 2006]. In fact, recent studies reported that carbon (C) processing in dry riverbed sediments can be maintained to some degree during river desiccation by the activity of well-adapted biofilms [Zoppini and Marxsen, 2011; Timoner *et al.*, 2012; Pohlen *et al.*, 2013]. Likewise, first estimates also showed that dry riverbeds are not inert but rather potentially active sites for CO₂ release to the atmosphere [Gallo *et al.*, 2013].

The C processed in dry streams and rivers has its particular history, since it either already left terrestrial ecosystems and entered the fluvial network, or was produced within the fluvial network [Steward *et al.*, 2012]. Therefore, emissions of CO₂ from dry riverbeds should not be considered terrestrial, but mostly as a fundamental biogeochemical component of fluvial networks under drought. Yet, little is known about the spatial variability and drivers of CO₂ emissions from dry riverbeds and the differences and similarities with respect to CO₂ emissions from terrestrial soils.

The aim of this study was to quantify CO₂ emissions from dry riverbeds of a temporary fluvial network, comparing them to those during the flowing period and to those from adjacent upland soils. We also looked for potential drivers regulating the CO₂ emissions by examining the main physical and chemical properties of dry riverbed sediments and adjacent upland soils. We predicted differences in both the magnitude and drivers controlling CO₂ emissions between dry riverbeds and the other investigated habitats because of strong dissimilarities in physicochemical properties and biogeochemical dynamics.

4.2 Materials and Methods

4.2.1 Study sites and sampling design

The Fluvià River (NE Iberian Peninsula; Figure 4.1) is 97-km long and drains a 990-km² catchment covered with mixed forests (78%), agricultural (19%) and urban (3%) areas (Land Cover Map of Catalonia 2009, Centre of Ecology and Forestry Research of Catalonia). The climate in the region is typically Mediterranean. Mean monthly air temperature ranges from 6°C in January to 26 °C in July. Mean annual precipitation is 660 mm, with

rainfall mainly occurring in autumn and spring (Data from 2004 to 2014, Catalan Water Agency). During the wet period (late autumn to early spring), hydrological connectivity is enhanced and most of the fluvial network area is covered with surface water. In contrast, during the dry period (late spring to early autumn) hydrological connectivity is reduced and the area of the fluvial network covered with surface water drastically decreases.

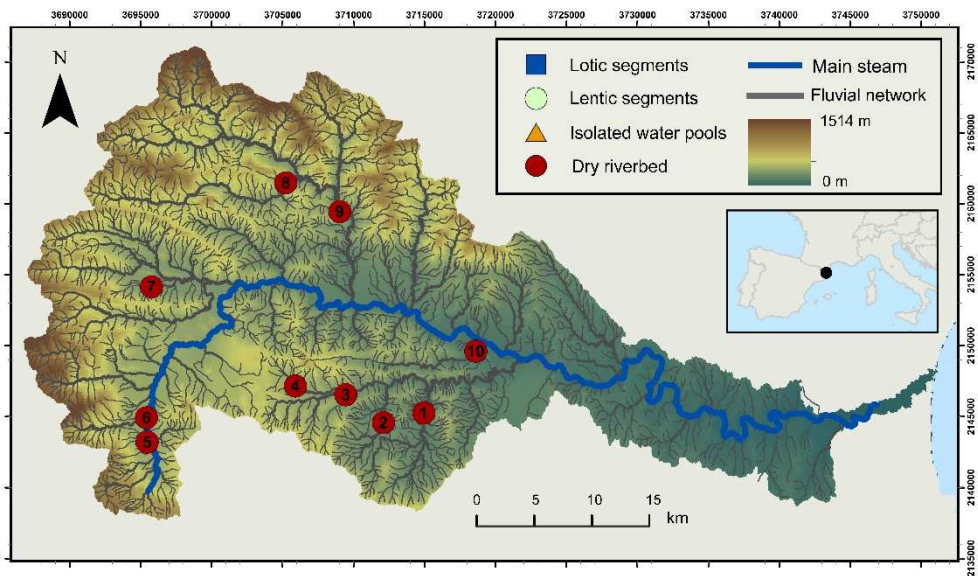


Figure 4.1 Location of the Fluvià River in Catalonia (NE Iberian Peninsula), with the corresponding position of the study sites ($n = 10$).

We conducted two samplings in 10 temporary tributaries of the Fluvià River spanning a wide range of physiographic and land use conditions (Figure 4.1 and Table 4.1). In the first sampling (dry period; August 2014), we measured CO₂ fluxes and took samples from the dry riverbed sediments and adjacent upland soils. In the second sampling (flowing period, March 2015), we measured the CO₂ fluxes from the riverbeds where flowing water was found (7 out of 10 rivers; see Figure A.4.1 in the Supporting information section for details).

Table 4.1 Physiographic and land use characteristics of the study sites and their corresponding subcatchments

Stream name	Stream code	Site-specific parameters						Catchment-specific parameters						
		Coordinates		Stream order ^a	Streambed grain sizes ^b (%)			Surface area ^c (ha)	Land uses ^c (%)				Lithology ^c (%)	
		x	y		Small fraction	Cobbles	Boulders		Scrubs	Pastures	Crops	Forest		
Riera de St. Miquel	1	473788	4663780	4	77.2	22.8	0.0	5191	1.2	2.6	10.7	84.6	Loams (66), conglomerates (17) and gravels (16)	
Riera de Mieres	2	470306	4663964	4	71.1	28.9	0.0	1825	1.1	5.1	18.4	72.9	Loams (65), gravels (22) and conglomerates (12)	
Torrent de Pujolars	3	464116	4665691	3	49.1	43.7	7.2	1219	0.2	0.1	7.9	91.7	Conglomerates (87) and gravels (13)	
Torrent de Rocanegra	4	464289	4665909	2	58.8	41.2	0.0	1252	1.7	3.7	27.6	59.4	Conglomerates (62), volcanic deposits (34) and gravels (23)	
Fluvià	5	454382	4662603	4	63.2	31.6	5.2	3078	0.9	10.7	16.9	70.2	Conglomerates (64), gravels (18), silt (7), sandstone (6) and gravels (5)	
Joanetes	6	453844	4663758	4	61.4	38.6	0.0	2954	1.3	4.1	11.4	81.9	Conglomerates (66), gravels (18) and loams (11)	
Torrent de St. Pere	7	453724	4673311	3	59.8	29.8	10.3	1480	0.2	2.1	10.5	86.2	Conglomerates (85), loams (9) and gravels (5)	
Riera d'Oix	8	462235	4680827	4	79.0	21.0	0.0	11085	4.4	1.4	1.9	92.2	Loams (49), conglomerates (33) gravels (16) and limestone (9)	
Llierca	9	466415	4679576	5	67.6	32.4	0.0	16743	5.9	2.8	1.5	89.7	Loams (59), limestone (23) and sandstone (18)	
Barranc de Junyell	10	476914	4671359	3	55.6	44.4	0.0	5238	0.5	0.3	1.9	97.3	Conglomerates (76), gravels (21) and sandstone (2)	

^a Stream order and subcatchment surface area were calculated with the Hydrological Extension in ESRI® ArcGIS v. 10.0 software. Data obtained from a 2-meter digital elevation model (Centre of Ecology and Forestry Research of Catalonia)

^b Surface grain-size characterization of studied streambeds was estimated following an image-processing-based procedure (Graham and others 2005). Results were obtained from an average of 3 high resolution photos along 50 m stream segments. Fraction classification was made according Wentworth (1922). Small fractions contain silt, clay, sand and gravel fractions.

^c Subcatchments land uses and lithologies (S=silt, L=loams, C=conglomerates, G=gravels, V=volcanic deposits, LS=limestone) were calculated with ESRI® ArcGIS v. 10.0 software from a Land cover map of Catalonia and a Lithological map of Catalonia, respectively (Centre of Ecology and Forestry Research of Catalonia)

4.2.2 Determination of CO₂ fluxes

In both dry riverbeds and upland soils, we applied the enclosed dynamic chamber method [Livingston and Hutchinson, 1995] to measure the CO₂ flux. Briefly, we monitored the gas concentration in an opaque chamber (SRC-1, PP-Systems, USA) every 4.8 s with an infrared gas analyser (EGM-4, PP-Systems, USA). Measurement accuracy of the EGM-4 is estimated to be within 1% over the calibrated range. In all the cases, flux measurements lasted until a change in CO₂ of at least 10 µatm was reached, with a maximum duration of 300 s and a minimum of 120 s. We calculated the CO₂ flux (F_{CO_2} , mmol m⁻² d⁻¹) from the rate of change of CO₂ inside the chamber:

$$F_{\text{CO}_2} = \left(\frac{dp_{\text{CO}_2}}{dt} \right) \left(\frac{V}{RTS} \right) \quad (1)$$

where $\frac{dp_{\text{CO}_2}}{dt}$ is the slope of the gas accumulation in the chamber along time in µatm s⁻¹, V is the volume of the chamber (1.171 dm³), S is the surface area of the chamber (0.78 dm²), T is the air temperature in Kelvin and R is the ideal gas constant in l atm K⁻¹ mol⁻¹. Positive F_{CO_2} values represent efflux of gas to the atmosphere, and negative F_{CO_2} values indicate influx of gas from the atmosphere. We performed 4 randomly distributed measurements within each site, 4 in dry riverbeds and 4 in upland soils.

In the flowing riverbeds we measured the CO₂ flux applying the Fick's First Law of gas diffusion:

$$F_{\text{CO}_2} = k_{\text{CO}_2} K_h \left(p_{\text{CO}_2, \text{w}} - p_{\text{CO}_2, \text{a}} \right) \quad (2)$$

where F_{CO_2} is the estimated CO₂ flux between the surface river water and the atmosphere (mmol m⁻² d⁻¹), K_h is the Henry's constant (mmol µatm⁻¹ m³) adjusted for salinity and temperature [Weiss, 1974; Millero, 1995], $p_{\text{CO}_2, \text{w}}$ and $p_{\text{CO}_2, \text{a}}$ are the surface water and the atmosphere partial pressures of CO₂ (µatm), respectively, and k_{CO_2} is the specific gas transfer velocity for CO₂ (m d⁻¹).

We measured $p_{\text{CO}_2, \text{w}}$ and $p_{\text{CO}_2, \text{a}}$ with an infrared gas analyser (EGM-4, PP-Systems, USA). In the case of $p_{\text{CO}_2, \text{w}}$ we coupled the gas analyzer to a membrane contactor (MiniModule, Liqui-Cel, USA). The water was circulated via gravity through the contactor at 300 mL min^{-1} , and the equilibrated gas was continuously recirculated into the infrared gas analyser for instantaneous p_{CO_2} measurements [Teodoru *et al.*, 2010].

We estimated the k_{CO_2} from the night-time drop in dissolved oxygen concentration [Hornberger and Kelly 1975], a method that has been extensively applied in ecosystem metabolism studies in rivers and streams (for example, Aristegi *et al.*, [2009]; Hunt *et al.*, [2012]; Riley and Dodds [2013]). Briefly, photosynthesis ceases from sunset to sunrise, thus night time dynamics of oxygen depend on respiration and reaeration. During the night, respiration reduces the oxygen levels until atmospheric equilibrium is reached. In parallel, reaeration approaches the oxygen concentration to saturation. Thus, when we plot the night time oxygen concentration per unit of time versus the oxygen saturation deficit, a linear trend is obtained. The intercept of the regression corresponds to the respiration ($\text{g O}_2 \text{ m}^{-2} \text{ h}^{-1}$), and the slope to the mean reaeration coefficient ($K_{\text{O}_2}; \text{d}^{-1}$). We corrected the K_{O_2} for depth to obtain the mean gas transfer velocity of oxygen ($k_{\text{O}_2}; \text{m d}^{-1}$) [Raymond *et al.*, 2012] and we further transformed to k_{CO_2} by applying equation (3).

$$k_{\text{CO}_2} = k_{\text{O}_2} \left(\frac{Sc_{\text{CO}_2}}{Sc_{\text{O}_2}} \right)^{-n}, \quad (3)$$

where k_{CO_2} is the mean gas transfer velocity of CO_2 (m d^{-1}), Sc_{CO_2} and Sc_{O_2} are the Schmidt numbers of respectively CO_2 and O_2 at a given water temperature [Wanninkhof, 1992]. Following Bade [2009], we set the exponent n to $1/2$ for turbulent environments (i.e., flowing waters). We obtained the diel cycles of dissolved oxygen concentration and temperature at each site at a frequency of 5 minutes with an optical dissolved oxygen sensor (MiniDot, PME, USA).

4.2.3 Physical and chemical characterization of dry riverbeds and upland soils

At each flux measurement location, we measured the substrate temperature by means of a portable soil probe (Decagon ECH₂O 10HS, Pullman, USA) and collected substrate samples (i.e., dry riverbed sediments and upland soils (0-10 cm depth)), after the flux measurements had been carried out. In the laboratory, we measured the substrate pH from a 1:1 sample:deionized water mixture [McLean 1982] with a hand-held pH meter (pH 3110, WTW, Germany). We also determined gravimetrically the substrate water content by drying a fresh subsample at 105 °C and the organic matter (OM) content by sample combustion following the loss on ignition method [Dean 1974]. We sieved the air-dried samples (2-mm mesh) and determined their main textural fractions (% sand, % silt and % clay) and their mean particle size with a laser-light diffraction instrument (Coulter LS 230, Beckman-Coulter, USA). We determined the percent of organic carbon (OC) and total nitrogen (TN) from a sieved and air-dried subsample on an Elemental Analyzer (Model 1108, Carlo-Erba, Italy) after grinding and eliminating the inorganic fraction (i.e., carbonates), by acidification (1.5N HCl) .

Water Extractable Organic Matter (WEOM), the fraction of DOM extracted with deionized water, and conceptually consisting of the mobile and available portion of the total DOM pool [Corvasce *et al.*, 2006; Vergnoux *et al.*, 2011], was obtained by shaking (100 rpm, 4°C) the air-dried, sieved and grinded samples with deionized water in the dark for 48h with a sample: water ratio of 1:10. After the extraction, we filtered the leachates through 0.70 and 0.45 µm pre-combusted glass microfiber filters (Whatman, USA). We determined their raw dissolved organic carbon (DOC) and total dissolved nitrogen (TDN) concentration with a total OC analyser (TOC-V CSH, Shimadzu, Japan). The detection limit of the analysis procedure was 0.05 mgC l⁻¹ for DOC and 0.005 mgN l⁻¹ for TDN. All samples were previously acidified with HCl 1.5 N and preserved at 4 °C until analysis. The extraction efficiencies were calculated as the ratio between the mass of WEOM recovered and the mass of the dry sample used for the extraction.

UV/Vis absorbance and fluorescence spectra were obtained from diluted WEOM extracts (DOC≈10 mg l⁻¹) [Anesio *et al.*, 2000]. We measured the UV/Vis absorbance spectra (200-800 nm) using a 1-cm quartz cuvette on a spectrophotometer (Shimadzu UV-1700,

Shimadzu, USA) with an analytical precision of 0.001 absorbance units. From the absorbance spectra, we calculated the specific UV absorbance at 254 nm ($SUVA_{254}$, $L\ mg^{-1}\ m^{-1}$) by dividing the absorbance at 254 nm by DOC concentration and cuvette path length (m). $SUVA_{254}$ is positively related with the aromaticity of DOM, with values generally ranging between 1 and 9 $L\ mg^{-1}\ m^{-1}$ [Weishaar *et al.*, 2003].

We obtained the excitation–emission matrices (EEM) on a spectrofluorometer (Shimadzu RF-5301PC, Shimadzu, USA) using a 1-cm quartz cuvette. We ran the EEM scans over an emission range of 270–630 nm (1-nm increments) and an excitation range of 240–400 (10-nm increments). A water blank (Milli-Q Millipore) EEM, recorded under the same conditions, was subtracted from each sample to eliminate Raman scattering. The area underneath the water Raman scan was used to normalize all sample intensities. All the EEMs were corrected for instrument-specific biases, and inner-filter effects corrections were applied according to Kothawala *et al.*, [2013]. From EEMs we calculated 3 indices: the fluorescence index (FI) as the ratio of the emission intensities at 470/520 nm for an excitation wavelength of 370 nm [Jaffé *et al.*, 2008]. FI is an indicator of terrestrial (low FI) or microbial (high FI) origin of DOM. The humification index (HIX) was calculated as the peak area under the emission spectrum 435–480 nm divided by that of 300–345 nm, at an excitation of 254 [Zsolnay *et al.*, 1999]. Higher values of HIX correspond to a higher degree of humification [Huguet *et al.*, 2009; Fellman *et al.*, 2010]. Finally, we calculated the biological index (BIX) as the ratio of the emission intensities at 380/430 nm for an excitation of 310 nm [Huguet *et al.*, 2009]. The BIX is an indicator of recent biological activity or recently produced DOM. Higher values of BIX correspond to a predominantly autochthonous origin of DOM and to the presence of OM freshly released into the sample, whereas a lower DOM production will lead to a low value of BIX [Huguet *et al.*, 2009].

4.2.4 Data analysis

We performed paired t-tests to test the differences in terms of CO_2 flux among habitats (i.e., dry riverbed vs. upland soil and dry riverbed vs. flowing riverbed).

We applied a principal component analysis (PCA) on the correlation matrix to ordinate the dry riverbeds ($n = 10$) and upland soil sites ($n = 10$) by their physical and chemical

properties. All the variables included in the analysis are described in Table 4.2. We also examined differences in physical and chemical properties of dry riverbed sediments and upland soils by means of paired t-tests.

We built two PLS regression models (projections of latent structures by means of partial least squares, *Wold et al.*, [2001]) to identify the potential physical and chemical drivers of CO₂ fluxes in dry riverbeds ($n = 35$) and upland soils ($n = 34$). All the variables included in the models are described in Table 4.2. PLS is a regression extension of PCA and allows the exploration of relationships between multiple, collinear data matrices of X' and Ys. The model performance is expressed by R²Y (explained variance) and by Q²Y (predictive power estimated by cross validation). The PLS model was validated by comparing the goodness of fit with models built from randomized Y-variables. To summarize the influence of every X-variable on the Y-variable, across the extracted PLS components, we used the variable influence on projection (VIP). The VIP scores of every model term (X-variables) are cumulative across components and weighted according to the amount of Y-variance explained in each component [*Wold et al.*, 2001]. X-variables with VIP > 1 are most influential on the Y-variable. A cut off around 0.8 separates moderately important X-variables, whereas those below this threshold can be regarded as less influential.

Table 4.2 Overview of X and Y variables included in the PCA and PLS models.

Variable	Description	PCA model	PLS models
<i>Fco₂</i>	CO ₂ flux (mmol m ⁻² d ⁻¹)	—	Y
<i>WC</i>	Water content (%)	X	X
<i>Temp</i>	Temperature (°C)	X	X
<i>Sand</i>	Sand fraction (%)	X	X
<i>Silt</i>	Sil fraction (%)	X	X
<i>Clay</i>	Clay fraction (%)	X	X
<i>P. Size</i>	Mean particle size (µm)	X	X
<i>OM</i>	Organic matter content (%)	X	X
<i>OC</i>	Organic carbon content (%)	X	X
<i>TN</i>	Nitrogen content (%)	X	X
<i>DOC</i>	Dissolved organic carbon concentration of WEOM (mg g ⁻¹)	X	X
<i>TDN</i>	Total dissolved nitrogen concentration of WEOM (mg g ⁻¹)	X	X
<i>SUVA</i>	SUVA ₂₅₄ index of WEOM (l mg ⁻¹ m ⁻¹)	X	X
<i>FI</i>	Fluorescence index of WEOM	X	X
<i>HIX</i>	Humification index of WEOM	X	X
<i>BIX</i>	Biological index of WEOM	X	X

All statistical analyses were conducted in the R statistical environment [R Core Team 2013] using the vegan package [Oksanen *et al.*, 2013], except for PLS analysis which was done with the software XLSAT (XLSTAT 2015.2.01, Addinsoft SRAL, Germany). Our data met the conditions of homogeneity of variance and normality. Statistical tests were considered significant at $p < 0.05$. Extreme outliers were excluded from the CO₂ flux data set after careful data exploration using numerical and graphical tools (i.e., Cook's influential outlier tests, boxplots, and Cleveland dotplots, following Zuur *et al.*, [2010])

4.3 Results

4.3.1 CO₂ effluxes

Dry riverbeds (mean \pm sd = 781.4 ± 390.2 mmol m⁻² d⁻¹), flowing riverbeds (305.6 ± 206.1 mmol m⁻² d⁻¹) and upland soils (896.1 ± 263.2 mmol m⁻² d⁻¹) were net emitters of CO₂ to the atmosphere (Figure 4.2). The CO₂ efflux from dry riverbeds experienced the highest intra-habitat variability and was significantly higher than the CO₂ efflux from flowing riverbeds (Paired t-test: $p = 0.043$, $n = 7$), but not statistically different than the CO₂ efflux from upland soils (Paired t-test: $p = 0.444$, $n = 10$).

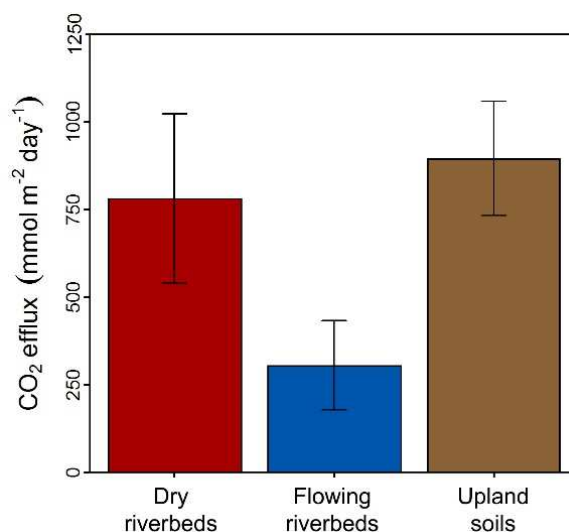


Figure 4.2 Mean CO₂ efflux from dry riverbeds ($n = 10$), flowing riverbeds ($n = 7$) and adjacent upland soils ($n = 10$) of the studied rivers. The error bars represent standard deviations.

4.3.2 Physical and chemical properties of dry riverbed sediments and upland soils

The principal component analysis (PCA) based on physical and chemical properties of the dry riverbed sediments and upland soils stressed differences between the two habitats (Figure 4.3). The two first axes of the PCA explained 71.6% of total variance. The first principal component (58.9% of total variance), clearly separated dry riverbeds and upland soils, and was related to texture properties, water content and OM quantity. The second principal component (12.7% of total variance), was mainly related to temperature and quality of the WEOM, and exerted a minor effect on the scores distribution along the 2 planes.

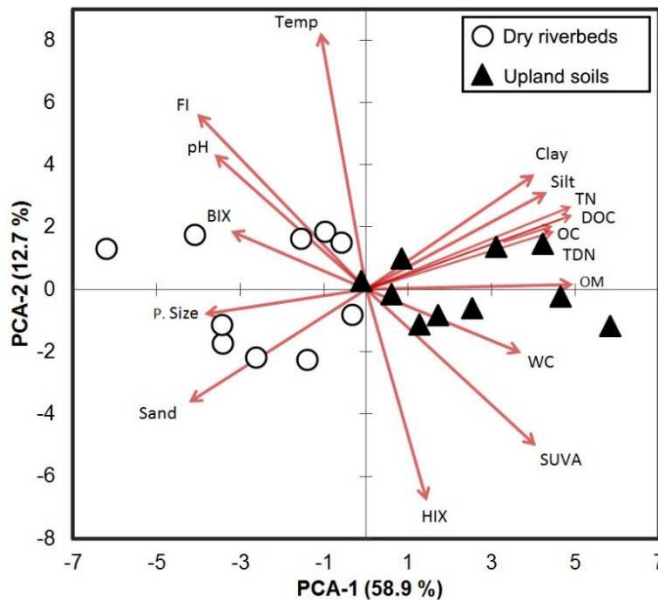


Figure 4.3 Multivariate ordination (PCA) of dry riverbed sediments and upland soils based on physical and chemical descriptors (See Table 2 for the explanation of the abbreviations). The percentage of explained variation for each component is shown in brackets. The symbols represent the scores of the samples for the first two axes and the arrows represent the loadings of each descriptor for the first two axes.

The paired t-tests further corroborated that dry riverbed sediments and upland soils differed in several physical and chemical properties (Table 4.3). Water content was

significantly lower in dry riverbeds than in upland soils. The substrate texture differed significantly between habitats. Dry riverbeds showed higher sand fraction and mean particle size, whereas upland soils had higher silt and clay fractions. The pH was significantly higher in dry riverbeds, whereas upland soils had higher organic matter, OC and TN content, both in the solid and in the extracted phase (WEOM). The SUVA₂₅₄ and FI indices indicated that the WEOM from dry riverbeds was less aromatic and had a more microbial-derived character than the WEOM from upland soils.

4.3.3 Drivers of CO₂ emissions from dry streambed sediments and upland soils

The PLS regression model for dry riverbed sediments (Figure 4.4) extracted two components from the data matrix that explained 40% of the variance ($R^2Y = 0.40$). The first (horizontal axis in Figure 4.4a) and the second PLS components (vertical axis in Figure 4.4a) respectively explained respectively 20.1% and 19.7% of the variance. This analysis stressed the relevance ($VIP > 1$) of sediment temperature, mean particle size, DOC, TDN and TN explaining the variance in the CO₂ efflux from dry riverbed sediments.

The PLS model for upland soils (Figure 4.4b) extracted two components that explained 42% of the variance ($R^2Y = 0.42$). The first and the second PLS components explained respectively, 24.0% and 17.6% of the variance. The pH, mean particle size, sand, silt and clay fractions, SUVA₂₅₄, FI and HIX were the most influential descriptors explaining the variance in the CO₂ efflux from upland soils ($VIP > 1$).

Table 4.3 Physical and chemical properties of the dry riverbed sediments and upland soils

Stream code	Habitat	Physical characteristics						Chemical characteristics									
		Temperature	Water content	Sand	Silt	Clay	Mean particle size	Solid phase				Extracted phase					
								pH	Organic matter	OC	TN	DOC	TDN	SUVA ₂₅₄	FI	HIX	BIX
1	Dry streambed	18.5 ± 0.3	5.5 ± 0.5	81.4 ± 1.4	11.2 ± 1.1	7.5 ± 0.4	1483.6 ± 168.5	8.49 ± 0.04	1.01 ± 0.18	0.94 ± 0.76	0.03 ± 0.01	0.06 ± 0.01	0.00 ± 0.00	3.12 ± 0.29	2.20 ± 0.17	7.62 ± 1.36	0.52 ± 0.06
	Upland soil	19.0 ± 0.0	16.4 ± 1.4	45.2 ± 9.4	34.8 ± 6.4	20.0 ± 3.2	407.7 ± 306.5	8.43 ± 0.05	6.68 ± 2.36	3.15 ± 2.05	0.20 ± 0.13	0.39 ± 0.12	0.03 ± 0.01	5.93 ± 1.05	2.08 ± 0.01	6.27 ± 0.70	0.54 ± 0.01
2	Dry streambed	19.8 ± 0.4	13.0 ± 6.2	38.9 ± 33.5	34.3 ± 16.5	26.8 ± 17.2	1326.4 ± 235.9	7.96 ± 0.17	2.50 ± 1.92	1.00 ± 0.44	0.09 ± 0.04	0.18 ± 0.08	0.01 ± 0.01	3.58 ± 1.00	2.29 ± 0.08	3.77 ± 0.78	0.57 ± 0.03
	Upland soil	19.9 ± 0.3	21.9 ± 3.8	59.8 ± 3.5	29.7 ± 2.6	10.5 ± 2.7	1239.3 ± 296.0	8.08 ± 0.07	10.10 ± 2.41	5.96 ± 1.32	0.36 ± 0.08	0.47 ± 0.02	0.05 ± 0.01	6.19 ± 0.79	2.09 ± 0.13	5.18 ± 1.61	0.50 ± 0.06
3	Dry streambed	17.7 ± 0.3	20.3 ± 5.6	72.5 ± 34.8	19.9 ± 26.2	7.6 ± 8.6	1039.1 ± 373.8	8.40 ± 0.13	3.79 ± 2.00	1.02 ± 1.07	0.08 ± 0.06	0.11 ± 0.07	0.01 ± 0.00	4.40 ± 0.50	2.14 ± 0.06	6.24 ± 0.65	0.54 ± 0.04
	Upland soil	18.3 ± 0.2	27.0 ± 6.2	48.6 ± 5.2	33.9 ± 4.6	17.5 ± 2.5	147.1 ± 12.7	8.27 ± 0.22	15.83 ± 8.53	6.05 ± 2.73	0.36 ± 0.14	0.55 ± 0.11	0.11 ± 0.01	5.86 ± 0.66	2.14 ± 0.11	5.40 ± 0.28	0.50 ± 0.03
4	Dry streambed	20.9 ± 1.1	10.0 ± 1.7	88.3 ± 7.9	6.7 ± 4.7	4.9 ± 3.3	1411.5 ± 217.6	7.94 ± 0.33	1.65 ± 0.57	0.37 ± 0.03	0.03 ± 0.00	0.07 ± 0.02	0.02 ± 0.00	5.48 ± 0.57	2.14 ± 0.05	7.00 ± 0.98	0.50 ± 0.01
	Upland soil	20.1 ± 0.5	15.3 ± 1.0	24.6 ± 2.4	48.2 ± 1.2	27.3 ± 1.8	855.7 ± 282.1	8.80 ± 0.29	11.07 ± 2.07	5.59 ± 1.50	0.39 ± 0.14	0.56 ± 0.13	0.12 ± 0.04	7.91 ± 0.55	2.04 ± 0.04	9.14 ± 1.37	0.47 ± 0.01
5	Dry streambed	21.2 ± 0.6	9.3 ± 1.9	89.1 ± 6.6	6.9 ± 3.9	4.0 ± 2.7	1305.0 ± 155.1	9.25 ± 0.06	1.11 ± 0.25	0.33 ± 0.14	0.03 ± 0.02	0.06 ± 0.02	0.01 ± 0.00	4.32 ± 0.55	2.18 ± 0.03	6.12 ± 1.00	0.53 ± 0.01
	Upland soil	21.0 ± 0.7	17.0 ± 1.4	55.7 ± 8.0	32.7 ± 6.2	11.5 ± 1.9	101.2 ± 18.7	8.14 ± 0.36	5.97 ± 0.70	1.85 ± 0.53	0.11 ± 0.07	0.30 ± 0.02	0.06 ± 0.01	4.88 ± 0.25	2.09 ± 0.02	5.65 ± 0.59	0.53 ± 0.02
6	Dry streambed	23.4 ± 1.1	15.4 ± 8.7	60.1 ± 30.7	28.0 ± 20.7	11.9 ± 10.0	686.1 ± 557.6	7.98 ± 0.05	4.25 ± 5.01	2.17 ± 2.22	0.15 ± 0.14	0.23 ± 0.16	0.05 ± 0.03	4.09 ± 0.66	2.27 ± 0.17	4.25 ± 0.59	0.53 ± 0.08
	Upland soil	21.1 ± 0.6	14.8 ± 1.1	60.4 ± 3.7	27.2 ± 2.5	12.4 ± 1.3	221.6 ± 49.6	7.78 ± 0.17	6.39 ± 1.39	1.50 ± 0.12	0.14 ± 0.02	0.28 ± 0.04	0.06 ± 0.02	5.60 ± 0.48	2.21 ± 0.03	5.73 ± 0.74	0.60 ± 0.04
7	Dry streambed	21.8 ± 0.7	9.2 ± 3.5	47.4 ± 11.1	36.3 ± 7.9	16.3 ± 3.2	440.2 ± 608.1	7.82 ± 0.26	2.05 ± 0.77	1.18 ± 0.52	0.10 ± 0.05	0.12 ± 0.02	0.02 ± 0.00	5.23 ± 0.47	2.15 ± 0.06	8.74 ± 1.20	0.51 ± 0.02
	Upland soil	22.1 ± 0.7	18.0 ± 2.5	25.0 ± 4.6	55.5 ± 3.7	19.5 ± 1.1	67.9 ± 26.9	7.13 ± 0.24	10.03 ± 3.12	5.17 ± 2.58	0.39 ± 0.18	0.52 ± 0.19	0.09 ± 0.01	5.14 ± 0.78	2.14 ± 0.02	6.14 ± 1.94	0.50 ± 0.03
8	Dry streambed	22.9 ± 1.4	7.2 ± 6.2	79.2 ± 7.9	14.8 ± 5.6	6.0 ± 2.3	1538.1 ± 238.8	8.14 ± 0.10	1.54 ± 1.03	2.13 ± 0.83	0.05 ± 0.04	0.10 ± 0.05	0.02 ± 0.01	2.83 ± 0.27	2.35 ± 0.10	4.64 ± 0.51	0.56 ± 0.01
	Upland soil	20.3 ± 0.4	24.2 ± 3.8	63.9 ± 2.0	24.5 ± 1.3	11.6 ± 0.8	242.4 ± 32.2	8.20 ± 0.14	8.56 ± 2.68	2.66 ± 0.83	0.13 ± 0.05	0.32 ± 0.05	0.03 ± 0.01	5.67 ± 0.68	2.07 ± 0.14	5.56 ± 1.07	0.43 ± 0.05
9	Dry streambed	22.1 ± 0.3	3.4 ± 1.2	96.5 ± 1.5	2.3 ± 0.9	1.3 ± 0.6	1886.6 ± 213.8	7.53 ± 0.52	0.52 ± 0.17	0.16 ± 0.04	0.01 ± 0.00	0.06 ± 0.02	0.00 ± 0.00	2.22 ± 0.16	2.36 ± 0.07	4.58 ± 0.82	0.60 ± 0.04
	Upland soil	22.0 ± 0.3	13.3 ± 1.0	23.4 ± 13.0	46.3 ± 6.2	30.3 ± 6.9	685.8 ± 286.5	8.40 ± 0.08	7.00 ± 1.95	5.02 ± 1.26	0.31 ± 0.09	0.57 ± 0.21	0.03 ± 0.01	4.53 ± 0.53	2.11 ± 0.16	7.54 ± 1.56	0.42 ± 0.05
10	Dry streambed	22.8 ± 0.2	16.1 ± 8.5	56.6 ± 27.7	29.3 ± 18.8	14.1 ± 8.9	800.9 ± 1093.9	8.41 ± 0.10	4.42 ± 2.87	2.87 ± 0.46	0.17 ± 0.05	0.32 ± 0.04	0.02 ± 0.00	3.90 ± 0.86	2.28 ± 0.13	4.93 ± 0.82	0.51 ± 0.03
	Upland soil	22.7 ± 0.3	11.6 ± 1.6	55.7 ± 4.9	29.7 ± 3.7	14.6 ± 1.7	683.5 ± 610.3	8.45 ± 0.16	7.24 ± 2.76	3.34 ± 1.46	0.20 ± 0.09	0.50 ± 0.18	0.04 ± 0.01	5.33 ± 0.57	2.14 ± 0.01	5.34 ± 0.53	0.47 ± 0.01
Mean ± sd	Dry streambed	21.1 ± 1.9	11.0 ± 5.2	71.0 ± 19.3	19.0 ± 12.4	10.0 ± 7.5	1191.7 ± 442.7	8.19 ± 0.48	2.28 ± 1.41	1.22 0.90	0.07 ± 0.05	0.13 ± 0.09	0.02 ± 0.01	3.92 ± 1.02	2.24 ± 0.08	5.79 ± 1.63	0.54 ± 0.03
Mean ± sd	Upland soil	20.6 ± 1.4	18.0 ± 4.9	46.2 ± 16.1	36.3 ± 10.2	17.5 ± 6.9	465.2 ± 387.6	8.17 ± 0.45	8.89 ± 3.01	4.03 1.73	0.26 ± 0.11	0.45 ± 0.11	0.06 ± 0.03	5.70 ± 0.93	2.11 ± 0.05	6.19 ± 1.24	0.50 ± 0.05
p value	dsb vs. us	0.220	< 0.001	0.020	0.009	0.040	< 0.001	0.009	< 0.001	< 0.001	< 0.001	< 0.001	0.019	< 0.001	< 0.001	0.472	0.105

Values reported means and standard deviations (mean ± sd; n=4). Results of the paired T-tests for differences between dry streambeds and upland soils are shown in the lower part of the table. Significant differences (p<0.05) are marked in bold.

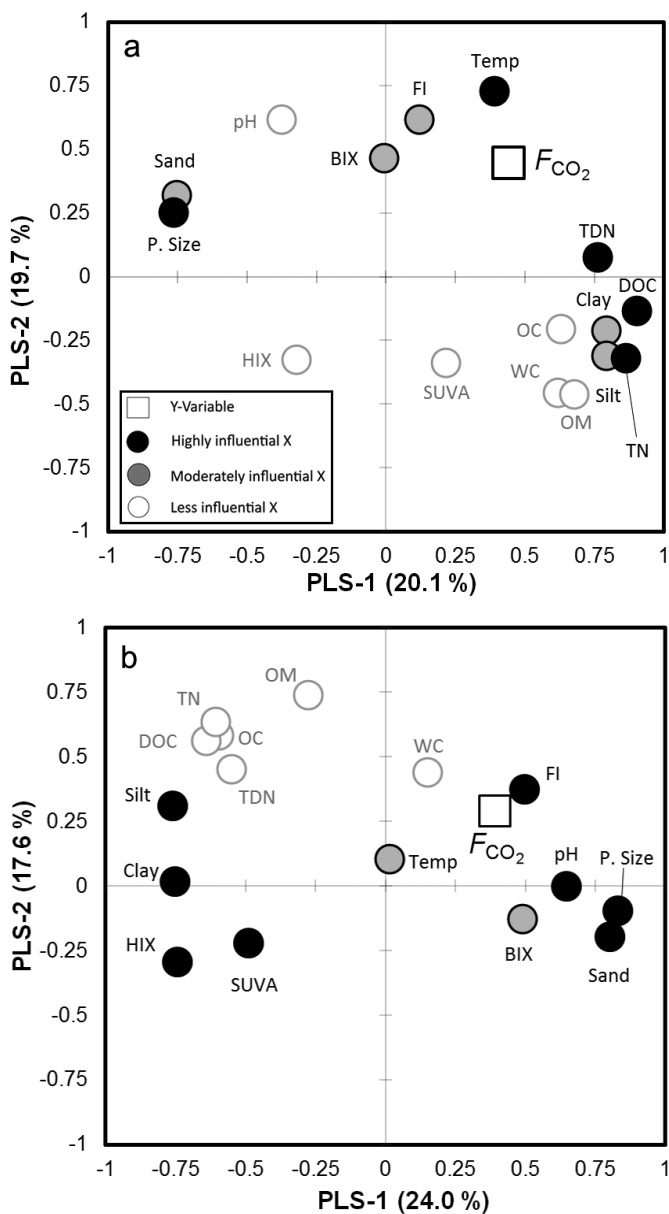


Figure 4.4 Loadings plot of the PLS regression analysis of the CO_2 emissions from dry riverbeds (a) and adjacent upland soils (b). The graph shows how the Y-variable (square) correlates with X-variables (circles) and the correlation structure of the X's. The X variables are classified according to their variable influence on projection value (VIP): highly influential (black circles), moderately influential (grey circles), and less influential (white circles). The X-variables situated near Y-variables are positively correlated to them and those situated on the opposite side are negatively correlated. See Table 4.2 for the explanation of the abbreviations.

4.4 Discussion

4.4.1 Magnitude of CO₂ emissions from dry riverbeds

Dry riverbeds from the studied temporary fluvial network emitted substantial amounts of CO₂ to the atmosphere. Our measurements of CO₂ efflux from dry riverbeds (mean = 781 mmol m⁻² d⁻¹, range = 342 to 1533 mmol m⁻² d⁻¹) are similar to those reported from a drying-rewetting experiment in dry desert streams in Arizona, USA (395 mmol m⁻² d⁻¹, range = 20 to 1531 mmol m⁻² d⁻¹; *Gallo et al.*, [2014]) and higher than others observed in the same geographical area of our study but with lower spatial coverage (mean = 209 mmol m⁻² d⁻¹, range = 189 to 220 mmol m⁻² d⁻¹; *von Schiller et al.*, [2014]). These are, to our knowledge, the only previous studies reporting CO₂ effluxes from dry riverbeds around the globe.

In the present study, we further show that the CO₂ efflux from dry streams and rivers was higher than the CO₂ efflux from the same aquatic system when they were flowing. On the one hand, this result indicates that energy flow, nutrient cycling and subsequent CO₂ production and efflux remain active after flow cessation [*Jacobson et al.*, 2000; *Boulton*, 2003; *Amalfitano et al.*, 2008]. On the other hand, this observation could be related to limitation of the CO₂ efflux in aquatic environments due to reduced gas diffusivity compared to dry riverbeds. Interestingly, these results agree with recent studies highlighting the relevance of the dry hydrological phases on the CO₂ fluxes from temporary systems of different nature, including temporary ponds [*Catalán et al.*, 2014] or reservoir beds found along Mediterranean fluvial networks [*Gómez-Gener et al.*, 2015; *Chapter 3*].

Contrary to our expectations, the CO₂ efflux from dry riverbeds was similar to the CO₂ efflux from adjacent upland soils. Similarly, *von Schiller et al.*, [2014] observed a comparable CO₂ efflux between dry riverbeds (median 212 mmol m⁻² d⁻¹; range 36–455 mmol m⁻² d⁻¹) and a compiled data set of Mediterranean soils (median 188 mmol m⁻² d⁻¹; range 44–371 mmol m⁻² d⁻¹). However, as our results show, a similar magnitude of CO₂ efflux from dry riverbeds and their adjacent upland soils does not necessarily imply that these habitats are equivalent in their physical and chemical structure and function, and therefore in the way they process and emit C.

4.4.2 Dry riverbeds as habitats in their own right

The studied riverbeds and their upland soils were very heterogeneous in terms of physical and chemical properties, but our results revealed a clear clustering of samples by habitat. In general, variables related to the textural composition and the OM content exerted the strongest influence on the differentiation between the two habitats. Specifically, dry riverbed sediments showed a higher mean particle size and a higher proportion of sand, whereas upland soils were associated to lower mean particle size and higher proportions of clay and silt fractions. Since they act as hydrological flow paths, riverbeds are more exposed to higher and recurrent surface stress in comparison to soils [Hickin 1995], making it more likely for water flow to initiate sediment erosion and transport. Thus, finer particles can be more easily mobilised in rivers, but tend to be more retained in soils [Jacobson *et al.*, 2000]. Dry riverbed sediments also contained less OM, OC, TN, DOC, TDN, in comparison to upland soils. Dry riverbeds and upland soils are subjected to different temporal and spatial dynamics of transport, retention, and processing of OM [Wagener *et al.*, 1998]. Accordingly we expect that recurrent periods of flow recession and subsequent reflowing in temporary streams and rivers may favour the oxidation and subsequent washing of OM from dry riverbeds, thus lowering its concentration of OM [Acuña *et al.*, 2007; Larned *et al.*, 2010].

Our results also show that dry riverbed sediments and upland soils were different in terms of the quality of WEOM. Significant differences in SUVA₂₅₄ and FI values between habitats indicate lower aromaticity and higher signal of in-situ produced OM from dry riverbed sediments. Mediterranean streams and rivers can receive a higher leaf input from the riparian forest (direct and lateral fluxes) in comparison to their upland soils during drought periods [Acuña *et al.*, 2007]. However, the recurrent periods of hydrological connections and disconnections, may prevent the stabilization and further humification of stored OM, thereby decreasing the signal of plant structural compounds such as lignin in the WEOM fraction. The dry riverbeds also showed higher BIX values than upland soils, pointing again towards a higher proportion of fresh DOM compounds likely derived from fluvial microbial sources [Birdwell and Engel, 2010]. The stronger microbial character of the WEOM from dry riverbed sediments compared to upland soils was likely due to the extracellular release and leachate from decaying bacteria and algae as a result of riverbed drying [Fierer and Schimel, 2003; Borken and Matzner, 2009; Kaiser *et al.*, 2015]

4.4.3 Regulation of CO₂ effluxes from dry riverbeds and upland soils

The physical and chemical variables that controlled the CO₂ efflux differed between dry riverbeds and upland soils, despite some variables (i.e., temperature and textural composition), were involved in the regulation of the efflux in both habitats. The positive relationship between temperature and many biogeochemical processes by stimulation of the microbial activity, for example, autotrophic and heterotrophic respiration, has been widely reported [Raich and Schlesinger, 1992; Mielnick and Dugas, 2000; Raich et al., 2002]. Soil texture also influenced the CO₂ efflux from dry riverbeds and from upland soils but in opposite directions in each habitat. The CO₂ efflux from dry riverbeds increased with decreasing mean particle size. Burke et al., [1989] and Buschiazzo et al., [2004] also reported that higher proportions of small particles (i.e., silt and clay fractions), correlated positively with DOC, TDN and TN concentrations and with water holding capacity, and Austin et al., [2004] showed that this promoted microbial heterotrophic respiration in soils of arid and semiarid ecosystems. On the contrary, our upland soils responded inversely to the textural properties and showed higher CO₂ efflux with increasing proportion of coarse-textured soils. This observation can be attributed to a higher diffusion of air and higher infiltration of water to the rooting zone of vegetated soils, resulting in a significant contribution of autotrophic respiration to the total CO₂ efflux in the investigated soils [Noy-Meir, 1973; Cable et al., 2008; Catalán et al., 2014]

Apart from these common drivers of the CO₂ efflux, some variables specifically regulated the efflux from dry riverbeds and upland soils. The concentration of the particulate and water extracted fractions of OC and TN were involved in the regulation of the CO₂ efflux from dry riverbeds. The availability of OM can be enhanced during drying periods by release of high amounts of fresh and labile materials to sediment interfaces through microbial cell lysis and physical processes [Fierer and Schimel, 2003; Borken and Matzner, 2009]. However, the microbial activity in dry riverbeds could be partially limited by the low concentration of DOC, TDN and TN in the substrate (Table 4.3), thus explaining the positive effect of OM concentration variables (TDN, DOC, TN) on the CO₂ efflux (Figure 4.3a). In contrast, the CO₂ efflux from upland soils was related to OM quality rather than to OM quantity (Figure 4.3b). Efflux from upland soils, which had a lower proportion of fresh and labile fractions in comparison to the dry riverbed sediments (Table 4.3), was

limited by the high aromaticity of the OM. Thus, low aromaticity and molecular complexity and high microbial signal were associated to high CO₂ efflux in the upland soils. The amount and composition of soil OM have been previously identified as important factors affecting CO₂ efflux from soils [Grogan and Jonasson, 2005; Casals *et al.*, 2009; Paré and Bedard-Haughn, 2013]

The PLS models only accounted for 50% of the total variance in CO₂ emissions, indicating that other factors involved in the production of CO₂ potentially contributed to the final CO₂ efflux. Such factors could include non-biotic CO₂-generating processes [Rey, 2015], reactions with the carbonate system [Angert *et al.*, 2014], photochemical degradation [Austin and Vivanco, 2006] or the effect of wind and air-pressure on the exchange of CO₂ [Suleau *et al.*, 2009; Redeker *et al.*, 2015]). Our results represent an initial attempt for the identification and quantification of the main drivers regulating CO₂ emissions from dry riverbeds.

4.5 Conclusions and implications

Temporary watercourses can be found in many areas of the world, and the spatial and temporal extent of the dry phase of these systems is increasing as a result of global change. Our study shows that streams and rivers do not turn into inert ecosystems when they become dry. On the contrary, they remain as active biogeochemical habitats processing and degassing significant amounts of C to the atmosphere comparable to those from upland soils. Our results also demonstrate that a similar magnitude of CO₂ emissions between dry riverbeds and upland soils does not imply that these habitats are equivalent in their physicochemical characteristics and in the variables driving CO₂ emissions. Further work is needed to provide a more conclusive understanding of the magnitude and regulation of CO₂ emissions occurring during the dry period of temporary streams and rivers, including the temporal patterns of the CO₂ efflux along the dry period. Nonetheless, available evidence so far suggests that neglecting CO₂ emissions from dry riverbeds may overlook a fundamental component of the C balance of fluvial networks.



**Effect of small water retention structures on diffusive
carbon emissions along a highly regulated river**

Abstract

Impoundment of running waters through the construction of large dams has been recognized as one of the most important factors determining the transport, transformation and emission dynamics of carbon (C) in fluvial networks. However, the effect of small and very small water retention structures (SWRS) on the magnitude and spatiotemporal patterns of C is still unknown, despite SWRS represent the most common type of water retention structure causing river fragmentation worldwide. Here, we investigated the effect of SWRS on the concentrations and air-water diffusive carbon dioxide (CO₂) and methane (CH₄) fluxes in an intensively regulated stretch of the Fluvia River (NE Iberian Peninsula). While the longitudinal pattern of dissolved CO₂ concentration along the investigated river stretch was relatively smooth, that of dissolved CH₄, exhibited a clear shifting pattern with substantial increases in impounded waters. The diffusive CO₂ efflux from impounded waters ($17.7 \pm 16.3 \text{ mmol m}^{-2} \text{ d}^{-1}$) was significantly lower than that from adjacent free-flowing river sections (230.6 ± 286.4 and $2.1 \pm 3.1 \text{ mmol m}^{-2} \text{ d}^{-1}$), because of the attenuated turbulent conditions in the former. On the contrary, no reduction in CH₄ efflux associated to the presence of SWRS was detected (0.7 ± 0.8 and $2.1 \pm 3.1 \text{ mmol m}^{-2} \text{ d}^{-1}$, for respectively impounded and free-flowing river sections), because the significant enrichment in CH₄ concentration in the impounded river sections compensated the lower turbulence. Overall, our results suggest that although the presence of SWRS might not significantly influence the C efflux of this highly-regulated river as a whole, these structures modify the local dynamics of C concentrations. Therefore, accounting for the effects of SWRS, together with that of larger dams, may be relevant for accurate estimations of C fluxes and transformation in fluvial networks.

Original publication:

Gómez-Gener, L., M. Gubau, D. von Schiller, R. Marcé, J. P. Casas-Ruiz, B. Obrador. Effect of small water retention structures on diffusive carbon emissions along a highly regulated river (to be submitted to Aquatic Sciences)

5.1 Introduction

Inland waters are active components of the global carbon (C) cycle that transform, store and emit more than half of the C they receive from terrestrial ecosystems [Cole *et al.*, 2007; Battin *et al.*, 2009a; Tranvik *et al.*, 2009; Aufdenkampe *et al.*, 2011]. Recent global estimates have shown that fluvial networks emit 2.1 Pg C y⁻¹ in the form of carbon dioxide (CO₂), of which 1.8 Pg C y⁻¹ is emitted from streams and rivers [Raymond *et al.*, 2013a] and 0.32 Pg C y⁻¹ from lakes and reservoirs [Raymond *et al.*, 2013a]. Similarly, fluvial networks emit 0.09 Pg C y⁻¹ in the form of methane (CH₄), of which 0.02 Pg C y⁻¹ is emitted from streams and rivers [Stanley *et al.*, 2016] and 0.07 Pg C y⁻¹ from lakes and reservoirs [Bastviken *et al.*, 2011; Deemer *et al.*, 2016]. The contribution of CH₄ is major (3.25 PgC-CO₂e y⁻¹) when considering the ~30-fold higher global warming potential of CH₄ compared to that of CO₂ over a 100-year time horizon [IPCC, 2013]. Nevertheless, despite the increasing availability of data covering both spatial and temporal variability, there are still fundamental uncertainties regarding the magnitude and spatiotemporal patterns of C emissions along highly regulated rivers where lotic and lentic sections inherently interact.

Due to the high human demand for energy and water, many fluvial networks worldwide have been regulated with a variety of hydraulic structures, ranging from very large dams to smaller reservoirs, impoundments and weirs [Nilsson *et al.*, 2005; Döll *et al.*, 2009]. Thus, the natural condition of fluvial networks as hierarchically organized and uninterrupted conduits draining water from the catchments to the ocean [Vannote *et al.*, 1980; Frissell *et al.*, 1986] has turned into an alternating series of lotic (i.e., running waters) and lentic (i.e., stagnant waters associated to a dam) reaches [Ward and Stanford, 1983; Stanford and Ward, 2001]. Disruption of water flow by dams changes the hydrological dynamics of rivers [Kondolf and Batalla, 2005; Grill *et al.*, 2015], thereby altering water physicochemistry [Ward and Stanford, 1983], the transport of suspended particles [Syvitski *et al.*, 2005; Houser *et al.*, 2010], and ultimately leading to multiple consequences on the composition and function of aquatic biological communities at different levels of organization [Haxton and Findlay, 2008; Ponsati *et al.*, 2015; von Schiller *et al.*, 2016; Proia *et al.*, 2016].

Sediments, organic matter (OM) and nutrients delivered from the inflowing river may accumulate upstream of water retention structures due to the higher deposition rates

typically occurring in lentic waterbodies [Syvitski *et al.*, 2005; Maeck *et al.*, 2013]. Such trapping of autochthonous and allochthonous OM typically leads to anaerobic environments that are ideal for active methanogenesis and subsequent CH₄ supersaturation of the water column and release of CH₄ to the atmosphere [Keller and Stallard, 1994; Giles, 2006; Delsontro *et al.*, 2010]. Likewise, the increase in water residence time (WRT) caused by river impoundment can favour the mineralization of OM and CO₂ supersaturation by increasing the interaction between organic substrates and biological actors [Battin *et al.*, 2009b; Acuña and Tockner, 2010; Crawford *et al.*, 2016].

Most of the quantitative estimates of C emissions from impounded waters have mainly been obtained for very large (> 10⁴ km²), large (10⁴ - 10² km²) and medium (100 - 1 km²) size reservoirs [St. Louis *et al.*, 2000; Barros *et al.*, 2011; Deemer *et al.*, 2016]. These estimates pointed out that the depositional zones close to the river inflow, where freshly allochthonous materials enter the reservoir (i.e., riverine-lacustrine transition zone, *sensu* Wetzel [2001]), remain a very active compartment in terms of CO₂ and CH₄ production and emission despite their relatively small areal coverage [Beaulieu *et al.*, 2016]. Recent research in small reservoirs (1 - 0.1 km²) has shown that the intense sedimentation of fresh OM in the riverine-lacustrine transition zone, which in the case of medium to small systems can cover a larger fraction of the reservoir's surface area, fuels intense CO₂ and CH₄ production, making these systems potential biogeochemical hotspots for C emission to the atmosphere [Maeck *et al.*, 2013].

Small water retention structures (SWRS) include weirs and small to very small impoundments with a surface impounded area < 0.1 km² and volume < 0.2 hm³ [Lehner *et al.*, 2011]. These structures, despite their small global areal extent (3.8% of the global reservoir surface area [Downing *et al.*, 2006; Lehner *et al.*, 2011]), represent one of the most common feature in freshwater landscapes (99.5% of the total number of reservoirs worldwide [Downing *et al.*, 2006; Lehner *et al.*, 2011]). However, they still remain underemphasized or even not considered in most of the biogeochemical studies in fluvial networks [Downing *et al.*, 2006].

SWRS have a profound effect on river fragmentation and generate substantial impacts on the spatial extent of flow alterations [Lehner *et al.*, 2011]. SWRS are also of increasing

concern because their cumulative effects may be considerable, yet they have so far remained underemphasized and unexamined [Downing *et al.*, 2006]. For example, Harrison *et al.*, [2009] showed that SWRS play an important regional and global role in the removal of nitrogen from surface water. Casas-Ruiz *et al.* [2015] pointed out that the presence of SWRS generate changes in the composition and degradation of dissolved organic matter (DOM) in rivers. In the same line, Proia *et al.* [2016] found that the presence of SWRS can also modify the natural dynamics of C processing along the fluvial network by altering the structure and activity of the microbial community. This previous knowledge leads to the intriguing question of whether SWRS can affect the magnitude and patterns of CO₂ and CH₄ similarly as larger impounded systems do.

Here, we investigate the effect of SWRS on the concentrations and air-water diffusive CO₂ and CH₄ fluxes in an intensively regulated stretch of a Mediterranean river. To this end, we measured the dissolved concentrations and fluxes of CO₂ and CH₄ in impounded and free-flowing riverine sections on a seasonal basis. We hypothesize that the presence of SWRS will lead to higher WRT and, in turn, higher accumulation rates of OM, thus enhancing aerobic heterotrophic respiration and anaerobic methanogenesis in both the water column and the sediments of impounded waters. We therefore expected higher concentrations and emission rates of CO₂ and CH₄ in the impounded water of SWRS in comparison to their upstream free-flowing waters. We also hypothesize that the CO₂ and CH₄ accumulated in the impounded waters will influence the emission dynamics of the lotic sections located downstream from the dams, being thus higher than in the upstream lotic sections.

5.2 Materials and Methods

5.2.1 Study sites and sampling design

The Fluvià River (NE Iberian Peninsula; Figure 5.1) is a 97-km long river, with a mean annual flow of 3.6 m³ s⁻¹ at the catchment outlet (Data from 2004 to 2014, Catalan Water Agency), that drains a 990-km² catchment covered with mixed forests (78%), agricultural (19%) and urban (3%) areas (Land Cover Map of Catalonia, Centre of Ecology and Forestry

Research of Catalonia, 2009). The catchment is mostly calcareous, with some areas (< 15%) of siliceous materials (Cartographic and Geological Institute of Catalonia, 2006). The climate in the area is typically Mediterranean; the mean monthly air temperature ranges from 6 °C in January to 26 °C in July and the mean annual precipitation is 660 mm, with rainfall primarily occurring in autumn and spring and occasional storms in summer (Data from 2004 to 2014, Catalan Water Agency). The water flow of Fluvià River has been deeply modified due to the high human demand for energy and water [García-Ruiz *et al.*, 2011]. Its fluvial network presents up to 61 SWRS that alter the flow dynamics from its headwaters to the river mouth [Pavón, 2010].

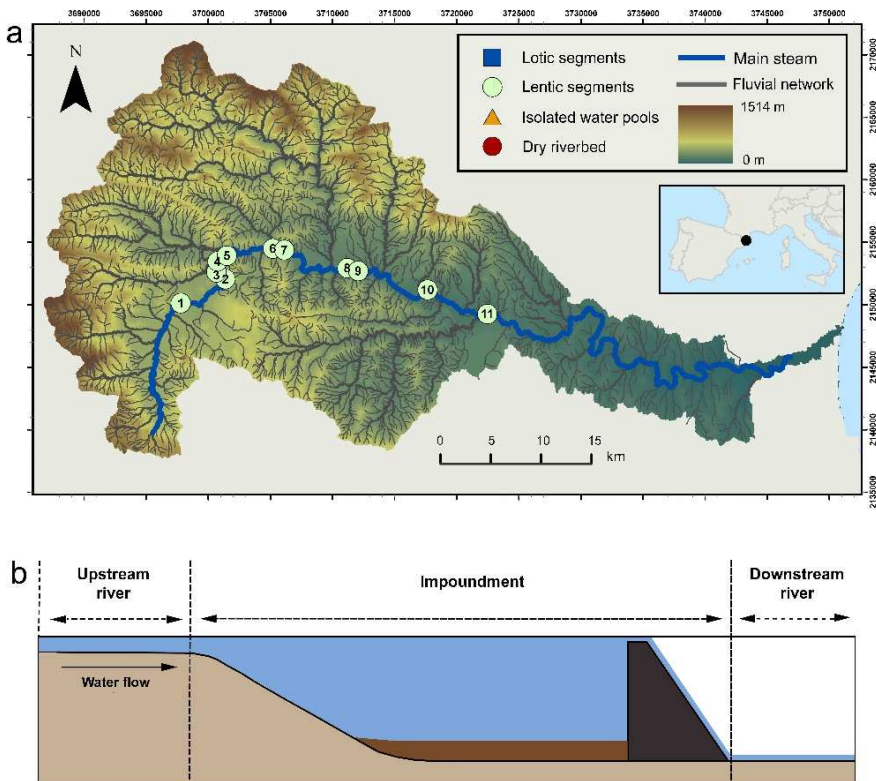


Figure 5.1 (a) Location of the Fluvià River catchment (NE Iberian Peninsula), with the position of the studied SWRS (black circles, $n = 11$). See Table A.5.1 in the Supporting information section for a detailed hydromorphological and physicochemical description of the selected SWRS (sorted by number). (b) Scheme of a SWRS sampling unit (i.e., upstream river, impoundment water and downstream river) sampled at each study site.

We focused this study on a highly regulated 36-km stretch situated in the upper part of the Fluvia River main stem (Figure 5.1a). To cover a wide spectrum of hydromorphological and trophic conditions (Table A.5.1 in the Supporting information section), we selected a total of 11 SWRS and we sampled them in spring (28 to 30 April), summer (2 to 4 September) and winter (9 to 11 December) 2014. At each site, we sampled the stagnant water impounded in the SWRS as well as the free-flowing river sections located upstream and downstream (Figure 5.1b). The distance between the SWRS and the downstream sampled free-flowing river section was between 20 and 380 meters.

5.2.2 Determination of CO₂ and CH₄ water-atmosphere fluxes

In the impounded river sections, we determined the CO₂ flux across the water-air interface by the enclosed chamber method [Frankignoulle 1988]. Briefly, we monitored the CO₂ gas concentration in an opaque floating chamber every 4.8 s with an infrared gas analyser (EGM-4, PP-Systems, USA). In all the cases, flux measurements lasted until a change in CO₂ of at least 10 µatm was reached, with a maximum duration of 600 s and a minimum of 300 s. We calculated the CO₂ flux from the rate of change of CO₂ inside the chamber as follows:

$$F_{\text{CO}_2} = \left(\frac{dp_{\text{CO}_2}}{dt} \right) \left(\frac{V}{RTS} \right) \quad (1)$$

where $\frac{dp_{\text{CO}_2}}{dt}$ is the change in CO₂ concentration in the chamber along time in µatm s⁻¹, V and S are the volume and surface area of the chamber (27.1 dm³ and 19.4 dm² respectively), T is the air temperature in Kelvin and R is the ideal gas constant (L atm K⁻¹ mol⁻¹). Positive F_{CO_2} values represent efflux of gas to the atmosphere while negative F_{CO_2} indicate influx of gas from the atmosphere. We performed 2 measurements in the central part of the impounded water after flushing the chamber with ambient air between consecutive measurements.

At each SWRS, we determined the partial pressure of CO₂ and CH₄ in the water ($p_{\text{CO}_2, \text{w}}$, $p_{\text{CH}_4, \text{w}}$) and in air ($p_{\text{CO}_2, \text{a}}$, $p_{\text{CH}_4, \text{a}}$) at the same location as the flux measurements. We

measured the $p_{\text{CO}_2, \text{w}}$ with an infrared gas analyser (EGM-4, PP-Systems, USA) coupled to a membrane contactor (MiniModule, Liqui-Cel, USA). The water was circulated by gravity through the contactor at 300 mL min^{-1} and the equilibrated gas was continuously recirculated into the infrared gas analyser for instantaneous p_{CO_2} measurements [Teodoru *et al.*, 2010]. For $p_{\text{CO}_2, \text{w}}$, the air samples were taken approximately one meter above the water surface layer and circulated through the gas analyzer. Measurement accuracy of the infrared gas analyser is estimated to be within 1% over the calibrated range. We determined the $p_{\text{CH}_4, \text{w}}$ and $p_{\text{CH}_4, \text{a}}$ by the headspace equilibrium technique and gas chromatography described by Striegl *et al.*, [2012]. Briefly, we collected 40 ml of water with a 60 ml polypropylene syringe creating a headspace with ambient air of 3:2 ratio (sampled water : ambient air). To facilitate the kinetics of equilibration between the liquid and the gas phase, we vigorously shook the syringe for 1 min and we submerged it for half an hour at constant water temperature. We then transferred the 20 mL of equilibrated gas to a pre-evacuated gas-tight glass tube (2-RV, Chromacol, USA). The CH_4 samples were analysed in the laboratory with a gas chromatograph coupled to a Flame Ionization Detector (Trace GC Ultra, Thermo Fisher Scientific, USA). Measurement accuracy of the gas chromatograph is estimated to be within 4% over the calibrated range.

We used the F_{CO_2} measured with the chamber to calculate the direct gas transfer velocity of CO_2 (k_{CO_2}) from Fick's law of gas diffusion:

$$F_{\text{CO}_2} = k_{\text{CO}_2} K_h (p_{\text{CO}_2, \text{w}} - p_{\text{CO}_2, \text{a}}) \quad (2)$$

where k_{CO_2} is the specific gas transfer velocity for CO_2 (m d^{-1}); F_{CO_2} is the chamber-measured F_{CO_2} between the surface water and the atmosphere ($\text{mmol m}^{-2} \text{d}^{-1}$), K_h is the Henry's constant ($\text{mmol } \mu\text{atm}^{-1} \text{ m}^{-3}$) adjusted for salinity and temperature [Weiss, 1974; Millero, 1995]. Because the gas transfer velocity is temperature- and gas-dependent, we standardized k_{CO_2} to a Schmidt number of 600 (k_{600} ; m d^{-1}), which corresponds to CO_2 at 20°C in freshwater:

$$k_{600} (\text{m d}^{-1}) = k_{\text{CO}_2} \left(\frac{600}{\text{Sc}}\right)^{-2/3} \quad (3)$$

where Sc is the Schmidt number of a given gas at a given water temperature [*Jähne and Münnich* [1987], *Bade* [2009], *Wanninkhof*, 1992].

At each SWRS, we derived the diffusive CH_4 flux across the water-air interface ($mmol\ m^{-2}\ d^{-1}$) following equation (2) and combining $p_{CH_4, w}$, $p_{CH_4, a}$ and the chamber derived k_{CH_4} obtained by applying equation (3).

In the riverine sections upstream and downstream the impounded water stored in the SWRS, we determined the diffusive CO_2 and CH_4 flux across the water-air interface ($mmol\ m^{-2}\ d^{-1}$) using equation (2). At each river section we determined $p_{CO_2, w}$, $p_{CO_2, a}$, $p_{CH_4, w}$ and $p_{CH_4, a}$ following the same technique described above and we estimated the reach gas transfer velocity from the segment slope (s ; $m\ m^{-1}$) and the mean segment water velocity (v ; $m\ s^{-1}$) with equation (4) in *Raymond et al.* [2012]:

$$k_{600} = 1162\ s^{0.77}\ v^{0.85} \quad (4)$$

The k_{600} was transformed to the k_{CO_2} and k_{CH_4} following equation (3).

5.2.3 Data analysis

We investigated the overall effect of the SWRS on the CO_2 and CH_4 fluxes, concentrations and gas transfer velocities in each season by using a one-way repeated measures analysis of variance (ANOVA). We performed subsequent post-hoc comparisons (Tukey's Honest Significant Differences test) to evaluate the specific effect of SWRS on i) the impounded water CO_2 and CH_4 fluxes, concentrations and gas transfer velocities (by comparing impounded waters and free flowing upstream reaches), and ii) the downstream C fluxes, concentrations and gas transfer velocities (by comparing upstream and downstream riverine reaches adjacent to the SWRS).

We assessed the relative control of $p_{CO_2, w}$ and k_{CO_2} on the CO_2 efflux using simple linear regression models. We used the same statistical approach to assess the relative control of $p_{CH_4, w}$ and k_{CH_4} on the CH_4 efflux.

We built two partial-least squares regression models (PLS) to identify the potential controls of both impounded water $p_{\text{CO}_2, \text{w}}$ and $p_{\text{CH}_4, \text{w}}$. The PLS is a regression extension of a principal component analysis (PCA) that allows the exploration of relationships between multiple and collinear independent (X; potential explanatory variables described in Table A.5.2 in the Supporting information section) and dependent (Y; $p_{\text{CO}_2, \text{w}}$ and $p_{\text{CH}_4, \text{w}}$) data matrices through a linear, multivariate model that produces latent variables (i.e.; PLS loadings) representing the combination of X variables that best describe the distribution of observations in 'Y space' [Eriksson *et al.*, 2006]. For each Y-variable, the best PLS model was selected by iteratively removing X-variables in order to maximize the goodness of fit (R_2Y) and the predictive ability (Q_2Y) of the model. In each case, Q_2Y was determined by comparing modelled and actual Y observations through an iterative, cross-validation process. We identified the influence of each X-variable by using variable influence on the projection (VIP) scores, calculated as the sum of square of the PLS weights across all components. Variables with high influence on impounded water $p_{\text{CO}_2, \text{w}}$ and $p_{\text{CH}_4, \text{w}}$ were identified as those having $\text{VIP} > 1$, while variables with moderate and low influence on impounded water $p_{\text{CO}_2, \text{w}}$ and $p_{\text{CH}_4, \text{w}}$ were those having VIP between 1 and 0.8 and $\text{VIP} < 0.8$, respectively [Eriksson *et al.*, 2006].

All statistical analyses were conducted in the R statistical environment [R Core Team 2013] using the vegan package [Oksanen *et al.*, 2013], except for PLS analysis which was done with the software XLSAT (XLSTAT 2015.2.01, Addinsoft SRAL, Germany). When necessary, we normalized data using log-transformations to meet parametric assumptions. In all cases, differences were considered statistically significant when $p < 0.05$.

5.3 Results

5.3.1 Diffusive CO₂ and CH₄ effluxes

The surface waters impounded in the 11 SWRS were net emitters of CO₂ (mean \pm SE = 17.7 ± 2.8 mmol m⁻² d⁻¹, range = -2.1–86.2 mmol m⁻² d⁻¹; Figure 5.2a) and CH₄ (0.66 ± 0.14 mmol m⁻² d⁻¹, range = 0.01–3.29 mmol m⁻² d⁻¹; Figure 5.2b) to the atmosphere in the three

studied seasons. The only exception to this pattern occurred at site N5, which acted as a sink of CO₂ in winter (-2.1 mmol m⁻² d⁻¹). Nonetheless, the CO₂ and CH₄ efflux from the impounded river sections never exceeded that from their adjacent free-flowing river sections, which were always net emitters of both C gases to the atmosphere (Figure 5.2a and 2b). More precisely, the efflux from impounded waters was significantly lower than their upstream and downstream free-flowing river sections in the case of CO₂ (ANOVA, $f = 10.26$, $p < 0.001$, $n = 33$; Figure 5.2a), but comparable in the case of CH₄ (ANOVA, $f = 4.82$, $p = 0.23$, $n = 33$; Figure 5.2b).

No significant differences among SWRS sampling units (i.e., upstream free-flowing river section, impounded river section and downstream free-flowing river section) in terms of $p_{\text{CO}_2, \text{w}}$ (ANOVA, $f = 0.08$, $p = 0.92$, $n = 33$; Figure 5.2c), were detected. In contrast, we detected significant differences among SWRS sampling units in terms of $p_{\text{CH}_4, \text{w}}$ (ANOVA, $f = 7.47$, $p < 0.001$, $n = 33$; Figure 5.2d). Specifically, we detected a significant increase in $p_{\text{CH}_4, \text{w}}$ in the impounded waters in relation to their upstream free-flowing river sections (ANOVA, post-hoc, $p < 0.001$, $n = 33$; Figure 5.2d). In spring, when this effect was more aggravated, it was translated into an increase of $p_{\text{CH}_4, \text{w}}$ in the flowing sections downstream the SWRS (ANOVA, post-hoc, $p = 0.01$, $n = 33$; Figure 5.2d). This impounded waters $p_{\text{CH}_4, \text{w}}$ increase, was however, not strong enough to cause a significant influence on the CH₄ efflux of the downstream riverine sections (ANOVA, post-hoc, $p = 0.18$, $n = 33$; Figure 5.2b).

Among the two main parameters directly driving the CO₂ and CH₄ fluxes (see Equation 2), the surface water turbulence (measured as k_{CO_2} and k_{CH_4}), which exhibited a significant positive relationship with both the CO₂ efflux (CO₂ efflux = $31.1 k_{\text{CO}_2} + 46.2$; $r^2 = 0.61$, $p < 0.001$, $n = 33$; Figure A.5.1a in the Supporting information section) and CH₄ efflux (CH₄ efflux = $31.1 k_{\text{CH}_4} + 46.2$; $r^2 = 0.61$, $p < 0.001$, $n = 33$; Figure A.5.1b in the Supporting information section). In addition, the k_{CO_2} (ANOVA, $f = 18.36$, $p < 0.001$, $n = 33$; Figure 5.2e) and k_{CH_4} (ANOVA, $f = 18.32$, $p < 0.001$, $n = 33$; Figure 5.2f) were significantly lower in the impounded river sections than in free-flowing river sections. Thus, surface water turbulence appeared to be the main responsible factor for the clear differences in CO₂ and CH₄ effluxes between impounded waters and riverine sections (Figure 5.2).

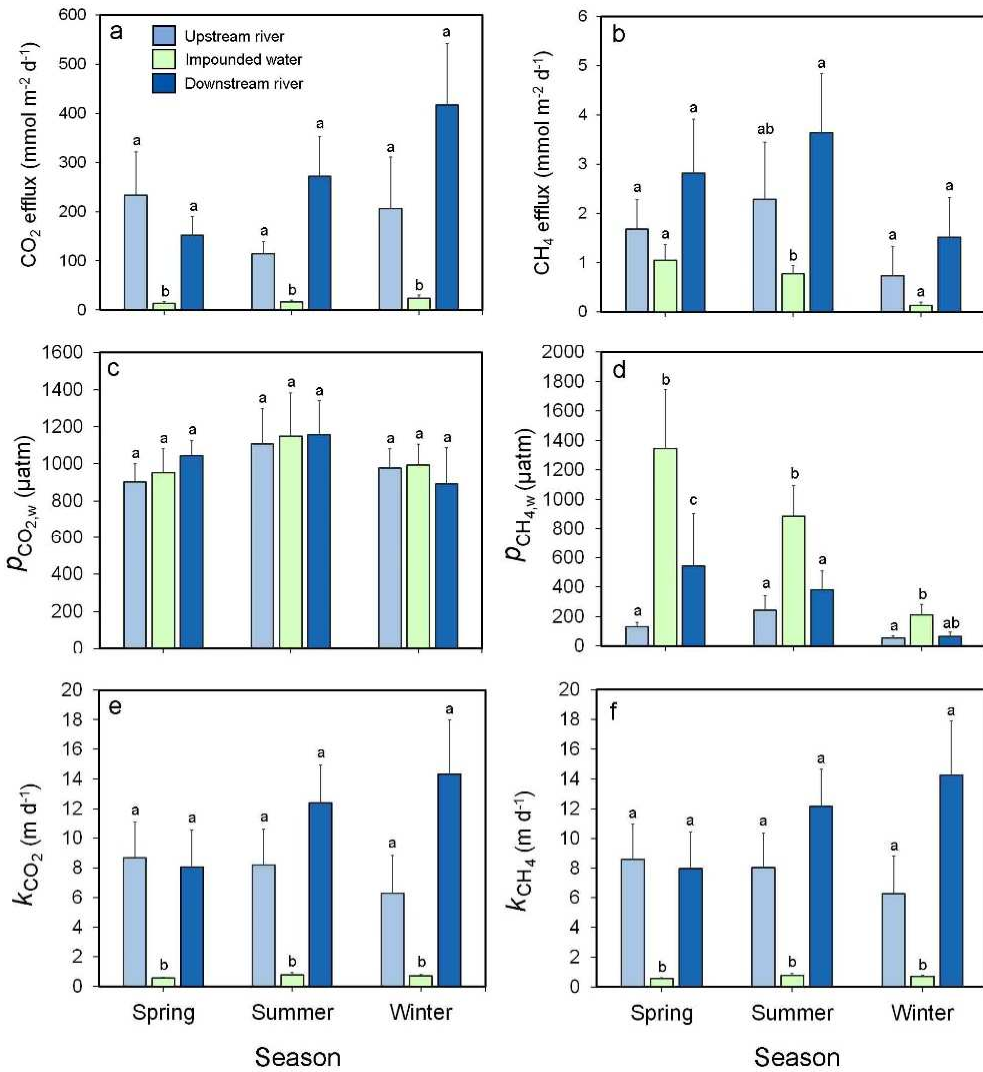


Figure 5.2 Mean (a) CO_2 efflux, (b) CH_4 efflux, (c) partial pressure of CO_2 in water ($p_{\text{CO}_2, \text{w}}$), (d) partial pressure of CH_4 in water ($p_{\text{CH}_4, \text{w}}$), (e) gas transfer velocity of CO_2 (k_{CO_2}) and (f) gas transfer velocity of CH_4 (k_{CH_4}) of the 11 SWRS grouped by sampling units (i.e., upstream river, impoundment water and downstream river) during the 3 sampled seasons (i.e., spring, summer and winter). Error bars represent standard error (SE) of the 11 studied SWRS. Significant differences of reported parameters between SWRS units ($p < 0.05$, Tukey's post-hoc test after repeated measures ANOVA) are marked with different letters above the bars.

5.3.2 Longitudinal patterns of $p_{\text{CO}_2, \text{w}}$ and $p_{\text{CH}_4, \text{w}}$

Distinct longitudinal patterns along the studied stretch were identified for $p_{\text{CO}_2, \text{w}}$ and $p_{\text{CH}_4, \text{w}}$ (Figure 5.3). The $p_{\text{CO}_2, \text{w}}$ showed a relatively smooth downstream pattern during the three investigated seasons (Figure 5.3a, 5.3b and 5.3c). On the contrary, the presence of SWRS not only influenced the dynamics of $p_{\text{CH}_4, \text{w}}$ at local scale (see previous section) but also led to abrupt fluctuations in the $p_{\text{CH}_4, \text{w}}$ longitudinal pattern (Figure 3). Even though this longitudinal $p_{\text{CH}_4, \text{w}}$ pattern was consistent in the three studied seasons, a more marked fluctuating pattern was observed during winter (Figure 3f).

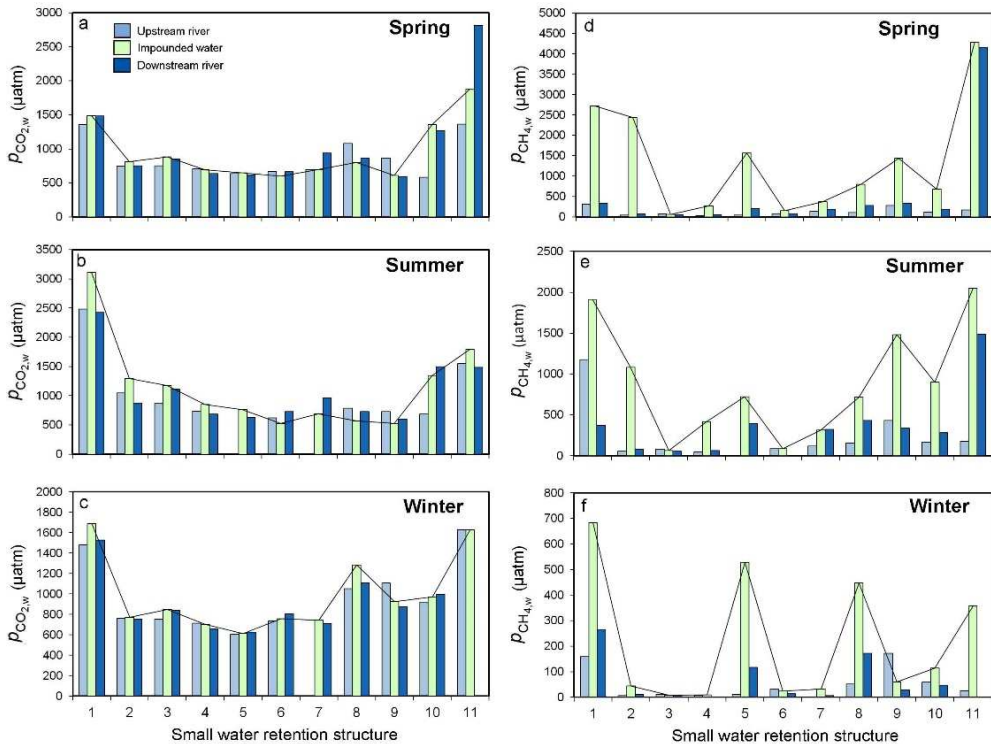


Figure 5.3 Downstream longitudinal patterns of the partial pressure of CO_2 in water ($p_{\text{CO}_2, \text{w}}$) in (a) spring, (b) summer and (c) winter and partial pressure of CH_4 in water ($p_{\text{CH}_4, \text{w}}$) in (d) spring, (e) summer and (f) winter for the 3 different SWRS units (i.e., upstream river, impoundment water and downstream river). The continuous solid lines represent the mean impoundment water $p_{\text{CO}_2, \text{w}}$ or $p_{\text{CH}_4, \text{w}}$. Water flow direction from N1.

5.3.3 Drivers of impounded water $p_{\text{CO}_2, \text{w}}$ and $p_{\text{CH}_4, \text{w}}$

The PLS models identified distinct combinations of factors as predictors of impounded water $p_{\text{CO}_2, \text{w}}$ and $p_{\text{CH}_4, \text{w}}$ (Figure 5.4a; Table A.5.3 in the Supporting information section).

The PLS model for $p_{\text{CO}_2, \text{w}}$ extracted two components from the data matrix that explained 68% of the variance (Figure 5.4a; Table A.5.3 in the Supporting information section). The most influential factors ($\text{VIP} > 1$) on $p_{\text{CO}_2, \text{w}}$ were surface area, WRT, $p_{\text{CH}_4, \text{w}}$, electrical conductivity and alkalinity, while the moderately influential factors (VIP between 0.8 and 1) on the $p_{\text{CO}_2, \text{w}}$ were surface water oxygen saturation, dissolved organic carbon concentration (DOC) and pH (see the direction and the relative strength of the effect of each factor on the $p_{\text{CO}_2, \text{w}}$ in Table A.5.3 in the Supporting information section).

The PLS model for $p_{\text{CH}_4, \text{w}}$ extracted two components from the data matrix that explained 69% of the variance (Figure 5.4b; Table A.5.3 in the Supporting information section). The most influential factors ($\text{VIP} > 1$) on $p_{\text{CH}_4, \text{w}}$ were surface area, WRT, total dissolved nitrogen concentration, DOC, surface water temperature and concentration of Chl-*a* in suspension (see the direction and the relative strength of the effect of each factor on the $p_{\text{CH}_4, \text{w}}$ in the Table A.5.3 in the Supporting information section), while no moderately influential factors was obtained from the PLS model for $p_{\text{CH}_4, \text{w}}$.

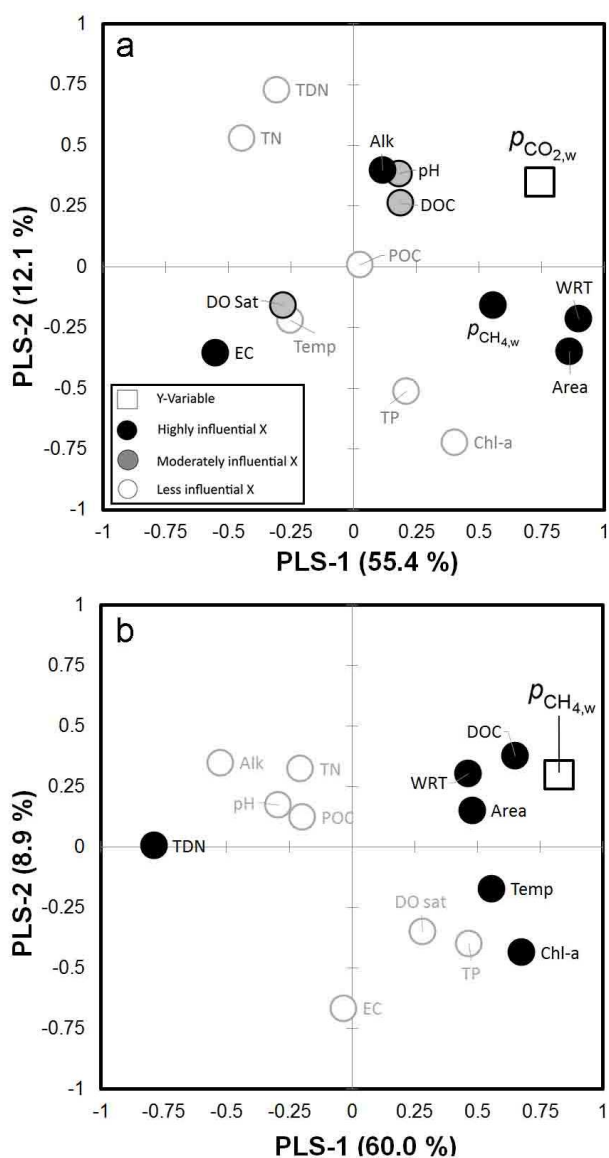


Figure 5.4 Loadings plot of the PLS regression analysis for (a) pressure of CO_2 in water ($p_{CO_2,w}$) and (b) partial pressure of CH_4 in water ($p_{CH_4,w}$). The graph shows how the Y-variable (squares) correlates with X-variables (circles) and the correlation structure of the X's. X-variables are classified according to their variable influence on projection value (VIP): highly influential (black circles), moderately influential (grey circles) and less influential (white circles). The X-variables situated near Y-variables are positively correlated to them and those situated on the opposite side are negatively correlated. See Table A.5.2 in the Supporting information section for the explanation of the abbreviations.

5.4 Discussion

5.4.1 Low diffusive CO₂ and CH₄ emissions from impounded waters

Disruption of water flow by SWRS changes the hydrological dynamics of rivers, leading to higher WRT and higher deposition rates of OM [Syvitski *et al.*, 2005; Acuña and Tockner, 2010; Maeck *et al.*, 2013]. Such trapping of autochthonous and allochthonous OM typically fuels aerobic and anaerobic heterotrophic processes, consequently favouring the enrichment of surface waters with CO₂ and CH₄ surface water concentrations and ultimately leading to higher emissions from impounded waters to the atmosphere [Cole, 2000; St. Louis *et al.*, 2000b; Duarte and Prairie, 2005; Giles, 2006]. Contrary to our expectations, the diffusive CO₂ and CH₄ emitted from impounded waters in our study never exceed the emissions from adjacent upstream riverine waters (treated as reference systems without SWRS influence). We attribute this finding to the higher turbulence induced by water currents in the free-flowing riverine sections. This physical control on C emissions was more evident in the case of CO₂, where differences in $p_{\text{CO}_2, \text{w}}$ were not even detected. Interestingly the physical control of emissions was also observed for CH₄, despite for this gas, the impounded waters did show a significant increase in CH₄ concentrations in relation to their upstream free-flowing river sections. Our results agree with previous findings that emphasized the importance of the gas transfer velocity as the major driver of diffusive CO₂ and CH₄ emissions from fluvial networks containing lakes and reservoirs [Guérin *et al.*, 2007; Lundin *et al.*, 2013; Crawford *et al.*, 2014a; Gómez-Gener *et al.*, 2015]. For CH₄, we must consider that our estimates did not account for the ebullitive efflux, which has been described to be a major pathway for total CH₄ efflux in very large, large and medium-size (> 1 km²) reservoirs [Delsontro *et al.*, 2010; Fearnside and Pueyo, 2012; Sobek *et al.*, 2012; Beaulieu *et al.*, 2016], small reservoirs (1 - 0.1 km²) [Maeck *et al.*, 2013] and SWRS (< 0.1 km²) previously examined in the same river [Gómez-Gener *et al.*, 2015]. Therefore, the inclusion of ebullition estimates (e.g. inverted funnel-style bubble traps) in our sampling design would have probably led to higher total CH₄ emission rates in the studied impounded waters compared to the river segments [Delsontro *et al.*, 2010].

5.4.2 Low effect of SWRS on downstream diffusive CO₂ and CH₄ emissions

Regulation by dams not only affects the C emissions from the surface waters of reservoirs but also influences the C dynamics in the riverine sections downstream the reservoir [Guérin *et al.*, 2006; Kemenes *et al.*, 2007]. Emissions downstream of reservoirs have generally been poorly studied and are usually not taken into account in reservoir C balances [Barros *et al.*, 2011]. The few works reporting C emissions downstream of reservoirs, mainly conducted in large reservoirs situated in the tropic region, showed that downstream C emissions can account for 7 to 25% of total CO₂ emissions from reservoirs [Abril, 2005; Guérin *et al.*, 2006] and 50 to 90% of total CH₄ emissions [Abril, 2005; Guérin *et al.*, 2006; Kemenes *et al.*, 2007].

In the present study, we did not find significant differences in CO₂ or CH₄ effluxes between free-flowing river sections located upstream and downstream of SWRS, despite the significant enrichment in CH₄ in the impounded surface water. Here, we propose that this finding may be due to a possible loss of CO₂ and CH₄ along the segment between the SWRS and the downstream sampling stations. We acknowledge that although the distance between the SWRS and the downstream sampling stations was relatively short (never exceed 380m), a non-quantifiable part of CO₂ and CH₄ could have been emitted along this distance (e.g., throughout the waterfall associated to the SWRS) [Galy-lacaux *et al.*, 1997; Wehrli, 2013; Deshmukh *et al.*, 2015].

5.4.3 Routing vs. local controls on the longitudinal patterns of $\rho_{\text{CO}_2, \text{w}}$ and $\rho_{\text{CH}_4, \text{w}}$

Conceptual models of longitudinal patterns in streams and rivers are framed by the interplay of two contrasting perspectives. On the one hand are those frameworks that emphasize flow as an integrator over space [Vannote *et al.*, 1980; Montgomery, 1999]. On the other hand, are those frameworks that highlight patchiness and abrupt spatial changes [Frisell *et al.*, 1986; Townsend 1989]. These models are based on gradient analysis in which rivers are ultimately viewed as uninterrupted continua. However, few fluvial networks remain free from flow regulation over the entire course, but contrarily, they typically result

in an alternating series of lentic and lotic reaches [Ward and Stanford, 1983; Nilsson *et al.*, 2005; Döll *et al.*, 2009].

Here, we show that the downstream longitudinal patterns of dissolved C gases in water differed considerably depending on the nature of the C gas. On the one hand, CO₂ concentrations varied softly and homogeneously both at local scale (i.e., across SWRS sampling units) and at fluvial network scale (i.e., along the 36-km study stretch). This pattern suggests that although localized controls may influence CO₂ concentrations in river water, the longitudinal dynamics of this gas have a routing control [Montgomery, 1999], where the CO₂ lost in riverine sections is constantly replenished by CO₂ produced internally or imported from the catchment [Hotchkiss *et al.*, 2015; Gómez Gener *et al.*, 2016]. On the other hand, CH₄ concentrations showed a more variable pattern both at local and fluvial network scales. This shifting longitudinal pattern suggests that the concentration of CH₄ is highly dominated by local controls such as the presence of SWRS [Stanley *et al.*, 2016]. Likewise, the difference in $p_{\text{CH}_4, \text{w}}$ between impounded and riverine sections also highlights the high reactivity and dynamism of this gas, which in few meters is generated and rapidly emitted or consumed [Guérin *et al.*, 2006; Kemenes *et al.*, 2007].

5.4.4 Regulation of $p_{\text{CO}_2, \text{w}}$ and $p_{\text{CH}_4, \text{w}}$ from impounded waters

Surface water supersaturation of dissolved CO₂ and CH₄ in impounded waters was persistent along the studied stretch and across seasons. Albeit, the results from the PLS-models suggest that the drivers of gas supersaturation in SWRS may differ between CO₂ and CH₄.

CO₂ supersaturation in impounded waters was explained by a combination of metabolically-related factors (i.e., oxygen saturation level, DOC, WRT and surface system area) and factors that may be related to hydrological inputs of CO₂ from soil respiration and mineral weathering within the catchment (i.e., surface water alkalinity, pH and electrical conductivity). These results confirm the idea that direct terrestrial or geological origin of river $p_{\text{CO}_2, \text{w}}$ [Stets *et al.*, 2009; McDonald *et al.*, 2013; Hotchkiss *et al.*, 2015a; Marcé *et al.*, 2015] is not in contradiction with the widespread notion of net heterotrophy

leading to CO₂ supersaturation in different aquatic ecosystems [Duarte and Prairie, 2005; Lapiere et al., 2013]. In the case of $p_{\text{CH}_4, \text{w}}$, our results support the idea that the presence of SWRS, despite their relative small water capacity, can still produce similar effects on their impounded water $p_{\text{CH}_4, \text{w}}$ than those previously found in larger impoundments [Delsontro et al., 2010; Maeck et al., 2013; Beaulieu et al., 2016]. This can occur, for example, by affecting internal metabolic processes in the sediments (i.e., attenuated hydrological conditions [Thornton 1990], altering temperature regimes [Delsontro et al., 2010] and by inducing higher input and concentration of autochthonous and allochthonous OM [Sobek et al., 2012]).

5.5 Conclusions and implications

Our results show that because of the attenuated turbulent conditions, the diffusive CO₂ efflux from impounded waters was significantly lower than that from free-flowing river sections. On the contrary, no reduction in CH₄ efflux associated to the presence of SWRS was detected because the significant enrichment in CH₄ concentration in the impounded river sections compared to the free-flowing river sections compensates the physical effect on CH₄ efflux. The significant increase in CH₄ concentration detected in the impounded waters was not high enough to imply a significantly increase in the diffusive CH₄ efflux from the free-flowing riverine sections adjacent to the SWRS; however, it influenced the overall longitudinal patterns of CH₄ along the study stretch. Local controls (e.g., higher WRT, higher sedimentation rates, higher temperatures) associated to the presence of SWRS shaped the longitudinal dynamics of CH₄ along this highly regulated river. Overall, these findings emphasize that the view of fluvial networks as a continuum is insufficient for describing the true spatial complexity of CH₄ dynamics.



**Low contribution of internal metabolism to carbon dioxide
emissions along lotic and lentic environments of a
Mediterranean fluvial network**

Abstract

Inland waters are significant sources of carbon dioxide (CO₂) to the atmosphere. CO₂ supersaturation and subsequent CO₂ emissions from inland waters can be driven by internal metabolism, external inputs of dissolved inorganic carbon (DIC) derived from the catchment and other processes (e.g., internal geochemical reactions of calcite precipitation or photochemical mineralization of organic solutes). However, the sensitivity of the magnitude and sources of CO₂ emissions to fluvial network hydromorphological alterations is still poorly understood. Here, we investigated both the magnitude and sources of CO₂ emissions from lotic (i.e., running waters) and lentic (i.e., stagnant waters associated to small dams or weirs) waterbodies of a Mediterranean fluvial network by computing segment-scale mass balances of CO₂. Our results showed that sources other than internal metabolism sustained most (82%) of the CO₂ emissions from the studied fluvial network. The magnitude and sources of CO₂ emissions in lotic waterbodies were highly dependent on hydrology, with higher emissions dominated by DIC inputs derived from the catchment during high flows, and lower emissions partially fuelled by CO₂ produced biologically within the river during low flows. In contrast, CO₂ emissions in lentic waterbodies were low, relatively stable over the time and the space, and dominated by DIC inputs from the catchment regardless of the different hydrological situations. Overall, our results stress the sensitivity of fluvial networks to human activities and climate change, and particularly highlight the role of hydromorphological conditions on modulating the magnitude and sources of CO₂ emissions from fluvial networks.

Original publication (*Appendix C in the Supporting information section*):

Gómez-Gener, L., D. von Schiller, R. Marcé, M. Arroita, J. P. Casas-Ruiz, P. A. Staehr, V. Acuña, S. Sabater, and B. Obrador (2016), Low contribution of internal metabolism to carbon dioxide emissions along lotic and lentic environments of a Mediterranean fluvial network, *J. Geophys. Res. Biogeosci.*, 121, doi:10.1002/2016JG003549

6.1 Introduction

Inland waters are active components of the global carbon (C) cycle that transform, store and emit more than half of the C they receive from terrestrial ecosystems [Cole *et al.*, 2007; Battin *et al.*, 2009a; Tranvik *et al.*, 2009; Aufdenkampe *et al.*, 2011]. Recent global estimates place the efflux of carbon dioxide (CO₂) emitted from streams and rivers at 1.8 Pg C y⁻¹ and from lakes and reservoirs at 0.32 Pg C y⁻¹, resulting in a global estimate of CO₂ emissions from fluvial networks of 2.1 Pg C y⁻¹ [Raymond *et al.*, 2013]. However, there are still fundamental uncertainties regarding the magnitude, spatiotemporal variation and sources of CO₂ emissions from fluvial networks [Raymond *et al.*, 2013; Wehrli, 2013; von Schiller *et al.*, 2014; Hotchkiss *et al.*, 2015].

A better understanding of the processes regulating CO₂ emissions from fluvial networks is essential to comprehend the present and thus predict the future role of freshwaters in the global C cycle and the climate system [Raymond *et al.*, 2013; Hotchkiss *et al.*, 2015]. The flux of CO₂ across the air–water interface depends on the gas transfer velocity and the supersaturation of CO₂ in the surface water [Bade, 2009]. While the gas transfer velocity is a physical factor mainly controlled by the turbulence at the air–water interface, there are two major processes that can lead to CO₂ supersaturation in aquatic ecosystems. The first is internal aquatic mineralization of organic matter (OM), which can result in an imbalance of net ecosystem production (NEP) towards net heterotrophy (respiration exceeding production) [Cole *et al.*, 2000; Duarte and Prairie, 2005]. The second is the input of surface and subsurface water with high dissolved inorganic carbon (DIC) content derived from soil respiration and mineral weathering within the catchment [Cole *et al.*, 2007; Humborg *et al.*, 2010b; Marcé *et al.*, 2015]. Among these, internal metabolism has classically been considered to be the main factor driving CO₂ supersaturation in lakes and rivers [Cole *et al.*, 2000; Duarte and Prairie, 2005]. Yet, recent studies have shown that external inputs dominate CO₂ supersaturation and thus CO₂ emissions from most streams and rivers [Borges *et al.*, 2015a; Hotchkiss *et al.*, 2015] as well as lakes and reservoirs [Stets *et al.*, 2009; McDonald *et al.*, 2013; Marcé *et al.*, 2015; Weyhenmeyer *et al.*, 2015; Wilkinson *et al.*, 2016a]. However, there is still little information about the relative contribution of these major sources to the CO₂ emissions from lotic and lentic waterbodies located within

fluvial networks. Likewise, the role of other less known processes such as internal geochemical reactions of calcite precipitation usually occurring in alkaline waterbodies [Otsuki and Wetzel, 1974; Stets *et al.*, 2009; Nōges *et al.*, 2016] or photochemical mineralization of organic solutes [Amon and Benner, 1996; Cory *et al.*, 2014; Vachon *et al.*, 2016] on sustaining CO₂ supersaturation and emission in aquatic ecosystems is still largely undefined.

Due to the high human demand for energy and water, many fluvial networks worldwide have been regulated with a variety of hydraulic structures, ranging from very large dams to smaller reservoirs, impoundments and small weirs [Nilsson *et al.*, 2005a; Döll *et al.*, 2009]. Mediterranean fluvial networks are no exception, having mainly been modified by small man-made flow discontinuities such as impoundments or weirs [García-Ruiz *et al.*, 2011]. Such anthropogenic changes combined with the naturally marked seasonality of river flow in Mediterranean regions [Gasith and Resh, 1999; Bernal *et al.*, 2013], modulate the fluvial network hydrological dynamics (i.e., flow conditions) that, in turn, govern the overall physicochemical [Friedl and Wüest, 2002; Poff and Hart, 2002], structural [Clavero *et al.*, 2004; Buffagni *et al.*, 2009] and functional [Ward and Stanford, 1983; Acuña and Tockner, 2010; Elosegi and Sabater, 2013; Abril *et al.*, 2015] attributes of these fluvial networks. As a consequence, strong changes in the magnitude and sources of CO₂ emissions in response to flow modification are expected for fluvial networks in this region.

Here we evaluated and compared the magnitude and sources of CO₂ emissions between lotic and lentic waterbodies within a Mediterranean fluvial network and investigated their response to different hydrological conditions. To test the overarching objectives, we measured CO₂ emissions and the underlying fluxes that drive variation in CO₂ concentration within studied segments. We then computed the relative contribution of the CO₂ production by internal metabolism, the hydrological flux of CO₂ and the CO₂ flux of other non-measured processes to the emitted CO₂ by solving segment-scale mass balances over one hydrological year. We hypothesized that the magnitude and the relative contribution of the different sources to CO₂ emissions in our fluvial network would strongly depend on the waterbody type (i.e., lotic or lentic) as well as on the hydrological conditions (i.e., high or low water flow). During high flows, we expected that higher gas exchange as well as greater hydrological connectivity would homogenize gas dynamics along the lotic

and lentic waterbodies of the fluvial network. Thus, we predicted generally higher fluvial network CO₂ emissions and similar rates of CO₂ emissions in lentic and lotic waterbodies, with dominant support of sources other than CO₂ produced by internal metabolism. In contrast, during low flows, we expected a general decrease in the gas exchange and hydrological connectivity, with an associated increased spatial heterogeneity in gas concentration and flux. Thus, we predicted generally lower fluvial network CO₂ emissions, and lower CO₂ emissions from lentic than from lotic segments, as well as a greater contribution of aquatic metabolic sources in lentic than in lotic waterbodies.

6.2 Materials and Methods

6.2.1 Study sites and sampling design

The Fluvià River (NE Iberian Peninsula; Figure 6.1) is a 97-km long river that drains a 990-km² catchment covered with mixed forests (78%), agricultural (19%) and urban (3%) areas (Land Cover Map of Catalonia, Centre of Ecology and Forestry Research of Catalonia, 2009). The catchment is mostly calcareous, with some areas (< 15%) of siliceous materials (Cartographic and Geological Institute of Catalonia, 2006). The climate in the area is typically Mediterranean; the mean monthly air temperature ranges from 6 °C in January to 26 °C in July and the mean annual precipitation is 660 mm, with rainfall primarily occurring in autumn and spring, with occasional storms in summer (Data from 2004 to 2014, Catalan Water Agency). The water flow of Fluvià River has been deeply modified due to the high human demand for energy and water [García-Ruiz *et al.*, 2011]. Its fluvial network presents up to 61 small to very small water retention structures (SWRS) such as weirs and small impoundments that cause flow interruptions from its headwaters to the river mouth [Pavón, 2010].

In order to cover the wide spectrum of hydrological conditions occurring in the Fluvià River fluvial network, we performed monthly samplings (December 2012 to November 2013) in a set of 12 segments situated throughout the fluvial network, from headwaters to lowlands (Figure 6.1). The segments included 8 lotic (i.e., running water reaches) and 4 lentic (i.e.,

stagnant waters associated to SWRS) segments.. The selected study segments were chosen as to avoid point source pollution, and their length was defined as a compromise between sufficient to detect changes in the variables of interest, while maintaining relative homogeneity of environmental conditions (i.e., canopy cover, morphology, and subcatchment land use). A detailed hydromorphological description of the selected segments along the sampling period is shown in Table A.6.1 in the Supporting information section.

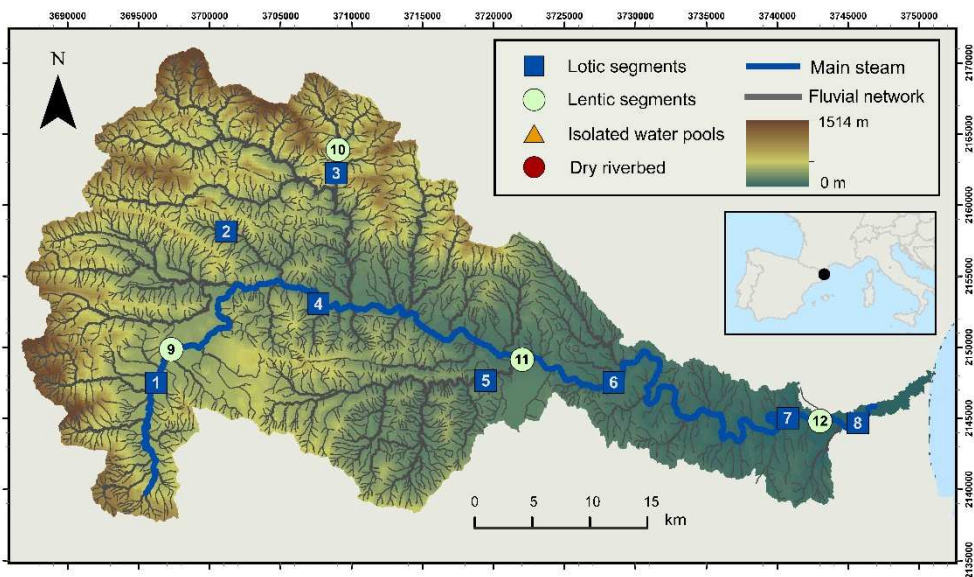


Figure 6.1 Location of the Fluvià River catchment in Catalonia (NE Iberian Peninsula), with the corresponding position of the study segments ($n = 12$). Dark blue circles indicate lotic segments ($n = 8$) and light green circles lentic segments ($n = 4$). See Table A.6.1 in the Supporting information section for a detailed description of the hydromorphological characteristics of the segments.

6.2.2 Hydromorphology

On each sampling date, we measured the cross-sectional water velocity (m s^{-1}) at the inlet and outlet of each segment with an acoustic-Doppler velocity meter (Sontek, YSI, USA), and we combined this with the cross-sectional depth (m) and width (m) to derive the water flow ($\text{m}^3 \text{s}^{-1}$). We used then the hydraulic modelling software HecRas 2.2 (US Army Corps

of Engineers, USA) to estimate the mean cross-sectional water velocity, the wet segment area and the water volume every ca. 100 m along the segments. The model was fed with the measured water flow and segment geometrical data provided by the Catalan Water Agency). We calculated the slope of each lotic segment as the elevation difference over the length of the segment with the geospatial-processing software (ArcMap v10, ESRI, USA) using a 2-meter digital elevation model (Cartographic and Geological Institute of Catalonia, 2006).

In lentic segments, we obtained the surface area, volume and mean and maximum depth from digitized bathymetric maps constructed with a geospatial-processing software (ArcMap v10, ESRI, USA) using in-situ morphological data obtained from different field surveys performed during 2013. The water residence time (WRT; h) in both lotic and lentic segments was calculated by dividing the segment volume by the segment average water flow.

6.2.3 Water-air flux of CO₂

In lotic segments we determined the CO₂ flux across the water-air interface ($F_{\text{CO}_2 \text{ emission}}$; mmol m⁻² d⁻¹) using Fick First Law of gas diffusion:

$$F_{\text{CO}_2 \text{ emission}} = k_{\text{CO}_2} K_h (p_{\text{CO}_2, \text{w}} - p_{\text{CO}_2, \text{a}}) \quad (1)$$

where K_h (mmol $\mu\text{atm}^{-1} \text{m}^{-3}$) is the Henry's constant for CO₂ adjusted for salinity and temperature [Weiss, 1974; Millero, 1995], $p_{\text{CO}_2, \text{w}}$ (μatm) and $p_{\text{CO}_2, \text{a}}$ (μatm) are the mean partial pressures of CO₂ in surface water and air, respectively, and the k_{CO_2} (m d⁻¹) is the specific gas transfer velocity for CO₂. Positive values of $F_{\text{CO}_2 \text{ emission}}$ represent gas efflux from the water to the atmosphere, and negative values indicate gas influx from the atmosphere to the water.

At the inlet and the outlet of each segment, we measured the $p_{\text{CO}_2, \text{w}}$ and $p_{\text{CO}_2, \text{a}}$ with an infrared gas analyzer (EGM-4, PP-Systems, USA). Measurement accuracy of the EGM-4 is estimated to be within 1% over the calibrated CO₂ range. For $p_{\text{CO}_2, \text{w}}$ measurements, the

water samples were circulated through a membrane contactor (MiniModule, Liqui-Cel, USA) coupled to the gas analyzer [Teodoru *et al.*, 2010] at 300 mL min⁻¹. For $p_{\text{CO}_2, a}$, the atmospheric air was taken approximately one meter above the water surface layer and circulated through the gas analyzer. We then averaged the $p_{\text{CO}_2, w}$ and $p_{\text{CO}_2, a}$ measured at the inlet and the outlet of each segment to obtain a mean segment $p_{\text{CO}_2, w}$ and $p_{\text{CO}_2, a}$.

We estimated a mean segment gas transfer velocity from the segment slope (s ; m m⁻¹) and the mean segment water velocity (v ; m s⁻¹) with equation (2) in Raymond *et al.* [2012]:

$$k_{600} = 1162 s^{0.77} v^{0.85} \quad (2)$$

where k_{600} (m d⁻¹) is the standardized gas transfer velocity at 20°C. The k_{600} was transformed to the k_{CO_2} following:

$$k_{\text{CO}_2} = k_{\text{O}_2} \left(\frac{Sc_{\text{CO}_2}}{Sc_{\text{O}_2}} \right)^{-n}, \quad (3)$$

where Sc (dimensionless) is the Schmidt number of CO₂ at the measured water temperature [Wanninkhof, 1992]. In addition, we compared our k_{CO_2} derived from equation (2) with the k_{CO_2} calculated from night-time oxygen dynamics (NTR method; [Hornberger and Kelly, 1972]; detailed description of the method in the Figure A.6.1 in the Supporting information section) and direct chamber measurements to ensure their applicability throughout the study (Figure A.6.1 in the Supporting information section). This validation exercise showed that the range where 95% of the y-observations (i.e., k_{CO_2} from equation (2)) fall (95th percentile) showed a clear linear relationship with the x-observations (i.e., k_{CO_2} from the NTR method and from chamber measurement made in lotic segments), with almost all the observations falling very close to the 1:1 reference line.

In lentic segments, we determined $F_{\text{CO}_2 \text{ emission}}$ by the enclosed chamber method [Frankignoulle 1988]. Briefly, we monitored the CO₂ gas concentration in an opaque floating chamber every 4.8 s with an infrared gas analyser (EGM-4, PP-Systems, USA). In all the cases, flux measurements lasted until a change in CO₂ of at least 10 µatm was

reached, with a maximum duration of 600 s and a minimum of 300 s. We calculated the $F_{\text{CO}_2 \text{ emission}}$ from the rate of change of CO_2 inside the chamber as follows:

$$F_{\text{CO}_2 \text{ emission}} = \left(\frac{dp_{\text{CO}_2}}{dt} \right) \left(\frac{V}{RTS} \right) \quad (4)$$

where $\frac{dp_{\text{CO}_2}}{dt}$ is the change in CO_2 concentration in the chamber along time in $\mu\text{atm s}^{-1}$, V and S are the volume and surface area of the chamber (27.1 dm^3 and 19.4 dm^2 respectively), T is the air temperature in Kelvin and R is the ideal gas constant ($\text{L atm K}^{-1} \text{ mol}^{-1}$). We performed and averaged a minimum of 3 measurements in the central part of the lentic segment after flushing the chamber with ambient air between consecutive measurements.

At each lentic segment, we determined the $p_{\text{CO}_2, \text{w}}$ and the $p_{\text{CO}_2, \text{a}}$ at the same location where flux was measured using the methodology described for lotic segments and we then derived the k_{CO_2} from equation (1).

6.2.4 Internal metabolic flux of CO_2

We estimated the internal metabolic flux of CO_2 ($F_{\text{CO}_2 \text{ metabolism}}$; $\text{mmol m}^2 \text{ d}^{-1}$) at each of the 12 segments from diel open-water dissolved oxygen (DO) variations [Odum 1956]. The diel DO data was obtained from automatic monitoring stations equipped with optical probes (YSI 600OMS V2, YSI 600XLM V2, Yellow Springs, USA, and MiniDOT, PME, USA). The YSI 600OMS V2, YSI 600XLM V2 and MiniDOT sensors have an accuracy of 0.1, 0.1 and 0.3 $\text{mg O}_2 \text{ L}^{-1}$, respectively. All the probes were intercalibrated before deployment.

The metabolic rates were determined for those days coincident with the $F_{\text{CO}_2 \text{ emission}}$ samplings. Specifically, in those segments where permanent monitoring stations were available (#8, #3 and #11, Figure 6.1) the metabolic rates were determined for all the monthly $F_{\text{CO}_2 \text{ emission}}$ samplings ($n = 12$). In the other segments, we used temporarily installed monitoring stations, and the metabolism was determined in two contrasted hydrological situations (high flow period, end of May 2013, and low flow period, end of August 2013; Figure 6.2a).

We obtained the solar irradiance reaching the surface (E ; $W\ m^{-2}$) from a nearby meteorological station (< 50 km away from the study segments) and converted it to photosynthetically active radiation (PAR; $mmol\ m^{-2}\ d^{-1}$) following Kirk [1994].

We calculated the gross primary production (GPP) and ecosystem respiration (ER) using a linear photosynthesis–irradiance relationship [Van der Bogert *et al.*, 2007; Hanson *et al.*, 2008; Holtgrieve *et al.*, 2010]:

$$DO_t = DO_{t-1} + \left(\frac{GPP}{z} \cdot \frac{PAR_{t-1}}{PAR_{24}} \right) - \left(\frac{ER}{z} \Delta t \right) + F_{O_2} \Delta t \quad (5)$$

where GPP is the rate of O_2 production by photosynthesis ($mmol\ O_2\ m^{-2}\ d^{-1}$), ER is the respiratory rate of O_2 consumption ($mmol\ O_2\ m^{-2}\ d^{-1}$), PAR_{t-1} is the instantaneous photosynthetically active radiation ($mmol\ m^{-2}\ d^{-1}$), PAR_{24} is the daily accumulated photosynthetically active radiation ($mmol\ m^{-2}\ d^{-1}$), z is mean water column depth (m), F_{O_2} is the exchange of O_2 between the water and the atmosphere ($mmol\ O_2\ m^{-2}\ d^{-1}$) and Δt is the time between measurements. F_{O_2} was calculated as $F_{O_2} = k_{O_2} (O_{2,w(t-1)} - O_{2,sat(t-1)})$, where k_{O_2} is the specific gas transfer velocity for O_2 ($m\ d^{-1}$), $O_{2,w}$ is the measured DO concentration in water, and $O_{2,sat}$ is the DO concentration in atmospheric equilibrium, calculated at each time step from temperature and corrected for barometric pressure from [Benson and Krause, 1984]. We obtained k_{O_2} from k_{CO_2} by applying equation (3).

We estimated GPP and ER by fitting Eq. 6 to the diel DO data for each day using a numerical minimization algorithm (the negative log likelihood function of a normal distribution), using the function `nlm` in R [R Core Team 2013]. Model performance (i.e., how well the model fitted observed diel changes in DO) was assessed both visually, and numerically through the coefficient of determination ($r^2 > 0.75$, see examples in Figure A.6.2 in the Supporting information section). Model fitting was generally good, and metabolic rates agreed with reported ranges for streams, rivers, lakes and reservoirs ([Hoellein *et al.*, 2013], Table A.6.2 and Figure A.6.23 in the Supporting information section).

We then calculated the net ecosystem production (NEP; $mmol\ O_2\ m^{-2}\ d^{-1}$) as:

$$\text{NEP} = \text{GPP} - \text{ER} \quad (6)$$

and we converted oxygen-based rates to C metabolic rates (expressed as mmol C m⁻² d⁻¹) using a CO₂:O₂ ratio of 138:106 [Torgersen and Branco, 2007]. For NEP > 0 (i.e., net autotrophy) there is more CO₂ being removed from the water column by photosynthesis than added by respiration, leading to negative $F_{\text{CO}_2 \text{ metabolism}}$. In contrast, NEP < 0 (i.e., net heterotrophy) implies higher respiration than photosynthesis, and therefore a positive $F_{\text{CO}_2 \text{ metabolism}}$.

6.2.5 Source apportionment of CO₂ emissions

In addition to the upstream inputs and internal metabolism, other processes (i.e., groundwater fluxes, lateral surface water fluxes and internal fluxes derived from geochemical reactions of calcite precipitation and photochemical mineralization of organic solutes), can contribute to CO₂ supersaturation in each segment. We derived the flux of CO₂ associated to these unmeasured sources ($F_{\text{CO}_2 \text{ others}}$; mmol m⁻² d⁻¹) by applying a mass balance approach of CO₂ assuming steady state in each individual segment:

$$\frac{d\text{CO}_2}{dx} = F_{\text{CO}_2 \text{ inflow}} - F_{\text{CO}_2 \text{ outflow}} \pm F_{\text{CO}_2 \text{ emission}} \pm F_{\text{CO}_2 \text{ metabolism}} \pm F_{\text{CO}_2 \text{ others}} \quad (7)$$

where $F_{\text{CO}_2 \text{ inflow}}$ (mmol m⁻² d⁻¹) is the measured flux of CO₂ imported from upstream surface waters, $F_{\text{CO}_2 \text{ outflow}}$ (mmol m⁻² d⁻¹) is the measured flux of CO₂ exported to downstream surface waters, $F_{\text{CO}_2 \text{ emission}}$ (mmol m⁻² d⁻¹) is the measured flux of CO₂ across the water-air interface and $F_{\text{CO}_2 \text{ metabolism}}$ is the measured flux of CO₂ derived from aerobic metabolic processes occurring in the segment. Not all the CO₂ derived from internal metabolism will remain in the water as CO₂ because a portion will be converted to carbonate or bicarbonate depending on water alkalinity and pH. Thus, we calculated $F_{\text{CO}_2 \text{ metabolism}}$ by considering the geochemical speciation of inorganic carbon (IC) once CO₂ from internal metabolism is added to the water. Concentrations of different DIC species were calculated from DIC, pH and temperature using the speciation software CO2SYS [Lewis and Wallace, 1998].

To assess the relative contribution (%) of each source to the total CO₂ inputs into the segment, we divided each of the contributing fluxes (i.e., $F_{\text{CO}_2 \text{ inflow}}$, $F_{\text{CO}_2 \text{ metabolism}}$ and $F_{\text{CO}_2 \text{ others}}$) by their sum.

6.2.6 Data analysis

We tested the effect of the segment type (i.e., lotic segments, n = 96; lentic segments, n = 48) on the mean WRT, $F_{\text{CO}_2 \text{ metabolism}}$, $p_{\text{CO}_2, w}$ and k_{CO_2} using one-way analysis of variance (ANOVA). We assessed the effect of the WRT on the $F_{\text{CO}_2 \text{ emission}}$, $p_{\text{CO}_2, w}$ and k_{CO_2} in both lotic and lentic segments using linear and non-linear regressions. To determine the importance of the two main parameters directly involved in the CO₂ emission (i.e., $p_{\text{CO}_2, w}$ and k_{CO_2}) we applied simple and multiple linear regression models.

We tested the effect of the segment type (i.e., lotic segments, n = 32; lentic segments, n = 10) on the CO₂ fluxes that determined CO₂ variations within segments (i.e., $F_{\text{CO}_2 \text{ emission}}$, $F_{\text{CO}_2 \text{ metabolism}}$, $F_{\text{CO}_2 \text{ inflow}}$, $F_{\text{CO}_2 \text{ outflow}}$ and $F_{\text{CO}_2 \text{ others}}$) using one-way ANOVA. We investigated the dependency of $F_{\text{CO}_2 \text{ metabolism}}$ on $F_{\text{CO}_2 \text{ emission}}$ and $p_{\text{CO}_2, w}$ in both lotic and lentic segments with linear and non-linear regression models. A similar approach was used to assess the effect of the WRT on the $F_{\text{CO}_2 \text{ metabolism}}$ and of the WRT on the relative contribution of $F_{\text{CO}_2 \text{ metabolism}}$, $F_{\text{CO}_2 \text{ inflow}}$ and $F_{\text{CO}_2 \text{ others}}$.

When the statistical tests required it, we transformed the variables by their natural logarithm to meet the conditions of homogeneity of variance, normality of residuals and to avoid the deleterious effect of extreme large values. All statistical analyses were conducted in the R statistical environment [R Core Team 2013] using the Vegan package [Oksanen *et al.* 2013]. Statistical tests were considered significant at $p < 0.05$.

6.3 Results

6.3.1 Hydrological regime

The WRT of lotic and especially that of lentic segments showed a wide annual variation, driven by changes in water flow (Figure 6.2a; Table A.6.1 in the Supporting information

section). Specifically, the first part of the monitored period (from December 2012 to March 2013) was characterized by low water flows. During this period, the average WRT in lotic segments was 10 h. In contrast, the presence of dams and weirs extended the WRT in lentic segments up to an average of 51 h. Subsequently, surface water flow in the fluvial network increased swiftly as a consequence of heavy rainfalls, leading to a minimum difference in WRT between segment types (mean WRT of lotic and lentic segments from April to May 2013 was 0.8 and 3.7 h, respectively). Following this hydrological peak (April 2013) the surface water flow gradually decreased until the end of the studied period (November 2013). Consequently, the mean fluvial network WRT increased progressively, and the difference in WRT between lotic and lentic segments increased again (mean WRT of lotic and lentic segments in November 2013 was 6.6 and 30.6 h, respectively).

6.3.2 CO₂ emissions

The $F_{\text{CO}_2 \text{ emission}}$ ranged from 627.2 to -11.2 mmol m⁻² d⁻¹ (mean = 131.9, n = 144) and showed a clear difference in magnitude and seasonal variation between lotic and lentic segments (Figure 6.2b). The lotic $F_{\text{CO}_2 \text{ emission}}$ was negatively related to WRT ($F_{\text{CO}_2 \text{ emission}} = -63.9 \ln(\text{WRT}) + 205.3$; $r^2 = 0.94$, $p < 0.001$, n = 12), indicating a strong dependency on hydrological dynamics. In contrast, a non-significant relationship between $F_{\text{CO}_2 \text{ emission}}$ and WRT was detected in lentic segments ($r^2 = 0.14$, $p = 0.29$, n = 12).

The $F_{\text{CO}_2 \text{ emission}}$ also showed a different spatial pattern in lotic and lentic segments (Figure A.6.4 in the Supporting information section). In lotic segments, both the magnitude and the temporal variability decreased from upstream segments (i.e., headwaters streams) to lowland segments (i.e., river mouth). In contrast, lentic segments showed the opposite pattern, and emitted more CO₂ and were more temporally variable when situated close to the river mouth, and emitted less CO₂ and were less variable when they were situated upstream on the fluvial network.

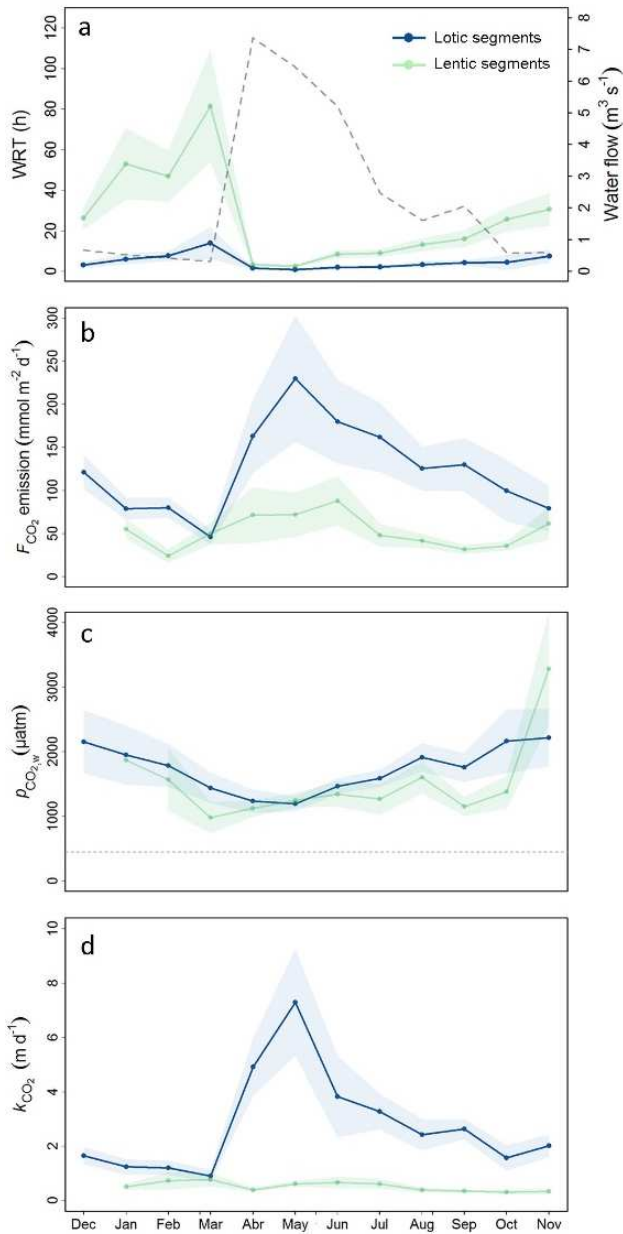


Figure 6.2 Temporal variation (from December 2012 to November 2013) of (a) water residence time (WRT), (b) CO_2 emissions ($F_{\text{CO}_2 \text{ emission}}$), (c) partial pressure of CO_2 in water ($p_{\text{CO}_2, \text{w}}$) and (d) specific gas transfer velocity for CO_2 (k_{CO_2}). Solid lines represent monthly averages for the lotic (blue, $n = 8$) and lentic (green, $n = 4$) segments. Shaded regions are monthly standard errors (SE) that represent spatial variations. The dashed grey line in panel (a) represents the water flow at the outlet of the catchment. The horizontal dashed line in panel (c) represents the average partial pressure of CO_2 in air ($p_{\text{CO}_2, \text{a}}$) for all the segments (418 μatm).

Most observations (142 out of 144) were supersaturated in dissolved CO₂ in relation to the atmosphere (Figure A.6.5 in the Supporting information section). The $p_{\text{CO}_2, \text{w}}$ ranged from 201 to 7213 μatm (mean = 1670, $n=144$). The $p_{\text{CO}_2, \text{w}}$ from lotic (range = 495 to 5274, mean = 1743, $n = 96$) and from lentic segments (range = 201 to 7313, mean = 1670, $n = 48$) did not differ significantly (ANOVA, $p = 0.216$; Figure 6.2c). The $p_{\text{CO}_2, \text{w}}$ from lotic segments showed a weak but statistically significant positive relationship with the WRT ($p_{\text{CO}_2, \text{w}} = 230.1 \ln(\text{WRT}) + 1446.5$; $r^2 = 0.26$, $p = 0.04$, $n = 12$), whereas such dependency was not observed for the lentic segments ($r^2 = 0.08$, $p = 0.39$, $n = 12$).

The k_{CO_2} ranged from 0.04 to 15.8 m d^{-1} (mean = 2.1, $n = 144$; Figure A.6.5 in the Supporting information section), and although variable, it was significantly higher (ANOVA, $p < 0.001$; Figure 6.2d) in lotic segments (range = 0.36 to 15.8 m d^{-1} , mean = 2.71, $n = 96$) than in lentic segments (range = 0.04 to 12.38 m d^{-1} , mean = 0.51, $n = 48$). Likewise, the k_{CO_2} from lotic segments clearly responded to the temporal hydrological fluctuations and gradually decreased with increasing WRT ($k_{\text{CO}_2} = -2.1 \ln(\text{WRT}) + 5.4$; $r^2 = 0.80$, $p < 0.001$, $n = 12$). In contrast, k_{CO_2} from lentic segments remained relatively stable along the WRT gradient ($r^2 = 0.03$, $p = 0.66$, $n = 12$).

Among the two main parameters directly driving $F_{\text{CO}_2 \text{ emission}}$ (i.e., $p_{\text{CO}_2, \text{w}}$ and k_{CO_2} ; Equation 1), the k_{CO_2} exhibited a significant positive relationship with the $F_{\text{CO}_2 \text{ emission}}$ ($F_{\text{CO}_2 \text{ emission}} = 31.1 k_{\text{CO}_2} + 46.2$; $r^2 = 0.61$, $p < 0.001$, $n = 144$; Figure A.6.5 in the Supporting information section), while no significant dependency between $p_{\text{CO}_2, \text{w}}$ and $F_{\text{CO}_2 \text{ emission}}$ was detected ($r^2 = 0.02$, $p = 0.080$, $n = 144$; Figure A.6.5 in the Supporting information section). The multiple regression analysis also revealed that k_{CO_2} and $p_{\text{CO}_2, \text{w}}$ explained respectively 86% and 0% of the total variation in $F_{\text{CO}_2 \text{ emission}}$. However, $p_{\text{CO}_2, \text{w}}$ explained a higher proportion of the variance of $F_{\text{CO}_2 \text{ emission}}$ (13.9%) when only lentic segments were included in the model.

6.3.3 Internal metabolism

While all segments where we estimated $F_{\text{CO}_2 \text{ metabolism}}$ ($n = 42$) were supersaturated in CO_2 , only 71% of them showed positive $F_{\text{CO}_2 \text{ metabolism}}$ values (i.e., internal metabolic production of CO_2 ; Figure 6.3 and Table A.6.2 in the Supporting information section). This discrepancy was more evident in lentic segments, of which only 40% showed positive $F_{\text{CO}_2 \text{ metabolism}}$, and even in most cases these were only slightly positive. $F_{\text{CO}_2 \text{ metabolism}}$ did not show any significant relationship with $F_{\text{CO}_2 \text{ emission}}$ or $p_{\text{CO}_2, \text{w}}$ (Figure 6.3), neither when pooling all the data nor when considering lotic and lentic segments separately.

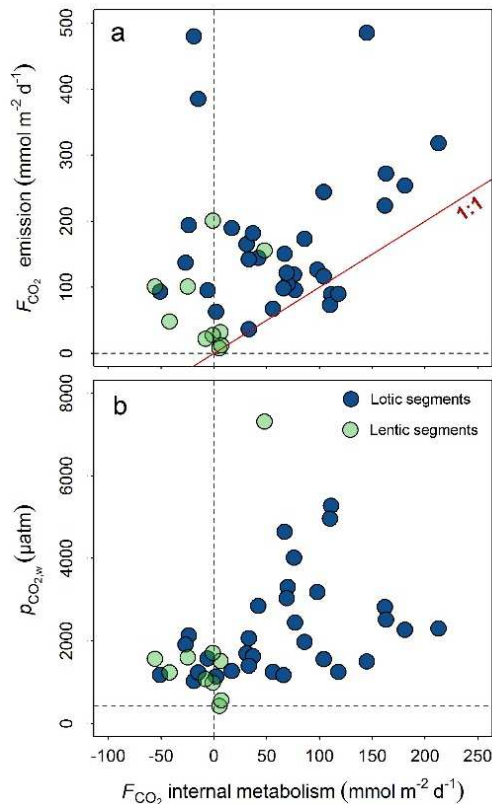


Figure 6.3 Relationship between the internal metabolic flux of CO_2 ($F_{\text{CO}_2 \text{ metabolism}}$) and (a) the CO_2 emissions ($F_{\text{CO}_2 \text{ metabolism}}$) and (b) the partial pressure of CO_2 in water ($p_{\text{CO}_2, \text{w}}$) for both lotic (dark blue circles; $n = 32$) and lentic segments (light green circles; $n = 10$). The vertical dashed lines represent $F_{\text{CO}_2 \text{ metabolism}} = 0$. The horizontal dashed line in panel (a) represents $F_{\text{CO}_2 \text{ metabolism}} = 0$. The horizontal dashed line in panel (b) represents the average partial pressure of CO_2 in air ($p_{\text{CO}_2, \text{a}}$) for all the segments (418 μatm). The 1:1 reference line is shown in panel (a).

$F_{\text{CO}_2 \text{ metabolism}}$ in both lotic segments ($r^2 = 0.62$, $p < 0.001$, $n = 30$) and lentic segments ($r^2 = 0.59$, $p = 0.008$, $n = 12$) showed a significant positive linear relationship with WRT (Figure 6.4). However, $F_{\text{CO}_2 \text{ metabolism}}$ increased more rapidly with increasing WRT in lotic (slope = 0.08 ± 0.01) than in lentic segments (slope = 0.02 ± 0.006).

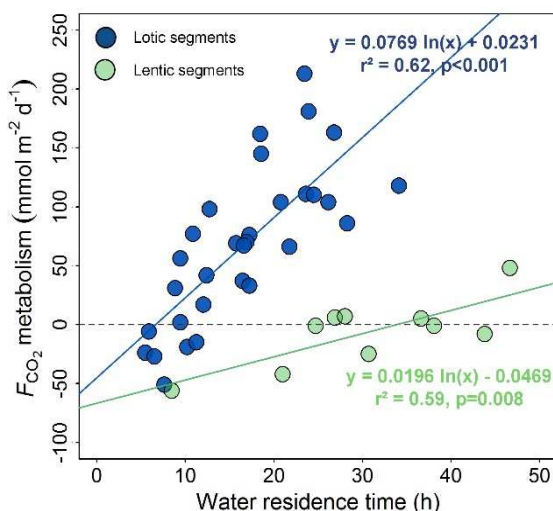


Figure 6.4 Internal metabolic flux of CO_2 ($F_{\text{CO}_2 \text{ metabolism}}$) as a function of water residence time for both lotic (dark blue circles) and lentic segments (light green circles). The horizontal dashed line represents $F_{\text{CO}_2 \text{ metabolism}} = 0$. The solid lines correspond to the regression model lines best fitting the data. Model equations are also shown close to model lines

6.3.4 Source apportionment of CO_2 emissions

The $F_{\text{CO}_2 \text{ inflow}}$ and the $F_{\text{CO}_2 \text{ others}}$ were the dominant sources of CO_2 that sustained the $F_{\text{CO}_2 \text{ emission}}$ in the fluvial network (50.2 and 31.9% on average, respectively; Figure 6.5). A similar influence of the $F_{\text{CO}_2 \text{ inflow}}$ and the $F_{\text{CO}_2 \text{ others}}$ on the $F_{\text{CO}_2 \text{ emission}}$ was detected in lotic segments (43.4 and 41.1%, respectively), whereas a stronger influence of upstream inputs on the $F_{\text{CO}_2 \text{ emission}}$ was detected in lentic segments (73.9%). We also detected differences in the contribution of $F_{\text{CO}_2 \text{ metabolism}}$ to the $F_{\text{CO}_2 \text{ emission}}$ between segment typologies. Whereas $F_{\text{CO}_2 \text{ metabolism}}$ contributed an average of 24% in lotic segments, the mean contribution of $F_{\text{CO}_2 \text{ metabolism}}$ to the $F_{\text{CO}_2 \text{ emission}}$ was negligible ($\sim 0\%$) in lentic segments (Figure 6.5).

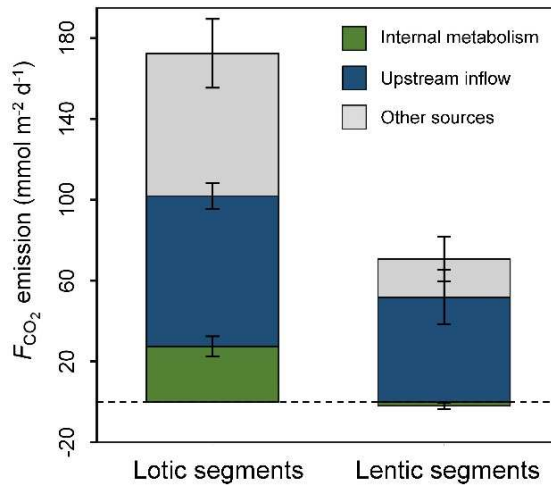


Figure 6.5 Source apportionment of CO_2 emissions ($F_{\text{CO}_2 \text{ emission}}$) for lotic (left) and lentic (right) segments. Columns represent averages and error bars standard errors for the different studied segments. The horizontal dashed line represents $F_{\text{CO}_2 \text{ emission}} = 0$.

The relative contribution of $F_{\text{CO}_2 \text{ metabolism}}$ to the $F_{\text{CO}_2 \text{ emission}}$ in lotic segments showed a positive relationship with WRT (contribution of $F_{\text{CO}_2 \text{ metabolism}} = 18.6 \ln(\text{WRT}) + 4.1$; $r^2 = 0.65$, $p < 0.001$, $n = 32$; Figure 6.6a), and contributed up to 40-70% of the emitted CO_2 in situations of high WRT. In contrast, no hydrological dependence of the contribution of $F_{\text{CO}_2 \text{ metabolism}}$ to the $F_{\text{CO}_2 \text{ emission}}$ was detected in the case of lentic segments. The contribution of $F_{\text{CO}_2 \text{ inflow}}$ to the $F_{\text{CO}_2 \text{ emission}}$ showed a negative relationship with the WRT (contribution of $F_{\text{CO}_2 \text{ inflow}} = 52.009 e^{-0.602 \ln(\text{WRT})}$; $r^2 = 0.44$, $p < 0.001$, $n = 32$; Figure 6.6b) in lotic segments, while no hydrological dependence of the contribution of $F_{\text{CO}_2 \text{ inflow}}$ to the $F_{\text{CO}_2 \text{ emission}}$ was detected in the case of lentic segments. Finally, the contribution of $F_{\text{CO}_2 \text{ others}}$ to the $F_{\text{CO}_2 \text{ emission}}$, which was highly variable along the fluvial network and during the studied period, was not related to the WRT, neither in lotic nor in lentic segments (Figure 6.6c).

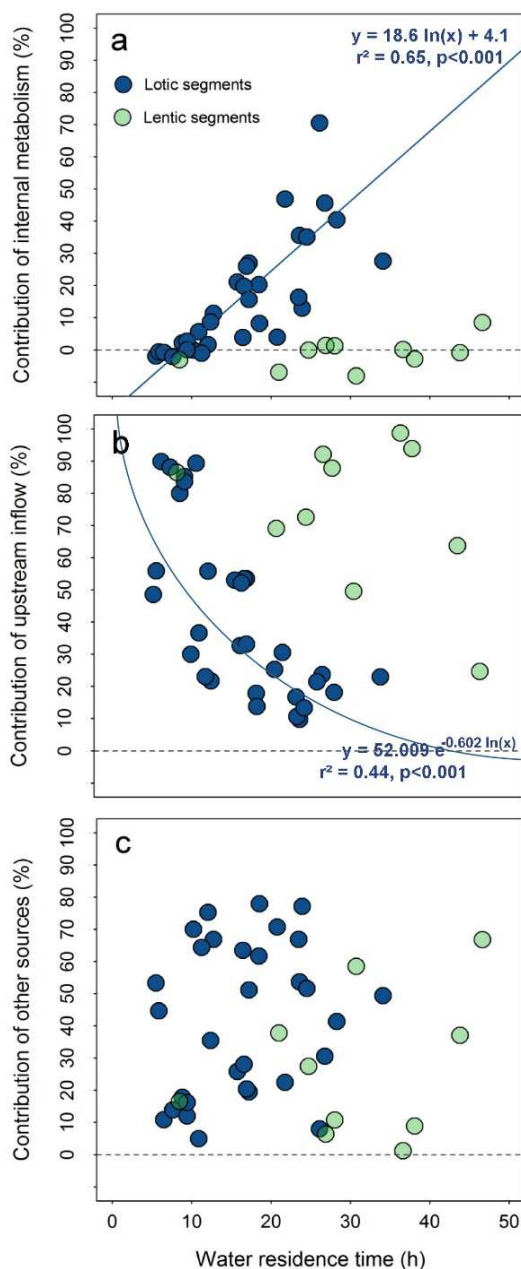


Figure 6.6 Relative contribution of (a) internal metabolism, (b) upstream inflow and (c) other non-measured sources to CO₂ emissions as a function of the water residence time for lotic (dark blue circles) and lentic segments (light green circles). The horizontal dashed lines represent reference lines for 0% contribution. The solid lines in panels (a) and (b) correspond to the regression lines best fitting the data (included when statistically significant). Model equations are also shown close to model lines.

6.4 Discussion

Here, we showed that the CO₂ emitted from the interconnected lotic and lentic waterbodies found along a Mediterranean fluvial network mostly derives from sources other than internal metabolism. Such sources may include surface and subsurface hydrological inputs of CO₂ derived from soil respiration and mineral weathering within the catchment, internal geochemical reactions of calcite precipitation and internal photochemical mineralization of organic solutes (see below). Furthermore, both the magnitude of CO₂ emissions and the relative contribution of the different sources strongly depended on the hydrological dynamics of the fluvial network, being particularly dependent on them in the lotic segments.

Our results highlight the importance of CO₂ emissions from running waters compared to slow-moving waterbodies associated to weirs and small impoundments. In general, low-order streams deserve special attention since they cover a large surface area [Butman and Raymond, 2011; Downing et al., 2012; Raymond et al., 2013]. Several studies have shown that stream emissions dominate total aquatic CO₂ emissions [Kokic et al., 2015] at regional [Lundin et al., 2013; Wallin et al., 2013] and global scales [Raymond et al., 2013]. Our study adds to current knowledge by accounting for the pronounced spatial and temporal variability in streams and impounded waterbodies within fluvial networks. Specifically, we show that CO₂ emissions from headwater streams dominate aquatic CO₂ loss, especially during periods of high flows, when most of the stream network is hydrologically connected [Benstead and Leigh, 2012; Downing, 2012; Bernal et al., 2013].

Our results also agree with previous findings on the importance of k_{CO_2} as the major driver of the spatial and temporal variability in fluvial network CO₂ emissions [Wallin et al., 2011; Gómez-Gener et al., 2015; Kokic et al., 2015; Long et al., 2015]. However, the complexity of the hydrological regime of Mediterranean fluvial networks leads to particular situations (in space and time) where the $p_{\text{CO}_2,w}$ can exert a significant control on CO₂ emissions. These situations mainly occurred in lentic segments during low flows, when dams and weirs create discontinuities that decreased k_{CO_2} and led to higher supersaturation of CO₂. Extended periods of low flows as a consequence of intensive use of the water resources or drought [Gasith and Resh, 1999; Gibson et al., 2005] may lead to a higher increase of lentic

habitats at the expenses of lotic environments in many fluvial networks [Sabater, 2008]. Consequently, the dominance of $p_{\text{CO}_2,w}$ on controlling the CO_2 emissions under situations of physical limitation induced by low flows [Demars and Manson, 2013; Gómez-Gener et al., 2015] will probably be more common in the future.

Internal biomineralization of aquatic and terrestrial OM (here referred to as internal metabolism), has commonly been considered to be the main factor driving CO_2 supersaturation in lakes and rivers [Cole et al., 2000; Duarte and Prairie, 2005]. Therefore, if no other processes are adding or removing CO_2 besides internal metabolism, the CO_2 present in the system and emitted to the atmosphere should be in line with the degree of net heterotrophy in the corresponding aquatic ecosystems. Our results showed a strong disagreement with this perspective, since the CO_2 produced by internal metabolism and both the CO_2 present in the segment and the CO_2 emitted to the atmosphere did not match (Figure 6.3). In fact, some of the supersaturated segments were actually net autotrophic, showing negative $F_{\text{CO}_2 \text{ metabolism}}$ values (overall, 60% of supersaturated lentic and 20% of lotic segments were found to have $F_{\text{CO}_2 \text{ metabolism}} < 0$; Figure 6.3b). In those situations, internal metabolism was acting as a net sink for IC, but the magnitude of this sink was not sufficient to maintain dissolved CO_2 concentrations below atmospheric levels. These results support previous findings that already indicated that sources other than internal metabolism can sustain CO_2 supersaturation in freshwaters [Stets et al., 2009; McDonald et al., 2013; Borges et al., 2015; Hotchkiss et al., 2015; Marcé et al., 2015].

Our mass balance of CO_2 (Table 6.1) highlights a crucial role of hydrological inputs and other sources on sustaining the CO_2 emissions along the fluvial network. Several studies in lentic systems point towards the same direction. For example, Stets et al. [2009] showed that the sum of surface and subsurface hydrological inputs of DIC accounted for 41% to 100% of the observed CO_2 release from two lakes situated in north-central Minnesota, USA. Likewise, McDonald et al. [2013] and Weyhenmeyer et al. [2015] showed that the surface and subsurface hydrological inputs of DIC accounted for a significant fraction of the total CO_2 emitted from a large number of lakes and reservoirs in the contiguous United States and Scandinavia, respectively. Similarly, Marcé et al. [2015] showed that in up to 57% of the lakes and reservoirs worldwide, CO_2 supersaturation could be related to

alkalinity inputs from the catchment, suggesting mineral weathering as a fundamental regulator of the DIC coming from terrestrial ecosystems. Also, *Wilkinson et al.* [2016] using high-frequency time series of O₂ and CO₂ confirmed the large influence of hydrological inputs on the CO₂ emissions, even in lakes where internal CO₂ uptake had been experimentally increased with nutrients. In the same direction, a recent study in lotic systems [*Hotchkiss et al.* 2015] showed that CO₂ produced by aquatic metabolism contributes on average to only 28% of CO₂ evasion from streams and rivers with flows ranging between 0.0001 and 19,000 m³ s⁻¹ in the contiguous United States. Our study adds to current knowledge by integrating the CO₂ fluxes determining CO₂ variation within lotic and lentic waterbodies that are interconnected in complex fluvial networks.

Table 6.1 Summary of the CO₂ fluxes determining CO₂ variations within the studied lotic (n = 32) and lentic segments (n = 10)

F_{CO_2} (mmol m ⁻² d ⁻¹) ^a	Lotic segments				Lentic segments				ANOVA test ^b
	Mean	Min	Max	n	Mean	Min	Max	n	p value
Emission	-172	-490	-40	32	-71	-203	-8	10	<0.001
Inflow	229	20	1230	32	273	37	630	10	0.65
Outflow	-279	-1280	-60	32	-290	-650	-40	10	0.91
Internal metabolism	68	-51	213	32	-7	-52	46	10	0.015
Other sources	188	30	1070	32	64	-160	250	10	0.07

^a Positive CO₂ fluxes indicate a gain of CO₂ within the segment (i.e. invasion from the atmosphere, upstream import, internal metabolic production or production from other sources). Negative CO₂ fluxes indicate a loss of CO₂ within the segment (i.e. emission to the atmosphere, downstream export, internal metabolic consumption or consumption by other sources)

^b Values in bold font indicate statistically significant differences (p<0.05) between lotic and lentic segments.

Despite the dominance of hydrological inputs and other sources to the net CO₂ emission, the contribution of internal metabolism was not negligible in lotic segments (Table 6.1; Figure 6.7), where we detected a predominance of net heterotrophy for most of the year. In contrast, lentic segments had much lower and balanced fluxes that varied between net autotrophy and heterotrophy, thus leading to a generally much smaller contribution of internal metabolism to the lentic CO₂ emissions (Table 6.1; Figure 6.7).

The relationships of the contribution of upstream inflow and internal metabolism to the CO₂ emissions with WRT in lotic segments reveals a clear coupling between the hydrological dynamics and the origin of CO₂ emissions (Figure 6.6a and 6b). During high flow periods, both the hydrological connectivity within the fluvial network and between the fluvial network and the catchment is maximized [Bernal *et al.*, 2013]. This favors longitudinal and lateral pathways of CO₂ supply along the fluvial network [Wallin *et al.*, 2010; Campeau and del Giorgio, 2013; Kokic *et al.*, 2015] and an efficient exchange between the adjacent terrestrial ecosystems and the stream channels [Stets *et al.*, 2009; Davidson *et al.*, 2010; McDonald *et al.*, 2013; Hotchkiss *et al.*, 2015]. At the same time, reduced WRT during high flows limits the capacity of the biota to interact with organic substrates [Battin *et al.*, 2009b], thereby constraining the internal metabolic pathway of CO₂ supply [Hotchkiss *et al.*, 2015]. Therefore, situations of high flows and short WRT lead to a higher contribution of externally derived CO₂ and a lower contribution of internal metabolically derived CO₂ to the finally emitted CO₂ (Figure 6.6). In contrast, during periods of low flows and long WRT, the reduced hydrological connectivity hampers the supply of CO₂ from upstream to downstream waters as well as from adjacent terrestrial ecosystems to the fluvial network. Additionally, OM processing is favored through increased interaction with biological actors [Battin *et al.*, 2009b]. Altogether, this leads to a higher contribution of internal metabolic CO₂ and a lower contribution of externally derived CO₂ to the finally emitted CO₂ during low flows and long WRT.

Interestingly, the above hydro-biogeochemical model does not apply to lentic waterbodies. Our results indicate that the contribution of the upstream inflow and internal metabolism to the CO₂ efflux from lentic waters was independent of hydrological variation (Figures 6.6a and 6.6b). The contribution of the upstream inflow was very variable and did not follow any trend along the WRT axis, while the contribution of the internal metabolism remained fairly constant and close to the 0% line. A balanced metabolism (i.e., NEP ~ 0) is expected in aquatic systems over longer durations and for larger spatial scales, if burial is minimal [Staeher *et al.*, 2012; Hotchkiss *et al.*, 2015]. Theoretically, this balance arises because, given sufficient time, any increase in primary production yields OM, which in a relatively closed system, will be proportionally respired. Alternatively, any increases in respiration will release inorganic nutrients that proportionally stimulate primary production [Staeher *et al.*,

2012]. The higher WRT in lentic segments combined with their higher resistance to hydrological perturbations will therefore favor a balanced metabolism that leads to a low contribution of internal metabolism to CO₂ emissions.

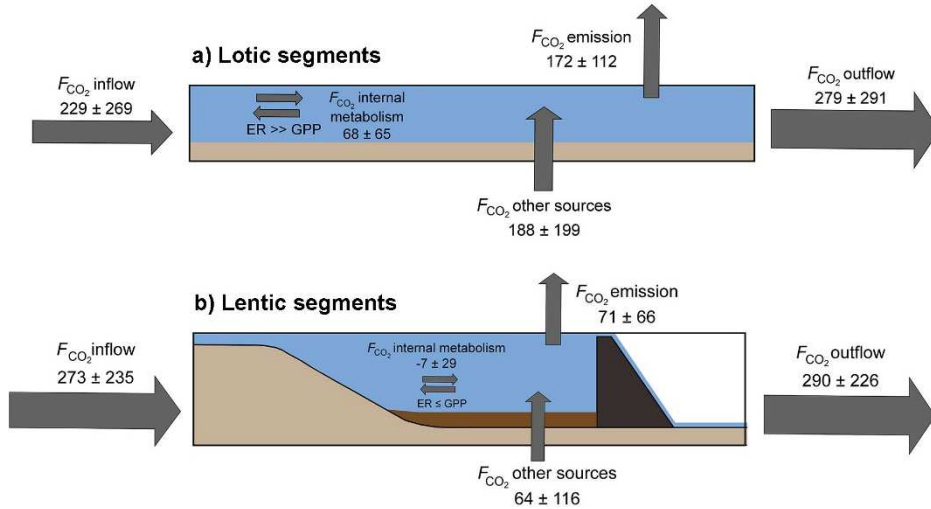


Figure 6.7 Summary of the CO₂ fluxes (mmol m⁻² d⁻¹) determining CO₂ variations within the studied (a) lotic and (b) lentic segments. Values are averages ± standard deviations from all studied segments. Note that the direction of the arrows indicate direction of the CO₂ within the segment (i.e., a gain when pointing to the segment and a loss when pointing out of the segment) and that the arrow size matches with the magnitude of the flux.

The variance around the contribution of other non-measured sources to the CO₂ emissions with WRT in both lotic and lentic waterbodies (Figure 6.6c) reveals a rather hydrological independence of this third component. The flux of CO₂ coming from these other non-estimated sources includes a set of diverse processes, apart from internal metabolism and upstream inputs, that can add or remove CO₂ to the studied segments (i.e., groundwater fluxes, lateral surface water fluxes and internal fluxes derived from geochemical reactions of calcite precipitation and photochemical mineralization of organic solutes). Therefore, being not surprising that such diverse set of CO₂ sources and sinks in origin and magnitude) may respond differently to hydrological variations.

Groundwater inputs, typically composed by high CO₂ and low O₂, can alter the chemistry of surface waters, especially of those small lotic [Öquist *et al.*, 2009; Hotchkiss *et al.*, 2015]

and lentic [Hanson *et al.*, 2006; López *et al.*, 2011] waterbodies situated along the fluvial network. Similarly, surface water lateral inputs (i.e., small low-order streams that flow into the segments) draining adjacent terrestrial ecosystems (i.e., riparian and upland) may also affect the CO₂ dynamics in the receiving waterbodies.

Precipitation and dissolution of carbonate minerals may, respectively, produce or consume CO₂ in fluvial networks. Considering the high alkalinity of our fluvial network (mean = 4.1 meq L⁻¹, n = 144), we suggest that calcite precipitation may be a relevant process contributing to the CO₂ supersaturation and emission [Otsuki and Wetzel, 1974; Stets *et al.*, 2009; Nõges *et al.*, 2016]. However, further investigation is needed in order to understand how and to what extent carbonate precipitation and dissolution reactions may potentially affect the CO₂ dynamics and further regulate the CO₂ emissions from fluvial network.

The photo-chemical mineralization of dissolved organic matter (DOM) can contribute to a great extent of the C processing [Cory *et al.*, 2014] and CO₂ emissions from inland waters [Koehler *et al.*, 2014]. This reaction also influence the O₂ dynamics of our fluvial network [Amon and Benner, 1996], and thus may contribute to the metabolism estimates calculated using diel changes in dissolved oxygen (O₂).

5.5 Conclusions and implications

The results of the present study show that sources other than internal metabolism (e.g., external inputs, internal geochemical reactions or photochemical mineralization) sustained most of the fluvial network CO₂ emissions. Internal metabolism accounted for a moderate proportion (24%) of CO₂ emissions in lotic segments, while it was insignificant in lentic ones. In addition, we also show that the magnitude and sources of CO₂ emissions depended on the WRT in lotic segments, while they remained relatively stable in lentic ones, suggesting a clear coupling between the hydrological dynamics and the origin of CO₂ emissions in lotic segments.

This work represents a novel attempt to integrate a mass balance of CO₂ fluxes into the complex temporal and spatial dynamism of an anthropogenically altered fluvial network.

Using a steady-state approach we were able to integrate most sources affecting CO₂ fluxes along the fluvial network. Still, uncertainty existed related to the substantial contribution of CO₂ from other non-measured sources. Solving this uncertainty would require further efforts to describe the drivers of the other sources (apart from internal metabolism and external surface hydrological) under non-steady state conditions, which would enable a better understanding of the conditions regulating the seasonal dynamics of CO₂ emissions at the fluvial network scale. Because of the high human demand for energy and water, few fluvial networks worldwide remain free from impoundment over the entire course, which typically results in an alternating series of lentic and lotic segments [*Ward and Stanford, 1983; Nilsson et al., 2005b; Döll et al., 2009*]. Therefore, we suggest that our findings should not be restricted to Mediterranean fluvial networks, but are also useful for predicting the integrated responses of fluvial networks that share similar spatial configurations.



Chapter 7

General discussion

The river discontinuum

A continuum is defined as “an extent, succession, or whole, no part of which can be distinguished from neighbouring parts except by arbitrary division” [*Dictionary of the Institute for Catalan Studies*; 2016]. The view of a river as a continuum from headwaters to mouth is exemplified by the River Continuum Concept [Vannote *et al.*, 1980], which assumes that the structure or function of a stream segment will always be most similar to that of neighbouring segments. Although this may be a useful and reasonable representation of a stream in general, no specific river is strictly a continuum. In fact, at any spatial scale, rivers are regularly divided into discrete parts based on non-arbitrary distinctions [Frissell *et al.*, 1986; Poole, 2002].

At the network scale, the presence or absence of flow paths between persistent fluvial patches modulates the transport of matter, energy, and organisms at different temporal and spatial scales [Fisher *et al.*, 2004; Freeman *et al.*, 2007; Larned *et al.*, 2010]. Thus, the view of a river as a discontinuum assumes that the flow paths between persistent fluvial patches might be laterally, vertically or longitudinally constrained over time [Stanley *et al.*, 1997; Stanford and Ward, 2001; Ward and Tockner, 2001; Fisher *et al.*, 2004; Larned *et al.*, 2010]. However, the discontinuum view does not reject the continuum but rather subsumes it. For instance, in some cases, the patchy arrangement of segments will happen to contain gradual downstream transitions between elements and will approximate the river continuum conditions.

During the last decades, some conceptual (e.g., [Ward and Stanford, 1983; Stanley *et al.*, 1997; Stanford and Ward, 2001; Fisher *et al.*, 2004; Battin *et al.*, 2009a; Larned *et al.*, 2010]) and empirical studies (e.g., [Dent and Grimm, 1999; McGuire *et al.*, 2014; Proia *et al.*, 2016]) have attempted to describe the biogeochemical patterns occurring in fluvial networks from the discontinuum point of view. Among them, particular attention has been paid to the understanding of the effects of artificial flow impoundment on biogeochemical patterns in fluvial networks. The “serial discontinuity concept”, originally formulated by Ward and Stanford [1983] and revised by Stanford and Ward [2001], views dams as longitudinal discontinuities within the river continuum. In this concept, biophysical responses are predicted in terms of ‘discontinuity distance’; thus, the higher the discontinuity distance

induced by the impoundment, the higher the upstream or downstream shift of a biogeochemical variable (e.g., Photosynthesis/Respiration) and the departure from the natural or reference condition. Similarly, some models have specifically focused on describing the influence of flow intermittency on biogeochemical patterns in fluvial networks. For instance, *Larned et al.*, [2010] proposed the “punctuated longitudinal reactor concept”, where flow discontinuities in temporary rivers lead to recurrent fluvial network heterogeneities in organic matter (OM) processing. Within this concept, the efficiency of OM processing is predicted to increase with the number of cycles of transport, deposition and processing that occur down the length of a temporary river.

A large number of empirical studies that focus on carbon (C) dynamics along fluvial networks [*Wallin et al.*, 2010; *Striegl et al.*, 2012; *Crawford et al.*, 2013; *Peter et al.*, 2014] cover a wide range of the temporal and spatial variability in C gas fluxes. However, most of these studies do not account for the effect of local discontinuities such as the presence of impoundments or the effect of flow intermittency. Consequently, they may be missing a portion of the complex spatial patterns in biogeochemical processes that is inherent to fluvial networks.

In this dissertation, we have intensively studied a Mediterranean fluvial network from December 2012 to March 2015 to examine how the discontinuities caused by river impoundment and flow intermittency affect the spatio-temporal patterns, controls and sources of C gas fluxes.

This general discussion focuses on the main outcomes of the present dissertation: (i) the effects of small retention structures on shaping the C gas fluxes along a Mediterranean fluvial network, (ii) the importance of dry riverbeds as hot spots for carbon dioxide (CO₂) emission, (iii) the role of physics as a valve modulating C gas exchange between fluvial networks and the atmosphere and (iv) the present and the future implications of integrating the effects of flow discontinuities on C emissions from fluvial networks.

7.1 The influence of small water retention structures on shaping carbon gas fluxes along a Mediterranean fluvial network

The construction and operation of over one million dams globally [Lehner *et al.*, 2011] has provided a variety of beneficial services to the growing human population (e.g., hydropower, flood control, navigation, and water supply), but has also significantly altered the natural longitudinal connectivity along fluvial networks [Ward and Stanford, 1983; Stanford and Ward, 2001]. Dams disrupt the fluvial continuum by changing hydrological dynamics (e.g., reduction of flood frequency, elimination of turbulent reaches, increased water residence time (WRT)), water physicochemistry [Ward and Stanford, 1983] and transport of suspended materials [Syvitski *et al.*, 2005; Maeck *et al.*, 2013bu]. These changes ultimately lead to severe impacts on the structure and functioning of ecological communities [Ward and Stanford, 1983; Stanford and Ward, 2001; Haxton and Findlay, 2008] and biogeochemical cycles at different levels of organization [Ward and Stanford, 1983; Stanford and Ward, 2001; Friedl and Wüest, 2002; Aristi *et al.*, 2014; von Schiller *et al.*, 2016; Proia *et al.*, 2016].

Although reservoirs are often seen as “green” or C-neutral sources of energy, a growing body of work has documented their role as greenhouse gas (GHG) sources [St. Louis *et al.*, 2000a; Barros *et al.*, 2011c; Deemer *et al.*, 2016]. However, most of the estimates of C emissions from reservoirs have been mainly obtained in very large ($> 10^4 \text{ km}^2$), large ($10^4 - 10^2 \text{ km}^2$), medium ($100 - 1 \text{ km}^2$) and small ($1 - 0.1 \text{ km}^2$) size reservoirs [Deemer *et al.*, 2016]. Small and very small water retention structures (SWRS; $< 0.1 \text{ km}^2$) have so far remained unexamined, although they represent the most common water retention structure causing river fragmentation worldwide [Downing *et al.*, 2006; Lehner *et al.*, 2011; Verpoorter *et al.*, 2014].

7.1.1 The effect of SWRS on the magnitude and variability of C gas fluxes along the fluvial network

The results in *Chapters 3, 5 and 6* of this dissertation show an overall significant reduction of the CO₂ efflux in those fluvial sections that are impounded with SWRS compared to

those that are free-flowing. These results are in line with other studies comparing larger stagnant waterbodies (e.g., lakes or reservoirs) with riverine waterbodies in fluvial networks [Lundin *et al.*, 2013; Kokic *et al.*, 2015]. Similarly, comparisons between lotic and lentic waterbodies at regional [Wallin *et al.*, 2013; Crawford *et al.*, 2014b] and global [Raymond *et al.*, 2013a; Lauerwald *et al.*, 2015] scales also point in the same direction. Together, these results support the idea that the presence of SWRS, despite their relatively small water capacity compared to larger systems, can still have a profound effect on attenuating the turbulence induced by water currents that typically drive the CO₂ efflux in the free-flowing river sections (*see section 7.3 below*).

Contrary to the effect observed for the CO₂ efflux, no reduction in methane (CH₄) efflux associated to the presence of SWRS was detected (*Chapters 3 and 5*). Our findings indicate that the significant increase in CH₄ production in impounded river sections compared to free-flowing river sections may compensate the physical effect on CH₄ emissions. Impounded river sections associated to SWRS always showed higher concentrations of CH₄ than free-flowing river sections; however, such impounded river sections did not show higher diffusive CH₄ emissions than their adjacent free-flowing river sections (*Chapters 5*). These results are consistent with observed trends across large and medium size systems [St. Louis *et al.*, 2000a; Deemer *et al.*, 2016]. Nonetheless, if we account for the ebullitive pathway of CH₄ emission, which in the Fluvia River contributed to more than 85 % of the total CH₄ efflux from impounded waters when the evasion of CH₄ was detected (CH₄ ebullition was only measured in *Chapter 3*), the total CH₄ emission flux from impounded river sections appears to be, on average, 70-fold higher than from their adjacent free-flowing river sections. Our results of ebullitive emission fluxes from impounded waterbodies are consistent with previous studies describing ebullition as the primary pathway for CH₄ efflux from large and medium reservoirs [Deemer *et al.*, 2016], small reservoirs [Maeck *et al.*, 2013] and natural lakes [Bastviken *et al.*, 2004]. Although CH₄ ebullition is highly variable in space and time [Beaulieu *et al.*, 2016; Wik *et al.*, 2016], the results shown in *Chapter 3* strongly emphasize that CH₄ ebullition makes a difference, claiming the need to include this pathway when assessing CH₄ emissions across the whole range of reservoir sizes [Deemer *et al.*, 2016].

Furthermore, in *Chapter 5* we also showed that the presence of SWRS, despite causing a significant enrichment of CH₄ in the impounded surface water, did not produce any effect on the CH₄ efflux at the downstream free-flowing river sections. Our result contrasts with those from the few other studies reporting C emissions downstream from reservoirs [Abril, 2005; Guérin *et al.*, 2006; Kemenes *et al.*, 2007]. These studies, which have mainly been conducted in large tropical systems, indicate that downstream C emissions can contribute significantly to C emissions associated to the reservoir: 7 to 25 % in the case of CO₂ [Abril, 2005; Guérin *et al.*, 2006] and 50 to 90% in the case of CH₄ [Abril, 2005; Guérin *et al.*, 2006; Kemenes *et al.*, 2007]. Our study contributes to current knowledge by accounting for the still poorly known downstream effects of SWRS in terms of C diffusive fluxes.

7.12 The effect of SWRS on the sources of C gas fluxes along the fluvial network

Over the last decades, a growing body of literature has recognized internal metabolism as the main factor driving CO₂ supersaturation in lakes and rivers [Cole *et al.*, 2000; Duarte and Prairie, 2005]. However, the mass balance of CO₂ shown in *Chapter 6* highlights the dominant role of sources other than internal metabolism (e.g., external inputs, internal geochemical reactions or photochemical mineralization) on sustaining CO₂ emissions from the Fluvià River network CO₂ emissions. Other recent studies based on temporally- and spatially-independent spot measurements made in lentic [Stets *et al.*, 2009; McDonald *et al.*, 2013; Marcé *et al.*, 2015; Wilkinson *et al.*, 2016b] and lotic [Hotchkiss *et al.*, 2015; Winterdahl *et al.*, 2016] systems point in the same direction. Hence, our study adds to current knowledge by integrating the CO₂ fluxes determining CO₂ variation within lotic and lentic waterbodies that are interconnected in complex fluvial networks.

In general terms, the common dominance of hydrological inputs and other sources among impounded and free-flowing river sections found in *Chapter 6* suggests a rather irrelevant effect of SWRS on the origin of the CO₂ emitted along the studied fluvial network. However, the presence of SWRS favoured a decoupling between the fluvial network hydrological dynamics and the local hydrological dynamics occurring in impounded waters (by attenuating the water currents in the impounded river sections). Thus the contribution of the different sources to the CO₂ efflux in impounded river sections remained stable and

independent of hydrological variation. In contrast, the presence of SWRS did not alter the hydrological conditions of the free-flowing river sections, which showed a clear coupling between the hydrological dynamics and the origin of CO₂ emissions. Specifically, during high flow conditions there is an efficient exchange of C along the fluvial network and between the fluvial network and the adjacent terrestrial ecosystems [Öquist *et al.*, 2009a; Stets *et al.*, 2009; Davidson *et al.*, 2010; Hotchkiss *et al.*, 2015c]. Also, reduced WRT during high flows limits the capacity of the biota to interact with organic substrates [Battin *et al.*, 2009b], thereby constraining the internal metabolic pathway of CO₂ supply [Hotchkiss *et al.*, 2015]. Therefore, situations of high flow and short WRT lead, in general, to a higher contribution of externally derived CO₂ and a lower contribution of internal metabolically derived CO₂ to the finally emitted CO₂. In contrast, during periods of low flow and long WRT, the reduced hydrological connectivity hampers the supply of CO₂ from upstream waters as well as from adjacent terrestrial ecosystems to the fluvial network. Additionally, OM processing is favoured through increased interaction with biological actors [Battin *et al.*, 2009b]. Altogether, this leads to a higher contribution of internal metabolic CO₂ and a lower contribution of externally derived CO₂ to the finally emitted CO₂ during low flow and long WRT periods.

Local conditions such as long WRT, high deposition rates of OM, high productivity or high temperature are required for CH₄ production [Zaiss *et al.* 1982, Dahm *et al.* 1991, Trimmer *et al.* 2012]. Results obtained in *Chapters 3 and 5*, which showed an enrichment of CH₄ in impounded waters, agree with findings found in other fluvial networks containing SWRS [Maeck *et al.*, 2013], and suggest that the presence of SWRS may favour proper conditions for CH₄ production and further emissions in the fluvial network. However, contrary to our expectations based on the established idea that CH₄ should be scarce in riverine sections because methanogenesis typically occurs at a low rate or not at all in these environments [Stanley *et al.*, 2016], in our fluvial network we found a persistent supersaturation of CH₄ in the free-flowing river sections (*Chapters 3 and 5*). We propose that the CH₄ present and emitted from the free-flowing river sections is probably imported from their adjacent impounded river sections. In fact, many studies indicate that hydrological linkage to suitable habitats can deliver CH₄ to the free-flowing river sections. Some examples include shallow groundwater flows that travel from CH₄ saturated soils or peat deposits to the river

[Jones and Mulholland, 1998; Hope et al., 2001; Crawford et al., 2014a] as well as connections to inundated river floodplains [Richey, 1988; Pullman, 1992; Teodoru et al., 2015] or adjacent wetlands [Crawford et al., 2015; Bresney et al. 2015]. Moreover, recent research has shown that the CH₄ emitted from free-flowing river sections can also be produced within the same channel [Crawford and Stanley, 2016], therefore adding a new pathway in the dynamic balance of CH₄ in fluvial networks.

7.1.3 Longitudinal patterns of C gas fluxes along the river discontinuum

Due to the high density of SWRS in the studied fluvial network, the local effect of SWRS on the impounded vs. free-flowing C gas dynamics, is transferred at the larger scale by modulating the longitudinal patterns of C effluxes, concentrations and their sources. Based on the results from *Chapters 3, 5 and 6* of this dissertation, we propose a conceptual model illustrating the longitudinal patterns in CO₂ and CH₄ fluxes in a hypothetic highly impounded segment of a Mediterranean fluvial network (Figure 7.1).

On the one hand, the conceptual model shows that the view of the fluvial network as a continuum [Vannote et al., 1980], where conditions are regulated primarily by external processes and thus, exhibit gradual routing control of downstream gradients [Montgomery, 1999], might be valid to approximate the patterns of CO₂ concentrations along highly impounded rivers with SWRS. The concentration of CO₂ showed a rather smooth pattern along the altering series of lotic and lentic waterbodies (Figure 7.1a). We suggest that this pattern is generated because the CO₂ consumed (e.g., metabolically or geochemically) or lost to the atmosphere (e.g., via diffusive emission) within the river is constantly replenished, mostly by CO₂ imported from the catchment via lateral, vertical or longitudinal pathways, with no clear differentiation between impounded and riverine sections (note that this is a general model but other processes such as internal production may also deliver CO₂ to the water column; *Chapter 6*). This phenomenon has been observed in larger stagnant waterbodies such as lakes and reservoirs [Stets et al., 2009; McDonald et al., 2013; Marcé et al., 2015], but also in other heavily impounded systems [Crawford et al., 2016]. Therefore, the results from this dissertation reinforce the crucial role of external

sources on modulating the longitudinal CO₂ patterns in fluvial networks, even when manmade small longitudinal discontinuities are included (*Chapter 6*).

On the other hand, the view of fluvial networks as a continuum is insufficient to describe the true spatial complexity of CH₄ concentrations (Figure 7.1b), where conditions are likely regulated by patches of intense CH₄ production (i.e., localized controls) such as the presence of SWRS that lead to ideal environments for active methanogenesis. Moreover, the view of the fluvial network as a continuum is also insufficient to characterize the longitudinal dynamics of CO₂ (Figure 7.1c) and CH₄ diffusive emissions (Figure 7.1d), which are controlled by the interplay between the attenuated hydrological conditions in impounded waterbodies and the turbulent conditions induced by the water currents typically driving the CO₂ and CH₄ efflux in the free-flowing riverine sections (see section 7.3, below). In the same line, a continuous view is not precise enough to describe ebullitive CH₄ emissions, which similarly to the CH₄ concentrations, are controlled by the presence of SWRS that lead to ideal redox conditions for CH₄ bubble formation in the sediments (Figure 7.1d).

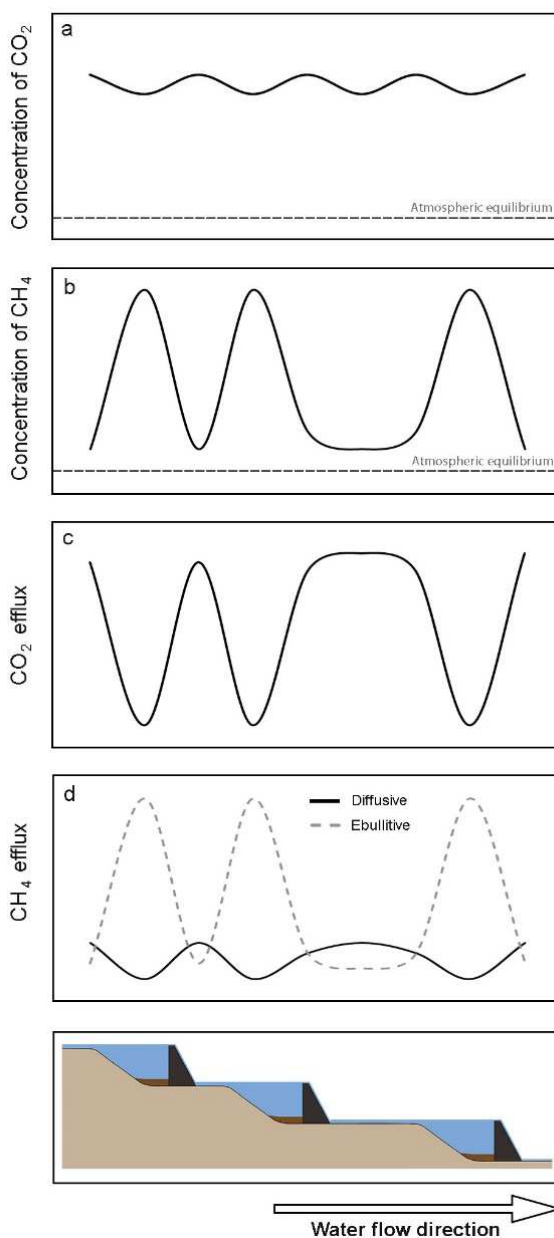


Figure 7.1 Conceptualization of the general longitudinal patterns in (a) concentration of dissolved CO_2 in water, (b) concentration of dissolved CH_4 in water, (c) CO_2 efflux and (d) CH_4 efflux (diffusive pathway represented as a continuous line and ebullitive pathway as dashed line) along a fluvial network integrating SWRS. Note that this is a general conceptual model which does not include temporal or spatial peculiarities. Distances between dams are not equal in order to simulate field conditions. The horizontal dashed line in panels (a) and (b) represents the atmospheric equilibrium concentration of CO_2 and CH_4 , respectively.

7.2 Dry riverbeds as hot spots for carbon dioxide emissions

In summer, fluvial networks in Mediterranean and other arid and semiarid regions are usually transformed into highly discontinuous riverscapes characterized by slow-moving waters, isolated river pools and large areas of dry riverbeds [Stanley *et al.*, 1997; von Schiller *et al.*, 2011; Bernal *et al.*, 2013]. River fragmentation as a consequence of flow intermittency has been recognized as one of the most important environmental pressures constraining the water-mediated transport of matter, energy, and organisms within or between elements along fluvial networks [Freeman *et al.*, 2007; Larned *et al.*, 2010; Acuña *et al.*, 2014; Datry *et al.*, 2014c]. At the fluvial network scale, dry riverbeds are not restricted to headwaters, but they can also be found in the mid-reaches and lowlands of fluvial networks [Steward *et al.*, 2012]. Hence, these environments can cover a substantial part of the fluvial network when drought conditions or water abstractions are severe [Datry *et al.*, 2014c]. Moreover, dry beds are not limited to the lotic sections of the fluvial network. Instead, they can also be found in the boundaries or belts of lentic waterbodies upstream from water retention structures which also dry up to some extent during certain moments of the year.

Dry riverbeds are highly dynamic habitats representing spatial (i.e., transitional zones between flowing streams and terrestrial habitats) and temporal (i.e., transitional periods between permanent and intermittent states) ecotones [Naiman and Decamps, 1997]. Thus, against the traditional view of being “biogeochemically inactive”, dry riverbeds are likely to be potential active sites for material transformations [McClain *et al.*, 2003]. However, our understanding of the biogeochemical processes that occur in the areas of temporary watercourses that recurrently run dry has been lagged well behind that of perennial watercourses [Leigh *et al.*, 2016].

7.2.1 Magnitude and variability of C gas fluxes from dry riverbeds

The measurements of dry riverbed CO₂ efflux and basal microbial respiration rates reported in *Chapters 3 and 4* of this dissertation confirm the active biogeochemical activity of this environment. The average CO₂ efflux from the Fluvia dry riverbeds was slightly

above that obtained in dry desert streams in Arizona, USA (Gallo *et al.*, [2013]; Figure 7.2a), to our knowledge, the only study reporting CO₂ emissions from dry riverbeds in other catchments. As indicated in some previous studies on biofilm functioning [Zoppini and Marxsen, 2011; Timoner *et al.*, 2012, 2014b], the energy flow, nutrient cycling and subsequent CO₂ production and efflux can remain active despite the lack of surface water.. A significant effect of drying on CO₂ loss has also been observed in dry reservoir belts (Figure 7.2b; [unpublished data]) and other aquatic ecosystems including wetlands (Moore and Knowles [1989]; Freeman *et al.* [1993]; Fenner and Freeman [2011]; Figure 7.2c) and temporary ponds (Catalán *et al.*, [2014]; Obrador *et al.*, [in prep] Figure 7.2d). Overall, these results emphasize the overlooked importance of the dry sections of freshwater ecosystems in terms of CO₂ effluxes, which may have potential implications for C budgets in fluvial networks.

Contrary to the CO₂ efflux, the CH₄ efflux from dry riverbeds was undetectable in almost all cases (Chapter 3). We associate this finding to the fact that recurrent cycles of flow recession and subsequent reflowing in temporary streams favours the aeration of dry riverbeds, thus limiting the redox requirements for CH₄ production.

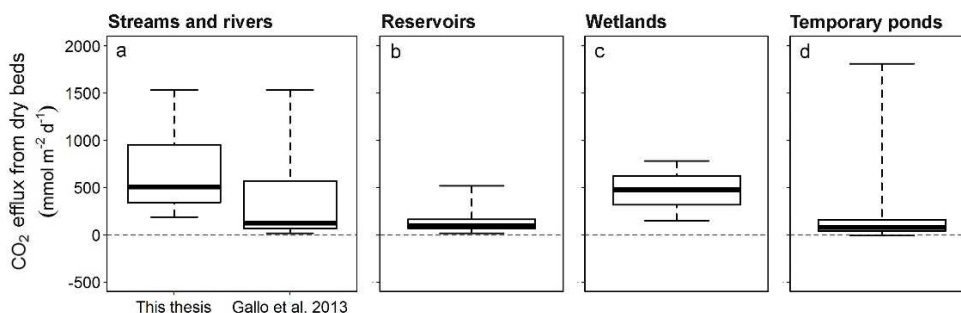


Figure 7.2 Comparison of CO₂ effluxes measured in the dry beds of 4 aquatic ecosystem types: (a) streams and rivers (b) reservoirs (c) wetlands and (d) temporary ponds. Data from streams and rivers was obtained both from this thesis (n=14) and from a study in dry desert streams in Arizona, USA (n=9) [Gallo *et al.*, 2013]. Data from dry belts of reservoirs was obtained from direct chamber field measurements in two reservoirs located in the Basque Country (NW Iberian Peninsula) [unpublished data]. Data from wetlands corresponds to a compilation of both field and laboratory measurements obtained from Moore and Knowles [1989] and Fenner and Freeman [2011]. Data from temporary ponds was obtained from Catalán *et al.* [2014] and Obrador *et al.*, [in prep]. Box plots display the 25th, 50th and 75th percentiles; whiskers display minimum and maximum values. The horizontal dashed line in all the panels corresponds to zero flux.

In *Chapter 4*, we further show that the CO₂ efflux from dry riverbeds was higher than the CO₂ efflux from the same streams when they were flowing. This observation could be related to limitation of the CO₂ efflux in aquatic environments due to reduced gas diffusivity compared to dry streambeds. This sudden change in terms of CO₂ efflux between dry and flowing riverbeds observed at local scale (*Chapter 4*), may influence the overall fluvial network spatiotemporal pattern in C gas flux, thereby emphasizing again how flow discontinuities (in this case, flow intermittency) may lead to a patchy and strongly heterogeneous pattern of C gas fluxes along the fluvial network.

The results from *Chapter 4* show that the CO₂ efflux from dry riverbeds was similar to the CO₂ efflux from adjacent upland soils. Consistent with this finding, *von Schiller et al.*, [2014] observed a comparable CO₂ efflux between dry riverbeds (median 212 mmol m⁻² d⁻¹; range 36–455 mmol m⁻² d⁻¹) and a compiled data set from Mediterranean soils (median 188 mmol m⁻² d⁻¹; range 44–371 mmol m⁻² d⁻¹; [Bond-Lamberty and Thomson, 2014]). The similar magnitude of CO₂ emissions from dry riverbeds and soils raises intriguing questions such as i) whether these environments are functionally equivalent in terms of C processing as well as ii) to what extent the C processed and further emitted from dry riverbeds can be considered terrestrial.

7.2.2 Sources of CO₂ emissions from dry riverbeds

Results in *Chapter 4* show that a similar magnitude of CO₂ efflux from dry riverbeds and their adjacent upland soils does not imply that these habitats are equivalent in their physical and chemical structure and function, and therefore they may differ in the sources that sustain their emissions. Our results suggest that part of the biologically derived CO₂ emissions from dry riverbeds could be fuelled by CO₂ produced from biological mineralization of fresh and labile water extractable organic matter (WEOM) fractions. In fact, dry conditions may enhance the release of high amounts of fresh and labile materials to sediment interfaces of dry riverbeds through microbial cell lysis and physical processes [Fierer and Schimel, 2003; Borken and Matzner, 2009]. Thus, at least part of the C emitted from dry riverbeds may have an internal in-stream origin. In contrast, CO₂ emissions from upland soils, which had a lower proportion of fresh and labile WEOM fractions in

comparison to the dry riverbeds, most likely rely on the biological mineralization of plant-derived aromatic and complex organic compounds [Casals *et al.*, 2009].

Our results suggest that at least part of the dry riverbed CO₂ emissions derives from biologically mineralized OM produced within the riverbed sediments. However, other non-biotic CO₂-generating processes such as reactions with the carbonate system [Angert *et al.*, 2014] or photochemical reactions [Austin and Vivanco, 2006] may also potentially contribute to the final CO₂ efflux [Rey, 2015]. Thus, further work is needed to provide a more conclusive understanding of the sources that sustain CO₂ emissions from dry riverbeds, including the temporal and spatial patterns and the processes of CO₂ production, transport and transfer.

7.2.3 Potential contribution of dry riverbeds to CO₂ emissions from fluvial networks

The CO₂ efflux measurements in our Mediterranean fluvial network (*Chapters 3 and 4*) indicate that dry riverbeds can play a relevant role in fluvial network C budgets. This is particularly important if we consider the expected increase in the spatial and temporal extent of temporary watercourses that will result from global change [Palmer *et al.*, 2008]. Yet, current global estimates of CO₂ emissions from fluvial networks do not consider the C emitted from the areas of temporary watercourses that recurrently run dry [Aufdenkampe *et al.*, 2011; Raymond *et al.*, 2013]. To explore the potential contribution of CO₂ emissions from dry riverbeds to the total CO₂ emissions from fluvial networks in both our study region and on a global basis, we carried out a simple upscaling approach combining our CO₂ effluxes with the mean annual global surface area occupied by dry watercourses derived from a global hydro-climatic model [Raymond *et al.*, 2013a] in each COastal Segmentation and related CATchments units (COSCAT, Meybeck *et al.*, [2006]). For a more detailed description of the upscaling procedure see von Schiller *et al.*, [2014].

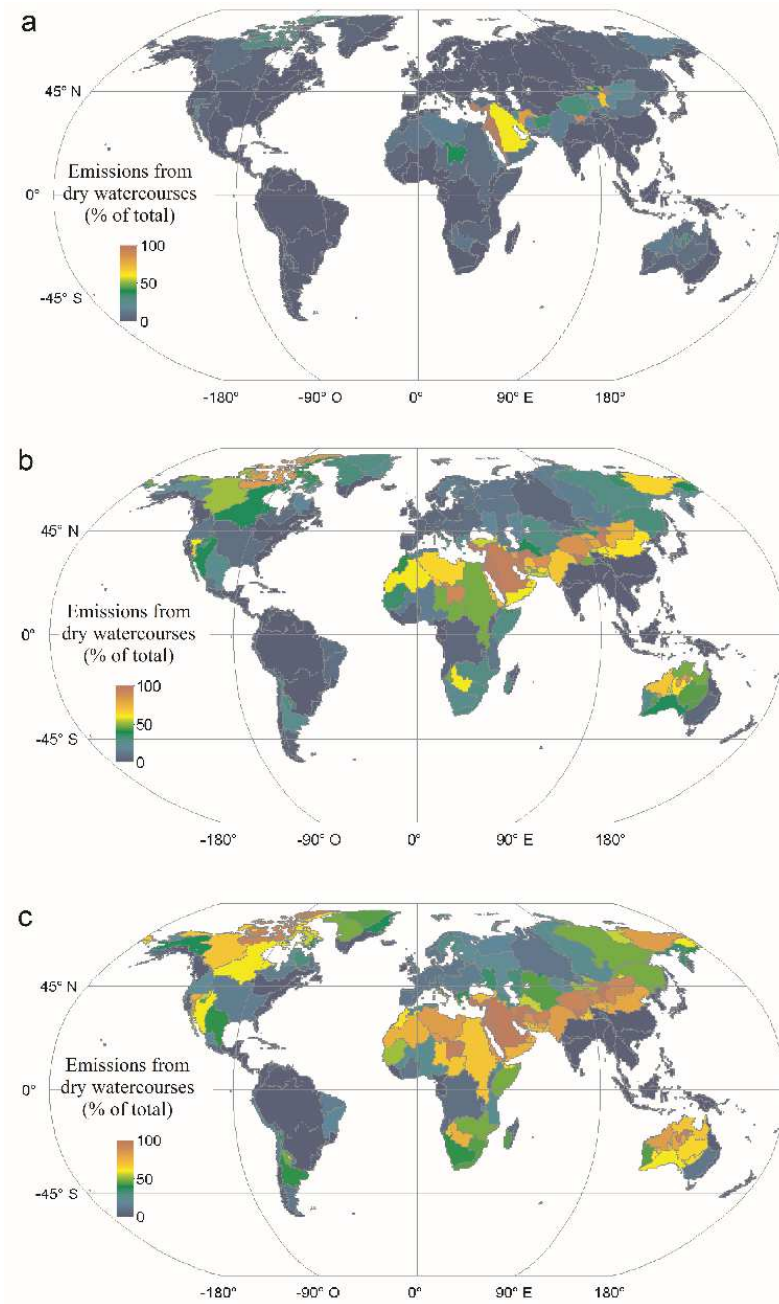


Figure 7.3 Estimated percentage contribution of the CO₂ efflux from dry watercourses to the total fluvial network CO₂ efflux in each COSCAT region. We built 3 scenarios using the (a) minimum, (b) median and (c) maximum CO₂ efflux from dry watercourses reported in the literature [Gallo *et al.*, 2013] and obtained in the Fluvia River network (Chapter 3 and 4). Figure extracted from von Schiller *et al.*, [2014]

The upscaling to our study region (COSCAT 418) indicates that including emissions from dry watercourses could increase the aquatic fluvial network estimate of CO₂ emissions by 0.6–15% [von Schiller *et al.*, 2014]. At the global scale, the upscaling approach shows that emissions from dry watercourses could be especially important in arid regions around 30°N and 30°S [von Schiller *et al.*, 2014], increasing the estimate of aquatic fluvial network CO₂ emissions [Raymond *et al.*, 2013a] by 0.4–9% (Figure 7.3). Although our results indicate that taking into account CO₂ emissions from dry watercourses may have only a small effect on the estimate of global CO₂ emissions from fluvial networks, they also point out to the fact that the efflux of CO₂ from dry watercourses may substantially contribute to, and even dominate, the CO₂ balance in many arid and semiarid fluvial networks (Figure 7.3).

We acknowledge that our results only represent a first rough estimate of the role of the dry phase of temporary watercourses on CO₂ effluxes from fluvial networks. Evidence so far shows highly intra- and inter-site variability in the CO₂ emissions from dry beds. This finding can probably be associated to the spatial gradients or shifts on the environmental conditions that drive CO₂ emissions from dry beds (see *Chapter 4* and *section 7.2.1* in the general discussion). Moreover, further work aimed to capture the temporal patterns of the CO₂ efflux along the dry period is also needed to provide a more conclusive understanding of the magnitude and variability of CO₂ emissions in these environments. We need, for example, to account for the potential loss of CO₂ from dry riverbeds as a response to hydrological pulses (e.g. precipitation events, channel reflooding), a phenomenon that has been extensively studied in soils [Birch, 1958; Austin *et al.*, 2004; Sponseller, 2007], but only to a limited extent in dry riverbeds [Gallo *et al.*, 2013]. In any case, our results indicate that neglecting CO₂ emissions from dry riverbeds may overlook a fundamental component of the C balance of fluvial networks. Thus, including CO₂ emissions from dry riverbeds may help to constrain the highly uncertain magnitude of the land C sink.

7.3 The role of physics as a valve regulating carbon gas exchange between fluvial networks and the atmosphere

The diffusion flux of C across the water- or soil-atmosphere interface only requires, in essence, a concentration difference between both phases (*Fick*, [1855]). However, this thesis clearly shows that what ultimately modulates the rate or intensity of the diffusion flux in the different aquatic and dry environments along the fluvial network are the physical mechanisms that either enhance or limit the gas exchange ability or gas transfer velocity across the boundary layer (i.e., k_{600}). Our results agree with general models of gas diffusion, where physical processes control the gas exchange between the atmosphere and aquatic ecosystems [*Zappa et al.*, 2007; *Bade*, 2009; *Raymond et al.*, 2012; *Long et al.*, 2015] and soils [*Smith et al.*, 2003; *Luo and Zhou*, 2010; *Blagodatsky and Smith*, 2012]. However, one of the most interesting findings unveiled in this dissertation is that the role of physics as the ultimate driver of the spatial and temporal variability of CO₂ and CH₄ emissions prevailed across wet and dry environments.

In the free-flowing running water sections, the CO₂ and CH₄ gas is rapidly emitted because the high turbulence induced by water currents disrupts the surface boundary layer (*Chapter 3, 5 and 6*). With similar (in the case of CO₂) and higher (in the case of CH₄) concentration gradients to those from running waters, the impounded waters showed an overall lower efflux of CO₂ and CH₄, indicating a physical limitation of the flux (*Chapter 3, 5 and 6*). An extreme effect of the physical limitation of CO₂ and CH₄ efflux occurred in the isolated river pools, where the diffusive CO₂ and CH₄ efflux was lowest despite showing the highest concentration gradients observed in the fluvial network (Figure 3.4). Moreover, in the dry riverbeds, the unexpected negative relationship between the basal respiration rates and the CO₂ efflux could suggest the existence of a physical factor restricting the evasion of CO₂ present in the sediment media (*Chapter 3*). Water content might be the factor modulating this uncoupling between CO₂ production and CO₂ emission in dry beds.

7.4 Integrating fluvial network discontinuities in a Mediterranean river: Implications for carbon gas emissions under present and future hydrological scenarios

The results of this dissertation emphasize the active role of dry riverbeds, running waters, and impounded waters in terms of C efflux (Table 7.1). An upscaling exercise was performed to examine the contribution of these different environments to the total annual C efflux of the entire fluvial network (see Text B.7.1. in the Supporting information section for a detailed description of the upscaling exercise). The results show that dry riverbeds and running waters contribute respectively to 60 and 38% of the total annual CO₂ efflux (Table 7.2). Interestingly, dry riverbeds dominate the total annual CO₂ efflux, even though this environment only covers 27% of the total fluvial network area (Table 7.2). A similar situation occurred for CH₄ in the lentic environments, which occupy only 6% of the total network area, but contributed up to 62% of the total annual CH₄ efflux (Table 7.2). Overall, the results from this upscaling exercise reinforce the established notion that running waters play a major role in fluvial network C budgets at different scales [Butman and Raymond, 2011; Lundin et al., 2013; Raymond et al., 2013a; Wallin et al., 2013; Crawford et al., 2014a]. However, more importantly, these results point to fluvial discontinuities as emerging components dominating the annual CO₂ (through dry beds) and CH₄ (through small impoundments) efflux in highly regulated networks. In line with Maeck et al., [2013] and other studies focused on other biogeochemical components or processes [Ward and Stanford, 1983; Stanford and Ward, 2001; Fisher et al., 2004; McGuire et al., 2014; Dent and Grimm, 2016], our upscaling results at annual and fluvial network scales together with those found along the previous chapters, point to the need for a shift away from a continuous and system-centric view to a more inclusive approach that incorporates the true spatiotemporal complexity (i.e., different environments, spatiotemporal discontinuities, lateral, vertical and longitudinal connections) of biogeochemical patterns and processes in fluvial networks.

Table 7.1 Summary of the areal CO₂, CH₄ and total C fluxes measured in the three types of environments studied along the Fluvia River network.

Environment	Areal CO ₂ Flux (mmol m ⁻² d ⁻¹)				Areal CH ₄ Flux (mmol m ⁻² d ⁻¹)				Total Areal C Flux (mmol m ⁻² d ⁻¹)		
	Mean	Min	Max	N	Mean	Min	Max	N	Total	Min	Max
Lotic	172.0	26.7	798.7	145	1.06	0.00	3.77	39	173.0	0.00	802.5
Lentic	44.1	-11.2	199.8	86	23.07	0.00	37.02	38	67.2	0.00	236.8
Dry	563.4	466.8	1046.0	13	0.56	0.00	5.83	3	563.9	0.00	1051.8

Mean, minimum (Min), maximum (Max) and number of observations (N) of the entire dataset (see Chapter 2 for a detailed description of the dataset) for the different environments (i.e., lotic, lentic and dry).

Table 7.2 Summary of upscaled surface areas and annual CO₂, CH₄ and total C fluxes for the entire Fluvia River network

Environment	Surface area (km ²)			CO ₂ Mass Flux (Gg CO ₂ y ⁻¹)				CH ₄ Mass Flux (Gg CO ₂ e y ⁻¹)				Total C Mass Flux (Gg CO ₂ e y ⁻¹)			
	Mean	Min	Max	Total annual	Mean	Min	Max	Total annual	Mean	Min	Max	Total annual	Mean	Min	Max
Lotic^a	8.0 (67)	6.0	11.2	22.6 (38)	1.9	0.5	5.0	5.9 (33)	0.5	0.3	0.8	28.5 (37)	2.4	0.9	5.7
Lentic^a	0.8 (6)	0.8	0.8	1.0 (2)	0.1	0.0	0.2	11.2 (62)	0.9	0.9	1.0	12.2 (16)	1.0	0.9	1.1
Dry^a	3.2 (27)	0.0	5.2	36.0 (60)	3.0	0.0	4.6	0.8 (4)	0.1	0.0	0.1	36.9 (49)	3.1	0.0	4.7
Total^b	11.9 (100)	6.8	17.1	59.7 (73)	-	9.5	146.0	17.9 (27)	-	4.8	26.2	77.6 (100)	-	14.3	172.2

^a Mean, minimum (Min) and maximum (Max) of the monthly estimates for the different environments (i.e., lotic, lentic and dry). Total annual values corresponds to the sum of the monthly estimates. The percentage contribution of each environment to the total fluvial network emission flux is shown in brackets.

^b Mean, minimum (Min) and maximum (Max) of the annual estimates. The percentage contribution of each gas (i.e., CO₂ and CH₄) to the total mass of C emitted is shown in brackets.

River desiccation and impoundment of running waters through the construction of dams or small weirs have been recognized as some of the most important environmental pressures in fluvial networks worldwide [Nilsson *et al.*, 2005a; Sabater, 2008; Vörösmarty *et al.*, 2010; Acuña *et al.*, 2014]. Future projections considering the combined effects of climate change [Hoerling *et al.*, 2012; IPCC, 2014] and human pressures [Iglesias *et al.*,

2007; Murray *et al.*, 2012] on water resources in the Mediterranean region indicate that they will have a relevant impact on regional hydrological regimes (e.g., [IPCC, 2014; Pascual *et al.*, 2015]). For instance, a case study in three Mediterranean basins (including the Fluvià River) showed that the mean annual discharge will decrease between 25 and 34% along the 21st century [Pascual *et al.*, 2015]. Similarly, a global reduction of the surface area of free-flowing river sections by about 21%, with SWRS being the most common impoundment structure, has been predicted by a recent review on global dam construction intentions [Zarfl *et al.*, 2014].

Here, we used simple empirical models (see Text B.7.2. in the Supporting information section for a detailed description of model development and related calculations) to predict how future hydrological alterations (projections for the coming 85 years in the Fluvià River network from Pascual *et al.*, [2015], see Table B.7.1 in the Supporting Information for a detailed description of the future hydrological scenarios) may influence the relative surface area of the different environments comprising the fluvial network and how this may, in turn, be translated into changes in the annual mass C fluxes. The outcome of this simulation is a negligible change in the total annual efflux of CO₂ (max of +1%), CH₄ (max of -2%), and total C (max of +0.3%) in scenarios 1 and 2 (Table 7.3). This result can be explained by the counterbalancing effect between lotic and dry CO₂ and CH₄ emissions observed in our fluvial network. Specifically, decreases in discharge increase the mean areal extent of dry riverbeds up to respectively +2.2 (+6.1%) and +5.8 (+15%) km² in scenarios 1 and 2 (Table 7.3). However, this areal increase in dry beds will be at the expense of a decrease of running water surface area. Therefore, the increase of the annual C mass flux from dry beds is at least partially compensated by the decrease of C emitted from the running water sections.

On the other hand, it is likely that an increase of the areal extent of impounded waters (+100%; from 0.75 km² to 1.5 km²) combined with a long term discharge reduction (Scenario 3; Table B.7.1 in the Supporting Information) would have a stronger influence on the total annual C emitted from the fluvial network (+11.3 Gg CO₂e y⁻¹; +15%). This predicted change seems to be related to a dramatic increase of +9.9 Gg CO₂e y⁻¹ (+55%) of the annual CH₄ emitted from impounded waters (Table 7.3, Scenario 3).

Additionally, it has to be noted that the predictions of fluvial networks C mass fluxes in our exercise, only depend on surface area changes as response to flow regime scenarios (Text B.7.2. in the Supporting information section). Therefore, our simulation does not consider changes in the areal C fluxes and their main drivers (i.e., $p_{CO_2,w}$, $p_{CH_4,w}$ and k_{600}). For example, increases in water temperature, OM availability or alteration of stream hydraulics can have significant implications for the total mass fluxes from fluvial networks [Campeau and del Giorgio, 2013]. Similarly, future modifications of DIC, DOC and CH₄ import and export dynamics may also influence the total mass fluxes from fluvial networks [Hope et al., 2004; Wallin et al., 2010; Regnier et al., 2013].

Table 7.3 Summary of expected changes in surface areas and annual CO₂, CH₄ and total C fluxes for the entire Fluvia River network under 3 future hydrological scenarios

Environment	Scenario 1 - Short term discharge reduction (2006-2030)															
	Annual surface area change (km ²)			Annual CO ₂ Mass Flux Change (Gg CO ₂ y ⁻¹)			Annual CH ₄ Mass Flux Change (Gg CO ₂ e y ⁻¹)			Annual Total C Mass Flux Change (Gg CO ₂ e y ⁻¹)						
	Mean	Min	Max	Mean	Min	Max	Mean	Min	Max	Mean	Min	Max				
Lotic	-2.2	(-2.4)	-2.8	-1.7	-1.8	(-8.1)	-2.4	-1.4	-0.2	(-3.0)	-0.2	-0.1	-2.0	(-7.0)	-2.5	-1.5
Lentic	0.0	(0)	0.0	0.0	0.0	(0)	0.0	0.0	0.0	(0)	0.0	0.0	0.0	(0)	0.0	0.0
Dry	+2.2	(+6.1)	+1.7	+2.8	+2.1	(+5.7)	+1.5	+2.6	+0.04	(+4.8)	+0.03	+0.05	+2.1	(+5.7)	+1.6	+2.6
Total	0.0	(0)	-1.1	+1.1	+0.3	(+0.5)	-0.9	+1.2	-0.14	(-0.8)	-0.17	-0.05	+0.1	(+0.1)	-0.9	+1.1
Scenario 2 - Long term discharge reduction (2076-2100)																
Lotic	-5.8	(-6)	-7.5	-4.1	-4.7	(-20.8)	-6.1	-3.3	-0.5	(-7.7)	-0.6	-0.3	-5.2	(-18.1)	-6.7	-3.7
Lentic	0.0	(0)	0.0	0.0	0.0	(0)	0.0	0.0	0.0	(0)	0.0	0.0	0.0	(0)	0.0	0.0
Dry	+5.8	(+6)	+4.1	+7.5	+5.3	(+14.7)	+3.8	+6.8	+0.10	(+12.4)	+0.07	+0.13	+5.4	(+14.7)	+3.9	+6.9
Total	0.0	(0)	-3.4	+3.4	+0.6	(+1.0)	-2.3	+3.5	-0.4	(-2.0)	-0.5	-0.2	+0.2	(+0.3)	-2.8	+3.2
Scenario 3 - Long term discharge reduction (2076-2100) + Intense dam construction (+100% area)																
Lotic	-6.2	(-7)	-8.3	-4.9	-5.0	(-24.3)	-7.3	-2.1	-1.3	(-20)	-1.1	-0.6	-6.3	(-25)	-8.4	-2.7
Lentic	+0.8	(+100)	+0.4	+1.2	+1.0	(+100)	+0.4	+1.6	+11.2	(+100)	+5.6	+17	+12.2	(+100)	+6.0	+18.6
Dry	+5.8	(+6)	+4.1	+7.5	+5.3	(+14.7)	+3.8	+6.8	+0.10	(+12.4)	+0.07	+0.13	+5.4	(+14.7)	+3.9	+6.9
Total	+0.4	(+3)	-4.2	+4.2	+1.3	(+2.2)	-3.9	+6.7	+9.9	(+55)	+9.5	+11.4	+11.3	(+6)	+1.5	+22.8

Mean, minimum (Min) and maximum (Max) absolute and relative (in brackets) change of the surface areas and annual mass C fluxes for the different environments (i.e., lotic, lentic and dry) and for the entire fluvial network (i.e., total) under 3 potential future scenarios. The 3 future scenarios proposed here are based on changes of the fluvial network surface area in response to short and long term hydrological predictions for the Fluvia catchment [Pascual et al., 2015; IPCC, 2014; Zarfl et al., 2014]. A detailed description of the calculations and the 3 different scenarios is shown in Appendix B in the Supporting Information section.

The results from this simulation show the rather low sensitivity of the annual CO₂, CH₄ and total C emissions to shifts in river discharge. In contrast, the simulation stresses the high sensitivity of annual CH₄ and total C emissions to shifts in the surface area of lentic waterbodies in fluvial networks. We advance that the combined effect of future dam construction [Zarfl *et al.*, 2014] and extended periods of low flows as a consequence of drought or intensive use of the water resources [Gasith and Resh, 1999; Gibson *et al.*, 2005] may lead to an increase of lentic and dry habitats at the expenses of lotic environments in many fluvial networks [Sabater, 2008]. These predictions emphasize the decisive role of lentic environments in shaping the C efflux from fluvial networks in response to global change.



Chapter 8

General conclusions

Overall, this dissertation contributes to a better understanding of how the presence of river discontinuities as a result of intense impoundment and flow intermittency alters the spatiotemporal patterns, controls and sources of C gas fluxes in fluvial networks. In this sense, **the main conclusions of this dissertation can be summarized as follows:**

- As a consequence of the attenuated turbulence in impounded waters associated to small water retention structures (SWRS), the diffusive carbon dioxide (CO₂) emissions from impounded river sections was significantly lower than that from free-flowing river sections.
- As a consequence of the higher CH₄ concentration at the impounded sections compensating the attenuated turbulence, no reduction in methane (CH₄) emissions from impounded river sections associated to SWRS was detected in relation to free-flowing river sections,
- The significant increase in CH₄ concentration detected in impounded river sections influenced the overall discontinuous longitudinal pattern of CH₄ along the study stretch but did not translate into a significant increase in the diffusive CH₄ efflux from the free-flowing riverine sections downstream the SWRS.
- As in larger reservoirs or lakes, the ebullitive pathway of CH₄ emission was the predominant pathway in our impounded river sections, contributing to more than 85% of the total CH₄ efflux when CH₄ emission was detected.
- Streams do not turn into inert ecosystems when they become dry. On the contrary, they remain as active biogeochemical habitats degassing significant amounts of CO₂ to the atmosphere.
- The CH₄ efflux from dry beds was undetectable in almost all cases, probably because of the high aeration limiting the redox requirements for microbial CH₄ production.
- The physical control on gas transfer prevailed across aquatic (i.e., water turbulence) and dry (i.e., water content) environments, ultimately driving the overall spatial and temporal variability of CO₂ and CH₄ emissions in the fluvial network.

- Sources other than internal metabolism (e.g., external inputs, internal geochemical reactions or photochemical mineralization) sustained most of the fluvial network CO₂ emissions. Internal metabolism accounted for a moderate proportion (24%) of CO₂ emissions in lotic segments, while its contribution was insignificant in lentic segments.
- The free-flowing river sections showed a clear coupling between the hydrological dynamics and the origin of CO₂ emissions. In contrast, the contribution of the different sources to the CO₂ efflux in impounded river sections associated to SWRS remained stable and independent of hydrological variation.
- The source of CO₂ emitted from dry riverbeds remains unclear, although CO₂ produced from biological mineralization of fresh and labile organic matter fractions could be an important source.
- The view of fluvial networks as a continuum cannot properly describe the spatial variability in CO₂ and CH₄ effluxes, highly driven by the presence of SWRS and dry riverbeds.
- Fluvial discontinuities are emerging components of the annual C emissions of the fluvial network, dominating the annual CO₂ (through dry riverbeds) and CH₄ (through small impoundments) efflux.
- Upscaling exercises combined with scenario analysis show that decreases in river discharge predicted by global change models for this region will not significantly alter the annual CO₂, CH₄ and total C emissions from the Fluvità River network. In contrast, annual CH₄ and total C emissions could be significantly enhanced in response to increases in the surface area of lentic waterbodies associated to SWRS.

References

- Abril, G. (2005), Carbon dioxide and methane emissions and the carbon budget of a 10-year old tropical reservoir (Petit Saut, French Guiana), *Global Biogeochem. Cycles*, 19(4), 1–16, doi:10.1029/2005GB002457.
- Abril, M., I. Muñoz, J. P. Casas-Ruiz, L. Gómez-Gener, M. Barceló, F. Oliva, and M. Menéndez (2015), Effects of water flow regulation on ecosystem functioning in a Mediterranean river network assessed by wood decomposition, *Sci. Total Environ.*, 517, 57–65, doi:10.1016/j.scitotenv.2015.02.015.
- Abril, M., I. Muñoz, and M. Menéndez (2016), Heterogeneity in leaf litter decomposition in a temporary Mediterranean stream during flow fragmentation, *Sci. Total Environ.*, 553, 330–339, doi:10.1016/j.scitotenv.2016.02.082.
- Acuña, V., and K. Tockner (2010), The effects of alterations in temperature and flow regime on organic carbon dynamics in Mediterranean river networks, *Glob. Chang. Biol.*, 16(9), 2638–2650, doi:10.1111/j.1365-2486.2010.02170.x.
- Acuña, V., A. Giorgi, I. Muñoz, F. Sabater, and S. Sabater (2007), Meteorological and riparian influences on organic matter dynamics in a forested Mediterranean stream, *J. North Am. Benthol. Soc.*, 26(1), 54–69, doi:10.1899/0887-3593(2007)26[54:MARIOO]2.0.CO;2.
- Acuña, V., T. Datry, J. Marshall, D. Barceló, C. N. Dahm, A. Ginebreda, G. McGregor, S. Sabater, K. Tockner, and M. . Palmer (2014), Why Should We Care About Temporary Waterways?, *Science* (80-.), 343, 1080–1082, doi:10.1126/science.1246666.
- Alin, S. R., M. D. F. F. L. Rasera, C. I. Salimon, J. E. Richey, G. W. Holtgrieve, A. V. Krusche, and A. Snidvongs (2011), Physical controls on carbon dioxide transfer velocity and flux in low-gradient river systems and implications for regional carbon budgets, *J. Geophys. Res.*, 116(G1), G01009, doi:10.1029/2010JG001398.
- Amalfitano, S., S. Fazi, A. Zoppini, A. B. Caracciolo, P. Grenni, and A. Puddu (2008), Responses of Benthic Bacteria to Experimental Drying in Sediments from Mediterranean Temporary Rivers, , 270–279, doi:10.1007/s00248-007-9274-6.
- Amon, R. M. W., and R. Benner (1996), Photochemical and microbial consumption of dissolved organic carbon and dissolved oxygen in the Amazon River system, *Geochim. Cosmochim. Acta*, 60(10), 1783–1792, doi:10.1016/0016-7037(96)00055-5.

- Anesio, A. M., J. Theil-Nielsen, and W. Graneli (2000), Bacterial growth on photochemically transformed leachates from aquatic and terrestrial primary producers, *Microb. Ecol.*, 40(3), 200–208, doi:10.1007/s002480000045.
- Angert, A., D. Yakir, M. Rodeghiero, Y. Preisler, E. A. Davidson, and T. Weiner (2014), Using O₂ to study the relationships between soil CO₂ efflux and soil respiration, *Biogeosciences Discuss.*, 11(8), 12039–12068, doi:10.5194/bgd-11-12039-2014.
- Anthony, S. E., F. G. Prahl, and T. D. Peterson (2012), Methane dynamics in the Willamette River, Oregon, *Limnol. Oceanogr.*, 57(5), 1517–1530, doi:10.4319/lo.2012.57.5.1517.
- Aristi, I., M. Arroita, A. Larrañaga, L. Ponsatí, S. Sabater, D. von Schiller, A. Elosegi, and V. Acuña (2014), Flow regulation by dams affects ecosystem metabolism in Mediterranean rivers, *Freshw. Biol.*, doi:10.1111/fwb.12385.
- Aristegi, L., O. Izagirre, and A. Elosegi (2009), Comparison of several methods to calculate reaeration in streams, and their effects on estimation of metabolism, *Hydrobiologia*, 635(1), 113–124, doi:10.1007/s10750-009-9904-8
- Aufdenkampe, A. K., E. Mayorga, P. a Raymond, J. M. Melack, S. C. Doney, S. R. Alin, R. E. Aalto, and K. Yoo (2011a), Riverine coupling of biogeochemical cycles between land, oceans, and atmosphere, *Front. Ecol. Environ.*, 9(1), 53–60, doi:10.1890/100014.
- Austin, A. T., L. Yahdjian, J. M. Stark, J. Belnap, A. Porporato, U. Norton, D. a Ravetta, and S. M. Schaeffer (2004), Water pulses and biogeochemical cycles in arid and semiarid ecosystems., *Oecologia*, 141(2), 221–35, doi:10.1007/s00442-004-1519-1.
- Austin, A. T., and L. Vivanco (2006), Plant litter decomposition in a semi-arid ecosystem controlled by photodegradation., *Nature*, 442(August), 555–558, doi:10.1038/nature05038.
- Bade, D. L. (2009), Gas exchange across the air-water interface, in *Encyclopedia of Inland Waters*, Academic Press: Oxford, 2009, edited by Gene, E. L., 70–78.
- Barros, N., J. J. Cole, L. J. Tranvik, Y. T. Prairie, D. Bastviken, V. L. M. Huszar, P. del Giorgio, and F. Roland (2011), Carbon emission from hydroelectric reservoirs linked to reservoir age and latitude, *Nat. Geosci.*, 4(9), 593–596, doi:10.1038/ngeo1211.
- Bastien, J., and M. Demarty (2013), Spatio-temporal variation of gross CO₂ and CH₄ diffusive emissions from Australian reservoirs and natural aquatic ecosystems, and estimation of net reservoir emissions, *Lakes Reserv. Res. Manag.*, 18(2), 115–127, doi:10.1111/lre.12028.
- Bastviken, D., J. Cole, M. Pace, and L. Tranvik (2004), Methane emissions from lakes: Dependence of lake characteristics, two regional assessments, and a

- global estimate, *Global Biogeochem. Cycles*, 18(4), 1–12, doi:10.1029/2004GB002238.
- Bastviken, D., L. J. Tranvik, J. A. Downing, P. M. Crill, and A. Enrich-Prast (2011), Freshwater Methane Emissions Offset the Continental Carbon Sink, *Science*, 331(6013), 50–50, doi:10.1126/science.1196808.
- Battin, T. J., S. Luyssaert, L. a. Kaplan, A. K. Aufdenkampe, A. Richter, and L. J. Tranvik (2009a), The boundless carbon cycle, *Nat. Geosci.*, 2(9), 598–600, doi:10.1038/ngeo618.
- Battin, T. J., L. a. Kaplan, S. Findlay, C. S. Hopkins, E. Marti, A. I. Packman, J. D. Newbold, and F. Sabater (2009b), Biophysical controls on organic carbon fluxes in fluvial networks, *Nat. Geosci.*, 2(8), 595–595, doi:10.1038/ngeo602.
- Baulch, H. M., P. J. Dillon, R. Maranger, and S. L. Schiff (2011), Diffusive and ebullitive transport of methane and nitrous oxide from streams: Are bubble-mediated fluxes important?, *J. Geophys. Res. Biogeosciences*, 116(4), doi:10.1029/2011JG001656.
- Beaulieu, J. J., W. D. Shuster, and J. a. Rebolz (2012), Controls on gas transfer velocities in a large river, *J. Geophys. Res. Biogeosciences*, 117(2), 1–13, doi:10.1029/2011JG001794.
- Beaulieu, J., M. McManus, and C. Nietch (2016), Estimates of reservoir methane emissions based on a spatially-balanced probabilistic-survey, *Limnol. Oceanogr.*, (Thornton 1990), doi:10.1109/JPHOT.2015.XXXXXXX
- Belger, L., B. R. Forsberg, and J. M. Melack (2010), Carbon dioxide and methane emissions from interfluvial wetlands in the upper Negro River basin, Brazil, *Biogeochemistry*, 105(1–3), 171–183, doi:10.1007/s10533-010-9536-0.
- Benson, B. B., and D. Krause (1984), The concentration and isotopic fractionation of oxygen dissolved in freshwater and seawater in equilibrium with the atmosphere, *Limnol. Oceanogr.*, 29(3), 620–632, doi:10.4319/lo.1984.29.3.0620.
- Benstead, J. P., and D. S. Leigh (2012), An expanded role for river networks, *Nat. Geosci.*, 5(10), 678–679, doi:10.1038/ngeo1593.
- Bergström, I., S. Mäkelä, P. Kankaala, and P. Kortelainen (2007), Methane efflux from littoral vegetation stands of southern boreal lakes: An upscaled regional estimate, *Atmos. Environ.*, 41(2), 339–351, doi:10.1016/j.atmosenv.2006.08.014.
- Bernal, S., D. Schiller, F. Sabater, and E. Martí (2013), Hydrological extremes modulate nutrient dynamics in mediterranean climate streams across different spatial scales, *Hydrobiologia*, 719(1), 31–42, doi:10.1007/s10750-012-1246-2.

- Birdwell, J. E., and A. S. Engel (2010), Characterization of dissolved organic matter in cave and spring waters using UV-Vis absorbance and fluorescence spectroscopy, *Org. Geochem.*, 41(3), 270–280, doi:10.1016/j.orggeochem.2009.11.002.
- Blagodatsky, S., and P. Smith (2012), Soil physics meets soil biology: Towards better mechanistic prediction of greenhouse gas emissions from soil, *Soil Biol. Biochem.*, 47, 78–92, doi:10.1016/j.soilbio.2011.12.015.
- Bonada, N., and V. H. Resh (2013), Mediterranean-climate streams and rivers: geographically separated but ecologically comparable freshwater systems, *Hydrobiologia*, 719(1), 1–29, doi:10.1007/s10750-013-1634-2.
- Bond-Lamberty, B., and A. Thomson (2010), A global database of soil respiration data, *Biogeosciences*, 7(6), 1915–1926, doi:10.5194/bg-7-1915-2010.
- Borges, A. V. et al. (2015), Globally significant greenhouse-gas emissions from African inland waters, *Nat. Geosci.*, 8(8), 637–642, doi:10.1038/ngeo2486.
- Borken, W., and E. Matzner (2009), Reappraisal of drying and wetting effects on C and N mineralization and fluxes in soils, *Glob. Chang. Biol.*, 15(4), 808–824, doi:10.1111/j.1365-2486.2008.01681.x.
- Boulton, A. J. (2003), Parallels and contrasts in the effects of drought on stream macroinvertebrate assemblages, *Freshw. Biol.*, 48(7), 1173–1185, doi:10.1046/j.1365-2427.2003.01084.x.
- Bresney, S. R., S. Moseman-Valtierra, and N. P. Snyder, (2015), Observations of greenhouse gases and nitrate concentrations in a Maine river and fringing wetland. *Northeastern Naturalist* 22:120–143.
- Buffagni, A., D. G. Armanini, and S. Erba (2009), Does the lentic-lotic character of rivers affect invertebrate metrics used in the assessment of ecological quality?, *J. Limnol.*, 68(1), 92–105, doi:10.4081/jlimnol.2009.92.
- Burke, I. C., C. M. Yonker, W. J. Parton, C. V. Cole, K. Flach, and D. S. Schimel (1989), Texture, climate, and cultivation effects on soil organic matter content in U.S. grassland soils, *Soil Sci. Soc. Am.*, 53(3), 800–805.
- Buschiazzo, D. E., H. D. Estelrich, S. B. Aimar, E. Viglizzo, and F. J. Babinec (2004), Soil texture and tree coverage influence on organic matter, *Rangel. Ecol. Manag.*, 57(5), 511, doi:10.2111/1551-5028(2004)057\ [0511:STATCI] 2.0.CO;2.
- Butman, D., and P. a. Raymond (2011), Significant efflux of carbon dioxide from streams and rivers in the United States, *Nat. Geosci.*, 4(12), 839–842, doi:10.1038/ngeo1294.
- Cable, J. M., K. Ogle, D. G. Williams, J. F. Weltzin, and T. E. Huxman (2008), Soil texture drives responses of soil respiration to precipitation pulses in the

- sonoran desert: Implications for climate change, *Ecosystems*, 11(6), 961–979, doi:10.1007/s10021-008-9172-x.
- Campbell, C., and S. Chapman (2003), A rapid microtiter plate method to measure carbon dioxide evolved from carbon substrate amendments so as to determine the physiological profiles of soil microbial, *Appl. Environ. Microbiol.*, 69(6), 3593–3599, doi:10.1128/AEM.69.6.3593.
- Campeau, A., and P. del Giorgio (2013), Patterns in CH₄ and CO₂ concentrations across boreal rivers: Major drivers and implications for fluvial greenhouse emissions under climate change scenarios., *Glob. Chang. Biol.*, 20(4), 1–14, doi:10.1111/gcb.12479.
- Campeau, A., and J. Lapierre (2014), Regional contribution of CO₂ and CH₄ fluxes from the fluvial network in a lowland boreal landscape of Québec, *Glob. Biogeochem. Cycles*, 28(1), 1–13, doi:10.1002/2013GB004685.
- Canadell, J. G. et al. (2000), Carbon metabolism of the terrestrial biosphere: A multitechnique approach for improved understanding, *Ecosystems*, 3(2), 115–130, doi:10.1007/s100210000014.
- Casals, P., C. Gimeno, A. Carrara, L. Lopez-Sangil, and M. Sanz (2009), Soil CO₂ efflux and extractable organic carbon fractions under simulated precipitation events in a Mediterranean Dehesa, *Soil Biol. Biochem.*, 41(9), 1915–1922, doi:10.1016/j.soilbio.2009.06.015.
- Casas-Ruiz, J. P., J. Tittel, D. von Schiller, N. Catalán, B. Obrador, L. Gómez-Gener, E. Zwirnmann, S. Sabater, and R. Marcé (2015), Drought-induced discontinuities in the source and degradation of dissolved organic matter in a Mediterranean river, *Biogeochemistry*, 127(1), 1–15, doi:10.1007/s10533-015-0173-5.
- Catalán, N., D. Von Schiller, R. Marcé, M. Koschorreck, L. Gomez-gener, and B. Obrador (2014), Carbon dioxide efflux during the flooding phase of temporary ponds, *Limnetica*, 33(2), 349–360.
- Clavero, M., F. Blanco-Garrido, and J. Prenda (2004), Fish fauna in Iberian Mediterranean river basins: Biodiversity, introduced species and damming impacts, *Aquat. Conserv. Mar. Freshw. Ecosyst.*, 14(6), 575–585, doi:10.1002/aqc.636.
- Cole, J. I., and N. F. Caraco (1998), Atmospheric exchange of carbon dioxide in a low-wind oligotrophic the addition of SF₆, lake measured by, *Limnol. Oceanogr.*, 43(4), 647–656, 10.4319/lo.1998.43.4.0647.
- Cole, J. J., M. L. Pace, S. R. Carpenter, and J. F. Kitchell (2000), Persistence of net heterotrophy in lakes during nutrient addition and food web manipulations, *Limnol. Oceanogr.*, 45(8), 1718–1730, doi:10.4319/lo.2000.45.8.1718.

- Cole, J. J. et al. (2007), Plumbing the Global Carbon Cycle: Integrating Inland Waters into the Terrestrial Carbon Budget, *Ecosystems*, 10(1), 172–185, doi:10.1007/s10021-006-9013-8.
- Cole, J. J., D. L. Bade, D. Bastviken, M. L. Pace, and M. Van De Bogert (2010), Multiple approaches to estimating air-water gas exchange in small lakes, *Limnol. Oceanogr. Methods*, 8, 285–293.
- Corvasce, M., A. Zsolnay, V. D’Orazio, R. Lopez, and T. M. Miano (2006), Characterization of water extractable organic matter in a deep soil profile., *Chemosphere*, 62(10), 1583–90, doi:10.1016/j.chemosphere.2005.07.065.
- Cory, R. M., C. P. Ward, B. C. Crump, and G. W. Kling (2014), Sunlight controls water column processing of carbon in arctic fresh waters, *Science*, 345(6199), 925–928, doi:10.1126/science.1253119.
- Cramer, W. et al. (2001), Global response of terrestrial ecosystem structure and function to CO₂ and climate change: Results from six dynamic global vegetation models, *Glob. Chang. Biol.*, 7(4), 357–373, doi:10.1046/j.1365-2486.2001.00383.x.
- Crawford, J. T., R. G. Striegl, K. P. Wickland, M. M. Dornblaser, and E. H. Stanley (2013), Emissions of carbon dioxide and methane from a headwater stream network of interior Alaska, *J. Geophys. Res. Biogeosciences*, 118(2), 482–494, doi:10.1002/jgrg.20034.
- Crawford, J. T., E. H. Stanley, S. a. Spawn, J. C. Finlay, L. C. Loken, and R. G. Striegl (2014a), Ebullitive methane emissions from oxygenated wetland streams., *Glob. Chang. Biol.*, 20(11), 3408–22, doi:10.1111/gcb.12614.
- Crawford, J. T., N. R. Lottig, E. H. Stanley, J. F. Walker, P. C. Hanson, J. C. Finlay, and R. G. Striegl (2014b), CO₂ and CH₄ emissions from streams in a lake-rich landscape: Patterns, controls and regional significance, *Global Biogeochem. Cycles*, 28(3), 197–210, doi:10.1002/2013GB004661.
- Crawford, J. T., L. C. Loken, E. H. Stanley, E. G. Stets, M. M. Dornblaser, and R. G. Striegl (2016), Basin scale controls on CO₂ and CH₄ emissions from the Upper Mississippi River, *Geophys. Res. Lett.*, 43(5), 1973–1979, doi:10.1002/2015GL067599.
- Crusius, J., and R. Wanninkhof (2003), Gas transfer velocities measured at low wind speed over a lake, *Limnol. Oceanogr.*, 48(3), 1010–1017, doi:10.4319/lo.2003.48.3.1010.
- Dahm, C. N., M. a. Baker, D. I. Moore, and J. R. Thibault (2003), Coupled biogeochemical and hydrological responses of streams and rivers to drought, *Freshw. Biol.*, 48(7), 1219–1231, doi:10.1046/j.1365-2427.2003.01082.x.
- Datry, T., S. T. Larned, and K. Tockner (2014), Intermittent rivers: A challenge for freshwater ecology, *Bioscience*, 64(3), 229–235, doi:10.1093/biosci/bit027.

- Davidson, E. A., R. O. Figueiredo, D. Markewitz, and A. K. Aufdenkampe (2010), Dissolved CO₂ in small catchment streams of eastern Amazonia: A minor pathway of terrestrial carbon loss, *J. Geophys. Res. Biogeosciences*, 115(4), 1–6, doi:10.1029/2009JG001202.
- Dean W.E., (1974), Determination of carbonate and organic matter in calcareous sediments and sedimentary rocks by loss on ignition: comparison with other method. *J Sediment Petrol* 44:242–248. doi: 10.1306/74D729D2-2B21-11D7-8648000102C1865D
- Deemer, B., J. Harrison, S. Li, J. J. Beaulieu, and T. Delsontro (2016), Greenhouse Gas Emissions from Reservoir Water Surfaces: A New Global Synthesis Manuscript, *Bioscience*, doi:10.1093/biosci/biw117.
- Delsontro, T., D. F. McGinnis, S. Sobek, I. Ostrovsky, and B. Wehrli (2010), Extreme methane emissions from a Swiss hydropower reservoir: contribution from bubbling sediments., *Environ. Sci. Technol.*, 44(7), 2419–25, doi:10.1021/es9031369.
- DelSontro, T., L. Boutet, A. St-Pierre, P. A. del Giorgio, and Y. T. Prairie (2016), Methane ebullition and diffusion from northern ponds and lakes regulated by the interaction between temperature and system productivity, *Limnol. Oceanogr.*, doi:10.1002/lno.10335.
- Demars, B. O. L., and J. R. Manson (2013), Temperature dependence of stream aeration coefficients and the effect of water turbulence: a critical review., *Water Res.*, 47(1), 1–15, doi:10.1016/j.watres.2012.09.054.
- Dent, C. L., and N. B. Grimm (1999), Spatial Heterogeneity of Stream Water Nutrient Concentrations over Successional Time, *Ecology*, 80(7), 2283–2298.
- Dent, C. L., and N. B. Grimm (2016), Spatial Heterogeneity of Stream Water Nutrient Concentrations over Successional Time Author (s): C . Lisa Dent and Nancy B . Grimm Published by: Wiley Stable URL : <http://www.jstor.org/stable/176910> REFERENCES Linked references are available on JSTOR f , , 80(7), 2283–2298.
- Deshmukh, C. et al. (2014), Physical controls on CH₄ emissions from a newly flooded subtropical freshwater hydroelectric reservoir: Nam Theun 2, *Biogeosciences*, 11(15), 4251–4269, doi:10.5194/bg-11-4251-2014.
- Deshmukh, C., F. Guérin, S. Pighini, A. Vongkhamsao, P. Guédant, W. Rode, A. Godon, V. Chanudet, S. Descloux, and D. Serça (2015), Low methane (CH₄) emissions downstream of a monomictic subtropical hydroelectric reservoir (Nam Theun 2, Lao PDR), *Biogeosciences*, 12(14), 11313–11347, doi:10.5194/bgd-12-11313-2015.
- Deutzmann, J. S., B. Schink, F. Bi, U. Konstanz, and D.- Constance (2011), Anaerobic Oxidation of Methane in Sediments of Lake Constance , an Oligotrophic Freshwater Lake, *Appl. Environ. Microbiol.*, 77, 4429–4436.

- Döll, P., K. Fiedler, and J. Zhang (2009), Global-scale analysis of river flow alterations due to water withdrawals and reservoirs, *Hydrol. Earth Syst. Sci. Discuss.*, 6(4), 4773–4812, doi:10.5194/hessd-6-4773-2009.
- Donelan M.A. (1990) Air–sea interaction. In LeMehaute, B. and Hanes D (eds) *The Sea: Ocean Engineering Science*, Wiley, New York, pp 239–292
- Downing, J. A. et al. (2006), Abundance and Size Distribution of Lakes, Ponds and Impoundments, *Limnol. Oceanogr.*, 51(5), 2388–2397, doi:10.1016/B978-0-12-409548-9.03867-7.
- Downing, J. A., J. J. Cole, J. J. Middelburg, R. G. Striegl, C. M. Duarte, P. Kortelainen, Y. T. Prairie, and K. a. Laube (2008), Sediment organic carbon burial in agriculturally eutrophic impoundments over the last century, *Global Biogeochem. Cycles*, 22(1), GB1018, doi:10.1029/2006GB002854.
- Downing, J. A., J. J. Cole, C. M. Duarte, J. J. Middelburg, J. M. Melack, Y. T. Prairie, P. Kortelainen, R. G. Striegl, W. H. McDowell, and L. J. Tranvik (2012), Global abundance and size distribution of streams and rivers, *Int. Waters*, 2(4), 229–236, doi:10.5268/IW-2.4.502.
- Duarte, C. M., and Y. T. Prairie (2005), Prevalence of Heterotrophy and Atmospheric CO₂ Emissions from Aquatic Ecosystems, *Ecosystems*, 8(7), 862–870, doi:10.1007/s10021-005-0177-4.
- Elosegi, A., and S. Sabater (2013), Effects of hydromorphological impacts on river ecosystem functioning: A review and suggestions for assessing ecological impacts, *Hydrobiologia*, 712(1), 129–143, doi:10.1007/s10750-012-1226-6.
- Fearnside, P. M., and S. Pueyo (2012), Greenhouse-gas emissions from tropical dams, *Nat. Clim. Chang.*, 2(6), 382–384, doi:10.1038/nclimate1540.
- Febria, C. M., J. D. Hosen, B. C. Crump, M. A. Palmer, and D. D. Williams (2015), Microbial responses to changes in flow status in temporary headwater streams: A cross-system comparison, *Front. Microbiol.*, 6(JUN), doi:10.3389/fmicb.2015.00522.
- Fellman, J. B., E. Hood, and R. G. M. Spencer (2010), Fluorescence spectroscopy opens new windows into dissolved organic matter dynamics in freshwater ecosystems: A review, *Limnol. Oceanogr.*, 55(6), 2452–2462, doi:10.4319/lo.2010.55.6.2452.
- Fenner, N., and C. Freeman (2011), Drought-induced carbon loss in peatlands, *Nat. Geosci.*, 4(12), 895–900, doi:10.1038/ngeo1323.
- Fick, A. (1855), Ueber Diffusion, *Ann. Phys.*, 170(1), 59–86, doi:10.1002/andp.18551700105.
- Fierer, N., and J. P. Schimel (2003), A Proposed Mechanism for the Pulse in Carbon Dioxide Production Commonly Observed Following the Rapid

- Rewetting of a Dry Soil, *Soil Sci. Soc. Am. J.*, 67(3), 798–805, doi:10.2136/sssaj2003.0798.
- Fisher, S. G., R. A. Sponseller, and J. B. Heffernan (2004), Horizons in stream biogeochemistry: Flowpaths to progress, *Ecology*, 85(9), 2369–2379, doi:10.1890/03-0244.
- Foley, J. A., I. C. Prentice, N. Ramankutty, S. Levis, D. Pollard, S. Sitch, and A. Haxeltine (1996), An integrated biosphere model of land surface processes, terrestrial carbon balance, and vegetation dynamics, *Global Biogeochem. Cycles*, 10(4), 603–628, doi:10.1029/96GB02692.
- Forzieri, G., L. Feyen, R. Rojas, M. Flörke, F. Wimmer, and A. Bianchi (2014), Ensemble projections of future streamflow droughts in Europe, *Hydrol. Earth Syst. Sci.*, 18(1), 85–108, doi:10.5194/hess-18-85-2014.
- Frankignoulle, M. (1988), Field measurements of air-sea CO₂ exchange, *Limnol. Ocean.*, 33(3), 313–322.
- Freeman, M. C., C. M. Pringle, and C. R. Jackson (2007), Hydrologic Connectivity and the Contribution of Stream Headwaters to Ecological Integrity at Regional Scales, *J. Am. Water Resour. Assoc.*, 43(1), 5–14, doi:10.1111/j.1752-1688.2007.00002.x.
- Friedl, G., and A. Wüest (2002), Disrupting biogeochemical cycles - Consequences of damming, *Aquat. Sci.*, 64(1), 55–65, doi:10.1007/s00027-002-8054-0.
- Frissell, C. A., W. J. Liss, C. E. Warren, and M. D. Hurley (1986), A hierarchical framework for stream habitat classification: Viewing streams in a watershed context, *Environ. Manage.*, 10(2), 199–214, doi:10.1007/BF01867358.
- Fujikawa, T., and T. Miyazaki (2005), Effects of Bulk Density and Soil Type on the Gas Diffusion Coefficient in Repacked and Undisturbed Soils, *Soil Sci.*, 170(11), 892–901, doi:10.1097/01.ss.0000196771.53574.79.
- Gallo, E. L., K. A. Lohse, C. M. Ferlin, T. Meixner, and P. D. Brooks (2013), Physical and biological controls on trace gas fluxes in semi-arid urban ephemeral waterways, *Biogeochemistry*, 1–19, doi:10.1007/s10533-013-9927-0.
- Galy-lacaux, C., R. Delmas, L. Labroue, and P. Gosse (1997), Gaseous emissions and oxygen consumption in hydroelectric dams: A case study in French Guyana, *Global Biogeochem. Cycles*, 11(4), 471–483.
- García-Ruiz, J. M., J. I. López-Moreno, S. M. Vicente-Serrano, T. Lasanta-Martínez, and S. Beguería (2011), Mediterranean water resources in a global change scenario, *Earth-Science Rev.*, 105(3–4), 121–139, doi:10.1016/j.earscirev.2011.01.006.

- Gasith, A., and V. H. Resh (1999), Streams in Mediterranean climate regions: Abiotic influences and biotic responses to predictable seasonal events, *Annu. Rev. Ecol. Syst.*, 30(1), 51–81.
- Gibson, C. A., J. L. Meyer, N. L. Poff, L. E. Hay, and A. Georgakakos (2005), Flow regime alterations under changing climate in two river basins: Implications for freshwater ecosystems, *River Res. Appl.*, 21(8), 849–864, doi:10.1002/rra.855.
- Giles, J. (2006), Methane quashes green credentials of hydropower, *Nature*, 444(7119), 524–525, doi:10.1038/444524a.
- Gómez-Gener, L., B. Obrador, D. von Schiller, R. Marcé, J. P. Casas-Ruiz, L. Proia, V. Acuña, N. Catalán, I. Muñoz, and M. Koschorreck (2015), Hot spots for carbon emissions from Mediterranean fluvial networks during summer drought, *Biogeochemistry*, 125(3), 409–426, doi:10.1007/s10533-015-0139-7.
- Grill, G., B. Lehner, A. E. Lumsdon, G. K. MacDonald, C. Zarfl, and C. Reidy Liermann (2015), Dams reshape the world's rivers, *Nature*, 517, 530.
- Grogan, P., and S. Jonasson (2005), Temperature and substrate controls on intra-annual variation in ecosystem respiration in two subarctic vegetation types, *Glob. Chang. Biol.*, 11(3), 465–475, doi:10.1111/j.1365-2486.2005.00912.x.
- Guérin, F., G. Abril, S. Richard, B. Burban, C. Reynouard, P. Seyler, and R. Delmas (2006), Methane and carbon dioxide emissions from tropical reservoirs: Significance of downstream rivers, *Geophys. Res. Lett.*, 33(21), 1–6, doi:10.1029/2006GL027929.
- Guérin, F., G. Abril, D. Serça, C. Delon, S. Richard, R. Delmas, A. Tremblay, and L. Varfalvy (2007a), Gas transfer velocities of CO₂ and CH₄ in a tropical reservoir and its river downstream, *J. Mar. Syst.*, 66(1–4), 161–172, doi:10.1016/j.jmarsys.2006.03.019.
- Guérin, F., and G. Abril (2007b), Significance of pelagic aerobic methane oxidation in the methane and carbon budget of a tropical reservoir, *J. Geophys. Res. Biogeosciences*, 112(3), 1–14, doi:10.1029/2006JG000393.
- Halbedel, S., and M. Koschorreck (2013), Regulation of CO₂ emissions from temperate streams and reservoirs, *Biogeosciences*, 10(11), 7539–7551, doi:10.5194/bg-10-7539-2013.
- Hanson, P. C., S. R. Carpenter, D. E. Armstrong, E. H. Stanley, and T. K. Kratz (2006), Lake dissolved inorganic carbon and dissolved oxygen: Changing drivers from days to decades, *Ecol. Monogr.*, 76(3), 343–363, doi:10.1177/0888325406287176.
- Hanson, P. C., S. R. Carpenter, N. Kimura, C. Wu, S. P. Cornelius, and T. K. Kratz (2008), Evaluation of metabolism models for free-water dissolved oxygen methods in lakes, *Limnol. Oceanogr. Methods*, 6(1956), 454–465, doi:10.4319/lom.2008.6.454.

- Harrison, J. A., R. J. Maranger, R. B. Alexander, A. E. Giblin, P. A. Jacinthe, E. Mayorga, S. P. Seitzinger, D. J. Sobota, and W. M. Wollheim (2009), The regional and global significance of nitrogen removal in lakes and reservoirs, *Biogeochemistry*, 93(1–2), 143–157, doi:10.1007/s10533-008-9272-x.
- Haxton, T. J., and C. S. Findlay (2008), Meta-analysis of the impacts of water management on aquatic communities, *Can. J. Fish. Aquat. Sci.*, 65(3), 437–447, doi:10.1139/f07-175.
- Heimann, M. (2009), Searching out the sinks, *Nat. Geosci.*, 2(1), 3–4, doi:10.1038/ngeo405.
- Hickin E.J. 1995. *River Geomorphology*. Chichester: Wiley.
- Ho, D. T., L. F. Bliven, R. Wanninkhof, and P. Schlosser (1997), The effect of rain on air-water gas exchange, *Tellus, Ser. B Chem. Phys. Meteorol.*, 49(2), 149–158, doi:10.1034/j.1600-0889.49.issue2.3.x.
- Ho, D. T., F. Veron, E. Harrison, L. F. Bliven, N. Scott, and W. R. McGillis (2007), The combined effect of rain and wind on air-water gas exchange: A feasibility study, *J. Mar. Syst.*, 66(1–4), 150–160, doi:10.1016/j.jmarsys.2006.02.012.
- Hoellein, T. J., D. A. Bruesewitz, and D. C. Richardson (2013), Revisiting Odum (1956): A synthesis of aquatic ecosystem metabolism, *Limnol. Oceanogr.*, 58(6), 2089–2100, doi:10.4319/lo.2013.58.6.2089.
- Hoerling, M., J. Eischeid, J. Perlwitz, X. Quan, T. Zhang, and P. Pegion (2012), On the Increased Frequency of Mediterranean Drought, *J. Clim.*, 25(6), 2146–2161, doi:10.1175/JCLI-D-11-00296.1.
- Holgerson, M. A., and P. A. Raymond (2016), Large contribution to inland water CO₂ and CH₄ emissions from very small ponds, *Nat. Geosci.*, 9(3), 222–226, doi:10.1038/ngeo2654.
- Holtgrieve, G. W., D. E. Schindler, T. a. Branch, and Z. T. A'mar (2010), Simultaneous quantification of aquatic ecosystem metabolism and reaeration using a Bayesian statistical model of oxygen dynamics, *Limnol. Oceanogr.*, 55(3), 1047–1062, doi:10.4319/lo.2010.55.3.1047.
- Hope, D., S. M. Palmer, M. F. Billett, and J. J. C. Dawson (2001), Carbon dioxide and methane evasion from a temperate peatland stream, *Limnol. Oceanogr.*, 46(4), 847–857, doi:10.4319/lo.2001.46.4.0847.
- Hope, D., S. M. Palmer, M. F. Billett, and J. J. C. Dawson (2004), Variations in dissolved CO₂ and CH₄ in a first-order stream and catchment: an investigation of soil-stream linkages, *Hydrol. Process.*, 18(17), 3255–3275, doi:10.1002/hyp.5657.
- Hornberger G.M, Kelly M.G (1975), Atmospheric reaeration in a river using productivity analysis. *Journal of the Environmental Engineering Division ASCE* 101: 729–739

- Hotchkiss, E. R., R. O. Hall Jr, R. A. Sponseller, D. Butman, J. Klaminder, H. Laudon, M. Rosvall, and J. Karlsson (2015), Sources of and processes controlling CO₂ emissions change with the size of streams and rivers, *Nat. Geosci.*, 8(9), 696–699, doi:10.1038/ngeo2507.
- Houser, J. N., D. W. Bierman, R. M. Burdis, and L. A. Soeken-Gittinger (2010), Longitudinal trends and discontinuities in nutrients, chlorophyll, and suspended solids in the Upper Mississippi River: Implications for transport, processing, and export by large rivers, *Hydrobiologia*, 651(1), 127–144, doi:10.1007/s10750-010-0282-z.
- Howard, D., and P. Howard (1993), Relationships between CO₂ evolution, moisture content and temperature for a range of soil types, *Soil Biol. Biochem.*, 25(1), 1537–1546, doi:10.1016/0038-0717(93)90008-Y.
- Huguet, A., L. Vacher, S. Relexans, S. Saubusse, J. M. Froidefond, and E. Parlanti (2009), Properties of fluorescent dissolved organic matter in the Gironde Estuary, *Org. Geochem.*, 40(6), 706–719, doi:10.1016/j.orggeochem.2009.03.002.
- Humborg, C., C.-M. Mörtz, M. Sundbom, H. Borg, T. Blenckner, R. Giesler, and V. Ittekkot (2010), CO₂ supersaturation along the aquatic conduit in Swedish watersheds as constrained by terrestrial respiration, aquatic respiration and weathering, *Glob. Chang. Biol.*, 16(7), 1966–1978, doi:10.1111/j.1365-2486.2009.02092.x.
- Hunt, R. J., T. D. Jardine, S. K. Hamilton, and S. E. Bunn (2012), Temporal and spatial variation in ecosystem metabolism and food web carbon transfer in a wet-dry tropical river, *Freshw. Biol.*, 57(3), 435–450, doi:10.1111/j.1365-2427.2011.02708.x.
- Iglesias, A., L. Garrote, F. Flores, and M. Moneo (2007), Challenges to manage the risk of water scarcity and climate change in the Mediterranean, *Water Resour. Manag.*, 21(5), 775–788, doi:10.1007/s11269-006-9111-6.
- IPCC (2001). *Climate Change 2001: Synthesis Report, A Contribution of Working Groups I, II, and III to the Third Assessment Report of the Intergovernmental Panel on Climate Change*, edited by: Watson, R. T. and the Core Writing Team, Cambridge University Press, Cambridge, United Kingdom, and New York, NY, USA, 398 pp., 2001.
- IPCC (2013). *Climate Change 2013: The Physical Science Basis. Contribution of Working Group I to the Fifth Assessment Report of the Intergovernmental Panel on Climate Change* [Stocker, T.F., D. Qin, G.-K. Plattner, M. Tignor, S.K. Allen, J. Boschung, A. Nauels, Y. Xia, V. Bex and P.M. Midgley (eds.)]. Cambridge University Press, Cambridge, United Kingdom and New York, NY, USA.

- Jacobson, P., K. . Jacobson, P. Angermeier, and D. Cherry (2000), Hydrologic influences on soil properties along ephemeral rivers in the Namib Desert, *J. Arid Environ.*, 45(1), 21–34, doi:10.1006/jare.1999.0619.
- Jaffé, R., D. McKnight, N. Maie, R. Cory, W. H. McDowell, and J. L. Campbell (2008), Spatial and temporal variations in DOM composition in ecosystems: The importance of long-term monitoring of optical properties, *J. Geophys. Res. Biogeosciences*, 113(4), 1–15, doi:10.1029/2008JG000683.
- Jähne, B., and K. Münnich (1987), On the parameters influencing air-water gas exchange, *J. Geophys. Res. Ocean.*, 92(2), 1937–1942, doi:10.1029/JC092iC02p01937.
- Jones, J. B., and P. J. Mulholland (1998), Methane input and evasion in a hardwood forest stream: Effects of subsurface flow from shallow and deep flowpaths, *Limnol. Oceanogr.*, 43(6), 1243–1250, doi:10.4319/lo.1998.43.6.1243.
- Jonsson, A., G. Algesten, A.K. Bergström, K. Bishop, S. Sobek, L. J. Tranvik, and M. Jansson (2007), Integrating aquatic carbon fluxes in a boreal catchment carbon budget, *J. Hydrol.*, 334(1–2), 141–150, doi:10.1016/j.jhydrol.2006.10.003.
- Kaiser, M., M. Kleber, and A. A. Berhe (2015), How air-drying and rewetting modify soil organic matter characteristics: An assessment to improve data interpretation and inference, *Soil Biol. Biochem.*, 80, 324–340, doi:10.1016/j.soilbio.2014.10.018.
- Keller, M., and R. F. Stallard (1994), Methane emission by bubbling from Gatun Lake, Panama, *J. Geophys. Res.*, 99(D4), 8307–8319, doi:10.1029/92JD02170.
- Kemenes, A., B. R. Forsberg, and J. M. Melack (2007), Methane release below a tropical hydroelectric dam, *Geophys. Res. Lett.*, 34(12), 1–5, doi:10.1029/2007GL029479.
- Kirschke, S. et al. (2013), Three decades of global methane sources and sinks, *Nat. Geosci.*, 6, 813–823, doi:10.1038/ngeo1955.
- Kling, G. W., G. W. Kipphut, and M. C. Miller (1991), Arctic lakes and streams as gas conduits to the atmosphere: implications for tundra carbon budgets., *Science*, 251(4991), 298–301, doi:10.1126/science.251.4991.298.
- Koehler, B., T. Landelius, G. A. Weyhenmeyer, N. Machida, and L. J. Tranvik (2014), Sunlight-induced carbon dioxide emissions from inland waters, *Glob. Biogeochem. Cycles*, 28, 696–711, doi:10.1002/2014GB004850.
- Kocic, J., and M. Wallin (2015), Carbon dioxide evasion from headwater systems strongly contributes to the total export of carbon from a small boreal lake catchment, *J. Geophys. Res. Biogeosciences*, 120(1), 13–28, doi:10.1002/2014JG002706.

- Kondolf, M. G., and R. J. Batalla (2005), Chapter 11 Hydrological effects of dams and water diversions on rivers of Mediterranean-climate regions: examples from California, *Dev. Earth Surf. Process.*, 7, 197–211, doi:10.1016/S0928-2025(05)80017-3.
- Koschorreck, M., and A. Darwich (2003), Nitrogen dynamics in seasonally flooded soils in the Amazon floodplain, *Wetl. Ecol. Manag.*, 11, 317–330, doi:10.1023/B:WETL.0000005536.39074.72.
- Kothawala, D. N., K. R. Murphy, C. A. Stedmon, G. A. Weyhenmeyer, and L. J. Tranvik (2013), Inner filter correction of dissolved organic matter fluorescence, *Limnol. Oceanogr. Methods*, 11(DEC), 616–630, doi:10.4319/lom.2013.11.616.
- Kirk J.T.O., (1994), *Light and photosynthesis in aquatic ecosystems*. Cambridge University Press, Cambridge
- Lapierre, J.-F., F. Guillemette, M. Berggren, and P. a Del Giorgio (2013), Increases in terrestrially derived carbon stimulate organic carbon processing and CO₂ emissions in boreal aquatic ecosystems., *Nat. Commun.*, 4, 2972, doi:10.1038/ncomms3972.
- Lake P. S. (2011), *Drought and aquatic ecosystems: effects and responses*. Wiley-Blackwell, Chichester
- Larned, S. T., T. Datry, D. B. Arscott, and K. Tockner (2010), Emerging concepts in temporary-river ecology, *Freshw. Biol.*, 55(4), 717–738, doi:10.1111/j.1365-2427.2009.02322.x.
- Lauerwald, R., G. G. Laruelle, J. Hartmann, P. Ciais, and P. a. G. Regnier (2015), Spatial patterns in CO₂ evasion from the global river network, *Global Biogeochem. Cycles*, n/a-n/a, doi:10.1002/2014GB004941.
- Laurion, I., W. F. Vincent, S. MacIntyre, L. Retamal, C. Dupont, P. Francus, and R. Pienitz (2010), Variability in greenhouse gas emissions from permafrost thaw ponds, *Limnol. Oceanogr.*, 55(1), 115–133, doi:10.4319/lo.2010.55.1.0115.
- Lehner, B. et al. (2011), High-resolution mapping of the world's reservoirs and dams for sustainable river-flow management, *Front. Ecol. Environ.*, 9(9), 494–502, doi:10.1890/100125.
- Leigh, C., A. J. Boulton, J. L. Courtwright, K. Fritz, C. L. May, R. H. Walker, and T. Datry (2016), Ecological research and management of intermittent rivers: an historical review and future directions, *Freshw. Biol.*, 61(8), 1181–1199, doi:10.1111/fwb.12646.
- Leith, F. I., K. J. Dinsmore, M. B. Wallin, M. F. Billett, K. V. Heal, H. Laudon, M. G. Öquist, and K. Bishop (2015), Carbon dioxide transport across the hillslope-riparian-stream continuum in a boreal headwater catchment, *Biogeosciences*, 12(6), 1881–1902, doi:10.5194/bg-12-1881-2015.

- Lewis, E., and D. W. R. Wallace (1998), Program Developed for CO₂ System Calculations. ORNL/CDIAC-105, Carbon dioxide Information Analysis Center, Oak Ridge Natl. Lab. Oak Ridge, Tenn.
- Liang, X., X. Zhang, Q. Sun, C. He, X. Chen, X. Liu, and Z. Chen (2016), The role of filamentous algae *Spirogyra* spp. in methane production and emissions in streams, *Aquat. Sci.*, 78(2), 227–239, doi:10.1007/s00027-015-0419-2.
- Likens, G. E., A. Enrich-Prast, D. Bastviken, and P. Crill (2009), Chemosynthesis, *Encycl. Inl. Waters*, (1), 211–225, doi:10.1016/B978-012370626-3.00126-5.
- Livingston GP, Hutchinson GL. (1995), Enclosure-based measurement of trace gas exchange: applications and sources of error. Matson PA, Harriss RC, editors. *Biogenic Trace Gases: Measuring Emissions From Soil and Water*. Oxford: Blackwell Scientific Publications. pp. 14–51
- Long, H., L. Vihermaa, S. Waldron, T. Hoey, S. Quemin, and J. Newton (2015), Hydraulics are a first-order control on CO₂ efflux from, doi:10.1002/2015JG002955. Received.
- López, P., R. Marcé, and J. Armengol (2011), Net heterotrophy and CO₂ evasion from a productive calcareous reservoir: Adding complexity to the metabolism-CO₂ evasion issue, *J. Geophys. Res.*, 116(G2), G02021, doi:10.1029/2010JG001614.
- Lowe, W. H., G. E. Likens, and M. E. Power (2006), Linking Scales in Stream Ecology, *Bioscience*, 56(7), 591, doi:10.1641/0006-3568(2006)56[591:LSISE]2.0.CO;2.
- Lulla, K., (1987), Mediterranean climate. In *Encyclopedia of Climatology*, ed. JE Oliver, RW Fairbridge, New York; Van Nostrand Reinhold, 986 pp.
- Lundin, E. J., R. Giesler, A. Persson, M. S. Thompson, and J. Karlsson (2013), Integrating carbon emissions from lakes and streams in a subarctic catchment, *J. Geophys. Res. Biogeosciences*, 118(3), 1200–1207, doi:10.1002/jgrg.20092.
- Luo, Y., and X. Zhou (2010), *Soil respiration and the environment*, edited by Academy Press, Elsevier.
- Maberly, S. C., P. a. Barker, A. W. Stott, and M. M. De Ville (2012), Catchment productivity controls CO₂ emissions from lakes, *Nat. Clim. Chang.*, 3(4), 391–394, doi:10.1038/nclimate1748.
- MacIntyre, S., W. Eugster, and G. W. Kling (2002), The Critical Importance of Buoyancy Flux for Gas Flux Across the Air-water Interface, *Gas Transf. Water Surfaces, Geophys. Monogr. Ser.*, vol. 127, 135–139, doi:10.1029/GM127.
- Maeck, A., T. Delsontro, D. F. McGinnis, H. Fischer, S. Flury, M. Schmidt, P. Fietzek, and A. Lorke (2013), Sediment trapping by dams creates methane

- emission hot spots., *Environ. Sci. Technol.*, 47(15), 8130–7, doi:10.1021/es4003907.
- Maeck, A., H. Hofmann, and A. Lorke (2014), Pumping methane out of aquatic sediments – ebullition forcing mechanisms in an impounded river, *Biogeosciences*, 11(11), 2925–2938, doi:10.5194/bg-11-2925-2014.
- Marcé, R., B. Obrador, J. Morguá, J. L. Riera, P. López, and J. Armengol (2015), Carbonate weathering as a driver of CO₂ supersaturation in lakes, *Nat. Geosci.*, 8, 107–111, doi:10.1038/NGEO2341.
- McClain, M. E. et al. (2003), Biogeochemical Hot Spots and Hot Moments at the Interface of Terrestrial and Aquatic Ecosystems, *Ecosystems*, 6(4), 301–312, doi:10.1007/s10021-003-0161-9.
- McDonald, C. P., E. G. Stets, R. G. Striegl, and D. Butman (2013), Inorganic carbon loading as a primary driver of dissolved carbon dioxide concentrations in the lakes and reservoirs of the contiguous United States, *Global Biogeochem. Cycles*, 27(2), 285–295, doi:10.1002/gbc.20032.
- McGinnis, D. F., G. Kirillin, K. W. Tang, S. Flury, P. Bodmer, C. Engelhardt, P. Casper, and H.-P. Grossart (2015), Enhancing Surface Methane Fluxes from an Oligotrophic Lake: Exploring the Microbubble Hypothesis, *Environ. Sci. Technol.*, 49(2), 873–880, doi:10.1021/es503385d.
- McGuire, K. J., C. E. Torgersen, G. E. Likens, D. C. Buso, W. H. Lowe, and S. W. Bailey (2014), Network analysis reveals multiscale controls on streamwater chemistry, *Proc Natl Acad Sci U S A*, 111(19), 7030–7035, doi:10.1073/pnas.1404820111\r1404820111 [pii].
- McIntyre, R. E. S., M. A. Adams, D. J. Ford, and P. F. Grierson (2009), Rewetting and litter addition influence mineralisation and microbial communities in soils from a semi-arid intermittent stream, *Soil Biol. Biochem.*, 41(1), 92–101, doi:10.1016/j.soilbio.2008.09.021.
- McLain, J. E. T., and D. a. Martens (2006), Moisture Controls on Trace Gas Fluxes in Semiarid Riparian Soils, *Soil Sci. Soc. Am. J.*, 70(2), 367, doi:10.2136/sssaj2005.0105.
- Megonigal, J. P., M. E. Hines, and P. T. Visscher (2004), Anaerobic Metabolism: Linkages to Trace Gases and Aerobic Processes, *Biogeochemistry*, 317–424..
- Meier, J. A., J. S. Jewell, C. E. Brennen, and J. Imberger (2011), Bubbles emerging from a submerged granular bed, *J. Fluid Mech.*, 666(1), 189–203, doi:10.1017/S002211201000443X.
- Melton, J. R. et al. (2013), Present state of global wetland extent and wetland methane modelling: Methodology of a model inter-comparison project (WETCHIMP), *Biogeosciences*, 10, 753–788, doi:10.5194/gmd-6-617-2013.

- Merbt, S. N., L. Proia, J. I. Prosser, E. Martí, E. O. Casamayor, and D. von Schiller (2016), Stream drying drives microbial ammonia oxidation and first-flush nitrate export, *Ecology*, 97(9), 2192–2198, doi:10.1002/ecy.1486.
- Meybeck, M., H. Dürr, and C. Vörösmarty (2006), Global coastal segmentation and its river catchment contributors: A new look at land-ocean linkage, *Global Biogeochem. Cycles*, 20(1), GB1S90, doi:10.1029/2005GB002540.
- Mielnick, P. C., and W. a. Dugas (2000), Soil CO₂ flux in a tallgrass prairie, *Soil Biol. Biochem.*, 32(2), 221–228, doi:10.1016/S0038-0717(99)00150-9.
- Millero, F. (1995), Thermodynamics of the carbon dioxide system in the oceans, *Geochim. Cosmochim. Acta*, 59(4), 661–677, doi:10.1016/0016-7037(94)00354-O.
- Milliman, J. D., K. L. Farnsworth, P. D. Jones, K. H. Xu, and L. C. Smith (2008), Climatic and anthropogenic factors affecting river discharge to the global ocean, 1951-2000, *Glob. Planet. Change*, 62(3–4), 187–194, doi:10.1016/j.gloplacha.2008.03.001.
- Mitchell, A. M., and D. S. Baldwin (1999), The effects of sediment desiccation on the potential for nitrification, denitrification, and methanogenesis in an Australian reservoir, (1973), 3–11.
- Mitsch, W. J., B. Bernal, A. M. Nahlik, Ü. Mander, L. Zhang, C. J. Anderson, S. E. Jørgensen, and H. Brix (2013), Wetlands, carbon, and climate change, *Landsc. Ecol.*, 28(4), 583–597, doi:10.1007/s10980-012-9758-8.
- Montgomery, D. R. (1999), Process domains and the river continuum, *J. Am. Water Resour. Assoc.*, 35(2), 397–410, doi:10.1111/j.1752-1688.
- Morales-Pineda, M. (2014), Daily, biweekly, and seasonal temporal scales of pCO₂ variability in two stratified Mediterranean reservoirs, *J. Geophys. Res. Biogeosciences*, 119(4), 1–12, doi:10.1002/2013JG002317.
- Mulholland, P. J., and J. W. Elwood (1982), The role of lake and reservoir sediments as sinks in the perturbed global carbon cycle, *Tellus A*, 34(5), 490–499, doi:10.3402/tellusa.v34i5.10834.
- Murray, S. J., P. N. Foster, and I. C. Prentice (2012), Future global water resources with respect to climate change and water withdrawals as estimated by a dynamic global vegetation model, *J. Hydrol.*, 448–449, 14–29, doi:10.1016/j.jhydrol.2012.02.044.
- Naiman, R. J., and H. Decamps (1997), The ecology of interfaces: Riparian zones, *Annu. Rev. Ecol. Syst.*, 28(102), 621–658, doi:10.1146/annurev.ecolsys.28.1.621.
- Nilsson, C., C. Reidy, M. Dynesius, and C. Revenga (2005), Fragmentation and flow regulation of the world's large river systems, *Science*, 266(5720), 405–408, doi:10.1126/science.1107887.

- Nõges, P., F. Cremona, A. Laas, T. Martma, E. I. Rõõm, K. Toming, M. Viik, S. Vilbaste, and T. Nõges (2016), Role of a productive lake in carbon sequestration within a calcareous catchment, *Sci. Total Environ.*, 550, 225–230, doi:10.1016/j.scitotenv.2016.01.088.
- Noy-Meir, I. (1973), Desert Ecosystems: Environment and Producers, *Annu. Rev. Ecol. Syst.*, 4(1), 25–51, doi:10.1146/annurev.es.04.110173.000325.
- Obrador, B., and J. L. Pretus (2013), Carbon and oxygen metabolism in a densely vegetated lagoon: implications of spatial heterogeneity, *Limnetica*, 32(2), 321–336.
- Oksanen, J., Blanchet FG, Kindt R, et al., (2016), *vegan: Community Ecology Package*. R package version 2.0-10. <http://CRAN.R-project.org/package=vegan>
- Öquist, M. G., M. Wallin, J. Seibert, K. Bishop, and H. Laudon (2009a), Dissolved inorganic carbon export across the soil/stream interface and its fate in a boreal headwater stream, *Environ. Sci. Technol.*, 43(19), 7364–7369, doi:10.1021/es900416h.
- Otsuki, A., and R. G. Wetzel (1974), Calcium and total alkalinity budgets and calcium carbonate precipitation in a small hardwater lake, *Arch. Hydrobiol.*, 73,14–30.
- Palmer, M. a., C. a. Reidy Liermann, C. Nilsson, M. Flörke, J. Alcamo, P. S. Lake, and N. Bond (2008), Climate change and the world’s river basins: Anticipating management options, *Front. Ecol. Environ.*, 6(2), 81–89, doi:10.1890/060148.
- Paré, M. C., and A. Bedard-Haughn (2013), Soil organic matter quality influences mineralization and GHG emissions in cryosols: A field-based study of sub- to high Arctic, *Glob. Chang. Biol.*, 19(4), 1126–1140, doi:10.1111/gcb.12125.
- Pascual, D., E. Pla, J. A. Lopez-Bustins, J. Retana, J. Terradas, T. Estrela, M. a Perez-Martin, and E. Vargas (2015), Impacts of climate change on water resources in the Mediterranean Basin: a case study in Catalonia, Spain, *Hydrol. Sci. J.*, 57(12), 1154–1167, doi:10.1080/02626667.2012.702213.
- Pavón, D. (2010), Desarrollo y decadencia hidroeléctrica en los pequeños ríos del litoral mediterráneo catalán. El caso de las cuencas del Fluvià y de la Muga, *Rev. Hist. Ind.*, 42(1), 43–87.
- Peter, H., G. Singer, C. Preiler, P. Chiffard, G. Steniczka, and T. J. Battin (2014), Scales and drivers of temporal pCO₂ dynamics in an Alpine stream, *J. Geophys. Res. Biogeosciences*, 120, 1–12, doi:10.1002/2013JG002552.Received.
- Poff, N. L., and D. D. Hart (2002), How Dams Vary and Why It Matters for the Emerging Science of Dam Removal, *Bioscience*, 52(8), 659–668, doi:10.1641/0006-3568(2002)052[0659:HDVAWI]2.0.CO;2.

- Pohlon, E., A. Ochoa Fandino, and J. Marxsen (2013), Bacterial Community Composition and Extracellular Enzyme Activity in Temperate Streambed Sediment during Drying and Rewetting., *PLoS One*, 8(12), e83365, doi:10.1371/journal.pone.0083365.
- Ponsatí, L., V. Acuña, I. Aristi, E. García-Berthou, D. von Schiller, A. Elosegí, and S. Sabater (2015), Biofilm Responses to Flow Regulation by Dams in Mediterranean Rivers, *River Res. Appl.*, 31, 1003–1016, doi:10.1002/rra.
- Poole, G. C. (2002), Fluvial landscape ecology: Addressing uniqueness within the river discontinuum, *Freshw. Biol.*, 47(4), 641–660, doi:10.1046/j.1365-2427.2002.00922.x.
- Prairie, Y., and P. del Giorgio (2013), A new pathway of freshwater methane emissions and the putative importance of microbubbles, *Inl. Waters*, 311–320, doi:10.5268/IW-3.3.542.
- Proia, L., D. von Schiller, C. Gutierrez, J. P. Casas-Ruiz, L. Gómez-Gener, R. Marcé, B. Obrador, V. Acuña, and S. Sabater (2016), Microbial carbon processing along a river discontinuum, *Freshw. Sci.*, 35, 000–000, doi:10.1086/689181.
- Pullman, W. M. (1992), Carbon dioxide and methane exports from a southeastern floodplain swamp, *Ecol. Monogr.*, 63(1), 29–53.
- Le Quéré, C. et al. (2016), Global Carbon Budget 2016, *Earth Syst. Sci. Data Discuss.*, 1–3, doi:10.5194/essd-2016-51.
- Raich, J., and W. Schlesinger (1992), The global carbon dioxide flux in soil respiration and its relationship to vegetation and climate, *Tellus B*, 44(2), 81–99, doi:10.1034/j.1600-0889.1992.t01-1-00001.x.
- Raich, J., C. Potter, and D. Bhagawati (2002), Interannual variability in global soil respiration, 1980–94, *Glob. Chang. Biol.*, 8(8), 800–812, doi:10.3334/CDIAC/lue.ndp081.
- Raymond, P. A., C. J. Zappa, D. Butman, T. L. Bott, J. Potter, P. Mulholland, A. E. Laursen, W. H. McDowell, and D. Newbold (2012), Scaling the gas transfer velocity and hydraulic geometry in streams and small rivers, *Limnol. Oceanogr. Fluids Environ.*, 2(0), 41–53, doi:10.1215/21573689-1597669.
- Raymond, P. A. et al. (2013), Global carbon dioxide emissions from inland water, *Nature*, 503(7476), 355–359, doi:10.1038/nature12760.
- Raymond, P. A., J. E. Saiers, and W. V Sobczak (2015), Hydrological and biogeochemical controls on watershed dissolved organic matter transport: Pulse-shunt concept, *Ecology*, doi:10.1890/14-1684.1.
- R Core Team (2016), R: A language and environment for statistical computing. R Foundation for Statistical Computing, Vienna, Austria. ISBN:3-900051-07-0, (URL: <http://www.R-project.org/>)

- Redeker, K. R., A. J. Baird, and Y. A. Teh (2015), Quantifying wind and pressure effects on trace gas fluxes across the soil–atmosphere interface, *Biogeosciences Discuss.*, 12(6), 4801–4832, doi:10.5194/bg-d-12-4801-2015.
- Reeburgh, W. (2007), Oceanic methane biogeochemistry, *Am. Chem. Soc.*, 107(2), 486–513, doi:10.1021/cr050362v.
- Regnier, P. et al. (2013), Anthropogenic perturbation of the carbon fluxes from land to ocean, *Nat. Geosci.*, 6(8), 597–607, doi:10.1038/ngeo1830.
- Rey, A. (2015), Mind the gap: Non-biological processes contributing to soil CO₂ efflux, *Glob. Chang. Biol.*, 21(5), 1752–1761, doi:10.1111/gcb.12821.
- Richey, J. E., A. H. Devol, S. C. Wofsy, R. Victoria, and M. N. G. Riberio (1988), Biogenic gases and the oxidation and reduction of carbon in Amazon River and floodplain waters, *Limnol. Oceanogr.*, 33(4), 551–561, doi:10.4319/lo.1988.33.4.0551.
- Richey, J. E., J. M. Melack, A. K. Aufdenkampe, V. M. Ballester, and L. L. Hess (2002), Outgassing from Amazonian rivers and wetlands as a large tropical source of atmospheric CO₂, *Nature*, 416(6881), 617–20, doi:10.1038/416617a.
- Riley, A. J., and W. K. Dodds (2013), Whole-stream metabolism: strategies for measuring and modeling diel trends of dissolved oxygen, *Freshw. Sci.*, 32(1), 56–69, doi:10.1899/12-058.1.
- Rutgersson, A., and A. Smedman (2010), Enhanced air-sea CO₂ transfer due to water-side convection, *J. Mar. Syst.*, 80(1–2), 125–134, doi:10.1016/j.jmarsys.2009.11.004.
- Sabater, S. (2008), Alterations of the global water cycle and their effects on river structure, function and services, *Freshw. Rev.*, 1(1), 75–88, doi:10.1608/FRJ-1.1.5.
- Siegenthaler, U., Sarmiento, J., (1993), Atmospheric carbon dioxide and the ocean. *Nature* 365, 119–125, doi:10.1038/365119a0.
- Tsivoglou, E. C., and L. A. Neal (1976), Tracer measurement of reaeration: III. Predicting the reaeration capacity of inland streams, *J. Water Pollut. Control Fed.*, 48(12), 2669–2689.
- Schindler, J. E., and D. P. Krabbenhoft (1998), The Hyporheic Zone as a Source of Dissolved Organic Carbon Gases to a Temperate Forest Stream, *Biogeochemistry*, 43(2), 157–174, doi:10.1023/A:1006005311257.
- Segarra, K. E. A., F. Schubotz, V. Samarkin, M. Y. Yoshinaga, K.-U. Hinrichs, and S. B. Joye (2015), High rates of anaerobic methane oxidation in freshwater wetlands reduce potential atmospheric methane emissions, *Nat. Commun.*, 6, 7477, doi:10.1038/ncomms8477.
- Sheldon, F., S. E. Bunn, J. M. Hughes, A. H. Arthington, S. R. Balcombe, and C. S. Fellows (2010), Ecological roles and threats to aquatic refugia in arid

- landscapes: Dryland river waterholes, *Mar. Freshw. Res.*, 61(8), 885–895, doi:10.1071/MF09239.
- Smith, K., T. Ball, and F. Conen (2003), Exchange of greenhouse gases between soil and atmosphere: interactions of soil physical factors and biological processes, *Eur. J. ...*, 54(4), 779–791, doi:10.1046/j.1365-2389.2003.00567.x.
- Sobek, S., and G. Algesten (2003), The catchment and climate regulation of pCO₂ in boreal lakes, *Glob. Chang. Biol.*, 9(4), 630–641, doi:10.1046/j.1365-2486.2003.00619.x.
- Sobek, S., R. Zurbrügg, and I. Ostrovsky (2011), The burial efficiency of organic carbon in the sediments of Lake Kinneret, *Aquat. Sci.*, 73(3), 355–364, doi:10.1007/s00027-011-0183-x.
- Sobek, S., T. DelSontro, N. Wongfun, and B. Wehrli (2012), Extreme organic carbon burial fuels intense methane bubbling in a temperate reservoir, *Geophys. Res. Lett.*, 39(1), 2–5, doi:10.1029/2011GL050144.
- Sponseller, R. (2007), Precipitation pulses and soil CO₂ flux in a Sonoran Desert ecosystem, *Glob. Chang. Biol.*, 426–436, doi:10.1111/j.1365-2486.2006.01307.x.
- Staehr, P. a., J. M. Testa, W. M. Kemp, J. J. Cole, K. Sand-Jensen, and S. V. Smith (2012), The metabolism of aquatic ecosystems: History, applications, and future challenges, *Aquat. Sci.*, 74(1), 15–29, doi:10.1007/s00027-011-0199-2.
- Stamp, I., A. J. Baird, and C. M. Heppell (2013), The importance of ebullition as a mechanism of methane (CH₄) loss to the atmosphere in a northern peatland, *Geophys. Res. Lett.*, 40(10), 2087–2090, doi:10.1002/grl.50501.
- Stanford, J. A., and J. V Ward (2001), Revisiting the serial discontinuity concept, *Regul. Rivers-Research Manag.*, 17(4–5), 303–310, doi:Doi 10.1002/Rrr.659.Abs.
- Stanley, E., S. Fisher, and N. Grimm (1997), Ecosystem expansion and contraction in streams, *Bioscience*, 47(1), 427–435, doi:10.2307/1313058.
- Stanley, E. H., N. J. Casson, C. S. T., J. T. Crawford, L. C. Loken, and S. K. Oliver (2016), The ecology of methane in streams and rivers : patterns , controls , and global significance, *Ecol. Monogr.*, 86, 146–171, doi:10.1890/15-1027.1.
- Stets, E. G., R. G. Striegl, G. R. Aiken, D. O. Rosenberry, and T. C. Winter (2009), Hydrologic support of carbon dioxide flux revealed by whole-lake carbon budgets, *J. Geophys. Res. Biogeosciences*, 114(1), 1–14, doi:10.1029/2008JG000783.
- Steward, A. L., D. von Schiller, K. Tockner, J. C. Marshall, and S. E. Bunn (2012), When the river runs dry: human and ecological values of dry riverbeds, *Front. Ecol. Environ.*, 10(4), 202–209, doi:10.1890/110136.

- St. Louis, V. L., C. a. Kelly, É. Duchemin, J. W. M. Rudd, and D. M. Rosenberg (2000), Reservoir Surfaces as Sources of Greenhouse Gases to the Atmosphere: A Global Estimate, *Bioscience*, 50(9), 766, doi:10.1641/0006-3568(2000)050[0766:RSASOG]2.0.CO;2.
- Striegl, R. G., M. M. Dornblaser, C. P. McDonald, J. R. Rover, and E. G. Stets (2012), Carbon dioxide and methane emissions from the Yukon River system, *Global Biogeochem. Cycles*, 26(4), GB0E05, doi:10.1029/2012GB004306.
- Suleau, M., A. Debacq, V. Dehaes, and M. Aubinet (2009), Wind velocity perturbation of soil respiration measurements using closed dynamic chambers, *Eur. J. Soil Sci.*, 60(4), 515–524, doi:10.1111/j.1365-2389.2009.01141.x.
- Syvitski, J., C. Vörösmarty, K. AJ, and P. Green (2005), Impact of Humans on the Flux of Terrestrial Sediment to the Global Coastal Ocean, *Science (80-.)*, 308(5720), 376–380.
- Tang, K. W., D. G. McGinnis, K. Frindte, V. Brüchert, and H.-P. Grossart (2014), Paradox reconsidered: Methane oversaturation in well-oxygenated lake waters, *Limnol. Oceanogr.*, 59(1), 275–284, doi:10.4319/lo.2014.59.1.0275.
- Tank, J. J. L., E. J. E. Rosi-Marshall, N. a. Griffiths, S. a. Entekin, and M. L. Stephen (2010), A review of allochthonous organic matter dynamics and metabolism in streams, *J. North Am. Benthol. Soc.*, 29(1), 118–146, doi:10.1899/08-170.1.
- Teodoru, C. R., Y. T. Prairie, and P. a. del Giorgio (2010), Spatial Heterogeneity of Surface CO₂ Fluxes in a Newly Created Eastmain-1 Reservoir in Northern Quebec, Canada, *Ecosystems*, 14(1), 28–46, doi:10.1007/s10021-010-9393-7.
- Teodoru, C. R., F. C. Nyoni, A. V. Borges, F. Darchambeau, I. Nyambe, and S. Bouillon (2015), Dynamics of greenhouse gases (CO₂, CH₄, N₂O) along the Zambezi River and major tributaries, and their importance in the riverine carbon budget, *Biogeosciences*, 12(8), 2431–2453, doi:10.5194/bg-12-2431-2015.
- Thornton KW, Kimmel BL, Payne FE (1990), *Reservoir limnology: Ecological perspectives*. JohnWiley, New York
- Timoner, X., V. Acuña, D. Von Schiller, and S. Sabater (2012), Functional responses of stream biofilms to flow cessation, desiccation and rewetting, *Freshw. Biol.*, 57(8), 1565–1578, doi:10.1111/j.1365-2427.2012.02818.x.
- Timoner, X., V. Acuña, L. Frampton, P. Pollard, S. Sabater, and S. E. Bunn (2014), Biofilm functional responses to the rehydration of a dry intermittent stream, *Hydrobiologia*, 727(1), 185–195, doi:10.1007/s10750-013-1802-4.
- Tockner, K., U. Uehlinger, C. T. Robinson, and J.-P. Descy (2009), *Rivers of Europe*, Elsevier.

- Tooth, S. (2000), Process, form and change in dry land rivers: a review of recent research, 51, 67–107.
- Torgersen, T., and B. Branco (2007), Carbon and oxygen dynamics of shallow aquatic systems: Process vectors and bacterial productivity, *J. Geophys. Res.*, 112(G3), G03016, doi:10.1029/2007JG000401.
- Townsend, C. R. (1989), The patch dynamics concept of stream community ecology. *Journal of the North American Benthological Society* 8:36–50.
- Tranvik, L., J. Downing, and J. Cotner (2009), Lakes and reservoirs as regulators of carbon cycling and climate, *Limnol. Oceanogr.*, 54(1), 2298–2314, doi:10.4319/lo.2009.54.6_part_2.2298.
- Trimmer, M., J. Grey, C. M. Heppell, A. G. Hildrew, K. Lansdown, H. Stahl, and G. Yvon-Durocher (2012), River bed carbon and nitrogen cycling: State of play and some new directions, *Sci. Total Environ.*, 434, 143–158, doi:10.1016/j.scitotenv.2011.10.074.
- Vachon, D., Y. T. Prairie, and J. J. Cole (2010), The relationship between near-surface turbulence and gas transfer velocity in freshwater systems and its implications for floating chamber measurements of gas exchange, *Limnol. Oceanogr.*, 55(4), 1723–1732, doi:10.4319/lo.2010.55.4.1723.
- Vachon, D., Y. Prairie, and R. Smith (2013), The ecosystem size and shape dependence of gas transfer velocity versus wind speed relationships in lakes, *Can. J. Fish. Aquat. Sci.*, 1764, 1757–1764.
- Vachon, D., J.-F. Lapierre, and P. A. del Giorgio (2016), Seasonality of photochemical dissolved organic carbon mineralization and its relative contribution to pelagic CO₂ production in northern lakes, *J. Geophys. Res. Biogeosciences*, , doi:10.1002/2015JG003244.
- Van de Bogert, M. C., S. R. Carpenter, J. J. Cole, and M. L. Pace (2007), Assessing pelagic and benthic metabolism using free water measurements, *Limnol. Oceanogr.*, 5, 145–155, doi:10.4319/lom.2007.5.145.
- Vannote, R. L., G. W. Minshall, K. W. Cummins, J. R. Sedell, and C. E. Cushing (1980), The River Continuum Concept, *Can. J. Fish. Aquat. Sci.*, 37(1), 130–137, doi:10.1139/f80-017.
- Vazquez, E., S. Amalfitano, S. Fazi, and A. Butturini (2010), Dissolved organic matter composition in a fragmented Mediterranean fluvial system under severe drought conditions, *Biogeochemistry*, 102(1–3), 59–72, doi:10.1007/s10533-010-9421-x.
- Vergnoux, A., R. Di Rocco, M. Domeizel, M. Guiliano, P. Doumenq, and F. Théraulaz (2011), Effects of forest fires on water extractable organic matter and humic substances from Mediterranean soils: UV-vis and fluorescence spectroscopy approaches, *Geoderma*, 160(3–4), 434–443, doi:10.1016/j.geoderma.2010.10.014.

- Verpoorter, C., T. Kutser, D. A. Seekell, and L. J. Tranvik (2014), A global inventory of lakes based on high-resolution satellite imagery, *Geophys. Res. Lett.*, 41(18), 6396–6402, doi:10.1002/2014GL060641.
- von Schiller, D., V. Acuña, D. Graeber, E. Martí, M. Ribot, S. Sabater, X. Timoner, and K. Tockner (2011), Contraction, fragmentation and expansion dynamics determine nutrient availability in a Mediterranean forest stream, *Aquat. Sci.*, 73(4), 485–497, doi:10.1007/s00027-011-0195-6.
- von Schiller, D., R. Marcé, B. Obrador, L. Gómez-Gener, J. P. Casas-Ruiz, V. Acuña, and M. Koschorreck (2014), Carbon dioxide emissions from dry watercourses, *Inl. Waters*, 4(4), 377–382, doi:10.5268/IW-4.4.746.
- von Schiller, D., D. Graeber, M. Ribot, X. Timoner, V. Acuña, E. Martí, S. Sabater, and K. Tockner (2015), Hydrological transitions drive dissolved organic matter quantity and composition in a temporary Mediterranean stream, *Biogeochemistry*, 1–18, doi:10.1007/s10533-015-0077-4.
- von Schiller, D., I. Aristi, L. Ponsatí, M. Arroita, V. Acuña, A. Elozegi, and S. Sabater (2016), Regulation causes nitrogen cycling discontinuities in Mediterranean rivers, *Sci. Total Environ.*, 540, 168–177, doi:10.1016/j.scitotenv.2015.07.017.
- Vörösmarty, C. J. et al. (2010), Global threats to human water security and river biodiversity., *Nature*, 467(7315), 555–61, doi:10.1038/nature09440.
- Wagener, S. M., M. W. Oswood, and J. P. Schimel (1998), Rivers and Soils: Parallels in Carbon and Nutrient Processing, *Bioscience*, 48(2), 104–108, doi:10.2307/1313135.
- Wallin, M., I. Buffam, M. Öquist, H. Laudon, and K. Bishop (2010), Temporal and spatial variability of dissolved inorganic carbon in a boreal stream network: Concentrations and downstream fluxes, *J. Geophys. Res.*, 115(Dic), 1–12, doi:10.1029/2009JG001100.
- Wallin, M. B., M. G. Öquist, I. Buffam, M. F. Billett, J. Nisell, and K. H. Bishop (2011), Spatiotemporal variability of the gas transfer coefficient (K_{CO_2}) in boreal streams: Implications for large scale estimates of CO_2 evasion, *Global Biogeochem. Cycles*, 25(3), n/a-n/a, doi:10.1029/2010GB003975.
- Wallin, M. B., T. Grabs, I. Buffam, H. Laudon, A. Ågren, M. G. Öquist, and K. Bishop (2013), Evasion of CO_2 from streams - The dominant component of the carbon export through the aquatic conduit in a boreal landscape, *Glob. Chang. Biol.*, 19, 785–797, doi:10.1111/gcb.12083.
- Wanninkhof, R. (1992), Relationship between wind speed and gas exchange over the ocean, *J. Geophys. Res. Ocean.*, 97(92), 7373–7382, doi:10.1029/92JC00188.
- Ward, and Tockner (2001), Biodiversity: Towards a unifying theme for river ecology, *Freshw. Biol.*, 46(6), 807–819, doi:10.1046/j.1365-2427.2001.00713.x.

- Ward, J. V., and J. a Stanford (1983), Serial Discontinuity Concept of Lotic Ecosystems, *Dyn. Lotic Syst. Ann Arbor Sci. Ann Arbor*, 29–42.
- Wehrli, B. (2013), Conduits of the carbon cycle, *Nature*, 503(21), 9–10, doi:10.1038/503346a.
- Weishaar, J., G. Aiken, B. BA, and F. MS (2003), Evaluation of specific ultraviolet absorbance as an indicator of the chemical content of dissolved organic carbon, *Environ. Chem.*, 41(2), 843–845.
- Weiss, R. (1974), Carbon dioxide in water and seawater: the solubility of a non-ideal gas, *Mar. Chem.*, 2(3), 203–215, doi:10.1016/0304-4203(74)90015-2.
- Wetzel, R. G. (2001), *Limnology: Lake and River Ecosystems*, 3rd ed., Academic, San Diego, Calif.
- Weyhenmeyer, G. A., S. Kosten, M. B. Wallin, L. J. Tranvik, E. Jeppesen, and F. Roland (2015), Significant fraction of CO₂ emissions from boreal lakes derived from hydrologic inorganic carbon inputs, *Nat. Geosci.*, 8, 933–936, doi:doi:10.1038/ngeo2582.
- Wik, M., B. F. Thornton, D. Bastviken, J. Uhlbäck, and P. M. Crill (2016), Biased sampling of methane release from northern lakes: A problem for extrapolation, *Geophys. Res. Lett.*, 43, 1256–1260, doi:10.1002/2015GL066501..
- Wilkinson, G. M., C. D. Buelo, J. J. Cole, and M. L. Pace (2016), Exogenously produced CO₂ doubles the CO₂ efflux from three north temperate lakes, *Geophys. Res. Lett.*, 43(5), 1996–2003, doi:10.1002/2016GL067732.
- Williams D.D., (2006) *The Biology of Temporary Waters*. Oxford University Press, Oxford.
- Winterdahl, M., M. B. Wallin, R. H. Karlson, H. Laudon, M. Öquist, and S. W. Lyon (2016), De-coupling of carbon dioxide and dissolved organic carbon in boreal headwater streams, *J. Geophys. Res. Biogeosciences*, doi:10.1002/2016JG003420.
- Wold, S., M. Sjöström, and L. Eriksson (2001), PLS-regression: A basic tool of chemometrics, *Chemom. Intell. Lab. Syst.*, 58(2), 109–130, doi:10.1016/S0169-7439(01)00155-1.
- Xiao, S., D. Liu, Y. Wang, Z. Yang, and W. Chen (2013), Temporal variation of methane flux from Xiangxi Bay of the Three Gorges Reservoir., *Sci. Rep.*, 3(1), 1–8, doi:10.1038/srep02500.
- Xu, L., D. D. Baldocchi, and J. Tang (2004), How soil moisture, rain pulses, and growth alter the response of ecosystem respiration to temperature, *Global Biogeochem. Cycles*, 18(4), n/a-n/a, doi:10.1029/2004GB002281.

- Yamamoto, S., J. B. Alcauskas, and T. E. Crozier (1976), Solubility of Methane in Distilled Water and Sea Water, *J. Chem. Eng. Data*, 21(1), 78–80, doi:10.1021/je60068a029.
- Yavitt J. B., and A. K. Knapp (1995), Methane emission to the atmosphere through emergent cattail (*Typha latifolia* L.) plants, *Tellus B*, 47(5), 521–534, doi:10.1034/j.1600-0889.47.issue5.1.x.
- Yvon-Durocher, G. et al. (2012), Reconciling the temperature dependence of respiration across timescales and ecosystem types., *Nature*, 487(7408), 472–6, doi:10.1038/nature11205.
- Zaiss, U., P. Winter, and H. Kaltwasser (1982), Microbial methane oxidation in the River Saar. *Zeitschrift für Allgemeine Mikrobiologie* 22:139–148.
- Zappa, C. J., W. R. McGillis, P. A. Raymond, J. B. Edson, E. J. Hints, H. J. Zemmelen, J. W. H. Dacey, and D. T. Ho (2007), Environmental turbulent mixing controls on air-water gas exchange in marine and aquatic systems, *Geophys. Res. Lett.*, 34(10), 1–6, doi:10.1029/2006GL028790.
- Zarfl, C., A. E. Lumsdon, J. Berlekamp, L. Tydecks, and K. Tockner (2014), A global boom in hydropower dam construction, *Aquat. Sci.*, 77(1), 161–170, doi:10.1007/s00027-014-0377-0.
- Zoppini, A., and J. Marxsen (2011), Importance of extracellular enzymes for biogeochemical processes in temporary river sediments during fluctuating dry-wet Conditions. In: *Soil Enzymology* (Eds G. Shukla & A. Varma), pp. 103–117. Springer Verlag, Berlin, Heidelberg, edited by G. Shukla and A. Varma, , 22, doi:10.1007/978-3-642-14225-3.
- Zsolnay, A., E. Baigar, M. Jimenez, B. Steinweg, and F. Saccomandi (1999), Differentiating with fluorescence spectroscopy the sources of dissolved organic matter in soils subjected to drying, *Chemosphere*, 38(1), 45–50, doi:10.1016/S0045-6535(98)00166-0.
- Zuur, A. F., E. N. Ieno, and C. S. Elphick (2010), A protocol for data exploration to avoid common statistical problems, *Methods Ecol. Evol.*, 1(1), 3–14, doi:10.1111/j.2041-210X.2009.00001.x

Supporting Information

This section contains supporting information for Chapter 3, Chapter 4, Chapter 5, and Chapter 6 (**Appendix A**), supporting information for the Chapter 7 (**Appendix B**) and also provides the original publications of Chapter 3, Chapter 4 and Chapter 6 (proof version) (**Appendix C**).

Appendix A

Table A.3.1 Location, surface water physicochemistry and hydromorphological characteristics of the studied sites.

Figure A.4.1 Schematic drawing and examples of different sites sampled in the dry and in the flowing period.

Table A.5.1 Hydromorphological and physicochemical characterization of the 11 studied impoundments.

Figure A.5.1 CO₂ emission flux (CO₂ flux) as a function of the gas transfer velocity of CO₂ (k_{CO_2}) and CH₄ emission flux (CH₄ flux) as a function of the gas transfer velocity of CO₂ (k_{CO_2}) of the 11 study sites for the three different impoundment units (i.e., upstream river, impounded water and downstream river) during the three sampled seasons (i.e., spring, summer and winter).

Table A.5.2 Overview of potential explanatory variables of $pCO_{2,w}$ and $pCH_{4,w}$ included in partial least square (PLS) models.

Table A.5.3 Summary of partial least square (PLS) models produced for $pCO_{2,w}$ and $pCH_{4,w}$.

Figure A.6.1. Relationship between the k_{CO_2} derived from both the night-time regression method (NTR method; open circles; n=151) and the chamber method (filled circles; n=18) and the k_{CO_2} obtained from equation (2) in *Raymond et al.*, [2012].

Figure A.6.2. Examples of diel dissolved oxygen dynamics (red points) and model fit (black continuous line) for representative examples of lotic (top) and lentic (bottom) segments.

Figure A.6.3. Comparison of metabolic rates obtained in Chapter 6 and global metabolic rates for lotic aquatic ecosystems (i.e., streams and rivers) and lentic aquatic ecosystems (i.e., lakes and reservoirs).

Figure A.6.4. Variation of CO₂ emissions in lotic and lentic segments along the river longitudinal continuum.

Figure A.6.5. CO₂ emissions as a function of k_{CO_2} and surface water $p_{\text{CO}_2,w}$ for both lotic (blue circles) and lentic segments (green circles). Horizontal dashed lines represent $F_{\text{CO}_2 \text{ emission}}=0$. Vertical dashed line in (b) represents the average $p_{\text{CO}_2,a}$ for all the segments.

Table A.6.1. Hydromorphological characteristics of the 12 studied segments

Table A.6.2. Summary of metabolic rates of the 12 studied segments

Table A.3.1 Location, surface water physicochemistry and hydromorphological characteristics of the studied sites

Environment	Location				Surface water physicochemistry								Hydromorphologic characteristics			
	X (UTM)	Y	(UTM)	Stream order	Water temp. (°C)	Cond. ($\mu\text{S cm}^{-1}$)	pH	O ₂ (%)	DOC (mg L ⁻¹)	DIC (mg L ⁻¹)	DIN (mg L ⁻¹)	P-PO ₄ ³⁻ (mg L ⁻¹)	Mean width (m)	Mean depth (m)	Mean velocity (m s ⁻¹)	Discharge (m ³ s ⁻¹)
Running waters	478288.00	4669565.00		4	19.3	809	8.29	89.3	1.8	56.5	2.8	0.03	6.9	0.21	0.30	0.12
	466173.50	4672993.31		5	19.2	828	8.29	110.8	1.7	55.3	3.6	0.23	12.7	0.14	0.62	0.88
	504755.14	4669171.03		5	20.3	908	7.79	83.1	1.0	47.6	1.0	0.00	22.7	0.24	0.64	2.65
	466139.00	4683037.00		2	16.7	674	7.72	92.9	0.6	36.4	0.0	0.00	4.1	0.11	0.09	0.03
	488016.15	4671133.08		5	22.3	906	8.40	104.3	2.0	48.2	1.7	0.08	23.7	0.31	0.54	2.72
	455646.68	4669068.73		3	16.1	492	8.29	93.9	1.3	62.8	4.5	0.01	3.4	0.163	0.4	0.12
													Surface area (hm ²)	Volume (hm ³)	Residence time (h)	Mean depth (m)
Impounded waters	456466.28	4669282.00		3	16.8	507	8.13	76.8	1.8	58.1	3.5	0.03	1.2	0.017	39.8	2.50
	466121.25	4683366.22		2	17.2	674	8.40	104.2	0.7	35.5	0.0	0.00	0.1	0.001	5.1	1.52
	480532.44	4670540.79		5	21.7	788	8.24	82.5	3.5	44.3	1.9	0.11	10.9	0.171	49.7	1.82
	502182.40	4668511.88		5	22.8	845	8.21	136.2	1.4	46.9	0.9	0.00	3.7	0.027	3.7	1.14
	485882.00	4688563.00		4	23.9	323	8.25	86.2	3.2	29.3	0.0	0.00	256.0	37.999	4247.6	16.50
Isolated pools	454538.81	4664338.02		3	17.2	271	7.11	28.6	5.7	26.0	1.3	0.16	length (m)	(5-10)		
	454516.45	4664288.20		2	17.6	251	7.57	40.9	5.4	23.8	1.2	0.18	width (m)	(2-5)		
	454465.20	4664244.11		2	17.8	239	7.51	32.5	4.9	21.8	1.3	0.19	depth (m)	(0.5-2)		
	454432.07	4664233.22		3	20.7	217	7.42	22.9	15.5	18.8	0.9	0.15				
	454415.45	4664220.38		2	18.1	229	7.53	40.9	7.2	20.9	1.2	0.19				
Dry beds	454536.99	4664335.08		2												
	454868.32	4661578.51		2												
	486488.53	4688216.26		2												

Reported surface water physicochemical parameters are means of three measurements (n=3) at the same location where the flux measurements were carried out

Surface water temperature (Water temp.) and conductivity (Cond.) were measured with a portable probe (Cond 3310, WTW, Germany)

pH was measured with a portable probe (pH 3110, WTW, Germany)

Oxygen saturation (O₂) was measured with a portable probe (YSI ProODO Handheld, Yellow Springs, USA)

Dissolved organic and inorganic carbon concentrations in water (DOC and DIC) were measured from 0.45 μm -filtered water samples with a total organic carbon analyser (TOC-V CSH, Shimadzu, Japan). The samples for DOC determination were previously acidified to eliminate dissolved inorganic constituents

Ammonium concentration (NH₄⁺) was analysed with ion chromatography (IC5000, DIONEX, USA) using an anion-exchange column (IonPac® AS18, DIONEX, USA) Dissolved nitrite (NO₂⁻), nitrate (NO₃⁻) and phosphate (PO₄³⁻) concentrations were analysed with ion chromatography (IC5000, DIONEX, USA) using a cation-exchange column (IonPac® CS16, DIONEX, USA). Dissolved inorganic nitrogen (DIN) concentration is the sum of NH₄⁺, NO₂⁻, and NO₃⁻ concentrations.

The methodology used to calculate the hydromorphological parameters is detailed in the manuscript.

The size range of isolated pools is approximated.

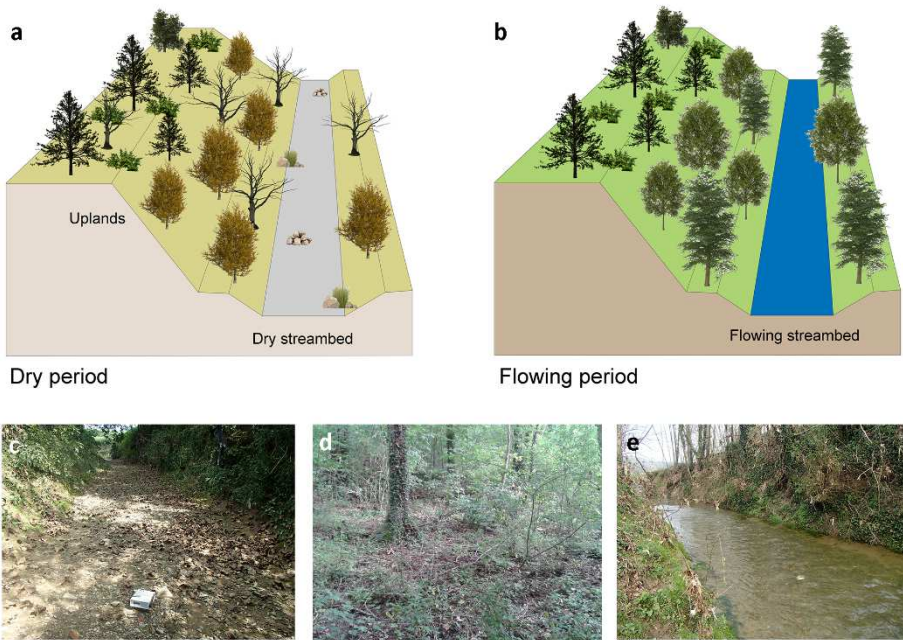


Figure A1 Schematic drawing and examples of different sites sampled in (a) the dry period (i.e., (c) dry riverbeds and (d) upland soils); and in (b) the flowing period (i.e., flowing riverbeds).

Table A.5.1 Hydromorphological and physicochemical characterization of the 11 studied impoundments

Impoundment	Hydro-morphological characteristics				Physico-chemical characteristics							
	Surface area (ha) ^a	Volume (hm ³) ^a	Mean depth (m) ^a	Water residence time (h) ^b	Temperature (°C) ^b	Conductivity (μS cm ⁻¹) ^b	DOC (mg L ⁻¹) ^b	TDN (mg L ⁻¹) ^b	Chlorophyll-a (μg L ⁻¹) ^b			
1	0.8	0.05	1.5	10.0 (6.9 - 13.2)	13.4 (7.8 - 18.4)	546 (480 - 623)	2.9 (2.1 - 4.0)	3.4 (1.4 - 4.8)	1.5 (1.0 - 2.1)			
2	0.2	0.01	1.1	0.6 (0.4 - 0.9)	9.9 (5.8 - 19.3)	550 (477 - 622)	2.8 (1.7 - 3.3)	3.4 (1.5 - 5.1)	1.9 (0.3 - 3.4)			
3	0.1	0.03	1.1	0.3 (0.2 - 0.4)	13.7 (6.7 - 20.3)	543 (472 - 627)	2.2 (1.4 - 2.8)	3.6 (1.9 - 4.9)	2.1 (0.2 - 3.5)			
4	0.2	0.03	1.3	1.3 (1.0 - 1.4)	14.9 (7.3 - 22.2)	751 (653 - 854)	2.2 (1.3 - 2.7)	3.8 (1.9 - 5.1)	3.3 (0.1 - 5.5)			
5	0.3	0.02	1.3	1.5 (0.9 - 2.0)	14.5 (7.6 - 21.6)	725 (663 - 762)	2.4 (1.5 - 2.9)	3.6 (1.9 - 4.7)	2.1 (0.3 - 4.5)			
6	0.2	0.02	0.8	0.6 (0.5 - 0.7)	15.9 (7.9 - 23.9)	813 (784 - 833)	2.1 (1.6 - 2.8)	3.0 (1.8 - 4.2)	1.8 (0.2 - 3.4)			
7	0.2	0.03	0.7	0.8 (0.3 - 1.6)	17.2 (9.4 - 24.9)	882 (821 - 946)	2.1 (1.7 - 2.7)	2.9 (1.8 - 3.9)	2.3 (1.6 - 3.0)			
8	1.9	0.04	1.8	10.0 (8.2 - 13.6)	21.2 (10.3 - 25)	933 (891 - 975)	2.0 (1.6 - 2.5)	2.8 (1.7 - 4.0)	4.0 (2.3 - 6.2)			
9	1.6	0.02	1.3	4.3 (2.6 - 5.2)	16.7 (9.3 - 23.6)	1038 (915 - 1170)	2.5 (2.0 - 3.1)	1.6 (1.4 - 1.8)	21.9 (1.2 - 48.1)			
10	2.7	0.01	0.6	3.2 (2.8 - 3.4)	12.9 (7.9 - 17.9)	682 (678 - 685)	2.0 (1.6 - 2.6)	2.3 (1.5 - 3.4)	6.1 (0.9 - 12.2)			
11	9.6	0.12	0.7	40.8 (37.0 - 45.5)	13.2 (6.4 - 20.0)	575 (516 - 634)	2.4 (2.0 - 2.7)	2.1 (1.1 - 3.2)	11.4 (0.6 - 27.6)			

^a Mean of the 3 sampling dates. The temporal variation was negligible for these parameters

^b Mean and range (in brackets) of the 3 sampling dates

Table A.5.2 Overview of potential explanatory variables of $p\text{CO}_{2,w}$ and $p\text{CH}_{4,w}$ included in partial least square (PLS) models.

Variable	Description	Units
<i>WRT</i>	Water residence time of the impounded water	hours
<i>Area</i>	Impounded water surface area	ha
<i>Volume</i>	Impounded water volume	hm ³
<i>Temp</i>	Surface water temperature	°C
<i>EC</i>	Electrical conductivity	μS cm ⁻¹
<i>Alk</i>	Surface water alkalinity	mg CaCO ₃ L ⁻¹
<i>pH</i>	Surface water pH	
<i>DO Sat</i>	Surface water oxygen saturation	%
<i>DOC</i>	Dissolved organic carbon concentration	mg L ⁻¹
<i>POC</i>	Water-suspended particulate organic carbon concentration	mg L ⁻¹
<i>TDN</i>	Total dissolved nitrogen concentration	mg L ⁻¹
<i>TN</i>	Total surface water nitrogen concentration	mg L ⁻¹
<i>TP</i>	Total surface water phosphorus concentration	mg L ⁻¹
<i>Chl-a</i>	Total surface water Chl-a concentration	μg L ⁻¹

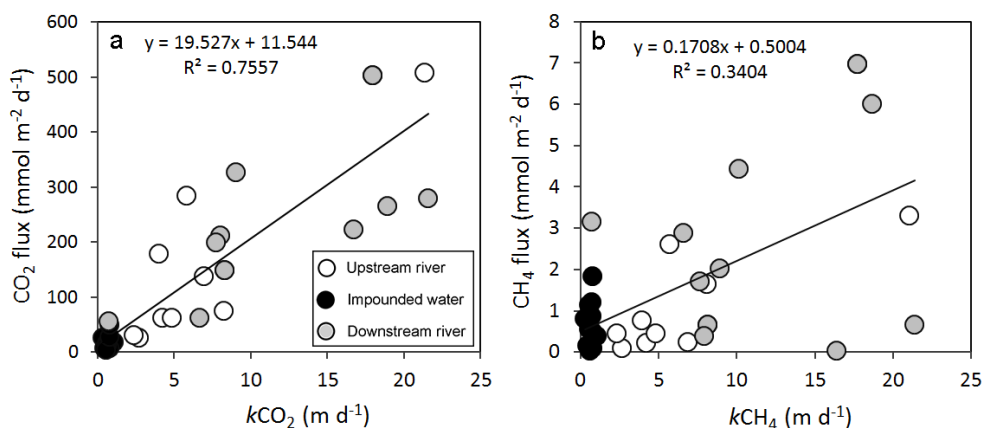


Figure A.5.1 (a) CO_2 emission flux (CO_2 flux) as a function of the gas transfer velocity of CO_2 ($k\text{CO}_2$) and (b) CH_4 emission flux (CH_4 flux) as a function of the gas transfer velocity of CO_2 ($k\text{CO}_2$) of the 11 study sites for the three different impoundment units (i.e., upstream river, impounded water and downstream river) during the three sampled seasons (i.e., spring, summer and winter). The solid lines correspond to the regression model lines best fitting the data. Model equations are also shown close to model lines.

Table A.5.3 Summary of partial least square (PLS) models produced for $p\text{CO}_{2,w}$ and $p\text{CH}_{4,w}$

$p\text{CO}_2$			$p\text{CH}_4$		
Variable	VIP value	Coefficient	Variable	VIP-value	Coefficient
WRT	1.8 **	0.24	DOC	1.7 **	0.35
Area	1.6 **	0.20	TDN	1.7 **	-0.26
EC	1.6 **	-0.31	WRT	1.2 **	0.22
$p\text{CH}_4$	1.2 **	0.18	Chl-a	1.1 **	0.09
Alk	1.0 **	0.24	Temp	1.1 **	0.13
DOC	0.9 *	0.20	Area	1.0 **	0.16
DO Sat	0.9 *	-0.17	Alk	0.7	0.03
Chl-a	0.6	0.01	TP	0.7	0.02
Temp	0.6	-0.10	pH	0.7	-0.15
TN	0.5	0.12	EC	0.6	-0.18
TDN	0.5	0.07	DO sat	0.5	0.02
pH	0.4	0.07	TN	0.3	0.08
TP	0.2	-0.05	POC	0.3	-0.01
<i>POC</i>	0.3	0.06			
	R²Y	0.68		R²Y	0.69
	Q²Y	0.34		Q²Y	0.41

Variable importance on the projection scores (VIP values in the table) indicate the partial influence of each explanatory variable (X-; see table S2 in the supporting information for the explanation of each abbreviation) on the response variables (Y-; $p\text{CO}_2$ and $p\text{CH}_4$). X-variables included in the PLS models are sorted according to their VIP's. Bold font is used to identify the top ones based on their VIP value. Among them, variables with two asterisks are highly influential (VIP>1) and variables with one asterisk are the moderately influential ones (VIP between 1 and 0.8). PLS models coefficients (coefficients in the table) describe the relationship (direction and relative strength) between X- and Y-variables.

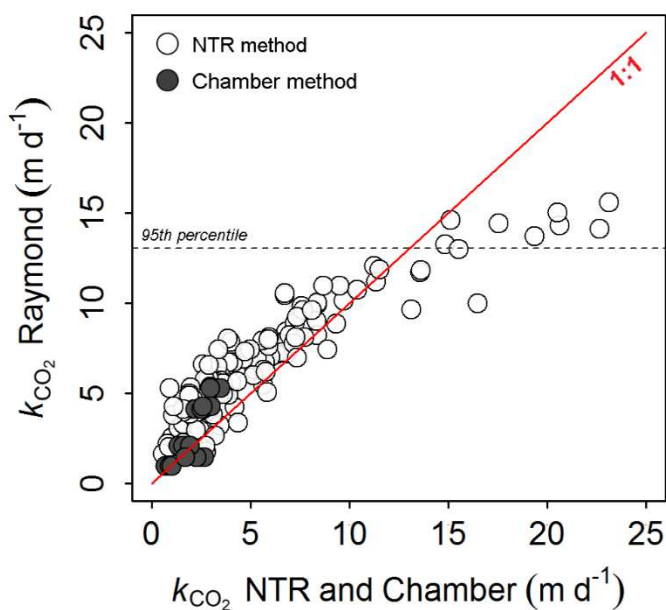


Figure A.6.1 Relationship between the k_{CO_2} derived from both the night-time regression method (NTR method; open circles; $n=151$) and the chamber method (filled circles; $n=18$) and the k_{CO_2} obtained from equation (2) in *Raymond et al.*, [2012]. Horizontal dashed line indicate 95th percentile boundary for the k_{CO_2} obtained from equation (2) in *Raymond et al.*, [2012]. The 1:1 reference line is shown as reference. The night-time regression method (NTR, Hornberger and Kelly [1975]) is based on the premise that the photosynthesis ceases from sunset to sunrise; thus night-time dynamics of oxygen depend on respiration and reaeration. During the night, respiration reduces the oxygen levels until atmospheric equilibrium is reached. In parallel, reaeration approaches the oxygen concentration to saturation. Thus, when we plot the night-time oxygen concentration per unit of time versus the oxygen saturation deficit, a linear trend is obtained. The intercept of the regression corresponds to the respiration rate and the slope to the mean reaeration coefficient (K_{O_2}) in d^{-1} . We corrected the K_{O_2} for depth to obtain the mean gas transfer velocity of oxygen (k_{O_2}) in $m\ d^{-1}$ and we further transformed k_{O_2} to k_{CO_2} by applying equation (3) in the manuscript.

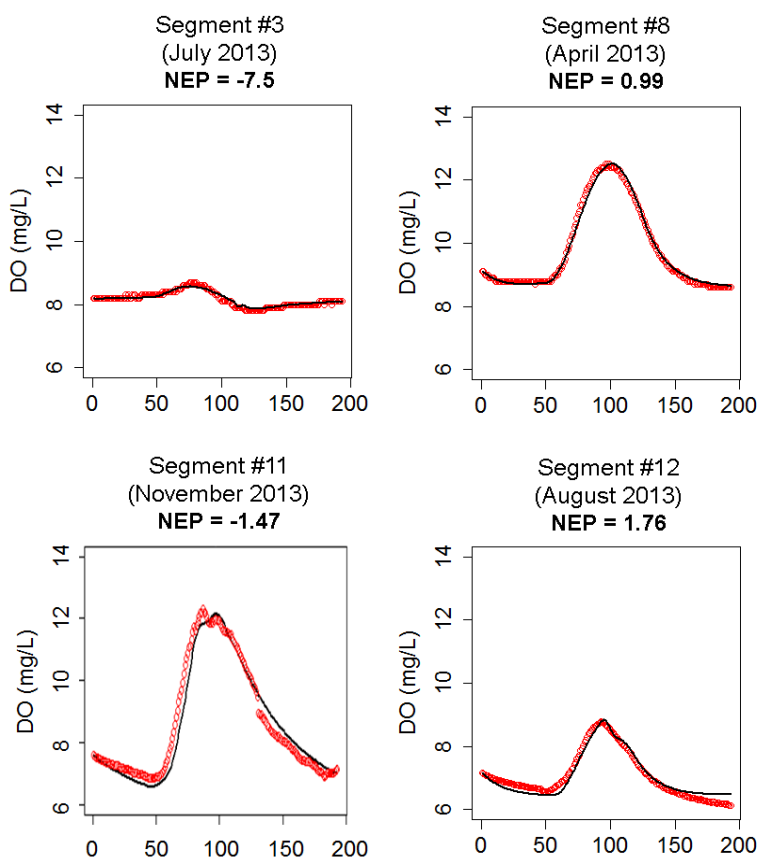


Figure A.6.2 Measured diel dissolved oxygen dynamics (red points) and model fit (black continuous line) for representative examples of lotic (top) and lentic (bottom) segments (see Figure 1 in the main text for the study segment location). Estimated net ecosystem production (NEP; $\text{mmol O}_2 \text{ m}^{-2} \text{ d}^{-1}$) is displayed above the curves. Y-axis (DO, mg L^{-1}) ranges are fixed to facilitate comparison among segments. Each DO curve correspond to a 24-hours period (X-axis) from sunrise to sunrise.

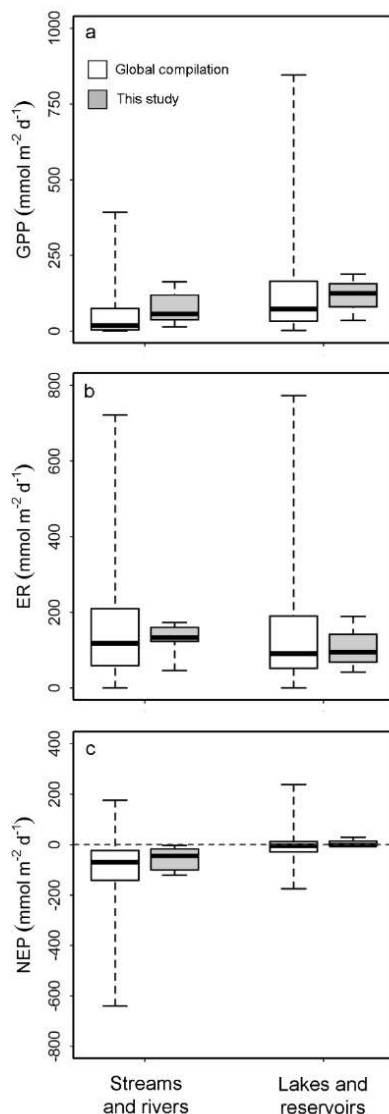


Figure A.6.3 Metabolic rates (in $\text{mmol m}^{-2} \text{d}^{-1}$) of (a) gross primary production (GPP), (b) ecosystem respiration (ER) and (c) net ecosystem production (NEP) across lotic aquatic ecosystems (i.e., streams and rivers) and lentic aquatic ecosystems (i.e., lakes and reservoirs). Box plots display the 25th, 50th and 75th percentiles; whiskers display minimum and maximum values. Grey boxes correspond to the metabolic rates obtained in our study, with data from 8 different lotic systems (32 observations) and 3 different lentic systems (10 observations) distributed along one fluvial network. White boxes correspond to the metabolic rates extracted from a global compilation made by *Hoellein et al.*, [2013], with data from 218 different lotic systems (626 observations) and 72 different lentic systems (1611 observations).

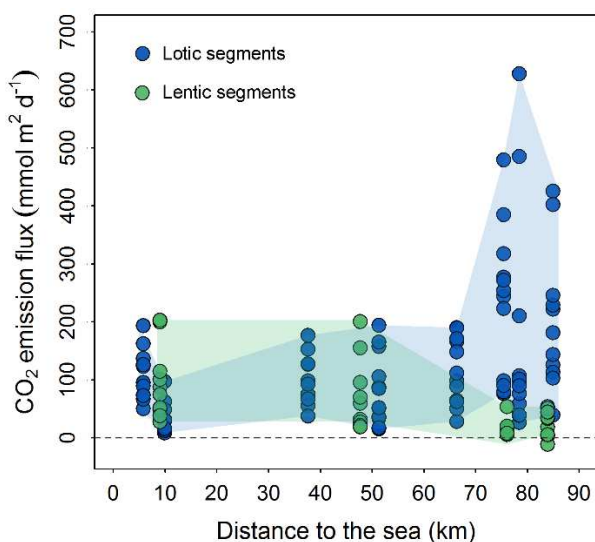


Figure A.6.4 Variation of the magnitude (solid line, segment means of the different dates) and standard deviation (shaded region, segment standard error of the different dates) of the $F_{\text{CO}_2 \text{ emission}}$ for the lotic (blue) and lentic (green) along the river longitudinal continuum. The horizontal dashed line represents $F_{\text{CO}_2 \text{ emission}}=0$. Spatial relationships shown in the Figure are statistically significant for lotic ($y = 0.0366x^2 - 1.6483x + 89.53$; $r^2 = 0.20$, $p < 0.001$, $n = 96$) and lentic ($y = -0.9525x + 103.39$; $r^2 = 0.29$, $p < 0.001$, $n = 48$) segments.

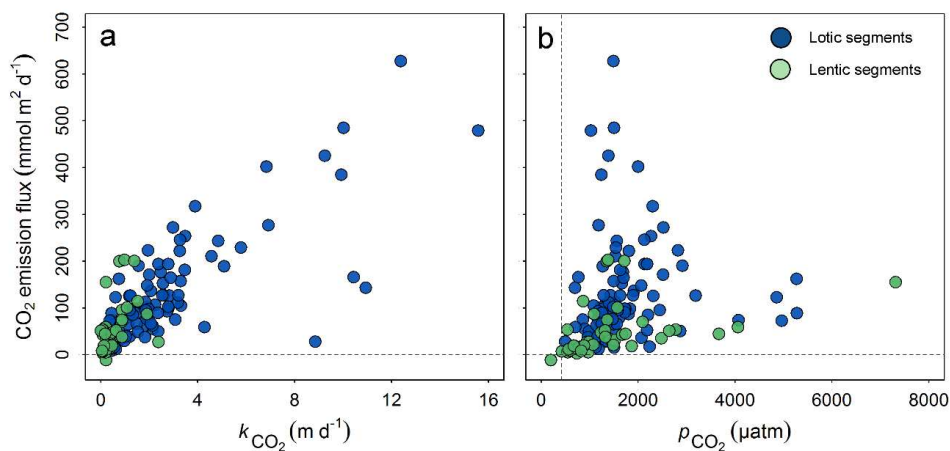


Figure A.6.5 $F_{\text{CO}_2 \text{ emission}}$ as a function of (a) k_{CO_2} and (b) surface water $p_{\text{CO}_2,w}$ for both lotic (blue circles) and lentic segments (green circles). Horizontal dashed lines represent $F_{\text{CO}_2 \text{ emission}}=0$. Vertical dashed line in (b) represents the average $p_{\text{CO}_2,a}$ for all the segments.

Table A.6.1 Hydromorphological characteristics of the 12 studied segments

Segment	Hydrological habitat	Stream order ^a	Length (m)	Slope (%)	Water flow (m ³ s ⁻¹) ^b	Velocity (m s ⁻¹) ^b	Width (m) ^b	Depth (m) ^b	Water residence time (hours) ^b
1	Lotic	4	2150	0.9	0.387 (0.02 - 1.84)	0.16 (0.034 - 0.433)	7.7 (5.7 - 11.3)	0.17 (0.08 - 0.37)	6.9 (1.4 - 17.4)
2	Lotic	2	660	3.7	0.012 (0.0004 - 0.05)	0.05 (0.004 - 0.176)	1.8 (1.1 - 2.4)	0.08 (0.06 - 0.12)	12.3 (1.0 - 45.7)
3	Lotic	3	340	2.1	0.117 (0.01 - 0.60)	0.07 (0.016 - 0.248)	5.6 (2.3 - 9.1)	0.16 (0.08 - 0.33)	2.5 (0.4 - 5.8)
4	Lotic	5	3810	0.2	2.569 (1.05 - 5.75)	0.22 (0.113 - 0.347)	26.4 (22.2 - 33.2)	0.12 (0.05 - 0.26)	2.0 (1.2 - 4.5)
5	Lotic	4	1720	0.3	0.422 (0.05 - 1.18)	0.22 (0.048 - 0.467)	7.5 (5.9 - 9.3)	0.15 (0.10 - 0.27)	3.5 (1.0 - 9.9)
6	Lotic	6	2360	0.7	0.482 (0.03 - 2.32)	0.18 (0.031 - 0.546)	9.9 (6.6 - 18.2)	0.08 (0.05 - 0.23)	6.6 (1.2 - 20.5)
7	Lotic	6	2450	0.2	3.170 (1.33 - 9.00)	0.25 (0.151 - 0.424)	32.6 (27.3 - 44.1)	0.29 (0.23 - 0.48)	2.9 (1.6 - 4.4)
8	Lotic	6	3220	0.1	2.349 (0.30 - 7.37)	0.21 (0.112 - 0.356)	35.2 (21.3 - 54.2)	0.19 (0.12 - 0.38)	5.0 (2.5 - 8.0)
9	Lentic	4	770	< 0.1	0.414 (0.02 - 1.83)	0.02 (0.001 - 0.080)	16.1 (16.1 - 16.1)	1.40 (1.40 - 1.40)	56.2 (2.6 - 215.2)
10	Lentic	3	80	< 0.1	0.098 (0.02 - 0.49)	0.01 (0.001 - 0.040)	10.4 (10.4 - 10.4)	1.14 (1.14 - 1.14)	7.5 (0.5 - 16.0)
11	Lentic	6	1640	< 0.1	2.717 (0.48 - 9.43)	0.03 (0.005 - 0.104)	66.4 (66.4 - 66.4)	1.36 (1.36 - 1.36)	35.1 (4.4 - 84.2)
12	Lentic	6	900	< 0.1	2.959 (0.46 - 8.78)	0.10 (0.016 - 0.291)	40.8 (40.8 - 40.8)	0.74 (0.74 - 0.74)	6.2 (0.8 - 15.8)

^a Stream order was calculated with the Hydrological Extension in ESRI® ArcGISTM v. 10.0. Data obtained from a 2-meter digital elevation model (Centre of Ecology and Forestry Research of Catalonia)

^b Mean and range (in brackets) of the 12 sampling dates

Table A.6.2 Summary of metabolic rates of the 12 studied segments

Segment	GPP (mmol m ⁻² d ⁻¹) ^a	ER (mmol m ⁻² d ⁻¹) ^a	NEP (mmol m ⁻² d ⁻¹) ^a	n
1	51.8 (27.7 - 75.9)	-156.5 (-219.1 - (-94.1))	-104.7 (-159.1 - (-50.2))	2
2	42.4 (13.4 - 71.4)	-163.1 (-216.0 - (-110.1))	-120.7 (-144.6 - (-96.7))	2
3	32.8 (13.81 - 68.0)	-129.9 (-281.0 - (-21.3))	-97.2 (-213.0 - 18.8)	10
4	162.2 (85.3 - 239.2)	-173.3 (-256.2 - (-90.4))	-11.0 (-16.9 - (-5.1))	2
5	14.0 (9.7 - 18.3)	-46.3 (-49.7 - (-43.0))	-32.3 (-33.2 - (-31.4))	2
6	127.5 (115.6 - 139.4)	-130.1 (-172.0 - (-88.2))	-2.6 (-56.4 - 51.2)	2
7	110.4 (56.8- 163.9)	-137.1 (-198.1 - (-76.0))	-26.7 (-58.9 - 6.8)	2
8	61.1 (12.4- 161.7)	-116.3 (-182.2 - (-71.1))	-55.2 (-111.1 - 26.6)	10
9 ^b	- -	- -	- -	0
10	35.6 (32.2 - 39.0)	-42.0 (-44.3 - (-39.6))	-6.3 (-7.3 - (-5.3))	2
11	188.3 (83.4 - 304.9)	-189.3 (-304.0 - (-75.4))	-1.0 (-35.4 - 25.2)	6
12	124.2 (49.0 - 199.4)	-95.2 (-157.0 - (-33.4))	29.0 (15.6 - 42.4)	2
Lotic segments	124.2 (9.7 - 239.2)	-125.2 (-281.0 - (-21.3))	-67.7 (-213.0 - 51.2)	32
Lentic segments	57.4 (32.2- 304.9)	-141.0 (-304.0 - (-33.4))	6.9 (-35.4 - 42.4)	10
All segments	78.3 (9.7- 304.9)	-129.0 (-304.0 - (-21.3))	-50.7 (-213 - 51.2)	42

^a Mean and range (in brackets) of the maximum available temporal data (n)

^b Before running the metabolism model, we examined the original data for anomalies that could have thwarted modeling efforts. Following this, we discarded the DO data from segment #9 because sensor malfunction lead to DO data anomalies.

Appendix B

Text B.7.1. Fluvial network upscaling of CO₂ and CH₄ emissions

Text B.7.2 Simulated change in fluvial network CO₂ and CH₄ emissions under future hydrological scenarios

Table B.7.1 Expected scenarios of short (2006-2030) and long term (2076-2100) streamflow and impounded surface area change (%) for the Fluvia River

B.7.1 Fluvial network upscaling of CO₂ and CH₄ emissions

Here, we combined a) the mean monthly areal CO₂ and CH₄ effluxes measured in the field for each environment (in mmol m⁻² d⁻¹) with b) the mean monthly surface area estimated for each environment (in m²) to derive a total annual mass of CO₂, CH₄ and total C (i.e., sum of CO₂ and CH₄) emitted from each environment (in Gg CO₂e y⁻¹).

B.7.1a Estimation of the areal CO₂ and CH₄ effluxes

We used the specific monthly areal CO₂ and CH₄ effluxes (both diffusive and ebullitive) for each environment (i.e., lotic, lentic and dry) and for each Strahler stream order obtained along the different chapters of this dissertation. Additionally, we used an ordinary resampling technique [Striegl *et al.*, 2012; Crawford *et al.*, 2016; Stanley *et al.*, 2016] to derive the CO₂ and CH₄ effluxes (and uncertainty) for those moments and those stream orders or which we lack field data. The bootstrapped CO₂ and CH₄ effluxes (means, standard deviations and confidence intervals) were obtained from 1000 simulated distributions based on the mean and 5th–95th percentiles from our dataset.

B.7.1b Estimation of the fluvial network surface area

Stream network length (in m) sorted by stream order was obtained from a high resolution map provided by the Catalan Water Agency (<http://aca-web.gencat.cat>). Further validation with a 2-m resolution digital elevation model (DEM) with the hydrology tools available in ArcGIS 10.2.1 was carried out. The mean monthly cross-sectional wetted width (and associated uncertainty; in m) at the same segments where we measured CO₂ and CH₄ fluxes was derived every ca. 100 m (i.e., 5–85 cross-sectional transects per segments) from the hydraulic modelling software HecRas 2.2 (US Army Corps of Engineers, USA). The model was fed with the measured water flow and segment geometrical data provided by the Catalan Water Agency. We then combined the mean monthly cross-sectional wetted width (sorted by stream order) with the stream length (sorted by stream order) to obtain an estimate of the mean monthly surface area occupied by aquatic environments (sorted by stream order; in m²). The surface area of lentic waterbodies associated to SWRS was estimated with the polygon tool of Google Earth Pro and applied to correct the surface area

occupied by aquatic environments. Based on visual inspection, we assumed no temporal variation of the water level in our lentic waterbodies. Finally, we derived the mean monthly surface area of dry riverbeds by subtraction of the total fluvial network surface area (i.e., surface area at the moment where the fluvial network was fully occupied (100%) by water - moment of maximum hydrological expansion) and the mean monthly surface area occupied by aquatic environments (for the 12 sampling campaigns). In a last step of our upscaling exercise, we multiplied the mean monthly areal CO₂ and CH₄ effluxes measured for each environment an stream order (in mmol m⁻² d⁻¹) by the mean monthly surface area estimated for each environment and stream order (in m²) to derivate a total annual mass of CO₂, CH₄ and total C (i.e., sum of CO₂ and CH₄) emitted from each environment (in Gg CO₂e y⁻¹). Similar fluvial network upscaling of CO₂ and CH₄ emissions exercises have been carried out in *Striegl et al.*, [2012] or *Crawford et al.*, [2013].

B.7.2. Simulated change in fluvial network CO₂ and CH₄ emissions under future hydrological scenarios

We used simple empirical models based on linear relationships between streamflow and surface area of the different environments (i.e., lotic, lentic and dry), in order to simulate how future streamflow changes in the Fluvià River (See Table S1 in the supporting information) may potentially change the relative surface area of the different environments and how this may, in turn, modify the total annual mass of CO₂, CH₄ and total C (i.e., sum of CO₂ and CH₄) emitted from each environment (in Gg CO₂e y⁻¹).

The 3 hydrological scenarios proposed here [*Pascual et al.*, 2015; Table S1 in the supporting information] have been obtained by simulating the Fluvià River hydrological cycle under different future scenarios that accounted for the impacts of climate change and antropogenic pressures on water resources [*IPCC*, 2014; *Zarfl et al.*, 2014]. By linear interpolation of the predicted streamflows in our river ([*Pascual et al.*, 2015]; Table S1 in the supporting information), we deterimned the total predicted area occupied by the different environments in the fluvial network. In Scenario 3 (Table S1 in the supporting information), apart from considering the effect of streamflow changes on the surface area

of the fluvial network, we have also considered the predicted dam construction intentions [Zarfl *et al.* 2014] and doubled the surface area of impounded waters accordingly.

Finally, we combined the mean monthly areal CO₂ and CH₄ effluxes measured in the field for each environment (in mmol m⁻² d⁻¹) with the predicted mean monthly surface area for each environment and for each scenario (in m²) to derivate a total simulated annual mass of CO₂, CH₄ and total C (i.e., sum of CO₂ and CH₄) emitted from each environment (in Gg CO₂e y⁻¹). We also computed the percentage change (%) between the present conditions and the outputs of the 3 simulated scenarios for the different environments and for the entire fluvial network (see Table S1 for further details).

Table B.7.1 Expected scenarios of short (2006-2030) and long term (2076-2100) streamflow and impounded surface area change (%) for the Fluvità River

Scenario	Description	Expected streamflow change (%)			Expected impounded water surface area change (%)		
		Mean	Min	Max	Mean	Min	Max
1	Short term discharge reduction (2006-2030)	-11.5	-9.0	-14.0	0.0	0.0	0.0
2	Long term discharge reduction (2076-2100)	-30.5	-22.0	-39.0	0.0	0.0	0.0
3	Long term discharge reduction (2076-2100) + Doubled surface area of impounded waters	-30.5	-22.0	-39.0	+100	+50	+150

Expected streamflow change (%) obtained from Pascual *et al.* [2014]. Relative change compared to the present period (1984–2008). Streamflow change predictions are for the river mouth.

Simulated impounded water surface area change (%) in the Fluvità river fluvial network based on Zarfl *et al.* [2014] global projection. Relative change compared to the present period (2013).

Mean, minimum (Min) and maximum (Max) for the different future projections

Appendix C

This Appendix provides the original publications of:

Chapter 3: Gómez-Gener, L., B. Obrador, D. von Schiller, R. Marcé, J. P. Casas-Ruiz, L. Proia, V. Acuña, N. Catalán, I. Muñoz, and M. Koschorreck (2015), Hot spots for carbon emissions from Mediterranean fluvial networks during summer drought, *Biogeochemistry*, 125(3), 409–426, doi:10.1007/s10533-015-0139-7.

Chapter 4: Gómez-Gener, L., B. Obrador, R. Marcé, V. Acuña, N. Catalán, J. P. Casas-Ruiz, S. Sabater, I. Muñoz, and D. von Schiller (2016), When water vanishes: magnitude and regulation of carbon dioxide emissions from dry temporary streams, *Ecosystems*, 19(4), 710–723, doi:10.1007/s10021-016-9963-4.

Chapter 6: Gómez-Gener, L., D. von Schiller, R. Marcé, M. Arroita, J. P. Casas-Ruiz, P. A. Staehr, V. Acuña, S. Sabater, and B. Obrador (2016), Low contribution of internal metabolism to carbon dioxide emissions along lotic and lentic environments of a Mediterranean fluvial network, *J. Geophys. Res. Biogeosci.*, 121, doi:10.1002/2016JG003549

Hot spots for carbon emissions from Mediterranean fluvial networks during summer drought

Lluís Gómez-Gener · Biel Obrador · Daniel von Schiller · Rafael Marcé ·
Joan Pere Casas-Ruiz · Lorenzo Proia · Vicenç Acuña ·
Núria Catalán · Isabel Muñoz · Matthias Koschorreck

Received: 9 March 2015 / Accepted: 14 September 2015
© Springer International Publishing Switzerland 2015

Abstract During summer drought, Mediterranean fluvial networks are transformed into highly heterogeneous landscapes characterized by different environments (i.e., running and impounded waters, isolated river pools and dry beds). This hydrological setting defines novel biogeochemically active areas that could potentially increase the rates of carbon emissions from the fluvial network to the atmosphere. Using chamber methods, we aimed to identify hot spots for carbon dioxide (CO₂) and methane (CH₄) emissions from two typical Mediterranean fluvial networks during summer drought. The CO₂ efflux from dry beds (mean ± SE = 209 ± 10 mmol CO₂ m⁻² d⁻¹) was comparable

to that from running waters (120 ± 33 mmol m⁻² d⁻¹) and significantly higher than from impounded waters (36.6 ± 8.5 mmol m⁻² d⁻¹) and isolated pools (17.2 ± 0.9 mmol m⁻² d⁻¹). In contrast, the CH₄ efflux did not significantly differ among environments, although the CH₄ efflux was notable in some impounded waters (13.9 ± 10.1 mmol CH₄ m⁻² d⁻¹) and almost negligible in the remaining environments (mean <0.3 mmol m⁻² d⁻¹). Diffusion was the only mechanism driving CO₂ efflux in all environments and was most likely responsible for CH₄ efflux in running waters, isolated pools and dry beds. In contrast, the CH₄ efflux in impounded waters was primarily ebullition-based. Using a simple heuristic approach to simulate potential changes in carbon emissions from Mediterranean fluvial networks under future hydrological scenarios, we show that an extreme drying out (i.e., a four-fold increase of the surface area

Responsible Editor: Jacques C Finlay.

Electronic supplementary material The online version of this article (doi:10.1007/s10533-015-0139-7) contains supplementary material, which is available to authorized users.

L. Gómez-Gener (✉) · B. Obrador · I. Muñoz
Department of Ecology, University of Barcelona, Av.
Diagonal 643, 08028 Barcelona, Spain
e-mail: lgomez@ub.edu

D. von Schiller
Department of Plant Biology and Ecology, Faculty of
Science and Technology, University of the Basque
Country, Apdo. 644, 48080 Bilbao, Spain

R. Marcé · J. P. Casas-Ruiz · L. Proia · V. Acuña
Catalan Institute for Water Research, Scientific and
Technological Park of the University of Girona, Carrer
Emili Grahit 101, 17003 Girona, Spain

N. Catalán
Limnology, Department of Ecology and Genetics,
Evolutionary Biology Centre, Uppsala University,
Norbyvägen 18 D, 75236 Uppsala, Sweden

M. Koschorreck
Department Lake Research, Helmholtz Centre for
Environmental Research, Brückstrasse 3a,
39114 Magdeburg, Germany

of dry beds) would double the CO₂ efflux from the fluvial network. Correspondingly, an extreme transformation of running waters into impounded waters (i.e., a twofold increase of the surface area of impounded waters) would triple the CH₄ efflux. Thus, carbon emissions from dry beds and impounded waters should be explicitly considered in carbon assessments of fluvial networks, particularly under predicted global change scenarios, which are expected to increase the spatial and temporal extent of these environments.

Keywords Greenhouse gas fluxes · Carbon dioxide · Methane · Fluvial network · Temporary rivers · Summer drought

Introduction

Increasing evidence has demonstrated the active role of inland waters in the global carbon (C) cycle and the capacity of these water bodies to emit significant amounts of carbon dioxide (CO₂) and methane (CH₄) to the atmosphere (Cole et al. 2007; Battin et al. 2009a). Recent global estimates of C emissions have shown that inland waters, including both running and impounded waters, emit approximately 2.1 Pg C year⁻¹ in the form of CO₂ (Raymond et al. 2013) and 0.10 Pg C year⁻¹ in the form of CH₄ (Bastviken et al. 2011). Expressed as CO₂ equivalents (Eq), these emissions correspond to 0.65 Pg C (CO₂ Eq) year⁻¹, assuming that 1 kg of CH₄ corresponds to 25 kg of CO₂ over a 100-year period (IPCC 2013). In this context, regional and local studies conducted in arctic and subarctic (Kling et al. 1991; Lundin et al. 2013), boreal (Jonsson et al. 2007; Campeau and Lapierre 2014), temperate (Hope et al. 2001; Halbedel and Koschorreck 2013) and tropical biomes (Abril 2005; Guérin et al. 2007; Fearnside and Pueyo 2012) have confirmed the role of streams, lakes and reservoirs as net emitters of CO₂ and CH₄ to the atmosphere. Nonetheless, there is limited information concerning the relevance of C release from inland waters to the atmosphere in arid and semiarid regions, such as the Mediterranean (López et al. 2011; Obrador and Pretus 2012; Morales-Pineda et al. 2014).

Because of the climatic conditions of Mediterranean regions, with warm, dry summers and mild, humid winters, Mediterranean fluvial networks are

characterized by a highly seasonal and intermittent hydrological regime (Gasith and Resh 1999). During the wet period (late autumn to early spring), the hydrological longitudinal connectivity increases, and most of the fluvial network area is covered with surface water. In contrast, during the dry period (from late spring to early autumn), the hydrological longitudinal connectivity decreases, and the area of the fluvial network covered with surface water is drastically reduced. Consequently, during summer drought, the fluvial network is converted into a fragmented heterogeneous landscape characterized by slow-moving waters, isolated river pools and dry beds (Bernal et al. 2013). Temporary rivers experiencing these patterns are not restricted to arid and semiarid regions, but they can be found in many areas of the world (Tooth 2000; Acuña et al. 2014; Datry et al. 2014). Moreover, as a consequence of climate change and water abstraction for socio-economic uses, their global surface area is expected to increase in the Mediterranean and other regions where a negative water flow trend has been predicted (Milliman et al. 2008; Tockner et al. 2009; Larned et al. 2010).

Dry beds are defined as the parts of the fluvial network exposed to air during dry periods (Steward et al. 2012). They are habitats in their own right and differ from adjacent riparian and other terrestrial habitats in their substrate composition, topography, microclimate, vegetation cover, inundation frequency, and biota (Steward et al. 2012). Dry river beds play an important role as dispersal corridors and contain a unique diversity of aquatic, amphibious, and terrestrial biota (Williams 2006; Lake 2011). Moreover, recent studies have reported that the energy flow, nutrient cycling and other biogeochemical processes also continue when the river runs dry. For example, Zoppini and Marxsen (2011), Timoner et al. (2014) and Pohlen et al. (2013) showed that extracellular enzymatic activities and carbon processing through sediment biofilms could be maintained to some degree during desiccation. Similarly, Gallo et al. (2014) and von Schiller et al. (2014) showed that temporary streams can release significant amounts of CO₂ when they are dry. Nevertheless, our understanding of the biogeochemical processes that occur in dry beds and the role of these environments as emitters of CO₂ and CH₄ to the atmosphere remains limited (Steward et al. 2012).

The hydrological contraction of the fluvial network also affects impounded waters stored in dams, weirs and small impoundments. These aquatic environments are abundant in Mediterranean regions because of the growing human demand for water and electricity (García-Ruiz et al. 2011). The reduction of the river flow as a consequence of seasonal drought prolongs the residence times of the water in impoundments, which favour C processing through the promotion of the interaction between organic matter and biological actors (Battin et al. 2009b; Acuña and Tockner 2010). As a result, C emissions from impounded waters might increase during hydrological contraction. Furthermore, the reduction of the volume and surface area during summer drought also increases the areal extent of exposed dry sediments along the shore of impounded waters, which are potentially active, but frequently neglected, sites for C emissions (Mitchell and Baldwin 1999; Forzieri et al. 2014).

Knowledge on the biogeochemistry of isolated river pools is also limited despite they are abundantly observed along temporary rivers during hydrological contraction (Bernal et al. 2013; Datry et al. 2014). Isolated pools show high residence times and potentially suitable conditions for methanogenesis (i.e., organic matter accumulation and low dissolved oxygen concentration) (Vazquez et al. 2010; von Schiller et al. 2011). Nevertheless, the hydrological isolation in these pools creates individual systems that are highly influenced through particular local conditions (Dahm et al. 2003; Bonada and Resh 2013; Fellman et al. 2010).

In the present study, we aimed to quantify C emissions and to identify C emission hot spots from Mediterranean fluvial networks during summer drought. To this end, we measured the CO₂ and CH₄ effluxes and their potential drivers in a variety of environments (i.e., running waters, impounded waters stored in reservoirs, weirs and small dams, isolated river pools and dry river and impoundment beds) typically observed in Mediterranean rivers during summer drought. We hypothesized that the reduction of flow during summer drought would promote the spatial heterogeneity of C fluxes along the fluvial network and enhance the contribution of dry beds, isolated pools and impounded waters to these fluxes. Moreover, we use a simple heuristic approach to explore the potential future implications of increasing river desiccation and impoundment of running waters

on the total C emissions from Mediterranean fluvial networks.

Methods

Study sites and sampling design

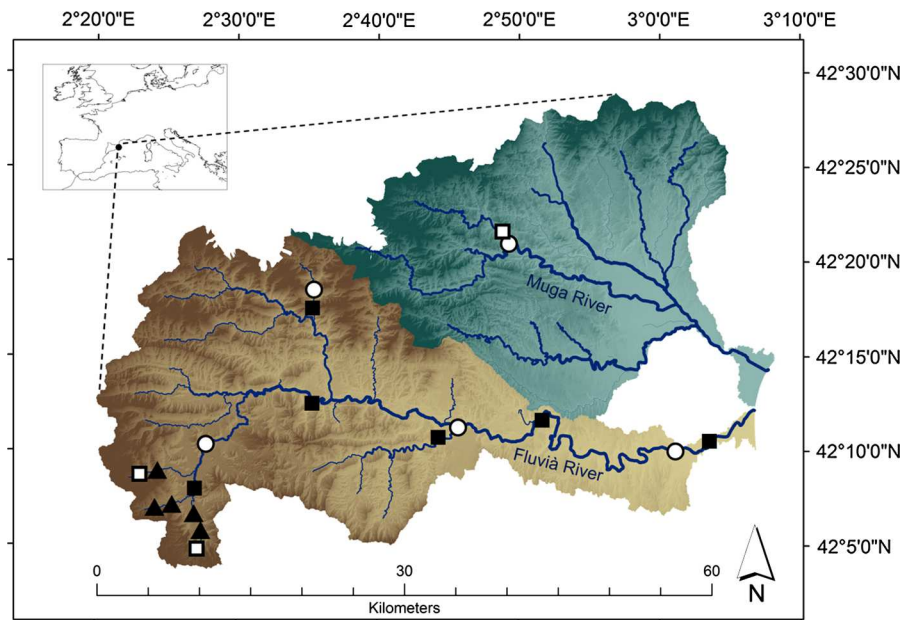
The Fluvià and Muga rivers are located in the NE of the Iberian Peninsula (Fig. 1). The Fluvià River is 97 km long and drains a 990 km² catchment covered with mixed forests (78 %), and agricultural (19 %) and urban (3 %) areas. The Muga River is 64 km long and drains a 853 km² catchment with a lower proportion of mixed forests (58 %) and a higher proportion of agricultural (37 %) and urban (5 %) areas (Land Cover Map of Catalonia 2009, Centre of Ecology and Forestry Research of Catalonia, <http://www.creaf.uab.es/mcsc/>).

The climate in this area is typically Mediterranean. The mean monthly air temperature ranges from 6 °C in January to 26 °C in July. The mean annual precipitation is 660 mm, with rainfall primarily occurring in autumn and spring, with occasional storms in summer (Data from 2004 to 2014, Catalan Water Agency, <http://aca-web.gencat.cat>).

The flow of both rivers has been highly regulated since the early 20th century due to the high human demand for energy and water in the area (García-Ruiz et al. 2011). A total of 61 and 18 manmade river interruptions (i.e., reservoirs, small impoundments and weirs) are present in the Fluvià and Muga rivers, respectively (Pavón 2010).

We conducted the sampling campaign at the end of summer (from 26 August to 6 September 2013), prior to the first post-summer rainfall events that typically occur in the region during autumn (Bernal et al. 2013). We sampled a total of 19 sites along the two fluvial networks to cover a wide spectrum of environments typically observed during summer drought (Fig. 1, Online Resource Table S1). The considered environments included running water reaches (n = 6), impounded waters stored in weirs and dams of different dimensions (n = 5), isolated river pools formed during the fragmentation of the fluvial network (n = 5) and dry beds (n = 3; two dry river beds and one dry impoundment bed). The dry beds in rivers had been dry for less than 4 weeks and the dry bed in the reservoir for approximately 2–3 months.

Fig. 1 Location of the Fluvià River and Muga River catchments in Catalonia (NE Iberian Peninsula), with the corresponding position of the study sites (n = 19). *Closed squares* indicate running waters (n = 6), *open circles* impounded waters (n = 5), *closed triangles* isolated river pools (n = 5) and *open squares* dry beds (n = 3; two dry river beds and one dry impoundment bed)



Determination of CO₂ and CH₄ fluxes

To guarantee the comparability of the flux measurements, we used the same approach (chamber method, Frankignoulle (1988)) to directly measure the CO₂ and CH₄ fluxes in all environments (Online Resource Fig. S1). We monitored the gas concentrations in the chamber every 30 s for a total of 10 min using a Fourier-Transform-Infrared (FTIR) Spectrometer (GASMET DX4000, Temet Instruments, Finland) after passing through an in-line moisture trap (Drierite, USA) at a rate of 2.9 L min⁻¹. Measurement accuracy of the GASMET DX4000 FTIR was within 2 % of the calibrated range. We calculated the total fluxes of both gases (F , mmol m⁻² d⁻¹) from the rate of change of CO₂ and CH₄ inside the chamber:

$$F = \left(\frac{dp}{dt} \right) \left(\frac{V}{RTS} \right) \quad (1)$$

where dp/dt is the slope of the gas accumulation in the chamber ($\mu\text{atm s}^{-1}$), V is the volume of the chamber (dm^3 ; aquatic chamber = 14.6 dm^3 , soil chamber = 2.2 dm^3), S is the surface area of the chamber (dm^2 ; aquatic chamber = 9.8 dm^2 , soil chamber = 2.0 dm^2), and T is the air temperature (K) and R is the ideal gas constant ($\text{L atm K}^{-1} \text{mol}^{-1}$). Positive F values represent gas evasion to the atmosphere, and negative F values indicate gas invasion from the

atmosphere. We calculated the diffusive flux of CO₂ and CH₄ from the linear concentration change of both gases in the chamber. We identified ebullitive episodes (bubbling), only in the case of CH₄, as notorious non-linear increases in the concentration of CH₄ during the course of chamber measurements. We estimated the ebullitive flux of CH₄ as the difference between the total and the diffusive flux (Campeau and Lapierre 2014).

The artificial enhancement of the gas transfer velocity through disturbance of the surface boundary layer during the chamber deployment and subsequent measurement could be a critical aspect (Guérin et al. 2007; Vachon et al. 2010). To minimize this, we carried out specific chamber deployment procedures in each environment. In running waters, we used a rope to deploy the chamber at a fixed position onto the water column. In impounded waters, we cautiously deployed the chamber from an anchored boat onto the water surface in the centre of the system. In isolated river pools, we slowly lowered the chamber onto the water surface in the central part of the pool using a rope. In the case of dry beds, we inserted the chamber into the exposed sediments. A total of 3 replicate measurements were obtained at every aquatic site. The number of replicate measurements was increased at each dry site (5–10) to cover the maximum spatial variability in terms of dry bed organic matter and

water content. In both the aquatic and the dry environments, we flushed the chamber with ambient air between consecutive measurements.

Determination of $p\text{CO}_2$, $p\text{CH}_4$ and k_{600}

At every aquatic site, we determined the partial pressure of CO_2 ($p\text{CO}_2$) and CH_4 ($p\text{CH}_4$) in water at the same location as flux measurements. We measured the $p\text{CO}_2$ using an infrared gas analyser (EGM-4, PP-Systems, USA) coupled to a membrane contactor (MiniModule, Liqui-Cel, USA). The water was circulated via gravity through the contactor at 300 mL min^{-1} , and the equilibrated gas was continuously recirculated into the infrared gas analyser for instantaneous $p\text{CO}_2$ measurements (Teodoru et al. 2010). The accuracy of the infrared gas analyser was estimated to be within 1 % over the calibrated range. We determined the $p\text{CH}_4$ using the headspace equilibrium technique and gas chromatography according to Striegl et al. (2012). Briefly, we collected 30 ml of water with a 60 ml polypropylene syringe, creating a headspace with ambient air of 1:1 ratio (sampled water:ambient air). To facilitate the kinetics of equilibration between the liquid and the gas phase, we shook the syringe for 1 min and submerged it in water at each sampling site for 30 min to maintain constant equilibrium temperature. The water temperature was recorded using a portable sensor, and no changes were observed during equilibration. Subsequently, we transferred the 30 mL of the equilibrated gas to a pre-evacuated gas-tight glass tube (2-RV, Chromacol, USA). The CH_4 samples were analysed in the laboratory using a gas chromatograph coupled to a Flame Ionization Detector (Trace GC Ultra, Thermo Fisher Scientific, USA). The measurement accuracy of the gas chromatograph was estimated to be within 4 % over the calibrated range. The water temperature during equilibration was used to calculate Henry's coefficient between the liquid and the gas phase (Stumm and Morgan 1996).

The CO_2 flux measured with the chamber was used to calculate the direct gas transfer velocity of CO_2 (k_{CO_2}) from Fick's law of gas diffusion:

$$F_{\text{CO}_2} = k_{\text{CO}_2} K_h (p\text{CO}_{2,w} - p\text{CO}_{2,a}) \quad (2)$$

where k_{CO_2} is the specific gas transfer velocity for CO_2 (m d^{-1}), F_{CO_2} is the chamber-measured CO_2 flux

between the surface water and the atmosphere ($\text{mmol m}^{-2} \text{ d}^{-1}$), K_h is Henry's constant ($\text{mmol } \mu\text{atm}^{-1} \text{ m}^{-3}$) adjusted for salinity and temperature (Weiss 1974; Millero 1995), and $p\text{CO}_{2,w}$ and $p\text{CO}_{2,a}$ are the surface water and the atmosphere partial pressures of CO_2 (μatm), respectively. Because the gas transfer velocity is temperature- and gas-dependent, we standardized k_{CO_2} to a Schmidt number of 600 (k_{600} ; m d^{-1}), which corresponds to CO_2 at 20°C in freshwater, following Jähne and Münnich (1987):

$$\text{Direct } k_{600} (\text{m d}^{-1}) = k_{\text{CO}_2} \left(\frac{600}{Sc} \right)^{-n} \quad (3)$$

where Sc is the Schmidt number of a given gas at a given water temperature (Wanninkhof 1992). In accordance with Bade (2009), the exponent n was set to $2/3$ at sites with a smooth water surface (sheltered impounded waters and isolated pools) and $1/2$ in the more turbulent environments (open impounded waters and running waters).

The k_{600} was also indirectly determined after applying different methods depending on the specific type of aquatic environment. In running waters, we obtained the indirect k_{600} from the night time drop in the oxygen concentration (Hornberger and Kelly 1975). Briefly, photosynthesis ceases from sunset to sunrise, thus night time dynamics are dependent on the respiration rate and reaeration coefficient. During the night, respiration reduces the oxygen levels until the atmosphere equilibrium is reached. In parallel, reaeration approaches the oxygen concentration to saturation. Thus, when we plot the night time oxygen concentration per unit of time versus the oxygen saturation deficit, a linear trend is obtained. The intercept of the regression corresponds to the respiration ($\text{g O}_2 \text{ m}^{-2} \text{ h}^{-1}$) and the slope to the mean gas transfer velocity of oxygen (k_{O_2} ; m d^{-1}). The k_{O_2} was transformed to indirect k_{600} using Eq. (3). The dissolved oxygen concentration and temperature used in the night time reduction in oxygen method, were obtained at the running water sites at a frequency of 10 min with a multiparameter probe (YSI 600 OMS V2, Yellow Springs, USA).

In impounded waters, we estimated the value of indirect k_{600} from the wind speed based Eq. (4) of Crusius and Wanninkhof (2003):

$$\text{Indirect } k_{600} (\text{m d}^{-1}) = 0.17 U_{10} \quad (4)$$

where U_{10} is the wind speed at 10 m above the surface (m s^{-1}). The wind speed at a given height (U_x ; m s^{-1}) was converted to that at 10 m (U_{10} ; m s^{-1}) from the equation described by Donelan (1990). The wind speed for these calculations was obtained from measurements during the chamber deployments using a portable anemometer (Kestrel 4000, Kestrel Meters, UK) fixed to a tripod at 2 m above the water surface.

In the case of isolated pools, we estimated the indirect k_{600} from a wind speed based model previously applied in small, shallow and low turbulence ponds (Laurion et al. 2010):

$$\text{Indirect } k_{600} (\text{m d}^{-1}) = 0.19 + 0.26 U_{10} + 0.02 U_{10}^2 \quad (5)$$

Due to the sheltered location, there was no noticeable wind in any of the isolated pools sites, resulting in a constant indirect k_{600} of 0.19 m d^{-1} (intercept of Eq. 5), a parameter reflecting the effect of the other physical processes occurring in addition to wind that cause turbulence at the air–water interface.

We acknowledge that the floating chamber approach could be problematic in some of our environments, particularly in running waters where the employed method might not capture the complex turbulence regime that characterizes this environment. To assess these potential biases, we compared the site-specific CO_2 and CH_4 fluxes obtained from the chamber method (direct) versus the system-integrated fluxes of CO_2 and CH_4 derived from the Fick's law of gas diffusion (indirect) using Eq. (2). We detected a good agreement between direct and indirect CO_2 fluxes ($\log(\text{indirect } \text{CO}_2 \text{ efflux}) = 1.096 (\log \text{direct } \text{CO}_2 \text{ efflux}) - 0.28$, $r^2 = 0.81$, $p < 0.001$, $n = 16$) and between direct and indirect CH_4 fluxes ($\log(\text{indirect } \text{CH}_4 \text{ efflux}) = 0.322 \log(\text{direct } \text{CH}_4 \text{ efflux}) - 0.647$, $r^2 = 0.33$, $p = 0.019$, $n = 16$). These significant relationships support the reliability of the chamber method for quantifying C emissions in our study. However, the slope < 1 for the CH_4 equation indicates the overestimation of the direct CH_4 efflux with respect to the indirect CH_4 efflux. Therefore, it is likely that, in addition to Fickian and ebullitive transport, other pathways of CH_4 efflux, such as microbubble release, were also involved in CH_4 emission (Beaulieu et al. 2012; Prairie and Del Giorgio 2013; Tang et al. 2014; McGinnis et al. 2015).

Physicochemical characteristics of sediments and dry beds

To characterize the inundated sediments of the impounded waters, we collected three replicates of sediment cores (diameter = 6 cm) from the deepest part of the impounded waters with a gravity corer (UWITEC, Austria). We sub-sampled the upper 5 cm of the sediment cores and determined the water content (%), dry bulk density (g cm^{-3}) and porosity (Sobek et al. 2011). We also determined its organic matter content (mg cm^{-3}) by sample combustion following the loss on ignition method (Dean 1974).

To characterize the dry river and impoundment beds, we first measured in situ the dry bed water content and temperature at the dry bed surface of every chamber location (upper 5 cm) along two dry sites (1 dry river bed and 1 dry impoundment bed) using a portable soil probe (Decagon ECH₂O 10HS, Pullman, USA). We then collected sediment samples (upper 5 cm) to determine the dry bed organic matter content using the loss on ignition method. We estimated the basal microbial respiration rate ($\mu\text{g CO}_2^{-1} \text{ h}^{-1}$) of the dry bed samples using a microrespirometry system (MicroResp, Macaulay Scientific Consulting Ltd, UK) according to Campbell and Chapman (2003). Briefly, four replicates of 0.5 g of the sample taken at the dry bed surface of every chamber location (upper 5 cm) were added to a deep well microplate. The samples were incubated for 6 h at 20 °C, and a colorimetric method was used to measure the evolution of CO_2 immediately before and after the incubation. The % change of CO_2 was converted to basal respiration ($\mu\text{g CO}_2^{-1} \text{ h}^{-1}$) considering the incubation time and temperature, the gas constant, the headspace volume and the soil dry weight as indicated in the MicroResp technical manual.

Hydromorphological characteristics

We measured the mean cross-sectional depth (m) and width (m) of the running water sites at the same location where the gas fluxes were measured. We measured the mean cross-sectional water velocity (m s^{-1}) with an acoustic-Doppler velocity metre (Sontek, YSI, USA), and we combined it with the measured section to derive the water discharge ($\text{m}^3 \text{ s}^{-1}$). The discharge data were used to obtain averages of water velocity and stream depth along a

1-km segment using the hydraulic modelling software HecRas 2.2 (US Army Corps of Engineers) and hydromorphological data from the Catalan Water Agency (<http://aca-web.gencat.cat>).

We estimated the surface area, volume, and mean and maximum depths of the impounded waters sites from digitized bathymetric maps using a geospatial-processing software (ArcMap 10, ArcGis, USA). We calculated the residence time combining the volume obtained from the bathymetric map and the measured inflow at each impounded water site.

Statistical analyses

We grouped the 19 studied sites into 4 major environments (i.e., running waters ($n = 6$), impounded waters ($n = 5$), isolated pools ($n = 5$) and dry river beds ($n = 3$)). We tested the effect of the factor environment on the CO_2 and CH_4 fluxes, $p\text{CO}_2$ and $p\text{CH}_4$, direct and indirect k_{600} and percentage molar ratio between CH_4 and CO_2 efflux ($(\text{CH}_4 \text{ efflux} / \text{CO}_2 \text{ efflux}) \times 100$) using one-way analysis of variance (ANOVA) and subsequent post hoc comparisons (Tukey's Honest Significant Differences test).

For the dry beds, we assessed the effect of dry bed basal respiration, water content and organic matter content on the CO_2 efflux using linear and non-linear regressions. For aquatic environments, we assessed the relative contributions of $p\text{CO}_2$ and indirect k_{600} on the CO_2 efflux using simple and multiple linear regressions. When the statistical techniques required it, we log-transformed the variables to meet the conditions of homogeneity of variance, normality and to avoid the deleterious effect of extreme large values. All statistical analyses were conducted in the R statistical environment (R Core Team 2013) using the Vegan package (Oksanen 2013).

Results

CO_2 and CH_4 effluxes along the fluvial network

The studied environments were net emitters of CO_2 (mean \pm SE = $95.7 \pm 43.9 \text{ mmol m}^{-2} \text{ d}^{-1}$, range = $17\text{--}219 \text{ mmol m}^{-2} \text{ d}^{-1}$) and CH_4 ($3.6 \pm 3.4 \text{ mmol m}^{-2} \text{ d}^{-1}$, $0.1\text{--}13.8 \text{ mmol m}^{-2} \text{ d}^{-1}$) to the atmosphere (Fig. 2, Table 1). However, significant differences among these environments, in terms of

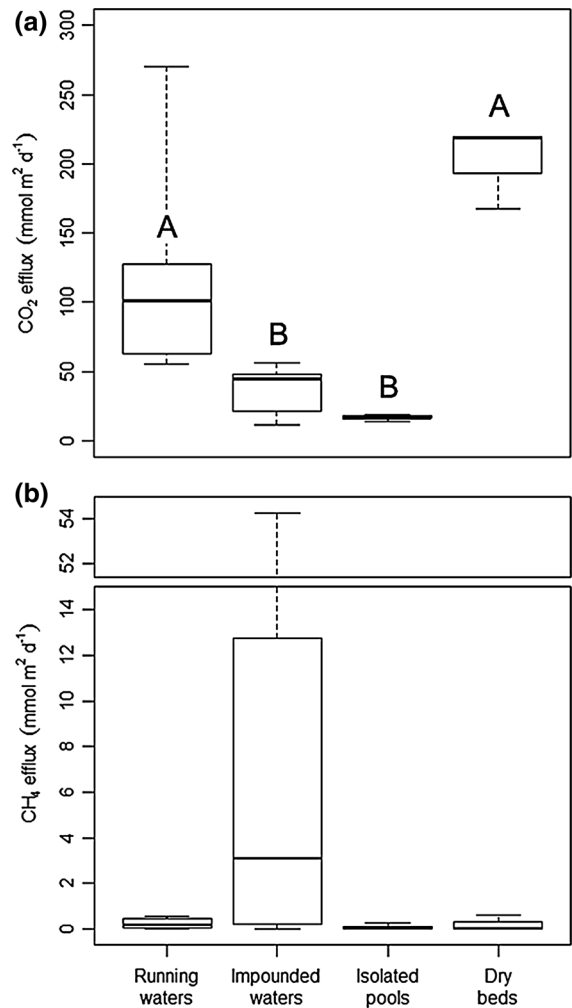


Fig. 2 Efflux of **a** CO_2 and **b** CH_4 measured from running waters ($n = 6$), impounded waters ($n = 5$), isolated pools ($n = 5$) and dry river and impoundment beds ($n = 3$). Box plots display the 25th, 50th and 75th percentiles; whiskers display minimum and maximum values. Significant differences of CO_2 and CH_4 efflux between environments ($p < 0.05$, Tukey's post hoc test) are marked with different capital letters above the box plots

CO_2 efflux (ANOVA, $F = 23.2$, $p < 0.001$, $n = 19$; Fig. 2a), were observed. The CO_2 efflux from dry beds (mean \pm SE = $209 \pm 10 \text{ mmol m}^{-2} \text{ d}^{-1}$) was statistically comparable to that from running waters ($120 \pm 33 \text{ mmol m}^{-2} \text{ d}^{-1}$) and significantly higher than the CO_2 efflux from impounded waters ($36.6 \pm 8.5 \text{ mmol m}^{-2} \text{ d}^{-1}$) and isolated pools ($17.2 \pm 0.9 \text{ mmol m}^{-2} \text{ d}^{-1}$). The intra-environment variability of the CO_2 efflux was highest in running waters and lowest in isolated pools (Fig. 2a, Table 1).

Table 1 Summary table showing the mean, the standard error (SE) and the total number of studied sites per environment (n) of the surface water partial pressures of CO₂ and CH₄ ($p\text{CO}_2$ and $p\text{CH}_4$), the direct and the indirect gas exchange coefficients (k_{600}), the total efflux of CO₂ and CH₄ and the percentage molar ratio between CH₄ and CO₂ flux (CH₄ flux : CO₂ flux) along the different studied environments

Parameter	Running waters			Impound waters			Isolated pools			Dry beds			ANOVA test <i>p</i> value
	Mean	SE	n	Mean	SE	n	Mean	SE	n	Mean	SE	n	
$p\text{ CO}_2$ ($\mu\text{ atm}$)	1841 ^A	242	6	1295 ^{AB}	228	5	2553 ^{AC}	224	5	NA	NA	NA	0.009
$p\text{ CH}_4$ ($\mu\text{ atm}$)	123	33	6	669	380	5	345	4.2	5	NA	NA	NA	0.12
Direct k_{600} (m d^{-1})	2.2 ^A	0.4	6	1.1 ^A	0.3	5	0.2 ^B	0.0	5	NA	NA	NA	<0.001
Indirect k_{600} (m d^{-1})	2.0 ^A	0.4	6	0.7 ^B	0.4	5	0.2 ^B	0.0	5	NA	NA	NA	<0.001
CO ₂ efflux ($\text{mmol m}^{-2} \text{ d}^{-1}$)	120 ^A (0)	32	6	36.6 ^B (0)	8.5	5	17.2 ^B (0)	0.9	5	209 ^A (0)	10	3	<0.001
CH ₄ efflux ($\text{mmol m}^{-2} \text{ d}^{-1}$)	0.2 (0)	0.1	6	13.8 (87)	10.1	5	0.1 (0)	0.0	5	0.2 (0)	0.5	3	0.089
CH ₄ efflux : CO ₂ efflux (%)	0.2 ^A	0.1	6	37.8 ^B	53.4	5	0.4 ^{AB}	2.4	5	0.2 ^{AB}	2.7	3	<0.001

Significant differences between environment types for each parameter were determined with a one-way ANOVA followed by Tukey's post hoc test and are displayed as different capital letters above the mean values

In brackets the percentages of ebullitive CO₂ and CH₄ effluxes in relation to the total CO₂ and CH₄ effluxes

NA not available

In contrast to CO₂, no significant differences in the CH₄ efflux were observed among the studied environments (ANOVA, $F = 2.62$, $p > 0.05$, $n = 19$; Fig. 2b). The CH₄ efflux from impounded waters ($14 \pm 10 \text{ mmol m}^{-2} \text{ d}^{-1}$) was the highest among the studied environments, but also showed the highest intra-environment variability (Fig. 2b, Table 1) and was thus, not significantly different from that of running waters ($0.2 \pm 0.1 \text{ mmol m}^{-2} \text{ d}^{-1}$), isolated pools ($0.10 \pm 0.05 \text{ mmol m}^{-2} \text{ d}^{-1}$) and dry beds ($0.2 \pm 0.2 \text{ mmol m}^{-2} \text{ d}^{-1}$).

Diffusion was the only mechanism driving CO₂ efflux in all studied environments (Table 1). Similarly, diffusion was most likely the only efflux mechanism for CH₄ in running waters, isolated pools and dry beds, while the predominant mechanism of CH₄ efflux in impounded waters was ebullition (>85 %; Table 1). Moreover, the percentage molar ratio between CH₄ and CO₂ efflux was significantly higher in impounded waters ($37.8 \pm 53.4 \%$) than in running waters ($0.2 \pm 0.1 \%$), isolated pools ($0.4 \pm 2.4 \%$) and dry beds ($0.2 \pm 2.7 \%$), where this ratio was nearly negligible (ANOVA, $F = 4.64$, $p < 0.001$, $n = 19$; Table 1).

Different spatial variation of CO₂ efflux, CO₂ concentration and O₂ concentration were observed in the aquatic environments sampled along a longitudinal gradient from headwaters to the mouth of the Fluvìà River (Online Resource Fig. S2)

Drivers of CO₂ and CH₄ effluxes

In dry beds, the basal respiration showed a significant positive linear relationship with both the dry bed water content ($r^2 = 0.72$, $p < 0.001$, $n = 10$; Fig. 3a) and the dry bed organic matter content ($r^2 = 0.71$, $p < 0.001$, $n = 10$; Fig. 3b). In contrast, the CO₂ efflux was inversely related to the dry bed water content ($r^2 = 0.75$, $p < 0.001$, $n = 10$; Fig. 3c) and showed no significant relationship with the dry bed organic matter content ($r^2 = 0.21$, $p > 0.05$, $n = 10$; Fig. 3d). This resulted in a significant negative exponential relationship between the basal respiration and CO₂ efflux in dry beds ($r^2 = 0.53$, $p < 0.001$, $n = 10$).

In aquatic environments, the two main parameters directly involved in the diffusion of CO₂ across the water-atmosphere boundary (i.e., surface water $p\text{CO}_2$ and k_{600} ; Eq. (2)) were directly related to the CO₂

efflux. When all aquatic environments were pooled together, the k_{600} and CO₂ efflux exhibited a significant positive relationship ($r^2 = 0.79$, $p < 0.001$, $n = 16$; Fig. 4a), while no dependency between surface water $p\text{CO}_2$ and the CO₂ efflux was detected ($p > 0.05$, $n = 16$; Fig. 4b). However, the CO₂ efflux and $p\text{CO}_2$ were positively related when the isolated pools were excluded from the model ($r^2 = 0.49$, $p = 0.015$, $n = 11$; Fig. 4b). The multiple regression analysis revealed that $p\text{CO}_2$ and k_{600} explained 0.1 and 86 % of the total variation in the CO₂ efflux, respectively, when all aquatic environments were included in the model. In contrast, when isolated pools were excluded from the multiple regression analysis, $p\text{CO}_2$ and k_{600} explained 49 and 38 % of the total variation in the CO₂ efflux, respectively ($r^2 = 0.87$, $p = 0.003$, $n = 11$).

A high contribution of ebullition to the CH₄ efflux was detected in the impounded waters, with increased residence time, higher sediment organic matter content and porosity and lower dry bulk density (Table 2). However, both the low number of study sites where ebullition of CH₄ was detected and the narrow range of ebullitive efflux values prevented a robust statistical analysis of the potential drivers that control the ebullitive CH₄ efflux.

The surface water physicochemical or hydromorphological variables (Online Resource Table S1) were not significantly related to the CO₂ and CH₄ effluxes or the $p\text{CO}_2$, $p\text{CH}_4$ and k_{600} in these aquatic environments.

Discussion

Hot spots for CO₂ and CH₄ effluxes

Among the different environments investigated in the present study, running waters and dry beds emitted significantly higher amounts of CO₂ than the other environments. Several studies have highlighted the importance of running waters as hot spots for CO₂ efflux (Cole et al. 2007; Battin et al. 2009a; Raymond et al. 2013). The results of the present study also show that the dry beds associated with the dry phase of Mediterranean temporary rivers are not only inert but also active sites in terms of CO₂ emissions to the atmosphere. The CO₂ efflux from dry beds (mean = $209 \text{ mmol m}^{-2} \text{ d}^{-1}$, range = $189\text{--}220 \text{ mmol m}^{-2} \text{ d}^{-1}$) was higher than that

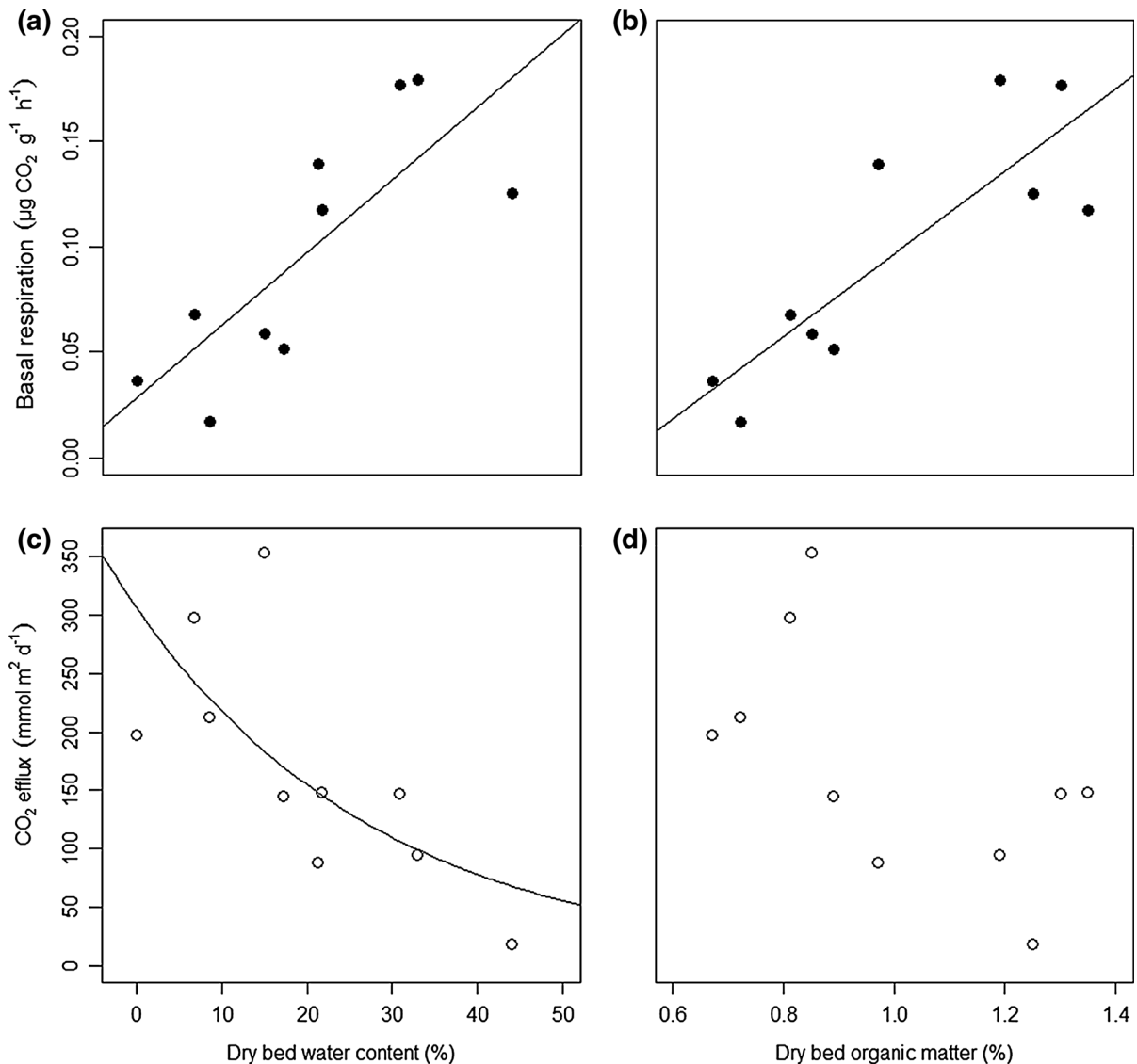


Fig. 3 Basal respiration as a function of **a** dry bed water content and **b** dry bed organic matter. Efflux of CO₂ as a function of **c** dry bed water content and **d** dry bed organic matter. The continuous line in **a** ($r^2 = 0.72$, $p < 0.001$, $n = 10$) and **b** ($r^2 = 0.71$, $p < 0.001$, $n = 10$) represent the linear regression model *fitting line* between predictor and response variables. The

continuous line in **c** ($r^2 = 0.65$, $p < 0.001$, $n = 10$) represents the exponential regression model *fitting line* between predictor and response variables. Absence of continuous line in **d** represents that no significant regression model fitted with the observed values

from dry desert streams in Arizona ($43.5 \text{ mmol m}^{-2} \text{ d}^{-1}$, range = $19.6\text{--}65 \text{ mmol m}^{-2} \text{ d}^{-1}$; Gallo et al. 2014), to our knowledge the only study reporting CO₂ emissions from dry beds in different catchments. The CO₂ efflux from dry beds was also higher than the global mean CO₂ efflux from soils ($123 \text{ mmol m}^{-2} \text{ d}^{-1}$, range = $121\text{--}125 \text{ mmol m}^{-2} \text{ d}^{-1}$; Raich et al. (2002)) and the regional mean CO₂ efflux from desert soils

($104 \text{ mmol m}^{-2} \text{ d}^{-1}$, range = $95\text{--}110 \text{ mmol m}^{-2} \text{ d}^{-1}$; Raich and Schlesinger (1992)), and it was in the upper range of values for the regional mean CO₂ efflux from Mediterranean soils ($188 \text{ mmol m}^{-2} \text{ d}^{-1}$, range = $44\text{--}371 \text{ mmol m}^{-2} \text{ d}^{-1}$; Bond-Lamberty and Thomson (2010)). Although the magnitude of CO₂ efflux from dry beds was within the range of reported soil emissions, the CO₂ from this environment should not be considered

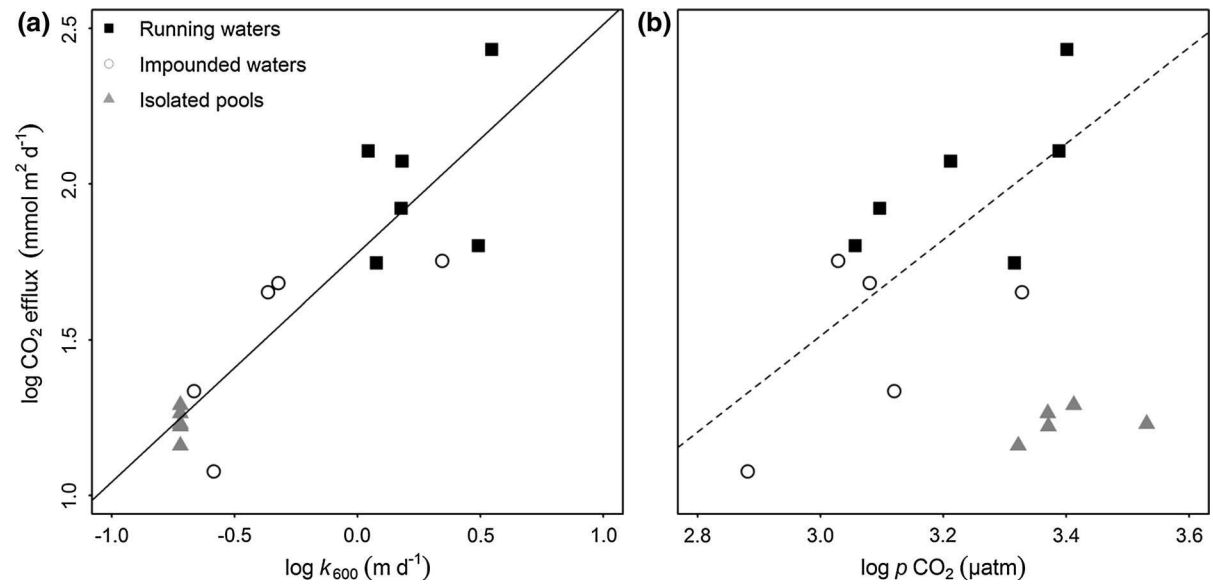


Fig. 4 Efflux of CO_2 as a function of **a** k_{600} and **b** surface water $p\text{CO}_2$ for all the aquatic study sites. *Squares* running waters; *circles* impounded waters; *triangles* isolated river pools. The *continuous line* in **a** represents the linear regression model fitting

line incorporating all the environments ($r^2 = 0.79$, $p < 0.001$, $n = 16$). The *dashed line* in **b** represents the linear regression model *fitting line* excluding isolated river pools ($r^2 = 0.49$, $p = 0.015$, $n = 11$)

Table 2 Hydromorphologic descriptors, and sediment physical and chemical properties of the different impounded waters

Site	Ebullition of CH_4		Hydromorphologic characteristics			Sediment properties			
	Detection (yes/no)	Flux (%)	Residence time (h)	Mean depth (m)	Max. depth (m)	Water content (%)	Dry bulk density (g cm^{-3})	Porosity	Organic matter (mg cm^{-3})
1	Yes	82	4247.6	16.5	45.5	0.69	0.41	0.84	26.2
2	Yes	87	49.7	1.8	5.7	0.63	0.51	0.77	35.5
3	Yes	90	39.8	2.5	5.4	0.58	0.62	0.69	29.8
4	No	0	5.1	1.5	3.6	0.41	1.00	0.41	18.7
5	No	0	3.7	1.1	2.6	NA	NA	NA	NA

Flux indicates the percentage of ebullitive efflux to the total CH_4 efflux

NA not available

terrestrial because the carbon processed in dry beds has either already left from the terrestrial ecosystems and entered into the fluvial network or has been produced within the fluvial network. In addition, the sediments from dry rivers and terrestrial soils are different environments in terms of physical structure and biogeochemical dynamics (McIntyre et al. 2009; Larned et al. 2010; Steward et al. 2012). Thus, we emphasize that dry beds should be included in CO_2 balances from fluvial networks, particularly in arid and semiarid

regions, such as the Mediterranean (von Schiller et al. 2014).

Despite the high variability of CH_4 efflux detected for impounded waters, this environment likely represents a hot spot for CH_4 efflux to the atmosphere. This result is consistent with the notion that impounded waters stored in dams and smaller impoundments play a prominent role in the CH_4 efflux from fluvial networks (Xiao et al. 2013; Maeck et al. 2013). Furthermore, the other three environments studied

(running waters, isolated pools and dry beds) were net emitters of CH₄. Although previous studies have detected CH₄ efflux from rivers (Striegl et al. 2012; Campeau and Lapierre 2014; Crawford et al. 2014) and dry beds (Gallo et al. 2014), this study provides to our knowledge the first evaluation of the CH₄ efflux from isolated river pools.

Ebullition was the primary pathway for CH₄ efflux from impounded waters. This finding is consistent with previous studies (Del Sontro et al. 2010; Maeck et al. 2013) and contrary to the efflux pathway of CO₂ which is a more soluble gas that primarily follows a strictly diffusive pathway of emission to the atmosphere (Belger et al. 2010). The ebullitive CH₄ efflux from impounded waters, as the only environment experiencing ebullition in the present study, contributed to more than 85 % of the total CH₄ efflux when the evasion of CH₄ was detected.

The CH₄ efflux was estimated using a floating chamber, reported as the most appropriate method for water-atmosphere diffusion flux measurements (Cole et al. 2010). Nonetheless, the floating chamber approach can be problematic in the case of ebullition measurements from aquatic systems (Bastviken et al. 2004; Del Sontro 2011; Crawford et al. 2014). The vast spatial and temporal heterogeneity of CH₄ ebullitive fluxes is generally not captured through short-term floating chamber experiments (10 min in our study). An inverted funnel survey designed to cover the maximum surface area of the impounded waters would likely have reduced potential sampling bias and increased the accuracy of the spatially and temporally integrated final dataset for CH₄ ebullitive fluxes (Bastien and Demarty 2013; Maeck et al. 2013). Although we did not observe ebullition in running waters and isolated pools (i.e., we never observed non-linearity in $d\text{CH}_4/dt$ during the chamber deployments or bubbles emerging from the stream or isolated pool sediments), a sampling design with inverted funnel-style bubble traps would have improved the characterization of CH₄ ebullitive fluxes from these environments (Baulch et al. 2011; Crawford et al. 2014). Despite the potential inaccuracies in capturing the temporal and spatial heterogeneity, the results indicate that the contribution of ebullitive efflux of CH₄ to the total CH₄ efflux is substantial in Mediterranean impounded waters during summer drought, and that they should be taken into account in CH₄ flux assessments.

Physical and biogeochemical regulation of CO₂ and CH₄ effluxes

The unexpected negative relationship between the basal respiration and CO₂ efflux indicates potential decoupling between CO₂ production and CO₂ emission from dry river and impoundment beds. This decoupling between processes suggests the existence of a physical factor restricting the evasion of the biologically produced CO₂. Based on the results obtained in the present study, the dry bed water content might play a dual role in the CO₂ generation-emission mechanism. On the one hand, higher water content enhances C respiration by facilitating the contact between microorganisms and available substrates (Koschorreck and Darwich 2003; Xu et al. 2004; Luo and Zhou 2010). On the other hand, higher water content diminishes the CO₂ efflux through the restriction of the gas diffusivity through the dry media, consistent with the results from Howard and Howard (1993) and Fujikawa and Miyazaki (2005) showing that the diffusivity of CO₂ and other gases in soils is strongly reduced when the air-filled porosity decreases with increasing water content. Taken together, these results suggest that the water content might modulate the uncoupling between CO₂ production and CO₂ emission from dry beds. However, it has to be noted that dry bed water content is highly dynamic in both space and time, and other non-biotic CO₂-generating processes (e.g., interactions with the groundwater system (Rey 2015), reactions with the carbonate system (Angert et al. 2014) or photochemical degradation reactions (Austin and Vivanco 2006) could potentially contribute to the observed uncoupling between the respiratory process and the emission of CO₂. Hence, further studies are required to understand the relative importance of environmental variables (e.g., air temperature, precipitation, vegetation) with respect to the role of local conditions (e.g., water content, temperature, organic matter content and type, grain size distribution of the substrate, light regime, and carbonate content) in driving the CO₂ efflux from dry beds.

In aquatic environments, the diffusive CO₂ efflux depends on both the surface water $p\text{CO}_2$, which is primarily regulated through biogeochemical processes (Sobek and Algesten 2003; Campeau and Del Giorgio 2014), and the k_{600} , which is a physical factor including the turbulent and molecular diffusion of

CO₂ (Bade 2009). However, the extent to which these two factors regulate the aquatic CO₂ efflux from Mediterranean fluvial networks during summer drought and whether there are shifts in the relative importance of these two parameters across the different aquatic environments remain unknown. The results of the present study show that k_{600} acts as the primary control for the CO₂ efflux along the studied aquatic environments. Although the three types of aquatic environments were supersaturated in terms of $p\text{CO}_2$, strong evidence for the active role of the physical turbulence (measured here as k_{600}) as a factor enhancing the exchange process between generated CO₂ and emitted CO₂ was observed (Halbedel and Koschorreck 2013). In running waters, the aquatic environment experiencing the highest CO₂ efflux, the CO₂ gas is immediately emitted because the high turbulence disrupts the surface boundary layer (Alin et al. 2011; Demars and Manson 2013). With values of $p\text{CO}_2$ similar to those from running waters, impounded waters showed a lower efflux of CO₂, suggesting a partial physical limitation of CO₂ gas. An extreme effect of the physical limitation of CO₂ efflux occurred in the isolated river pools, where CO₂ efflux was lowest despite showing the highest $p\text{CO}_2$.

Because of the unbalanced contribution of diffusion and ebullition to the total CH₄ efflux in the different environments, any statistical assessment of the factors controlling the CH₄ efflux could not be performed. In any case, the total CH₄ efflux was detectable, but low, from all environments, except impounded waters, where the dominant efflux pathway was the ebullitive one (see above). Nonetheless, our results are consistent with those of previous studies showing that both the residence time and the sediment physical and chemical composition also play a crucial role in controlling the biological activity involved in the generation of CH₄ in the sediment layer (Sobek et al. 2012; Maeck et al. 2013). The amount and composition of stored organic matter are key factors affecting the biological activity in sediments and, therefore, the CH₄ efflux (Mulholland and Elwood 1982; Downing et al. 2008; Sobek et al. 2012). Moreover, the porosity of the sediment plays an important role by limiting or favouring the diffusion of CH₄, the shape of CH₄ bubbles and the capacity for CH₄ to escape from or be retained in the sediment media (Del Sontro 2011; Meier et al. 2011).

Unexpectedly, the CH₄ efflux in isolated pools was low, despite the high water residence time and optimum redox conditions for methanogenic activity, suggesting that these systems contain much less stored organic matter compared with impounded waters which are more active organic matter traps. Thus, we speculate that the amount of organic matter could be a limiting factor for the CH₄ generation in the sediments of isolated pools. Nevertheless, the hydrological isolation in the pools generates individual systems highly influenced through particular local conditions (Bonada and Resh 2013; Fellman et al. 2010; von Schiller et al. 2011). For example, these observations would likely differ under contrasting situations, such as increased canopy cover and higher leaf input. Thus, further investigation of the hydrological and biogeochemical processes in isolated pools over time and across contrasting systems is needed to better understand the dynamics of C emissions from these systems.

Potential changes in C emissions from Mediterranean fluvial networks under future hydrological scenarios

River desiccation and impoundment of running waters through the construction of dams or small weirs have been recognized as some of the most important environmental pressures on fluvial networks worldwide (Nilsson et al. 2005; Sabater 2008; Vörösmarty et al. 2010; Steward et al. 2012). The influence and interplay between these two processes largely determines the relative surface area of the different environments comprising the fluvial network. Estimation of the areal extent and distribution of different environments along the fluvial network is key aspect when upscaling specific biogeochemical processes to the entire fluvial network (Benstead and Leigh 2012). However, the high temporal and spatial dynamism of Mediterranean rivers makes these estimations extremely difficult and subject to high inaccuracies (Benstead and Leigh 2012; Detry et al. 2014).

Herein, we applied a simple heuristic approach using different potential scenarios to evaluate how river desiccation and running water impoundment might affect the C emissions from fluvial networks. We combined the mean CO₂ and CH₄ effluxes measured for each environment with the relative surface area (%) of each environment in each scenario to obtain a mean fluvial network efflux of CO₂, CH₄, and total C (i.e., sum of CO₂ and CH₄), and the total C considering the global warming potential (i.e., C_{GWP} ;

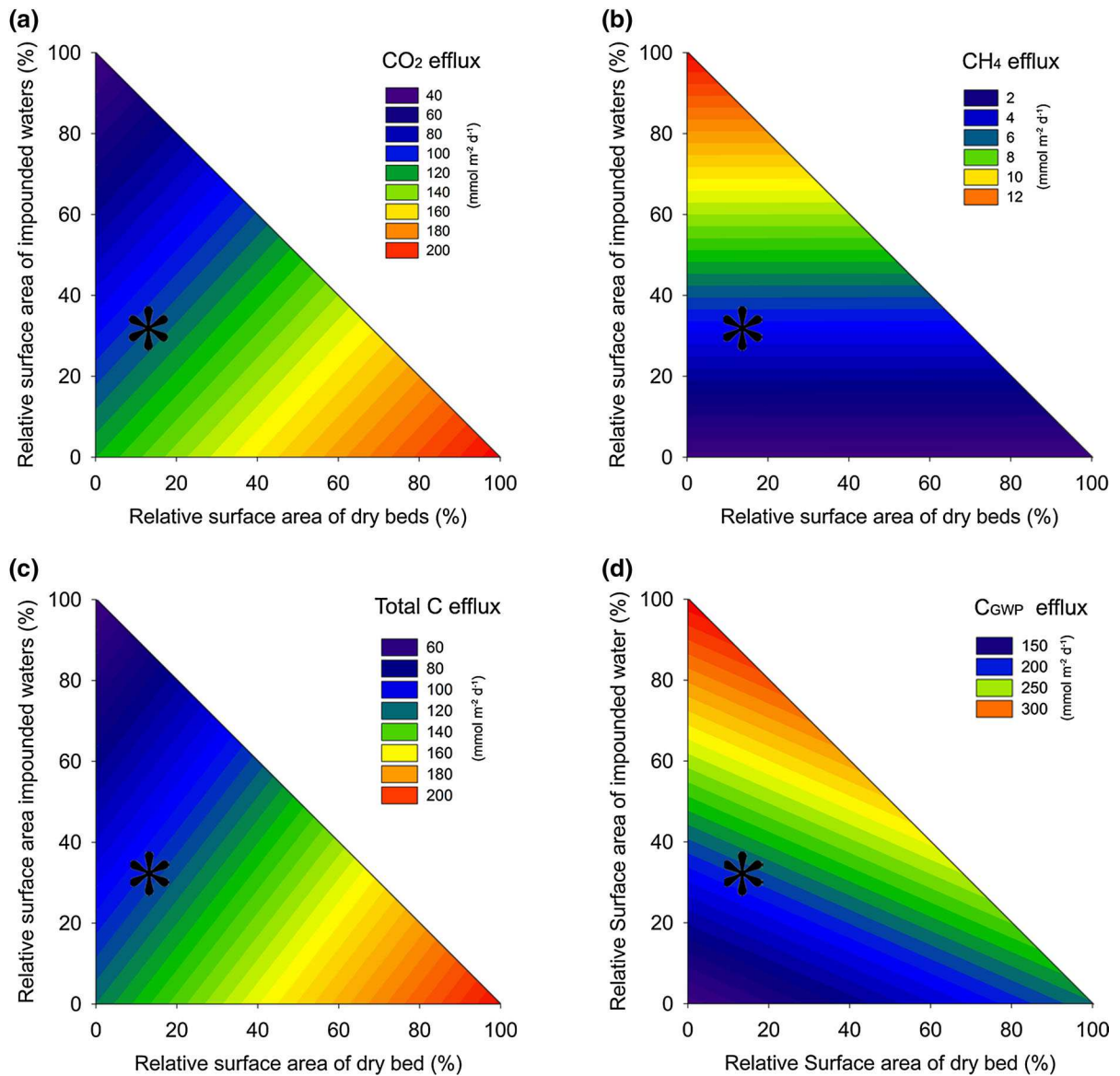


Fig. 5 Contour plots simulating the effect of a broad spectrum of potential hydrological scenarios of river desiccation and transformation of running waters into impounded waters of an hypothetical Mediterranean fluvial network during summer drought (expressed in terms of relative surface area of dry bed (x -axis) and relative surface area of impounded waters (y -axis))

expressed as CO_2 Eq (Fig. 5). We then combined the annual mean relative area per environment from the COastal Segmentation analysis and the related CATchments regions for the study region (Meybeck et al. (2006), COSCAT Region 418) with the data from the dry and total river effective areas from the same

on **a** the mean fluvial network CO_2 efflux, **b** the mean fluvial network CH_4 efflux, **c** the mean total fluvial network C efflux and **d** the mean total C efflux considering the global warming potential of CH_4 . The marked asterisks represent an idealized Western Mediterranean fluvial network. Details of calculations are provided in the text

region (Raymond et al. 2013) to situate an idealized Western Mediterranean fluvial network in the scenarios contour map (Fig. 5). The idealized fluvial network (with an annual mean relative surface area of running waters, impounded waters and dry river and impoundment beds of 54.8, 30.7 and 14.5 %,

respectively) emits $107 \text{ mmol m}^{-2}\text{d}^{-1}$ of CO_2 , $4.4 \text{ mmol m}^{-2} \text{ d}^{-1}$ of CH_4 , $112 \text{ mmol m}^{-2} \text{ d}^{-1}$ of total C and $217 \text{ mmol m}^{-2} \text{ d}^{-1}$ of total C_{GWP} .

The results from this heuristic approach showed that the potential scenarios with the highest mean CO_2 and total C effluxes were those in which the relative surface area of dry beds was highest (Fig. 5a, c). In contrast, the results also showed that the potential scenarios with the highest mean CH_4 and total C_{GWP} effluxes were those in which the relative surface area of the impounded waters dominated the fluvial network (Fig. 5b, d).

According to these scenarios, in the idealized fluvial network, (i) an extreme drying out (i.e., a fourfold increase of the surface area of dry beds) doubled the CO_2 and the total C effluxes, (ii) an extreme transformation of running waters into impounded waters (i.e., a twofold increase of the surface area of impounded waters) tripled the CH_4 and the total C_{GWP} effluxes and (iii) a proportional drying out and transformation of running waters into impounded waters increased the emission of all CO_2 , CH_4 , total C and total C_{GWP} . Despite the methodological uncertainties of this approach, the results clearly illustrate that global change could have a relevant impact on C emissions from fluvial networks in arid and semi-arid regions, such as the Mediterranean.

Conclusions

The results of the present study show that dry beds and running waters (for CO_2) and impounded waters (for CH_4) are hot spots for C efflux from Mediterranean fluvial networks during summer drought. These results suggest dry beds as active sites in terms of C emissions, which should be considered in C balances from fluvial networks in arid and semiarid areas. The CO_2 efflux, which was only mediated via diffusion, is most physically limited in both dry and aquatic environments. In contrast, the CH_4 efflux, which is predominantly mediated through ebullition, is primarily controlled through the biological activity in the sediments. The duration, spatial extent and severity of flow intermittency and the degree of river impoundment will play a decisive role in shaping the C efflux from fluvial networks in response to global change.

Acknowledgments All the data used for the results of this paper is available upon request to the corresponding author. We thank P. A. Raymond for providing data of the effective area occupied by dry rivers in our COSCAT region. This research was funded by the Spanish Ministry of Economy and Competitiveness through the projects CGL2011-30474-C02-01 and CGL2014-58760-C3-1-R. Ll. Gómez-Gener and J. P. Casas-Ruiz were additionally supported by FPI predoctoral grants (BES-2012-059743 and BES-2012-059655) and D. von Schiller by a “Juan de la Cierva” postdoctoral grant (JCI-2010-06397). We thank Carmen Gutiérrez, Mertixell Abril and Susanne Halbedel, for the lab and field assistance. We also thank the Scientific and Technical Service Department of the Catalan Institute for Water research (ICRA) for the lab assistance.

References

- Abril G (2005) Carbon dioxide and methane emissions and the carbon budget of a 10-year old tropical reservoir (Petit Saut, French Guiana). *Global Biogeochem Cycles* 19:1–16. doi:[10.1029/2005GB002457](https://doi.org/10.1029/2005GB002457)
- Acuña V, Tockner K (2010) The effects of alterations in temperature and flow regime on organic carbon dynamics in Mediterranean river networks. *Global Chang Biol* 16:2638–2650. doi:[10.1111/j.1365-2486.2010.02170.x](https://doi.org/10.1111/j.1365-2486.2010.02170.x)
- Acuña V, Detry T, Marshall J et al (2014) Why should we care about temporary waterways? *Science* 343:1080–1082. doi:[10.1126/science.1246666](https://doi.org/10.1126/science.1246666)
- Alin SR, Rasera MDFFL, Salimon CI et al (2011) Physical controls on carbon dioxide transfer velocity and flux in low-gradient river systems and implications for regional carbon budgets. *J Geophys Res* 116:G01009. doi:[10.1029/2010JG001398](https://doi.org/10.1029/2010JG001398)
- Angert A, Yakir D, Rodeghiero M et al (2014) Using O_2 to study the relationships between soil CO_2 efflux and soil respiration. *Biogeosciences Discuss* 11:12039–12068. doi:[10.5194/bgd-11-12039-2014](https://doi.org/10.5194/bgd-11-12039-2014)
- Austin AT, Vivanco L (2006) Plant litter decomposition in a semi-arid ecosystem controlled by photodegradation. *Nature* 442:555–558. doi:[10.1038/nature05038](https://doi.org/10.1038/nature05038)
- Bade DL (2009) Gas exchange across the air-water interface. In: Gene EL (ed) *Encyclopedia of inland waters*. Academic Press, Oxford, pp 70–78
- Bastien J, Demarty M (2013) Spatio-temporal variation of gross CO_2 and CH_4 diffusive emissions from Australian reservoirs and natural aquatic ecosystems, and estimation of net reservoir emissions. *Lakes Reserv Res Manag* 18:115–127. doi:[10.1111/lre.12028](https://doi.org/10.1111/lre.12028)
- Bastviken D, Cole J, Pace M, Tranvik LJ (2004) Methane emissions from lakes: dependence of lake characteristics, two regional assessments, and a global estimate. *Global Biogeochem Cycles* 18:1–12. doi:[10.1029/2004GB002238](https://doi.org/10.1029/2004GB002238)
- Bastviken D, Tranvik LJ, Downing JA et al (2011) Freshwater methane emissions offset the continental carbon sink. *Science* 331:50–57. doi:[10.1126/science.1196808](https://doi.org/10.1126/science.1196808)
- Battin TJ, Luyssaert S, Kaplan LA et al (2009a) The boundless carbon cycle. *Nat Geosci* 2:598–600. doi:[10.1038/ngeo618](https://doi.org/10.1038/ngeo618)

- Battin TJ, Kaplan LA, Findlay S et al (2009b) Biophysical controls on organic carbon fluxes in fluvial networks. *Nat Geosci* 2:95–100. doi:[10.1038/ngeo602](https://doi.org/10.1038/ngeo602)
- Baulch HM, Dillon PJ, Maranger R, Schiff SL (2011) Diffusive and ebullitive transport of methane and nitrous oxide from streams: are bubble-mediated fluxes important? *J Geophys Res Biogeosciences* 116:1–15. doi:[10.1029/2011JG001656](https://doi.org/10.1029/2011JG001656)
- Beaulieu JJ, Shuster WD, Rebolz JA (2012) Controls on gas transfer velocities in a large river. *J Geophys Res Biogeosciences* 117:1–13. doi:[10.1029/2011JG001794](https://doi.org/10.1029/2011JG001794)
- Belger L, Forsberg BR, Melack JM (2010) Carbon dioxide and methane emissions from interfluvial wetlands in the upper Negro River basin, Brazil. *Biogeochemistry* 105:171–183. doi:[10.1007/s10533-010-9536-0](https://doi.org/10.1007/s10533-010-9536-0)
- Benstead JP, Leigh DS (2012) An expanded role for river networks. *Nat Geosci* 5:678–679. doi:[10.1038/ngeo1593](https://doi.org/10.1038/ngeo1593)
- Bernal S, von Schiller D, Sabater F, Martí E (2013) Hydrological extremes modulate nutrient dynamics in mediterranean climate streams across different spatial scales. *Hydrobiologia* 719:31–42. doi:[10.1007/s10750-012-1246-2](https://doi.org/10.1007/s10750-012-1246-2)
- Bonada N, Resh VH (2013) Mediterranean-climate streams and rivers: geographically separated but ecologically comparable freshwater systems. *Hydrobiologia* 719:1–29. doi:[10.1007/s10750-013-1634-2](https://doi.org/10.1007/s10750-013-1634-2)
- Bond-Lamberty B, Thomson A (2010) A global database of soil respiration data. *Biogeosciences* 7:1915–1926. doi:[10.5194/bg-7-1915-2010](https://doi.org/10.5194/bg-7-1915-2010)
- Campbell C, Chapman S (2003) A rapid microtiter plate method to measure carbon dioxide evolved from carbon substrate amendments so as to determine the physiological profiles of soil microbial. *Appl Environ Microbiol* 69:3593–3599. doi:[10.1128/AEM.69.6.3593](https://doi.org/10.1128/AEM.69.6.3593)
- Campeau A, Del Giorgio PA (2014) Patterns in CH₄ and CO₂ concentrations across boreal rivers: major drivers and implications for fluvial greenhouse emissions under climate change scenarios. *Glob Chang Biol* 20:1–14. doi:[10.1111/gcb.12479](https://doi.org/10.1111/gcb.12479)
- Campeau A, Lapierre J (2014) Regional contribution of CO₂ and CH₄ fluxes from the fluvial network in a lowland boreal landscape of Québec. *Glob Biogeochem Cycles* 28:1–13. doi:[10.1002/2013GB004685](https://doi.org/10.1002/2013GB004685)
- Cole JJ, Prairie YT, Caraco NF et al (2007) Plumbing the global carbon cycle: integrating inland waters into the terrestrial carbon budget. *Ecosystems* 10:172–185. doi:[10.1007/s10021-006-9013-8](https://doi.org/10.1007/s10021-006-9013-8)
- Cole JJ, Bade DL, Bastviken D et al (2010) Multiple approaches to estimating air-water gas exchange in small lakes. *Limnol Oceanogr Methods* 8:285–293. doi:[10.4319/lom.2010.8.285](https://doi.org/10.4319/lom.2010.8.285)
- Crawford JT, Stanley EH, Spawn SA et al (2014) Ebullitive methane emissions from oxygenated wetland streams. *Global Chang Biol* 20:3408–3422. doi:[10.1111/gcb.12614](https://doi.org/10.1111/gcb.12614)
- Crusius J, Wanninkhof R (2003) Gas transfer velocities measured at low wind speed over a lake. *Limnol Oceanogr* 48:1010–1017. doi:[10.4319/lo.2003.48.3.1010](https://doi.org/10.4319/lo.2003.48.3.1010)
- Dahm CN, Baker MA, Moore DI, Thibault JR (2003) Coupled biogeochemical and hydrological responses of streams and rivers to drought. *Freshw Biol* 48:1219–1231. doi:[10.1046/j.1365-2427.2003.01082.x](https://doi.org/10.1046/j.1365-2427.2003.01082.x)
- Datry T, Larned ST, Tockner K (2014) Intermittent rivers: a challenge for freshwater ecology. *Bioscience* 64:229–235. doi:[10.1093/biosci/bit027](https://doi.org/10.1093/biosci/bit027)
- Dean WE (1974) Determination of carbonate and organic matter in calcareous sediments and sedimentary rocks by loss on ignition: comparison with other method. *J Sediment Petrol* 44:242–248. doi:[10.1306/74D729D2-2B21-11D7-864800102C1865D](https://doi.org/10.1306/74D729D2-2B21-11D7-864800102C1865D)
- Del Sontro T (2011) Quantifying methane emissions from reservoirs: from Basin-scale to discrete analyses with a focus on ebullition dynamics. PhD dissertation, Eidgenössische Technische Hochschule ETH Zürich, Zürich. doi: <http://dx.doi.org/10.3929/ethz-a-006725547>
- Del Sontro T, McGinnis DF, Sobek S et al (2010) Extreme methane emissions from a Swiss hydropower reservoir: contribution from bubbling sediments. *Environ Sci Technol* 44:2419–2425. doi:[10.1021/es9031369](https://doi.org/10.1021/es9031369)
- Demars BOL, Manson JR (2013) Temperature dependence of stream aeration coefficients and the effect of water turbulence: a critical review. *Water Res* 47:1–15. doi:[10.1016/j.watres.2012.09.054](https://doi.org/10.1016/j.watres.2012.09.054)
- Donelan MA (1990) Air–sea interaction. In: LeMehaute B, Hanes D (eds) *The sea: ocean engineering science*. Wiley, New York, pp 239–292
- Downing JA, Cole JJ, Middelburg JJ et al (2008) Sediment organic carbon burial in agriculturally eutrophic impoundments over the last century. *Global Biogeochem Cycles* 22:GB1018. doi:[10.1029/2006GB002854](https://doi.org/10.1029/2006GB002854)
- Fearnside PM, Pueyo S (2012) Greenhouse-gas emissions from tropical dams. *Nat Clim Chang* 2:382–384. doi:[10.1038/nclimate1540](https://doi.org/10.1038/nclimate1540)
- Fellman JB, Hood E, Spencer RGM (2010) Fluorescence spectroscopy opens new windows into dissolved organic matter dynamics in freshwater ecosystems: a review. *Limnol Oceanogr* 55:2452–2462. doi:[10.4319/lo.2010.55.6.2452](https://doi.org/10.4319/lo.2010.55.6.2452)
- Forzieri G, Feyen L, Rojas R et al (2014) Ensemble projections of future streamflow droughts in Europe. *Hydrol Earth Syst Sci* 18:85–108. doi:[10.5194/hess-18-85-2014](https://doi.org/10.5194/hess-18-85-2014)
- Frankignoulle M (1988) Field measurements of air-sea CO₂ exchange. *Limnol Oceanogr* 33:313–322
- Fujikawa T, Miyazaki T (2005) Effects of bulk density and soil type on the gas diffusion coefficient in repacked and undisturbed soils. *Soil Sci* 170:892–901. doi:[10.1097/01.ss.0000196771.53574.79](https://doi.org/10.1097/01.ss.0000196771.53574.79)
- Gallo EL, Lohse KA, Ferlin CM et al (2014) Physical and biological controls on trace gas fluxes in semi-arid urban ephemeral waterways. *Biogeochemistry* 121:189–207. doi:[10.1007/s10533-013-9927-0](https://doi.org/10.1007/s10533-013-9927-0)
- García-Ruiz JM, López-Moreno JJ, Vicente-Serrano SM et al (2011) Mediterranean water resources in a global change scenario. *Earth-Sci Rev* 105:121–139. doi:[10.1016/j.earscirev.2011.01.006](https://doi.org/10.1016/j.earscirev.2011.01.006)
- Gasith A, Resh VH (1999) Streams in mediterranean climate regions: abiotic influences and biotic responses to predictable seasonal events. *Annu Rev Ecol Syst* 30:51–81. doi:[10.1146/annurev.ecolsys.30.1.51](https://doi.org/10.1146/annurev.ecolsys.30.1.51)
- Guérin F, Abril G, Serça D et al (2007) Gas transfer velocities of CO₂ and CH₄ in a tropical reservoir and its river downstream. *J Mar Syst* 66:161–172. doi:[10.1016/j.jmarsys.2006.03.019](https://doi.org/10.1016/j.jmarsys.2006.03.019)

- Halbedel S, Koschorreck M (2013) Regulation of CO₂ emissions from temperate streams and reservoirs. *Biogeosciences* 10:7539–7551. doi:[10.5194/bg-10-7539-2013](https://doi.org/10.5194/bg-10-7539-2013)
- Hope D, Palmer SM, Billett MF, Dawson JJC (2001) Carbon dioxide and methane evasion from a temperate peatland stream. *Limnol Oceanogr* 46:847–857. doi:[10.4319/lo.2001.46.4.0847](https://doi.org/10.4319/lo.2001.46.4.0847)
- Hornberger GM, Kelly MG (1975) Atmospheric reaeration in a river using productivity analysis. *J Environ Eng Div ASCE* 101:729–739
- Howard D, Howard P (1993) Relationships between CO₂ evolution, moisture content and temperature for a range of soil types. *Soil Biol Biochem* 25:1537–1546. doi:[10.1016/0038-0717\(93\)90008-Y](https://doi.org/10.1016/0038-0717(93)90008-Y)
- IPCC 2013: Climate Change 2013: The physical science basis. Contribution of Working Group I to the fifth assessment report of the Intergovernmental Panel on climate change. Stocker TF, Qin D, Plattner G-K, Tignor M, Allen SK, Boschung J, Nauels A, Xia Y, Bex V, Midgley PM (eds). Cambridge University Press, Cambridge and New York, 1535 pp
- Jähne B, Münnich K (1987) On the parameters influencing air-water gas exchange. *J Geophys Res Ocean* 92:1937–1942. doi:[10.1029/JC092iC02p01937](https://doi.org/10.1029/JC092iC02p01937)
- Jonsson A, Algesten G, Bergström AK et al (2007) Integrating aquatic carbon fluxes in a boreal catchment carbon budget. *J Hydrol* 334:141–150. doi:[10.1016/j.jhydrol.2006.10.003](https://doi.org/10.1016/j.jhydrol.2006.10.003)
- Kling GW, Kipphut GW, Miller MC (1991) Arctic lakes and streams as gas conduits to the atmosphere: implications for tundra carbon budgets. *Science* 251(4991):298–301. doi:[10.1126/science.251.4991.298](https://doi.org/10.1126/science.251.4991.298)
- Koschorreck M, Darwich A (2003) Nitrogen dynamics in seasonally flooded soils in the Amazon floodplain. *Wetl Ecol Manag* 11:317–330. doi:[10.1023/B:WETL.0000005536.39074.72](https://doi.org/10.1023/B:WETL.0000005536.39074.72)
- Lake PS (2011) Drought and aquatic ecosystems: effects and responses. Wiley-Blackwell, Chichester
- Larned ST, Dattray T, Arscott DB, Tockner K (2010) Emerging concepts in temporary-river ecology. *Freshw Biol* 55:717–738. doi:[10.1111/j.1365-2427.2009.02322.x](https://doi.org/10.1111/j.1365-2427.2009.02322.x)
- Laurion I, Vincent W, McIntyre S (2010) Variability in greenhouse gas emissions from permafrost thaw ponds. *Limnol Oceanogr* 55:115–133. doi:[10.4319/lo.2010.55.1.0115](https://doi.org/10.4319/lo.2010.55.1.0115)
- López P, Marcé R, Armengol J (2011) Net heterotrophy and CO₂ evasion from a productive calcareous reservoir: adding complexity to the metabolism-CO₂ evasion issue. *J Geophys Res Biogeosciences* 116:G02021. doi:[10.1029/2010JG001614](https://doi.org/10.1029/2010JG001614)
- Lundin EJ, Giesler R, Persson A et al (2013) Integrating carbon emissions from lakes and streams in a subarctic catchment. *J Geophys Res Biogeosciences* 118:1–8. doi:[10.1002/jgrg.20092](https://doi.org/10.1002/jgrg.20092)
- Luo Y, Zhou X (2010) Soil respiration and the environment. Elsevier Academy Press, Amsterdam
- Maeck A, Del Sontro T, McGinnis DF et al (2013) Sediment trapping by dams creates methane emission hot spots. *Environ Sci Technol* 47:8130–8137. doi:[10.1021/es4003907](https://doi.org/10.1021/es4003907)
- McGinnis DF, Kirillin G, Tang KW et al (2015) Enhancing surface methane fluxes from an Oligotrophic lake: exploring the microbubble hypothesis. *Environ Sci Technol* 49:873–880. doi:[10.1021/es503385d](https://doi.org/10.1021/es503385d)
- McIntyre RES, Adams MA, Ford DJ, Grierson PF (2009) Rewetting and litter addition influence mineralisation and microbial communities in soils from a semi-arid intermittent stream. *Soil Biol Biochem* 41:92–101. doi:[10.1016/j.soilbio.2008.09.021](https://doi.org/10.1016/j.soilbio.2008.09.021)
- Meier JA, Jewell JS, Brennen CE, Imberger J (2011) Bubbles emerging from a submerged granular bed. *J Fluid Mech* 666:189–203. doi:[10.1017/S002211201000443X](https://doi.org/10.1017/S002211201000443X)
- Meybeck M, Dürr H, Vörösmarty C (2006) Global coastal segmentation and its river catchment contributors: A new look at land-ocean linkage. *Global Biogeochem Cycles* 20:GB1S90. doi:[10.1029/2005GB002540](https://doi.org/10.1029/2005GB002540)
- Millero F (1995) Thermodynamics of the carbon dioxide system in the oceans. *Geochim Cosmochim Acta* 59:661–677. doi:[10.1016/0016-7037\(94\)00354-O](https://doi.org/10.1016/0016-7037(94)00354-O)
- Milliman JD, Farnsworth KL, Jones PD et al (2008) Climatic and anthropogenic factors affecting river discharge to the global ocean, 1951–2000. *Glob Planet Chang* 62:187–194. doi:[10.1016/j.gloplacha.2008.03.001](https://doi.org/10.1016/j.gloplacha.2008.03.001)
- Mitchell AM, Baldwin DS (1999) The effects of sediment desiccation on the potential for nitrification, denitrification, and methanogenesis in an Australian reservoir. *Hydrobiologia* 392:3–11. doi:[10.1023/A:1003589805914](https://doi.org/10.1023/A:1003589805914)
- Morales-Pineda M, Cózar A, Laiz I et al (2014) Daily, biweekly, and seasonal temporal scales of pCO₂ variability in two stratified Mediterranean reservoirs. *J Geophys Res Biogeosciences* 119:1–12. doi:[10.1002/2013JG002317](https://doi.org/10.1002/2013JG002317)
- Mulholland PJ, Elwood JW (1982) The role of lake and reservoir sediments as sinks in the perturbed global carbon cycle. *Tellus A* 34:490–499. doi:[10.3402/tellusa.v34i5.10834](https://doi.org/10.3402/tellusa.v34i5.10834)
- Nilsson C, Reidy C, Dynesius M, Revenga C (2005) Fragmentation and flow regulation of the world's large river systems. *Science* 308:405–408. doi:[10.1126/science.1107887](https://doi.org/10.1126/science.1107887)
- Obrador B, Pretus JL (2012) Budgets of organic and inorganic carbon in a Mediterranean coastal lagoon dominated by submerged vegetation. *Hydrobiologia* 699:35–57. doi:[10.1007/s10750-012-1152-7](https://doi.org/10.1007/s10750-012-1152-7)
- Oksanen, J, Blanchet FG, Kindt R et al. (2013). Vegan: community ecology package. R package version 2.0-10. <http://CRAN.R-project.org/package=vegan>
- Pavón D (2010) Desarrollo y decadencia hidroeléctrica en los pequeños ríos del litoral mediterráneo catalán. El caso de las cuencas del Fluvià y de la Muga. *Revista de Historia Industrial* 42:43–87
- Pohlon E, Ochoa Fandino A, Marxsen J (2013) Bacterial community composition and extracellular enzyme activity in temperate streambed sediment during drying and rewetting. *PLoS One* 8:e83365. doi:[10.1371/journal.pone.0083365](https://doi.org/10.1371/journal.pone.0083365)
- Prairie Y, Del Giorgio PA (2013) A new pathway of freshwater methane emissions and the putative importance of microbubbles. *Inl Waters* 3:311–320. doi:[10.5268/IW-3.3.542](https://doi.org/10.5268/IW-3.3.542)
- R Core Team (2013). R: a language and environment for statistical computing. R Foundation for Statistical Computing, Vienna. ISBN:3-900051-07-0, <http://www.R-project.org/>
- Raich J, Schlesinger W (1992) The global carbon dioxide flux in soil respiration and its relationship to vegetation and

- climate. *Tellus B* 44:81–99. doi:[10.1034/j.1600-0889.1992.t01-1-00001.x](https://doi.org/10.1034/j.1600-0889.1992.t01-1-00001.x)
- Raich J, Potter C, Bhagwati D (2002) Interannual variability in global soil respiration, 1980–94. *Global Chang Biol* 8:800–812. doi:[10.3334/CDIAC/lue.ndp081](https://doi.org/10.3334/CDIAC/lue.ndp081)
- Raymond PA, Hartmann J, Lauerwald R et al (2013) Global carbon dioxide emissions from inland waters. *Nature* 503:355–359. doi:[10.1038/nature12760](https://doi.org/10.1038/nature12760)
- Rey A (2015) Mind the gap: non-biological processes contributing to soil CO₂ efflux. *Global Chang Biol* 21:1752–1761. doi:[10.1111/gcb.12821](https://doi.org/10.1111/gcb.12821)
- Sabater S (2008) Alterations of the global water cycle and their effects on river structure, function and services. *Freshw Rev* 1:75–88. doi:[10.1608/FRJ-1.1.5](https://doi.org/10.1608/FRJ-1.1.5)
- Sobek S, Algesten G (2003) The catchment and climate regulation of pCO₂ in boreal lakes. *Global Chang Biol* 9:630–641. doi:[10.1046/j.1365-2486.2003.00619.x](https://doi.org/10.1046/j.1365-2486.2003.00619.x)
- Sobek S, Zurbrügg R, Ostrovsky I (2011) The burial efficiency of organic carbon in the sediments of Lake Kinneret. *Aquat Sci* 73:355–364. doi:[10.1007/s00027-011-0183-x](https://doi.org/10.1007/s00027-011-0183-x)
- Sobek S, Del Sontro T, Wongfun N, Wehrli B (2012) Extreme organic carbon burial fuels intense methane bubbling in a temperate reservoir. *Geophys Res Lett* 39:2–5. doi:[10.1029/2011GL050144](https://doi.org/10.1029/2011GL050144)
- Steward AL, von Schiller D, Tockner K et al (2012) When the river runs dry: human and ecological values of dry riverbeds. *Front Ecol Environ* 10:202–209. doi:[10.1890/110136](https://doi.org/10.1890/110136)
- Striegl RG, Dornblaser MM, McDonald CP et al (2012) Carbon dioxide and methane emissions from the Yukon River system. *Global Biogeochem Cycles* 26:GB0E05. doi:[10.1029/2012GB004306](https://doi.org/10.1029/2012GB004306)
- Stumm W, Morgan JJ (1996) *Aquatic chemistry: chemical equilibria and rates in natural waters*. Wiley, Hoboken
- Tang KW, McGinnis DG, Frindte K et al (2014) Paradox reconsidered: methane oversaturation in well-oxygenated lake waters. *Limnol Oceanogr* 59:275–284. doi:[10.4319/lo.2014.59.1.0275](https://doi.org/10.4319/lo.2014.59.1.0275)
- Teodoru CR, Prairie YT, Del Giorgio PA (2010) Spatial Heterogeneity of Surface CO₂ Fluxes in a newly created eastmain-1 reservoir in Northern Quebec, Canada. *Ecosystems* 14:28–46. doi:[10.1007/s10021-010-9393-7](https://doi.org/10.1007/s10021-010-9393-7)
- Timoner X, Acuña V, Frampton L et al (2014) Biofilm functional responses to the rehydration of a dry intermittent stream. *Hydrobiologia* 727:185–195. doi:[10.1007/s10750-013-1802-4](https://doi.org/10.1007/s10750-013-1802-4)
- Tockner K, Uehlinger U, Robinson CT (2009) *Rivers of Europe*. Academic Press, San Diego
- Tooth S (2000) Process, form and change in dry land rivers: a review of recent research. *Earth Sci Rev* 51:67–107. doi:[10.1016/S0012-8252\(00\)00014-3](https://doi.org/10.1016/S0012-8252(00)00014-3)
- Vachon D, Prairie YT, Cole JJ (2010) The relationship between near-surface turbulence and gas transfer velocity in freshwater systems and its implications for floating chamber measurements of gas exchange. *Limnol Oceanogr* 55:1723–1732. doi:[10.4319/lo.2010.55.4.1723](https://doi.org/10.4319/lo.2010.55.4.1723)
- Vazquez E, Amalfitano S, Fazi S, Butturini A (2010) Dissolved organic matter composition in a fragmented Mediterranean fluvial system under severe drought conditions. *Biogeochemistry* 102:59–72. doi:[10.1007/s10533-010-9421-x](https://doi.org/10.1007/s10533-010-9421-x)
- Von Schiller D, Acuña V, Graeber D et al (2011) Contraction, fragmentation and expansion dynamics determine nutrient availability in a Mediterranean forest stream. *Aquat Sci* 73:485–497. doi:[10.1007/s00027-011-0195-6](https://doi.org/10.1007/s00027-011-0195-6)
- Von Schiller D, Marcé R, Obrador B et al (2014) Carbon dioxide emissions from dry watercourses. *Inland waters* 4:377–382. doi:[10.5268/IW-4.4.746](https://doi.org/10.5268/IW-4.4.746)
- Vörösmarty CJ, McIntyre PB, Gessner MO et al (2010) Global threats to human water security and river biodiversity. *Nature* 467:555–561. doi:[10.1038/nature09440](https://doi.org/10.1038/nature09440)
- Wanninkhof R (1992) Relationship between wind speed and gas exchange over the ocean. *J Geophys Res Ocean* 97:7373–7382. doi:[10.1029/92JC00188](https://doi.org/10.1029/92JC00188)
- Weiss R (1974) Carbon dioxide in water and seawater: the solubility of a non-ideal gas. *Mar Chem* 2:203–215. doi:[10.1016/0304-4203\(74\)90015-2](https://doi.org/10.1016/0304-4203(74)90015-2)
- Williams DD (2006) *The biology of temporary waters*. Oxford University Press, Oxford
- Xiao S, Liu D, Wang Y et al (2013) Temporal variation of methane flux from Xiangxi Bay of the three gorges reservoir. *Sci Rep* 3:2500. doi:[10.1038/srep02500](https://doi.org/10.1038/srep02500)
- Xu L, Baldocchi DD, Tang J (2004) How soil moisture, rain pulses, and growth alter the response of ecosystem respiration to temperature. *Global Biogeochem Cycles* 18:GB4002. doi:[10.1029/2004GB002281](https://doi.org/10.1029/2004GB002281)
- Zoppini A, Marxsen J (2011) Importance of extracellular enzymes for biogeochemical processes in temporary river sediments during fluctuating dry-wet Conditions. In: Shukla G, Varma A (eds) *Soil enzymology*. Springer, Berlin, pp 103–117

When Water Vanishes: Magnitude and Regulation of Carbon Dioxide Emissions from Dry Temporary Streams

Lluís Gómez-Gener,^{1*} Biel Obrador,¹ Rafael Marcé,² Vicenç Acuña,² Núria Catalán,³ Joan Pere Casas-Ruiz,² Sergi Sabater,² Isabel Muñoz,¹ and Daniel von Schiller⁴

¹Department of Ecology, University of Barcelona, Av. Diagonal 643, 08028 Barcelona, Barcelona, Spain; ²Catalan Institute for Water Research, Scientific and Technological Park of the University of Girona, Carrer Emili Grahit 101, 17003 Girona, Spain; ³Limnology, Department of Ecology and Genetics, Evolutionary Biology Centre, Uppsala University, Norbyvägen 18 D, 75236 Uppsala, Sweden; ⁴Department of Plant Biology and Ecology, Faculty of Science and Technology, University of the Basque Country, Apdo. 644, 48080 Bilbao, Spain

ABSTRACT

Most fluvial networks worldwide include watercourses that recurrently cease to flow and run dry. The spatial and temporal extent of the dry phase of these temporary watercourses is increasing as a result of global change. Yet, current estimates of carbon emissions from fluvial networks do not consider temporary watercourses when they are dry. We characterized the magnitude and variability of carbon emissions from dry watercourses by measuring the carbon dioxide (CO₂) flux from 10 dry streambeds of a fluvial network during the dry

period and comparing it to the CO₂ flux from the same streambeds during the flowing period and to the CO₂ flux from their adjacent upland soils. We also looked for potential drivers regulating the CO₂ emissions by examining the main physical and chemical properties of dry streambed sediments and adjacent upland soils. The CO₂ efflux from dry streambeds (mean ± SD = 781.4 ± 390.2 mmol m⁻² day⁻¹) doubled the CO₂ efflux from flowing streambeds (305.6 ± 206.1 mmol m⁻² day⁻¹) and was comparable to the CO₂ efflux from upland soils (896.1 ± 263.2 mmol m⁻² day⁻¹). However, dry streambed sediments and upland soils were physicochemically distinct and differed in the variables regulating their CO₂ efflux. Overall, our results indicate that dry streambeds constitute a unique and biogeochemically active habitat that can emit significant amounts of CO₂ to the atmosphere. Thus, omitting CO₂ emissions from temporary streams when they are dry may overlook the role of a key component of the carbon balance of fluvial networks.

Key words: greenhouse gas emissions; fluxes; streams; intermittent; fluvial network; drought; dry streambeds.

Received 30 September 2015; accepted 7 December 2015;

Electronic supplementary material: The online version of this article (doi:10.1007/s10021-016-9963-4) contains supplementary material, which is available to authorized users.

Author contributions D.v.S., B.O., R.M., V.A., S.S., I.M. and L.G. conceived and designed the study. L.G., D.v.S. and V.A. conducted field work. L.G., N.C. and J.C. performed laboratory and data analyses. L.G., D.v.S. and B.O. wrote the paper with inputs from the rest of co-authors. *Corresponding author; e-mail: gomez.gener87@gmail.com

INTRODUCTION

Fluvial networks emit significant amounts of carbon dioxide (CO₂) to the atmosphere (Raymond and others 2013; Lauerwald and others 2015). However, considerable uncertainties regarding the magnitude and controls of CO₂ emitted from fluvial networks still exist (Wehrli 2013). For instance, current global estimates do not accurately consider the CO₂ emitted from expanded areas of rivers and streams during floods, which can increase the areal extent of fluvial networks by several orders of magnitude (Richey and others 2002). Also, these estimates, based on continuous models, do not include the CO₂ emitted from local discontinuities along the fluvial network, such as weirs, rapids, waterfalls or turbine releases in hydropower plants (Wehrli 2013). Finally, current estimates do not consider the CO₂ emitted from the areas of temporary watercourses that recurrently desiccate (Raymond and others 2013; von Schiller and others 2014).

Temporary watercourses are found worldwide (Acuña and others 2014; Leigh and others 2015). In Australia, roughly 70% of the 3.5 million kilometres of watercourses are considered temporary (Sheldon and others 2010), and more than half of the total length of watercourses in the United States, Greece and South Africa are also temporary (Larned and others 2010). Temporary watercourses can also be found in humid areas such as Antarctica (McKnight and others 1999) and Amazonia (Chapman and Kramer 1991). Low-order streams deserve special attention, since they account for more than 70% of fluvial networks surface area and are particularly prone to flow intermittency (Lowe and others 2006). These are dynamic systems in time and space, and analysing their spatial coverage is particularly difficult to detect by traditional mapping techniques (Benstead and Leigh 2012). We can therefore suspect that the surface area of temporary watercourses in the global fluvial network can be higher than 50% (Datry and others 2014), whereas their importance is increasing as a result of the combined effects of climate and land-use changes (Palmer and others 2008; Larned and others 2010; Hoerling and others 2012).

The dry streambeds of temporary streams, also commonly referred to as dry riverbeds (Steward and others 2012), are dynamic habitats (Stanley and others 1997; Boulton 2003), representing transitional zones between dissimilar habitats, and transitional periods between persistent and dissimilar states (Naiman and Decamps 1997). These

systems are constrained by the strength of interactions with their adjacent ecosystems. Thus, despite being traditionally neglected by aquatic and terrestrial ecologists and biogeochemists, dry streambeds are likely to be unique biogeochemical hotspots for materials transformations (McClain and others 2003). In fact, recent studies reported that carbon processing in dry streambed sediments can be maintained to some degree during stream desiccation by the activity of well-adapted biofilms (Zoppini and Marxsen 2011; Timoner and others 2012; Pohlen and others 2013). Likewise, first estimates also showed that dry streambeds are not inert but rather active sites for CO₂ release to the atmosphere (Gallo and others 2014; von Schiller and others 2014, Gómez-Gener and others 2015).

The carbon processed in dry streams has its own particular history, because it has either already left terrestrial ecosystems and entered the fluvial network or was produced within the fluvial network (Steward and others 2012). Therefore, emissions of CO₂ from dry streambeds should not be considered terrestrial, but mostly as a fundamental biogeochemical component of fluvial networks that experience large, often seasonal, hydrological expansions and contraction. Yet, there is an important lack of knowledge regarding the spatial variability and drivers of CO₂ emissions from dry streambeds and the differences and similarities with respect to CO₂ emissions from terrestrial soils.

The aim of this study was to quantify CO₂ emissions from dry streambeds of temporary streams within a fluvial network and to compare them to those during the period with flow and to those from adjacent upland soils. We also looked for potential drivers regulating the CO₂ emissions by examining the main physical and chemical properties of dry streambed sediments and adjacent upland soils. We predicted differences in both the magnitude and drivers controlling CO₂ emissions between dry streambeds and the other investigated habitats because of strong dissimilarities in physicochemical properties and biogeochemical dynamics.

METHODS

Study Site and Sampling Design

The Fluvià River (NE Iberian Peninsula) is 97 km long and drains a 990-km² catchment covered with mixed forests (78%), agricultural (19%) and urban (3%) areas (Land Cover Map of Catalonia 2009, Centre of Ecology and Forestry Research of Catalonia, <http://www.creaf.uab.es/mcsc/>). The

climate in the region is typically Mediterranean. Mean monthly air temperature ranges from 6°C in January to 26°C in July. Mean annual precipitation is 660 mm, with rainfall mainly occurring in autumn and spring (Data from 2004 to 2014, Catalan Water Agency, <http://aca-web.gencat.cat>). During the wet period (late autumn to early spring), hydrological connectivity is enhanced and most of the fluvial network area is covered with surface water. In contrast, during the dry period (late spring to early autumn) hydrological connectivity is reduced and the area of the fluvial network covered with surface water drastically decreases.

We conducted two samplings in 10 temporary tributaries of the Fluvià River spanning a wide range of physiographic and land-use conditions (Table 1; see Appendix 1 in Supplementary Materials for details). In the first sampling (dry period; August 2014), we measured CO₂ fluxes and took samples from the dry streambed sediments and adjacent upland soils. The upland was defined as the area occupied by terrestrial vegetation located close to the stream but beyond the strip of riparian vegetation. In the second sampling (flowing period, March 2015), we measured the CO₂ fluxes from the streambeds where flowing water was found, that is, 7 out of 10 streams (see Appendix 2 in Supplementary Materials for details). All the CO₂ flux measurements and associated sampling were carried out at each stream only once during the day.

Determination of CO₂ Fluxes

In both dry streambeds and upland soils, we applied the enclosed dynamic chamber method (Livingston and Hutchinson 1995) to measure the CO₂ flux. Briefly, we monitored the gas concentration in an opaque chamber (SRC-1, PP-Systems, USA) every 4.8 s with an infrared gas analyser (EGM-4, PP-Systems, USA). According to the manufacturer's specifications, the measurement accuracy of the EGM-4 is estimated to be within 1% over the calibrated range. In all cases, flux measurements lasted until a change in CO₂ of at least 10 µatm was reached, with a maximum duration of 300 s and a minimum of 120 s. We calculated the CO₂ flux (F_{CO_2} , mmol m⁻² day⁻¹) from the rate of change of CO₂ inside the chamber:

$$F_{\text{CO}_2} = \left(\frac{dp_{\text{CO}_2}}{dt} \right) \left(\frac{V}{RTS} \right), \quad (1)$$

where dp_{CO_2}/dt is the slope of the gas accumulation in the chamber along time in µatm s⁻¹, V is the volume of the chamber (1.171 dm³), S is the sur-

face area of the chamber (0.78 dm²), T is the air temperature in Kelvin and R is the ideal gas constant in l atm K⁻¹ mol⁻¹. Positive F_{CO_2} values represent efflux of gas to the atmosphere, and negative F_{CO_2} values indicate influx of gas from the atmosphere. We performed 4 randomly distributed measurements within each site, that is, 4 in dry streambeds and 4 in upland soils.

In the flowing streambeds, we measured the CO₂ flux applying the Fick's First Law of gas diffusion:

$$F_{\text{CO}_2} = k_{\text{CO}_2} K_h (p_{\text{CO}_{2,w}} - p_{\text{CO}_{2,a}}), \quad (2)$$

where F_{CO_2} is the estimated CO₂ flux between the surface stream water and the atmosphere in mmol m⁻² day⁻¹, K_h is the Henry's constant in mmol µatm⁻¹ m⁻³ adjusted for salinity and temperature (Weiss 1974; Millero 1995), $p_{\text{CO}_{2,w}}$ and $p_{\text{CO}_{2,a}}$ are the surface water and the atmosphere partial pressures of CO₂ in µatm, respectively, and k_{CO_2} is the specific gas transfer velocity for CO₂ in m day⁻¹.

We measured $p_{\text{CO}_{2,w}}$ and $p_{\text{CO}_{2,a}}$ with an infrared gas analyser (EGM-4, PP-Systems, USA). In the case of $p_{\text{CO}_{2,w}}$ we coupled the gas analyser to a membrane contactor (MiniModule, Liqui-Cel, USA). The water was circulated via gravity through the contactor at 300 mL min⁻¹, and the equilibrated gas was continuously recirculated into the infrared gas analyser for instantaneous p_{CO_2} measurements (Teodoru and others 2010).

We followed the approach used by Gómez-Gener and others (2015) to estimate the k_{CO_2} from the night-time drop in dissolved oxygen concentration (Hornberger and Kelly 1972), a method that has been extensively applied in ecosystem metabolism studies in rivers and streams (for example, Aristegi and others 2009; Hunt and others 2012; Riley and Dodds 2013). Briefly, photosynthesis ceases from sunset to sunrise; thus night-time dynamics of oxygen depend on respiration and reaeration. During the night, respiration reduces the oxygen levels until atmospheric equilibrium is reached. In parallel, reaeration approaches the oxygen concentration to saturation. Thus, when we plot the night-time oxygen concentration per unit of time versus the oxygen saturation deficit, a linear trend is obtained. The intercept of the regression corresponds to the respiration rate in g O₂ m⁻² h⁻¹, and the slope to the mean reaeration coefficient (K_{O_2}) in day⁻¹. We corrected the K_{O_2} for depth to obtain the mean gas transfer velocity of oxygen (k_{O_2}) in m day⁻¹ (Raymond and others 2012) and we further transformed k_{O_2} to k_{CO_2} by applying equation (3).

Table 1. Physiographic and Land-Use Characteristics of the Study Sites and Their Corresponding Subcatchments

Stream name	Stream code	Site-specific parameters						Catchment-specific parameters					
		Coordinates		Stream order ^a	Streambed grain sizes ^b (%)			Surface area ^a (ha)	Land uses ^c (%)				Lithology ^c (%)
		x	y		Small fractions	Cobbles	Boulders		Scrubs	Pastures	Crops	Forest	
Riera de St. Miquel	1	473788	4663780	4	77.2	22.8	0.0	5191	1.2	2.6	10.7	84.6	L(66), C(17), G(16)
Riera de Mieres	2	470306	4663964	4	71.1	28.9	0.0	1825	1.1	5.1	18.4	72.9	L(65), G(22), C(12)
Torrent de Pujolars	3	464116	4665691	3	49.1	43.7	7.2	1219	0.2	0.1	7.9	91.7	C(87), G(13)
Torrent de Rocanegra	4	464289	4665909	2	58.8	41.2	0.0	1252	1.7	3.7	27.6	59.4	C(62), V(34), G(23)
Fluvià	5	454382	4662603	4	63.2	31.6	5.2	3078	0.9	10.7	16.9	70.2	C(64), G(18), S(7), SS(6), G(5)
Joanetes	6	453844	4663758	4	61.4	38.6	0.0	2954	1.3	4.1	11.4	81.9	C(66), G(18), L(11)
Torrent de St. Pere	7	453724	4673311	3	59.8	29.8	10.3	1480	0.2	2.1	10.5	86.2	C(85), L(9), G(5)
Riera d'Oix	8	462235	4680827	4	79.0	21.0	0.0	11085	4.4	1.4	1.9	92.2	L(49), C(33), G(16), LS(9)
Llierca	9	466415	4679576	5	67.6	32.4	0.0	16743	5.9	2.8	1.5	89.7	L(59), LS(23), SS(18)
Barranc de Junyell	10	476914	4671359	3	55.6	44.4	0.0	5238	0.5	0.3	1.9	97.3	C(76), G(21), SS(2)

^aStream order and subcatchment surface area were calculated with the Hydrological Extension in ESRI® ArcGISTM v. 10.0 software. Data obtained from a 2-meter digital elevation model (Centre of Ecology and Forestry Research of Catalonia)

^bSurface grain-size characterization of studied streambeds was estimated following an image-processing-based procedure (Graham and others 2005). Results were obtained from an average of 3 high resolution photos along 50 m stream segments. Fraction classification was made according Wentworth (1922). Small fractions contain silt, clay, sand and gravel fractions.

^cSubcatchments land uses and lithologies (S = silt, L = loams, C = conglomerates, G = gravels, V = volcanic deposits, LS = limestone) were calculated with ESRI® ArcGISTM v. 10.0 software from a Land cover map of Catalonia and a Lithological map of Catalonia, respectively (Centre of Ecology and Forestry Research of Catalonia)

$$k_{\text{CO}_2} = k_{\text{O}_2} \left(\frac{S_{\text{CCO}_2}}{S_{\text{CO}_2}} \right)^{-n}, \quad (3)$$

where k_{CO_2} is the mean gas transfer velocity of CO_2 in m day^{-1} , S_{CCO_2} and S_{CO_2} are the Schmidt numbers of CO_2 and O_2 , respectively, at a given water temperature (Wanninkhof 1992). Following Bade (2009), we set the exponent n to 1/2 for turbulent environments, that is, flowing waters. Our k_{CO_2} ranged from 0.075 to 15.21 m day^{-1} . We obtained the diel cycles of dissolved oxygen concentration and temperature at each site at a frequency of 5 min with an optical dissolved oxygen sensor (MiniDot, PME, USA). The oxygen probes were inter-calibrated before the sampling campaign.

Physical and Chemical Characterization of Dry Streambeds and Upland Soils

At each flux measurement location, we measured the substrate temperature by means of a portable soil probe (Decagon ECH₂O 10HS, Pullman, USA) and collected substrate samples, that is, dry streambed sediments and upland soils (0–10 cm depth), after the flux measurements had been carried out. In the laboratory, we measured the substrate pH from a 1:1 sample:deionized water mixture (McLean 1982) with a hand-held pH meter (pH 3110, WTW, Germany). We also determined, gravimetrically, the substrate water content by drying a fresh subsample at 105°C and the organic matter content by sample combustion following the loss on ignition method (Dean 1974). We sieved the air-dried samples (2-mm mesh) and determined their main textural fractions (% sand, % silt and % clay) and their mean particle size with a laser-light diffraction instrument (Coulter LS 230, Beckman-Coulter, USA). We determined the percentage of organic carbon (OC) and total nitrogen (TN) from a sieved and air-dried subsample on an Elemental Analyzer (Model 1108, Carlo-Erba, Italy) after grinding and eliminating the inorganic fraction by acidification (HCl 1.5 N).

Water Extractable Organic Matter (WEOM), the fraction of DOM extracted with deionized water and conceptually consisting of the mobile and available portion of the total DOM pool (Corvasce and others 2006; Vergnoux and others 2011), was obtained by shaking (100 rpm, 4°C) the air-dried, sieved and ground samples with deionized water in the dark for 48 h with a sample:water ratio of 1:10. After the extraction, we filtered the leachates through 0.70- and 0.45- μm pre-combusted glass microfiber filters (Whatman, USA). We determined their raw dissolved organic carbon (DOC) and total

dissolved nitrogen (TDN) concentration with a total organic carbon analyser (TOC-V CSH, Shimadzu, Japan). The detection limit of the analysis procedure was 0.05 mg C l^{-1} for DOC and 0.005 mg N l^{-1} for TDN. All samples were previously acidified with HCl 1.5 N and preserved at 4°C until analysis. The extraction efficiencies were calculated as the ratio between the mass of WEOM recovered and the mass of the dry sample used for the extraction.

UV/Vis absorbance and fluorescence spectra were obtained from diluted WEOM extracts (DOC $\approx 10 \text{ mg l}^{-1}$) (Anesio and others 2000). We measured the UV/Vis absorbance spectra (200–800 nm) using a 1-cm quartz cuvette on a spectrophotometer (Shimadzu UV-1700, Shimadzu, USA) with an analytical precision of 0.001 absorbance units. From the absorbance spectra, we calculated the specific UV absorbance at 254 nm (SUVA₂₅₄, $\text{L mg}^{-1} \text{ m}^{-1}$) by dividing the absorbance at 254 nm by DOC concentration and cuvette path length (m). SUVA₂₅₄ is positively related with the aromaticity of DOM, with values generally ranging between 1 and 9 $\text{L mg}^{-1} \text{ m}^{-1}$ (Weishaar and others 2003).

We obtained the excitation–emission matrices (EEM) on a spectrofluorometer (Shimadzu RF-5301PC, Shimadzu, USA) using a 1-cm quartz cuvette. We ran the EEM scans over an emission range of 270–630 nm (1-nm increments) and an excitation range of 240–400 (10-nm increments). A water blank (Milli-Q Millipore) EEM, recorded under the same conditions, was subtracted from each sample to eliminate Raman scattering. The area underneath the water Raman scan was used to normalize all sample intensities. All the EEMs were corrected for instrument-specific biases, and inner-filter effects corrections were applied according to Kothawala and others (2013). From the EEMs, we calculated 3 indices: the fluorescence index (FI) as the ratio of the emission intensities at 470/520 nm for an excitation wavelength of 370 nm (Jaffé and others 2008). FI is an indicator of terrestrial (low FI) or microbial (high FI) origin of DOM. The humification index (HIX) was calculated as the peak area under the emission spectrum 435–480 nm divided by that of 300–345 nm, at an excitation of 254 (Zsolnay and others 1999). Higher values of HIX correspond to a higher degree of humification (Huguet and others 2009; Fellman and others 2010). Finally, we calculated the biological index (BIX) as the ratio of the emission intensities at 380/430 nm for an excitation of 310 nm (Huguet and others 2009). The BIX is an indicator of recent biological activity or recently

produced DOM. Higher values of BIX correspond to a predominantly autochthonous origin of DOM and to the presence of OM freshly released into the sample, whereas a lower DOM production will lead to a low value of BIX (Huguet and others 2009).

Data Analysis

We performed paired *t* tests to test the differences in terms of CO₂ flux among habitats, that is, dry streambed versus upland soil and dry streambed versus flowing streambed.

We applied a principal component analysis (PCA) on the correlation matrix to ordinate the dry streambeds (*n* = 10) and upland soil sites (*n* = 10) by their physical and chemical properties. All the variables included in the analysis are described in Table 2. We also examined differences in physical and chemical properties of dry streambed sediments and upland soils by means of paired *t* tests.

We built two PLS regression models (projections of latent structures by means of partial least squares, Wold and others 2001) to identify the potential physical and chemical drivers of CO₂ fluxes in dry streambeds (*n* = 35) and upland soils (*n* = 34). All the variables included in the models are described in Table 2. PLS is a regression extension of PCA and allows the exploration of relationships between multiple, collinear data matrices of *X'* and *Y's*. The model performance is expressed by R²Y (explained variance) and by Q²Y (predictive power estimated by cross validation). The PLS model was validated by comparing the goodness of fit with models built from randomized *Y*-variables. To summarize the influence of every *X*-variable on the *Y*-variable, across the extracted

PLS components, we used the variable influence on projection (VIP). The VIP scores of every model term (*X*-variables) are cumulative across components and weighted according to the amount of *Y*-variance explained in each component (Eriksson and others 2006). *X*-variables with VIP > 1 are most influential on the *Y*-variable. A cutoff around 0.8 separates moderately important *X*-variables, whereas those below this threshold can be regarded as less influential.

All statistical analyses were conducted in the R statistical environment (R Core Team 2013) using the vegan package (Oksanen and others 2013), except for PLS analysis which was done with the software XLSAT (XLSTAT 2015.2.01, Addinsoft SRAL, Germany). Our data met the conditions of homogeneity of variance and normality. Statistical tests were considered significant at *p* < 0.05. Extreme outliers were excluded from the CO₂ flux dataset after careful data exploration using numerical and graphical tools, that is, Cook's influential outlier tests, boxplots, and Cleveland dotplots, following Zuur and others (2010).

RESULTS

CO₂ Emissions

Dry streambeds (mean ± SD = 781.4 ± 390.2 mmol m⁻² day⁻¹), flowing streambeds (305.6 ± 206.1 mmol m⁻² day⁻¹) and upland soils (896.1 ± 263.2 mmol m⁻² day⁻¹) were net emitters of CO₂ to the atmosphere (Figure 1). The CO₂ efflux from dry streambeds experienced the highest intra-habitat variability and was significantly higher than the CO₂ efflux from flowing streambeds (Paired *t*

Table 2. Overview of *X*- and *Y*-Variables Included in the PCA and PLS Models

Variable	Description	PCA model	PLS models
Fco ₂	CO ₂ flux (mmol m ⁻² day ⁻¹)	–	<i>Y</i>
WC	Water content (%)	<i>X</i>	<i>X</i>
Temp	Temperature (°C)	<i>X</i>	<i>X</i>
Sand	Sand fraction (%)	<i>X</i>	<i>X</i>
Silt	Silt fraction (%)	<i>X</i>	<i>X</i>
Clay	Clay fraction (%)	<i>X</i>	<i>X</i>
P. Size	Mean particle size (µm)	<i>X</i>	<i>X</i>
OM	Organic matter content (%)	<i>X</i>	<i>X</i>
OC	Organic carbon content (%)	<i>X</i>	<i>X</i>
TN	Nitrogen content (%)	<i>X</i>	<i>X</i>
DOC	Dissolved organic carbon concentration of WEOM (mg g ⁻¹)	<i>X</i>	<i>X</i>
TDN	Total dissolved nitrogen concentration of WEOM (mg g ⁻¹)	<i>X</i>	<i>X</i>
SUVA	SUVA ₂₅₄ index of WEOM (l mg ⁻¹)	<i>X</i>	<i>X</i>
FI	Fluorescence index of WEOM	<i>X</i>	<i>X</i>
HIX	Humification index of WEOM	<i>X</i>	<i>X</i>
BIX	Biological index of WEOM	<i>X</i>	<i>X</i>

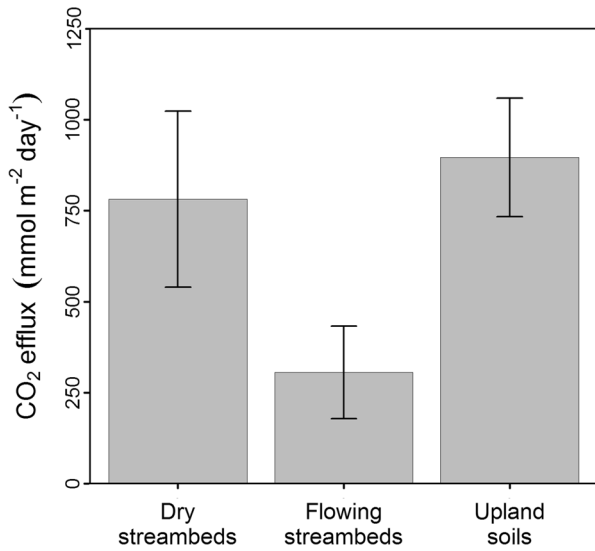


Figure 1. Mean CO₂ efflux from dry streambeds ($n = 10$), flowing streambeds ($n = 7$) and adjacent upland soils ($n = 10$) of the studied streams. The error bars represent standard deviations.

test: $p = 0.043$, $n = 7$), but not statistically different than the CO₂ efflux from upland soils (Paired t test: $p = 0.444$, $n = 10$).

Physical and Chemical Properties of Dry Streambed Sediments and Upland Soils

The principal component analysis (PCA) based on physical and chemical properties of the dry streambed sediments and upland soils stressed differences between the two habitats (Figure 2). The two first axes of the PCA explained 71.6% of total variance. The first principal component (58.9% of total variance), clearly separated dry streambeds and upland soils, and was related to texture properties, water content and organic matter quantity. The second principal component (12.7% of total variance) was mainly related to temperature and quality of the WEOM, and exerted a minor effect on the scores distribution along the 2 planes.

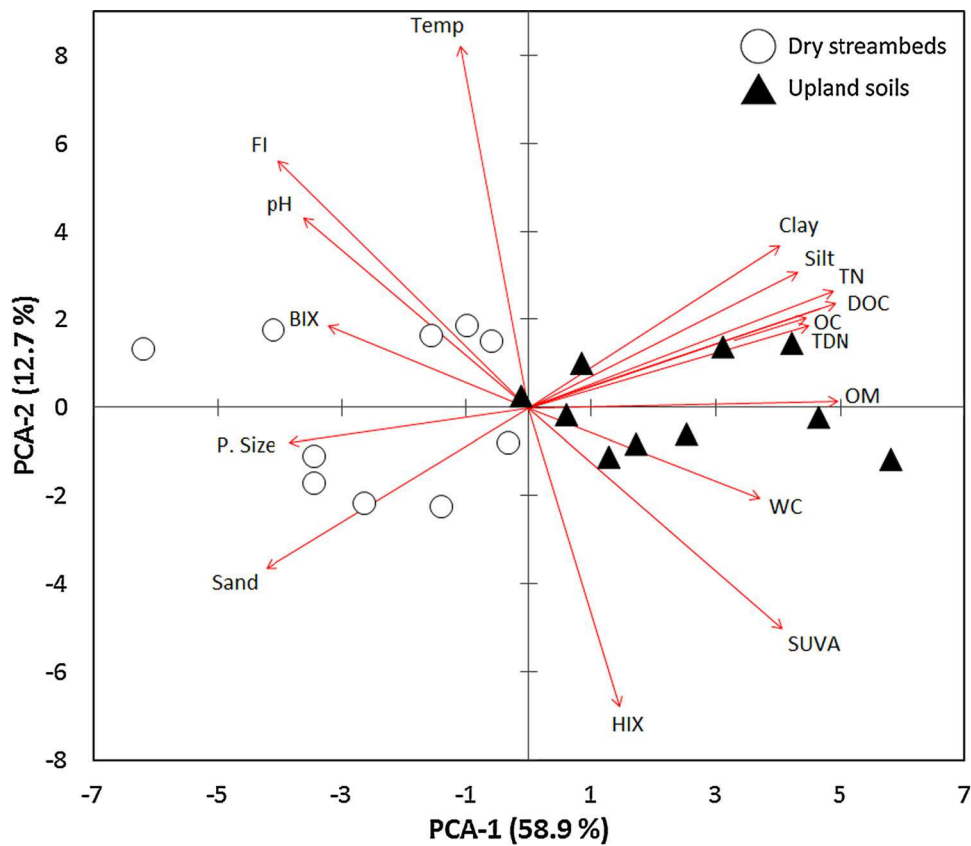


Figure 2. Multivariate ordination (PCA) of dry streambed sediments and upland soils based on physical and chemical descriptors (see Table 2 for the explanation of the abbreviations). The percentage of explained variation for each component is shown in brackets. The symbols represent the scores of the samples for the first two axes and the arrows represent the loadings of each descriptor for the first two axes.

The paired *t* tests further corroborated that dry streambed sediments and upland soils differed in several physical and chemical properties (Table 3). Water content was significantly lower in dry streambeds than in upland soils. The substrate texture differed significantly between habitats with dry streambeds having a higher sand fraction and mean particle size, whereas upland soils had higher silt and clay fractions. The pH was significantly higher in dry streambeds, whereas upland soils had higher organic matter, organic carbon and nitrogen contents, both in the solid and in the extracted phase (WEOM). The SUVA₂₅₄ and FI indices indicated that the WEOM from dry streambeds was less aromatic and had a more microbial-derived character than the WEOM from upland soils.

Drivers of CO₂ Emissions from Dry Streambed Sediments and Upland Soils

The PLS regression model for dry streambed sediments (Figure 3A) extracted two components from the data matrix that explained 40% of the variance ($R^2Y = 0.40$). The first (horizontal axis in Figure 3A) and the second PLS components (vertical axis in Figure 3A) explained, respectively, 20.1 and 19.7% of the variance. This analysis stressed the relevance (VIP > 1) of sediment temperature, mean particle size, DOC, TDN and TN explaining the variance in the CO₂ efflux from dry streambed sediments.

The PLS model for upland soils (Figure 3B) extracted two components that explained 42% of the variance ($R^2Y = 0.42$). The first and the second PLS components explained, respectively, 24.0 and 17.6% of the variance. The pH, mean particle size, sand, silt and clay fractions, SUVA₂₅₄, FI and HIX were the most influential descriptors explaining the variance in the CO₂ efflux from upland soils (VIP > 1).

DISCUSSION

Magnitude of CO₂ Emissions from Dry Streambeds

Dry streambeds from the studied fluvial network emitted substantial amounts of CO₂ to the atmosphere. Our measurements of CO₂ efflux from dry streambeds (mean = 781 mmol m⁻² day⁻¹, range = 342–1533 mmol m⁻² day⁻¹) are similar to those reported from a drying-rewetting experiment in dry desert streams in Arizona, USA (395 mmol m⁻²

day⁻¹, range = 20–1531 mmol m⁻² day⁻¹; Gallo and others 2014) and higher than others observed in the same geographical area of our study but with lower spatial coverage (mean = 209 mmol m⁻² day⁻¹, range = 189–220 mmol m⁻² day⁻¹; von Schiller and others 2014; Gómez-Gener and others 2015). These are, to our knowledge, the only previous studies reporting CO₂ effluxes from dry streambeds.

In the present study, we further show that the CO₂ efflux from dry streams was higher than the CO₂ efflux from the same streams when they were flowing. This result indicates that energy flow, nutrient cycling and subsequent CO₂ production and efflux remain active after flow cessation (Boulton 1991; Jacobson and others 2000); Amalfitano and others 2008). This observation could be related to limitation of the CO₂ efflux due to reduced gas diffusivity and the likely higher uptake of CO₂ by primary producers in aquatic environments compared to dry streambeds. Interestingly, these results agree with recent studies highlighting the relevance of the dry hydrological phases on the CO₂ fluxes from temporary systems of different nature, including temporary ponds (Catalan and others 2014) or reservoir beds found along Mediterranean fluvial networks (Gómez-Gener and others 2015).

Contrary to our expectations, the CO₂ efflux from dry streambeds was similar to the CO₂ efflux from adjacent upland soils. Similarly, von Schiller and others (2014) observed a comparable CO₂ efflux between dry streambeds (median 212 mmol m⁻² day⁻¹; range 36–455 mmol m⁻² day⁻¹) and a compiled dataset of Mediterranean soils (median 188 mmol m⁻² days⁻¹; range 44–371 mmol m⁻² day⁻¹). However, as our results show, a similar magnitude of CO₂ efflux from dry streambeds and their adjacent upland soils does not necessarily imply that these habitats are equivalent in their physical and chemical structure and function, and therefore in the way they process and emit carbon.

Dry Streambeds as Unique Biogeochemical Hotspots

The studied streambeds and their upland soils were heterogeneous in terms of physical and chemical properties, but our results revealed a clear clustering of samples by habitat. In general, variables related to the textural composition and the organic matter content exerted the strongest influence on the differentiation between the two habitats. Specifically, dry streambed sediments showed a

Table 3. Physical and Chemical Properties of the Dry Streambed Sediments and Upland Soils at Each Study Site

Stream code	Habitat	Physical characteristics						Chemical characteristics										
		Temperature °C	Water content %	Sand %	Silt %	Clay %	Mean particle size µm	Solid phase				Extracted phase						
								pH	Organic matter %	OC %	TN %	DOC mg g DW ⁻¹	TDN mg g DW ⁻¹	SUVA ₂₅₄ L mg ⁻¹ m ⁻¹	FI	HIX	BIX	
1	Dry streambed	18.5 ± 0.3	5.5 ± 0.5	81.4 ± 1.4	11.2 ± 1.1	7.5 ± 0.4	1483.6 ± 168.5	8.49 ± 0.04	1.01 ± 0.18	0.94 ± 0.76	0.03 ± 0.01	0.06 ± 0.01	0.00 ± 0.00	3.12 ± 0.29	2.20 ± 0.17	7.62 ± 1.36	0.52 ± 0.06	
	Upland soil	19.0 ± 0.0	16.4 ± 1.4	45.2 ± 9.4	34.8 ± 6.4	20.0 ± 3.2	407.7 ± 306.5	8.43 ± 0.05	6.68 ± 2.36	3.15 ± 2.05	0.20 ± 0.13	0.39 ± 0.12	0.03 ± 0.01	5.93 ± 1.05	2.08 ± 0.01	6.27 ± 0.70	0.54 ± 0.01	
2	Dry streambed	19.8 ± 0.4	13.0 ± 6.2	38.9 ± 33.5	34.3 ± 16.5	26.8 ± 17.2	1326.4 ± 235.9	7.96 ± 0.17	2.50 ± 1.92	1.00 ± 0.44	0.09 ± 0.04	0.18 ± 0.08	0.01 ± 0.01	3.58 ± 1.00	2.29 ± 0.08	3.77 ± 0.78	0.57 ± 0.03	
	Upland soil	19.9 ± 0.3	21.9 ± 3.8	59.8 ± 3.5	29.7 ± 2.6	10.5 ± 2.7	1239.3 ± 296.0	8.08 ± 0.07	10.10 ± 2.41	5.96 ± 1.32	0.36 ± 0.08	0.47 ± 0.02	0.05 ± 0.01	6.19 ± 0.79	2.09 ± 0.13	5.18 ± 1.61	0.50 ± 0.06	
3	Dry streambed	17.7 ± 0.3	20.3 ± 5.6	72.5 ± 34.8	19.9 ± 26.2	7.6 ± 8.6	1039.1 ± 373.8	8.40 ± 0.13	3.79 ± 2.00	1.02 ± 1.07	0.08 ± 0.06	0.11 ± 0.07	0.01 ± 0.00	4.40 ± 0.50	2.14 ± 0.06	6.24 ± 0.65	0.54 ± 0.04	
	Upland soil	18.3 ± 0.2	27.0 ± 6.2	48.6 ± 5.2	33.9 ± 4.6	17.5 ± 2.5	147.1 ± 12.7	8.27 ± 0.22	15.83 ± 8.53	6.05 ± 2.73	0.36 ± 0.14	0.55 ± 0.11	0.11 ± 0.01	5.86 ± 0.66	2.14 ± 0.11	5.40 ± 0.28	0.50 ± 0.03	
4	Dry streambed	20.9 ± 1.1	10.0 ± 1.7	88.3 ± 7.9	6.7 ± 4.7	4.9 ± 3.3	1411.5 ± 217.6	7.94 ± 0.33	1.65 ± 0.57	0.37 ± 0.03	0.03 ± 0.00	0.07 ± 0.02	0.02 ± 0.00	5.48 ± 0.57	2.14 ± 0.05	7.00 ± 0.98	0.50 ± 0.01	
	Upland soil	20.1 ± 0.5	15.3 ± 1.0	24.6 ± 2.4	48.2 ± 1.2	27.3 ± 1.8	855.7 ± 282.1	8.80 ± 0.29	11.07 ± 2.07	5.59 ± 1.50	0.39 ± 0.14	0.56 ± 0.13	0.12 ± 0.04	7.91 ± 0.55	2.04 ± 0.04	9.14 ± 1.37	0.47 ± 0.01	
5	Dry streambed	21.2 ± 0.6	9.3 ± 1.9	89.1 ± 6.6	6.9 ± 3.9	4.0 ± 2.7	1305.0 ± 155.1	9.25 ± 0.06	1.11 ± 0.25	0.33 ± 0.14	0.03 ± 0.02	0.06 ± 0.02	0.01 ± 0.00	4.32 ± 0.55	2.18 ± 0.03	6.12 ± 1.00	0.53 ± 0.01	
	Upland soil	21.0 ± 0.7	17.0 ± 1.4	55.7 ± 8.0	32.7 ± 6.2	11.5 ± 1.9	101.2 ± 18.7	8.14 ± 0.36	5.97 ± 0.70	1.85 ± 0.53	0.11 ± 0.07	0.30 ± 0.02	0.06 ± 0.01	4.88 ± 0.25	2.09 ± 0.02	5.65 ± 0.59	0.53 ± 0.02	
6	Dry streambed	23.4 ± 1.1	15.4 ± 8.7	60.1 ± 30.7	28.0 ± 20.7	11.9 ± 10.0	686.1 ± 557.6	7.98 ± 0.05	4.25 ± 5.01	2.17 ± 2.22	0.15 ± 0.14	0.23 ± 0.16	0.05 ± 0.03	4.09 ± 0.66	2.27 ± 0.17	4.25 ± 0.59	0.53 ± 0.08	
	Upland soil	21.1 ± 0.6	14.8 ± 1.1	60.4 ± 3.7	27.2 ± 2.5	12.4 ± 1.3	221.6 ± 49.6	7.78 ± 0.17	6.39 ± 1.39	1.50 ± 0.12	0.14 ± 0.02	0.28 ± 0.04	0.06 ± 0.02	5.60 ± 0.48	2.21 ± 0.03	5.73 ± 0.74	0.60 ± 0.04	
7	Dry streambed	21.8 ± 0.7	9.2 ± 3.5	47.4 ± 11.1	36.3 ± 7.9	16.3 ± 3.2	440.2 ± 608.1	7.82 ± 0.26	2.05 ± 0.77	1.18 ± 0.52	0.10 ± 0.05	0.12 ± 0.02	0.02 ± 0.00	5.23 ± 0.47	2.15 ± 0.06	8.74 ± 1.20	0.51 ± 0.02	
	Upland soil	22.1 ± 0.7	18.0 ± 2.5	25.0 ± 4.6	55.5 ± 3.7	19.5 ± 1.1	67.9 ± 26.9	7.13 ± 0.24	10.03 ± 3.12	5.17 ± 2.58	0.39 ± 0.18	0.52 ± 0.19	0.09 ± 0.01	5.14 ± 0.78	2.14 ± 0.02	6.14 ± 1.94	0.50 ± 0.03	
8	Dry streambed	22.9 ± 1.4	7.2 ± 6.2	79.2 ± 7.9	14.8 ± 5.6	6.0 ± 2.3	1538.1 ± 238.8	8.14 ± 0.10	1.54 ± 1.03	2.13 ± 0.83	0.05 ± 0.04	0.10 ± 0.05	0.02 ± 0.01	2.83 ± 0.27	2.35 ± 0.10	4.64 ± 0.51	0.56 ± 0.01	
	Upland soil	20.3 ± 0.4	24.2 ± 3.8	63.9 ± 2.0	24.5 ± 1.3	11.6 ± 0.8	242.4 ± 32.2	8.20 ± 0.14	8.56 ± 2.68	2.66 ± 0.83	0.13 ± 0.05	0.32 ± 0.05	0.03 ± 0.01	5.67 ± 0.68	2.07 ± 0.14	5.56 ± 1.07	0.43 ± 0.05	
9	Dry streambed	22.1 ± 0.3	3.4 ± 1.2	96.5 ± 1.5	2.3 ± 0.9	1.3 ± 0.6	1886.6 ± 213.8	7.53 ± 0.52	0.52 ± 0.17	0.16 ± 0.04	0.01 ± 0.00	0.06 ± 0.02	0.00 ± 0.00	2.22 ± 0.16	2.36 ± 0.07	4.58 ± 0.82	0.60 ± 0.04	
	Upland soil	22.0 ± 0.3	13.3 ± 1.0	23.4 ± 13.0	46.3 ± 6.2	30.3 ± 6.9	685.8 ± 286.5	8.40 ± 0.08	7.00 ± 1.95	5.02 ± 1.26	0.31 ± 0.09	0.57 ± 0.21	0.03 ± 0.01	4.53 ± 0.53	2.11 ± 0.16	7.54 ± 1.56	0.42 ± 0.05	
10	Dry streambed	22.8 ± 0.2	16.1 ± 8.5	56.6 ± 27.7	29.3 ± 18.8	14.1 ± 8.9	800.9 ± 1093.9	8.41 ± 0.10	4.42 ± 2.87	2.87 ± 0.46	0.17 ± 0.05	0.32 ± 0.04	0.02 ± 0.00	3.90 ± 0.86	2.28 ± 0.13	4.93 ± 0.82	0.51 ± 0.03	
	Upland soil	22.7 ± 0.3	11.6 ± 1.6	55.7 ± 4.9	29.7 ± 3.7	14.6 ± 1.7	683.5 ± 610.3	8.45 ± 0.16	7.24 ± 2.76	3.34 ± 1.46	0.20 ± 0.09	0.50 ± 0.18	0.04 ± 0.01	5.33 ± 0.57	2.14 ± 0.01	5.34 ± 0.53	0.47 ± 0.01	
Mean ± sd	Dry streambed	21.1 ± 1.9	11.0 ± 5.2	71.0 ± 19.3	19.0 ± 12.4	10.0 ± 7.5	1191.7 ± 442.7	8.19 ± 0.48	2.28 ± 1.41	1.22	0.90	0.07 ± 0.05	0.13 ± 0.09	0.02 ± 0.01	3.92 ± 1.02	2.24 ± 0.08	5.79 ± 1.63	0.54 ± 0.03
Mean ± sd	Upland soil	20.6 ± 1.4	18.0 ± 4.9	46.2 ± 16.1	36.3 ± 10.2	17.5 ± 6.9	465.2 ± 387.6	8.17 ± 0.45	8.89 ± 3.01	4.03	1.73	0.26 ± 0.11	0.45 ± 0.11	0.06 ± 0.03	5.70 ± 0.93	2.11 ± 0.05	6.19 ± 1.24	0.50 ± 0.05
<i>p</i> value	dsb vs. us	0.220	< 0.001	0.020	0.009	0.040	< 0.001	0.009	< 0.001	< 0.001	< 0.001	< 0.001	< 0.001	0.019	< 0.001	< 0.001	0.472	0.105

Values reported means and standard deviations (mean ± sd; n=4). Results of the paired T-tests for differences between dry streambeds and upland soils are shown in the lower part of the table. Significant differences (p<0.05) are marked in bold.

higher mean particle size and a higher proportion of sand, whereas upland soils were associated with lower mean particle size and higher proportions of clay and silt fractions. Because they act as hydrological flow paths, streambeds are more exposed to higher and recurrent surface stress in comparison to soils (Hickin 1995), making it more likely for water flow to initiate sediment erosion and transport. Thus, finer particles can be more easily mobilized in streams, but tend to be more retained in soils (Jacobson and others 2000). Dry streambed sediments also contained less organic matter, that is, OM, OC, TN, DOC, TDN, in comparison to upland soils. Dry streambeds and upland soils are subject to different temporal and spatial dynamics of transport, retention and processing of organic matter (Wagener and others 1998). Accordingly, we expect that recurrent periods of flow recession and subsequent reflowing in temporary streams may favour the oxidation and subsequent washing of OM from dry streambeds, thus lowering its concentration of OM (Acuña and others 2007; Larned and others 2010).

Our results also show that dry streambed sediments and upland soils were different in terms of the quality of organic matter. Significant differences in SUVA₂₅₄ and FI values between habitats indicate lower aromaticity and a higher signal of in situ produced OM from dry streambed sediments. Mediterranean streams can receive a higher leaf input from the riparian forest (direct and lateral fluxes) in comparison to their upland soils during drought periods (Acuña and others 2007). However, the recurrent periods of hydrological connections and disconnections may prevent the stabilization and further humification of stored OM, thereby decreasing the signal of plant structural compounds such as lignin in the WEOM fraction. The dry streambeds also showed higher BIX values than upland soils, pointing again towards a higher proportion of fresh DOM compounds likely derived from fluvial microbial sources (Birdwell and Engel 2010). The stronger microbial character of the WEOM from dry streambed sediments compared to upland soils was likely due to the extracellular release and leachate from decaying bacteria and algae as a result of stream drying (Fierer and Schimel 2003; Boroken and Matzner 2009; Kaiser and others 2015).

Regulation of CO₂ Effluxes from Dry Streambeds and Upland Soils

The physical and chemical variables that controlled the CO₂ efflux differed between dry streambeds

and upland soils, despite some variables, that is, temperature and textural composition, being involved in the regulation of the efflux in both habitats. The positive relationship between temperature and many biogeochemical processes by stimulation of the microbial activity, for example, autotrophic and heterotrophic respiration, has been widely reported (Raich and Schlesinger 1992; Mielnick and Dugas 2000; Raich and others 2002). Soil texture also influenced the CO₂ efflux from dry streambeds and from upland soils but in opposite directions in each habitat. The CO₂ efflux from dry streambeds increased with decreasing mean particle size. Burke and others (1989) and Buschiazzo and others (2004) also reported that higher proportions of small particles, that is, silt and clay fractions, correlated positively with DOC, TDN and TN concentrations and with water holding capacity, while Austin and others (2004) showed that this promoted microbial heterotrophic respiration in soils of arid and semiarid ecosystems. On the contrary, our upland soils responded inversely to the textural properties and showed higher CO₂ efflux with increasing proportion of coarse-textured soils. This observation can be attributed to a higher diffusion of air and higher infiltration of water to the rooting zone of vegetated soils, resulting in a significant contribution of autotrophic respiration to the total CO₂ efflux in the investigated soils (Noy-Meir 1973; Cable and others 2008; Catalán and others 2014).

Apart from these common drivers of the CO₂ efflux, some variables specifically regulated the efflux from dry streambeds and upland soils. The concentration of the particulate and water extracted fractions of organic carbon and nitrogen were involved in the regulation of the CO₂ efflux only in dry streambeds. The availability of OM can be enhanced during drying periods by release of high amounts of fresh and labile materials to sediment interfaces through microbial cell lysis and physical processes (Fierer and Schimel 2003; Boroken and Matzner 2009). However, the microbial activity in dry streambeds could be partially limited by the low concentration of DOC, TDN and TN in the substrate (Table 3), thus explaining the positive effect of OM concentration variables (TDN, DOC, TN) on the CO₂ efflux (Figure 3A). In contrast, the CO₂ efflux from upland soils was related to OM quality rather than to OM quantity (Figure 3B). Efflux from upland soils, which had a lower proportion of fresh and labile fractions in comparison to the dry streambed sediments (Table 3), was limited by the high aromaticity of the OM. Thus, low aromaticity and molecular complexity and high microbial signal

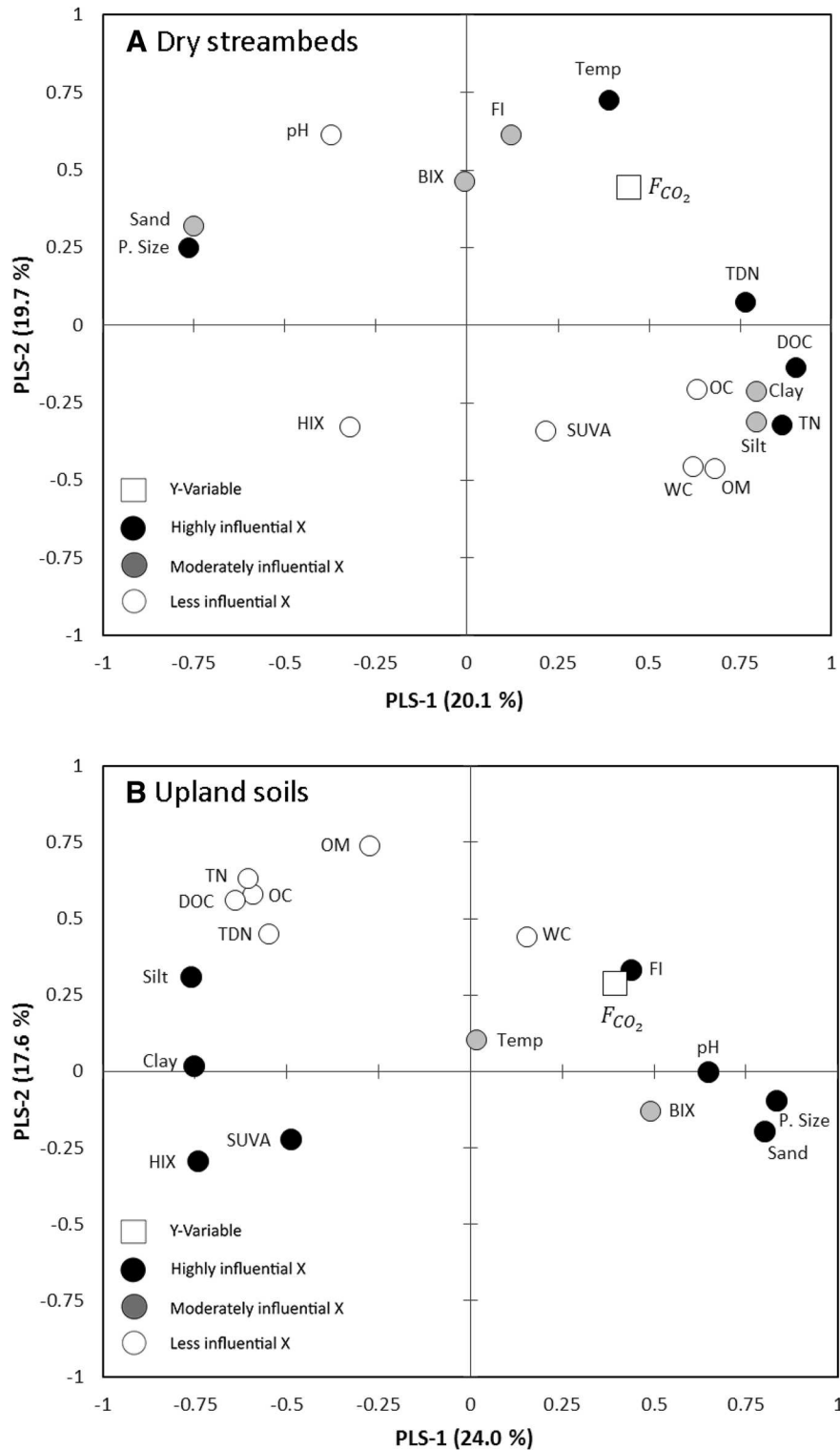


Figure 3. Loadings plot of the PLS regression analysis of the CO_2 emissions from dry streambeds (**A**) and adjacent upland soils (**B**). The graph shows how the Y -variable (*square*) correlates with X -variables (*circles*) and the correlation structure of the X 's. The X -variables are classified according to their variable influence on projection value (VIP): highly influential (*black circles*), moderately influential (*grey circles*) and less influential (*white circles*). The X -variables situated near Y -variables are positively correlated to them and those situated on the opposite side are negatively correlated. See Table 2 for the explanation of the abbreviations.

were associated with high CO₂ efflux in the upland soils. The amount and composition of soil organic matter have been previously identified as important factors affecting CO₂ efflux from soils (Casals and others 2009, Grogan and Jonasson 2005; Paré and Bedard-Haughn 2013).

The PLS models only accounted for 50% of the total variance in CO₂ emissions, indicating that other factors involved in the production of CO₂ potentially contributed to the final CO₂ efflux. Such factors could include differences in microbial community structure, biomass and activity (Amalfitano and others 2008), or non-biotic CO₂-generating processes, such as groundwater CO₂ import (Rey 2015), reactions with the carbonate system (Angert and others 2014), photochemical degradation (Austin and Vivanco 2006) or the effect of wind and air-pressure on the exchange of CO₂ (Suleau and others 2009; Redeker and others 2015). Our results represent an initial attempt at identifying and quantifying the main drivers regulating CO₂ emissions from dry streambeds.

CONCLUSIONS

Temporary watercourses can be found worldwide, and the spatial and temporal extent of the dry phase of these systems is increasing as a result of global change. Despite the prevalence of temporary watercourses, most knowledge in stream ecosystem ecology has been exclusively derived from studies in perennial streams. Thus, fundamental concepts, including the role of fluvial networks in global biogeochemical cycles, may be challenged when temporary watercourses are considered. Our study shows that streams do not turn into inert ecosystems when they become dry. On the contrary, they remain as unique biogeochemical hotspots processing and degassing significant amounts of carbon to the atmosphere comparable to those from upland soils. Our results strongly suggest that not considering streams when they are dry will lead to inaccurate estimates of CO₂ emissions from fluvial networks.

ACKNOWLEDGEMENTS

This research was funded by the Spanish Ministry of Economy and Competitiveness through the Projects CGL2011-30474-C02-01 and CGL2014-58760-C3-1-R. Ll. Gómez-Gener and J. P. Casas-Ruiz were additionally supported by FPI predoctoral grants (BES-2012-059743 and BES-2012-059655). N. Catalán hold a Wenner-Gren postdoctoral grant (Sweden). We thank Maria Caselles,

Sílvia de Castro and Marina Gubau, for field and laboratory assistance.

REFERENCES

- Acuña V, Giorgi A, Muñoz I, Sabater F, Sabater S. 2007. Meteorological and riparian influences on organic matter dynamics in a forested Mediterranean stream. *J N Am Benthol Soc* 26:54–69.
- Acuña V, Datry T, Marshall J, Barceló D, Dahm CN, Ginebreda A, McGregor G, Sabater S, Tockner K, Palmer M. 2014. Why should we care about temporary waterways? *Science* 343:1080–2.
- Amalfitano S, Fazi S, Zoppini A, Caracciolo AB, Grenni P, Puddu A. 2008. Responses of benthic bacteria to experimental drying in sediments from mediterranean temporary rivers. *Microb Ecol* 55:270–9.
- Anesio AM, Theil-Nielsen J, Graneli W. 2000. Bacterial growth on photochemically transformed leachates from aquatic and terrestrial primary producers. *Microb Ecol* 40:200–8.
- Angert A, Yakir D, Rodeghiero M, Preisler Y, Davidson EA, Weiner T. 2014. Using O₂ to study the relationships between soil CO₂ efflux and soil respiration. *Biogeosci Discuss* 11:12039–68.
- Aristegi L, Izagirre O, Elozegi A. 2009. Comparison of several methods to calculate reaeration in streams, and their effects on estimation of metabolism. *Hydrobiologia* 635:113–24.
- Austin AT, Yahdjian L, Stark JM, Belnap J, Porporato A, Norton U, Ravetta DA, Schaeffer SM. 2004. Water pulses and biogeochemical cycles in arid and semiarid ecosystems. *Oecologia* 141:221–35.
- Austin AT, Vivanco L. 2006. Plant litter decomposition in a semi-arid ecosystem controlled by photodegradation. *Nature* 442:555–8.
- Bade DL. 2009. Gas exchange across the air-water interface. In: Gene EL, Ed. *Encyclopedia of Inland waters*. Oxford: Academic Press. p 70–78.
- Belnap J, Welter JR, Grimm NB, Barger N, Ludwig JA. 2005. Linkages between microbial and hydrologic processes in arid and semiarid watersheds. *Ecology* 86:298–307.
- Benstead JP, Leigh DS. 2012. An expanded role for river networks. *Nat Geosci* 5:678–9.
- Birdwell JE, Engel AS. 2010. Characterization of dissolved organic matter in cave and spring waters using UV-Vis absorbance and fluorescence spectroscopy. *Org Geochem* 41:270–80.
- Borken W, Matzner E. 2009. Reappraisal of drying and wetting effects on C and N mineralization and fluxes in soils. *Glob Change Biol* 15:808–24.
- Boulton AJ. 1991. Eucalypt leaf decomposition in an intermittent stream in South-Eastern Australia. *Hydrobiologia* 211:123–36.
- Boulton AJ. 2003. Parallels and contrasts in the effects of drought on stream macroinvertebrate assemblages. *Freshw Biol* 48:1173–85.
- Burke IC, Yonker CM, Parton WJ, Cole CV, Flach K, Schimel DS. 1989. Texture, climate, and cultivation effects on soil organic matter content in U.S. grassland soils. *Soil Sci Soc Am J* 53:800–5.
- Buschiazzo DE, Estelrich HD, Aymar SB, Viglizzo E, Babinec FJ. 2004. Soil texture and tree coverage influence on organic matter. *Rangel Ecol Manag* 57:511–16.

- Cable JM, Ogle K, Williams DG, Weltzin JF, Huxman TE. 2008. Soil texture drives responses of soil respiration to precipitation pulses in the Sonoran desert: implications for climate change. *Ecosystems* 11:961–79.
- Casals P, Gimeno C, Carrara A, Lopez-Sangil L, Sanz M. 2009. Soil CO₂ efflux and extractable organic carbon fractions under simulated precipitation events in a Mediterranean Dehesa. *Soil Biol Biochem* 41:1915–22.
- Catalán N, von Schiller D, Marcé R, Koschorreck M, Gómez-Gener L, Obrador B. 2014. Carbon dioxide efflux during the flooding phase of temporary ponds. *Limnetica* 33:349–60.
- Chapman LJ, Kramer DL. 1991. The consequences of flooding for the dispersal and fate of poeciliid fish in an intermittent tropical stream. *Oecologia* 87:299–306.
- Corvasce M, Zsolnay A, D’Orazio V, Lopez R, Miano TM. 2006. Characterization of water extractable organic matter in a deep soil profile. *Chemosphere* 62:1583–90.
- Datry T, Larned ST, Tockner K. 2014. Intermittent rivers: a challenge for freshwater ecology. *Bioscience* 64:229–35.
- Dean WE. 1974. Determination of carbonate and organic matter in calcareous sediments and sedimentary rocks by loss on ignition: comparison with other method. *J Sediment Petrol* 44:242–8.
- Eriksson L, Johansson E, Kettaneh-Wold N, Wold S. 2001. Multi- and megavariable data analysis: principles and applications. Umea, Sweden: Umetrics AB.
- Fellman JB, Hood E, Spencer RGM. 2010. Fluorescence spectroscopy opens new windows into dissolved organic matter dynamics in freshwater ecosystems: a review. *Limnol Oceanogr* 55:2452–62.
- Fierer N, Schimel JP. 2003. A proposed mechanism for the pulse in carbon dioxide production commonly observed following the rapid rewetting of a dry soil. *Soil Sci Soc Am J* 67:798–805.
- Gallo EL, Lohse KA, Ferlin CM, Meixner T, Brooks PD. 2014. Physical and biological controls on trace gas fluxes in semi-arid urban ephemeral waterways. *Biogeochemistry* 121:189–207.
- Gómez-Gener L, Obrador B, von Schiller D, Marcé R, Casas Ruiz JP, Proia L, Acuña V, Catalán N, Muñoz I, Koschorreck M. 2015. Hot spots for carbon emissions from Mediterranean fluvial networks during summer drought. *Biogeochemistry* 19:1–18.
- Grogan P, Jonasson S. 2005. Temperature and substrate controls on intra-annual variation in ecosystem respiration in two subarctic vegetation types. *Glob Change Biol* 11:465–75.
- Hickin EJ. 1995. *River geomorphology*. Chichester: Wiley.
- Hoerling M, Eischeid J, Perlwitz J, Quan X, Zhang T, Pegion P. 2012. On the increased frequency of Mediterranean drought. *J Clim* 25:2146–61.
- Hornberger GM, Kelly MG. 1972. The determination of primary production in a stream using an exact solution to the oxygen balance equation. *Water Resour Bull* 8:795–801.
- Huguet A, Vacher L, Relexans S, Saubusse S, Froidefond JM, Parlanti E. 2009. Properties of fluorescent dissolved organic matter in the Gironde Estuary. *Org Geochem* 40:706–19.
- Hunt RJ, Jardine TD, Hamilton SK, Bunn SE. 2012. Temporal and spatial variation in ecosystem metabolism and food web carbon transfer in a wet-dry tropical river. *Freshw Biol* 57:435–50.
- Jacobson PJ, Jacobson KM, Angermeier PL, Cherry DS. 2000. Hydrologic influences on soil properties along ephemeral rivers in the Namib desert. *J Arid Environ* 45:21–34.
- Jaffé R, McKnight D, Maie N, Cory R, McDowell WH, Campbell JL. 2008. Spatial and temporal variations in DOM composition in ecosystems: the importance of long-term monitoring of optical properties. *J Geophys Res: Biogeosci* 113:1–15.
- Kaiser M, Kleber M, Berhe AA. 2015. How air-drying and rewetting modify soil organic matter characteristics: an assessment to improve data interpretation and inference. *Soil Biol Biochem* 80:324–40.
- Kothawala DN, Murphy KR, Stedmon CA, Weyhenmeyer GA, Tranvik LJ. 2013. Inner filter correction of dissolved organic matter fluorescence. *Limnol Oceanogr: Methods* 11:616–30.
- Larned ST, Datry T, Arscott DB, Tockner K. 2010. Emerging concepts in temporary-river ecology. *Freshw Biol* 55:717–38.
- Lauerwald R, Laruelle GG, Hartmann J, Ciais P, Regnier G. 2015. Spatial patterns in CO₂ evasion from the global river network. *Global Biogeochem Cycl* 29:534–54.
- Leigh C, Boulton AJ, Courtwright JL, Fritz K, May CL, Walker RH, Datry T. 2015. Ecological research and management of intermittent rivers: an historical review and future directions. *Freshwater Biology*. doi:10.1111/fwb.12646.
- Livingston GP, Hutchinson GL. 1995. Enclosure-based measurement of trace gas exchange: applications and sources of error. In: Matson PA, Harris RC, Eds. *Biogenic trace gases: measuring emissions from soil and water*. Oxford: Blackwell Scientific Publications. p 14–51.
- Lowe WH, Likens GE, Power ME. 2006. Linking scales in stream ecology. *Bioscience* 56:591–7.
- McClain ME, Boyer EW, Dent CL, Gergel SE, Grimm NB, Groffman PM, Hart SC, Harvey JW, Johnston CA, Mayorga E, McDowell WH, Pinay G. 2003. Biogeochemical hot spots and hot moments at the interface of terrestrial and aquatic ecosystems. *Ecosystems* 6:301–12.
- Mcknight DM, Niyogi DK, Alger AS, Bombles A, Peter A, Tate CM, Conovitz A, Mcknight DM, Niyogi DEVK, Bombles A, Tate M. 2008. Valley streams Antarctica: ecosystems waiting for water. *Bioscience* 49:985–95.
- McKnight DM, Boyer EW, Westerhoff PK, Doran PT, Kulbe T, Andersen DT. 2001. Spectrofluorometric characterization of dissolved organic matter for indication of precursor organic material and aromaticity. *Limnol Oceanogr* 46:38–48.
- McLean EO. 1982. Soil pH and lime requirement. In: Page AL, Ed. *Methods of soil analysis, part 2: chemical and microbiological properties*. Madison: American Society of Agronomy Inc. p 199–224.
- Mielnick PC, Dugas WA. 2000. Soil CO₂ flux in a tallgrass prairie. *Soil Biol Biochem* 32:221–8.
- Millero F. 1995. Thermodynamics of the carbon dioxide system in the oceans. *Geochim Cosmochim Acta* 59:661–77.
- Naiman RJ, Decamps H. 1997. The ecology of interfaces: riparian zones. *Annu Rev Ecol Syst* 28:621–58.
- Noy-Meir I. 1973. Desert ecosystems: environment and producers. *Annu Rev Ecol Syst* 4:25–51.
- Oksanen, J, Blanchet FG, Kindt R, Legendre P, Minchin PR, O’Hara RB, et al. 2013. *Vegan: community ecology package*. R package version 2.0–10. <http://CRAN.R-project.org/package=vegan>.
- Palmer MA, Reidy Liermann CA, Nilsson C, Flörke M, Alcamo J, Lake PS, Bond N. 2008. Climate change and the world’s river basins: anticipating management options. *Front Ecol Environ* 6:81–9.
- Paré MC, Bedard-Haughn A. 2013. Soil organic matter quality influences mineralization and GHG emissions in cryosols: a

- field-based study of sub- to high Arctic. *Glob Change Biol* 19:1126–40.
- Pohlon E, Ochoa Fandino A, Marxsen J. 2013. Bacterial community composition and extracellular enzyme activity in temperate streambed sediment during drying and rewetting. *PLoS One* 8:e83365.
- Raich J, Potter C, Bhagawati D. 2002. Interannual variability in global soil respiration, 1980–94. *Glob Chang Biol* 8:800–12.
- Raich J, Schlesinger W. 1992. The global carbon dioxide flux in soil respiration and its relationship to vegetation and climate. *Tellus B* 44:81–99.
- Raymond PA, Zappa CJ, Butman D, Bott TL, Potter J, Mulholland P, Laursen AE, McDowell WH, Newbold D. 2012. Scaling the gas transfer velocity and hydraulic geometry in streams and small rivers. *Limnol Oceanogr: Fluids Environ* 2:41–53.
- Raymond PA, Hartmann J, Lauerwald R, Sobek S, McDonald C, Hoover M, Butman D, Striegl R, Mayorga E, Humborg C, Kortelainen P, Dürr H, Meybeck M, Ciais P, Guth P. 2013. Global carbon dioxide emissions from inland water. *Nature* 503:355–9.
- Redeker KR, Baird AJ, Teh YA. 2015. Quantifying wind and pressure effects on trace gas fluxes across the soil–atmosphere interface. *Biogeosci Discuss* 12:4801–32.
- Rey A. 2015. Mind the gap: non-biological processes contributing to soil CO₂ efflux. *Glob Change Biol* 21:1752–61.
- Richey JE, Melack JM, Aufdenkampe AK, Ballester VM, Hess LL. 2002. Outgassing from Amazonian rivers and wetlands as a large tropical source of atmospheric CO₂. *Nature* 416:617–20.
- Riley AJ, Dodds WK. 2013. Whole-stream metabolism: strategies for measuring and modeling diel trends of dissolved oxygen. *Freshw Sci* 32:56–69.
- Sheldon F, Bunn SE, Hughes JM, Arthington AH, Balcombe SR, Fellows CS. 2010. Ecological roles and threats to aquatic refugia in arid landscapes: dryland river waterholes. *Mar Freshw Res* 61:885–95.
- Stanley E, Fisher S, Grimm N. 1997. Ecosystem expansion and contraction in streams. *Bioscience* 47:427–35.
- Steward AL, von Schiller D, Tockner K, Marshall JC, Bunn SE. 2012. When the river runs dry: human and ecological values of dry riverbeds. *Front Ecol Environ* 10:202–9.
- Suleau M, Debaq A, Dehaes V, Aubinet M. 2009. Wind velocity perturbation of soil respiration measurements using closed dynamic chambers. *Eur J Soil Sci* 60:515–24.
- Teodoru CR, Prairie YT, Del Giorgio PA. 2010. Spatial heterogeneity of surface CO₂ fluxes in a newly created eastmain-1 reservoir in Northern Quebec, Canada. *Ecosystems* 14:28–46.
- Timoner X, Acuña V, von Schiller D, Sabater S. 2012. Functional responses of stream biofilms to flow cessation, desiccation and rewetting. *Freshw Biol* 57:1565–78.
- von Schiller D, Marcé R, Obrador B, Gómez-Gener L, Casas-Ruiz JP, Acuña V, Koschorreck M. 2014. Carbon dioxide emissions from dry watercourses. *Inland Water* 4:377–82.
- Vergnoux A, Di Rocco R, Domeizel M, Guiliano M, Doumenq P, Théraulaz F. 2011. Effects of forest fires on water extractable organic matter and humic substances from Mediterranean soils: UV-vis and fluorescence spectroscopy approaches. *Geoderma* 160:434–43.
- Wagner SM, Oswood MW, Schimel JP. 1998. Rivers and soils: parallels in carbon and nutrient processing. *Bioscience* 48:104–8.
- Wanninkhof R. 1992. Relationship between wind speed and gas exchange over the ocean. *J Geophys Res: Oceans* 97:7373–82.
- Wehrli B. 2013. Conduits of the carbon cycle. *Nature* 503:9–10.
- Weishaar JL, Aiken GR, Bergamaschi BA, Fram MS, Fujii R, Mopper K. 2003. Evaluation of specific ultra-violet absorbance as an indicator of the chemical content of dissolved organic carbon. *Environ Chem* 41:843–5.
- Weiss R. 1974. Carbon dioxide in water and seawater: the solubility of a non-ideal gas. *Mar Chem* 2:203–15.
- Wold S, Sjöström M, Eriksson L. 2001. PLS-regression: a basic tool of chemometrics. *Chemometr Intell Lab Syst* 58:109–30.
- Zoppini A, Marxsen J. 2011. Importance of extracellular enzymes for biogeochemical processes in temporary river sediments during fluctuating dry-wet conditions. In: Shukla G, Varma A, Eds. *Soil enzymology*. Berlin: Springer. p 103–17.
- Zsolnay A, Baigar E, Jimenez M, Steinweg B, Saccomandi F. 1999. Differentiating with fluorescence spectroscopy the sources of dissolved organic matter in soils subjected to drying. *Chemosphere* 38:45–50.
- Zuur AF, Ieno EN, Elphick CS. 2010. A protocol for data exploration to avoid common statistical problems. *Methods Ecol Evol* 1:3–14.

Low contribution of internal metabolism to carbon dioxide emissions along lotic and lentic environments of a Mediterranean fluvial network

Lluís Gómez-Gener¹, Daniel von Schiller², Rafael Marcé³, Maite Arroita², Joan Pere Casas-Ruiz³, Peter Anton Staehr⁴, Vicenç Acuña³, Sergi Sabater^{3,5} and Biel Obrador¹

¹ Department of Ecology, University of Barcelona, Av. Diagonal 643, ES-08028 Barcelona, Spain.

² Department of Plant Biology and Ecology, University of the Basque Country, Apdo. 644, ES-48080 Bilbao, Spain.

³ Catalan Institute for Water Research (ICRA), Carrer Emili Grahit 101, ES-17003 Girona, Spain.

⁴ Institute of Bioscience, Aarhus University, Frederiksborgvej 399, PO Box 358, 4000 Roskilde, Denmark

⁵ GRECO, Institute of Aquatic Ecology, University of Girona, Girona, Spain.

Corresponding author: Ll. Gómez-Gener, e-mail: lgomez@ub.edu, Tel: +34 934021509

Key Points:

- Sources other than internal metabolism (e.g., external inputs, internal geochemical reactions or photochemical mineralization) sustained most of the fluvial network CO₂ emissions.
- Internal metabolism accounted for a moderate proportion (24%) of CO₂ emissions in lotic segments, while it was insignificant in lentic ones.
- The magnitude and sources of CO₂ emissions depended on the water residence time in lotic segments, while they remained relatively stable in lentic ones.

This article has been accepted for publication and undergone full peer review but has not been through the copyediting, typesetting, pagination and proofreading process which may lead to differences between this version and the Version of Record. Please cite this article as doi: 10.1002/2016JG003549

Abstract

Inland waters are significant sources of carbon dioxide (CO₂) to the atmosphere. CO₂ supersaturation and subsequent CO₂ emissions from inland waters can be driven by internal metabolism, external inputs of dissolved inorganic carbon (DIC) derived from the catchment and other processes (e.g., internal geochemical reactions of calcite precipitation or photochemical mineralization of organic solutes). However, the sensitivity of the magnitude and sources of CO₂ emissions to fluvial network hydromorphological alterations is still poorly understood. Here, we investigated both the magnitude and sources of CO₂ emissions from lotic (i.e., running waters) and lentic (i.e., stagnant waters associated to small dams) waterbodies of a Mediterranean fluvial network by computing segment-scale mass balances of CO₂. Our results showed that sources other than internal metabolism sustained most (82%) of the CO₂ emissions from the studied fluvial network. The magnitude and sources of CO₂ emissions in lotic waterbodies were highly dependent on hydrology, with higher emissions dominated by DIC inputs derived from the catchment during high flows, and lower emissions partially fueled by CO₂ produced biologically within the river during low flows. In contrast, CO₂ emissions in lentic waterbodies were low, relatively stable over the time and the space, and dominated by DIC inputs from the catchment regardless of the different hydrological situations. Overall, our results stress the sensitivity of fluvial networks to human activities and climate change, and particularly highlight the role of hydromorphological conditions on modulating the magnitude and sources of CO₂ emissions from fluvial networks.

Key Words: Greenhouse gas, emission, carbon dioxide, metabolism, fluvial network, hydrology

1. Introduction

Inland waters are active components of the global carbon (C) cycle that transform, store and outgas more than half of the C they receive from terrestrial ecosystems [Cole *et al.*, 2007; Battin *et al.*, 2009a; Tranvik *et al.*, 2009; Aufdenkampe *et al.*, 2011]. Recent global estimates place the efflux of CO₂ emitted from streams and rivers at 1.8 Pg C year⁻¹ and from lakes and reservoirs at 0.32 Pg C year⁻¹, resulting in a global estimate of CO₂ emissions from fluvial networks of 2.1 Pg C year⁻¹ [Raymond *et al.*, 2013]. However, there are still fundamental uncertainties regarding the magnitude, spatiotemporal variation and sources of CO₂ emissions from fluvial networks [Raymond *et al.*, 2013; Wehrli, 2013; von Schiller *et al.*, 2014; Hotchkiss *et al.*, 2015].

A better understanding of the processes regulating CO₂ emissions from fluvial networks is essential to comprehend the present and thus predict the future role of freshwaters in the global C cycle and the climate system [Raymond *et al.*, 2013; Hotchkiss *et al.*, 2015]. The flux of CO₂ across the air–water interface depends on the gas transfer velocity and the supersaturation of CO₂ in the surface water [Bade, 2009]. While the gas transfer velocity is a physical factor mainly controlled by the turbulence at the air–water interface, there are two major processes that can lead to CO₂ supersaturation in aquatic ecosystems. The first is internal aquatic mineralization of organic matter, which can result in an imbalance of net ecosystem production (NEP) towards net heterotrophy (respiration exceeding production) [Cole *et al.*, 2000; Duarte and Prairie, 2005]. The second is the input of surface and subsurface water with high dissolved inorganic carbon (DIC) content derived from soil respiration and mineral weathering within the catchment [Cole *et al.*, 2007; Humborg *et al.*, 2010; Marcé *et al.*, 2015]. Among these, internal metabolism has classically been considered to be the main factor driving CO₂ supersaturation in lakes and rivers [Cole *et al.*, 2000; Duarte and Prairie, 2005]. Yet, recent studies have shown that external inputs dominate CO₂

supersaturation and thus CO₂ emissions from most streams and rivers [Borges *et al.*, 2015a; Hotchkiss *et al.*, 2015] as well as lakes and reservoirs [Stets *et al.*, 2009; McDonald *et al.*, 2013; Marcé *et al.*, 2015; Weyhenmeyer *et al.*, 2015; Wilkinson *et al.*, 2016]. However, there is still little information about the relative contribution of these major sources to the CO₂ emissions from lotic and lentic waterbodies located within fluvial networks. Likewise, the role of other less known processes such as internal geochemical reactions of calcite precipitation usually occurring in alkaline waterbodies [Otsuki and Wetzel, 1974; Stets *et al.*, 2009; Nõges *et al.*, 2016] or photochemical mineralization of organic solutes [Amon and Benner, 1996; Cory *et al.*, 2014; Vachon *et al.*, 2016] on sustaining CO₂ supersaturation and emission in aquatic ecosystems is still largely undefined.

Due to the high human demand for energy and water, many fluvial networks worldwide have been regulated with a variety of hydraulic structures, ranging from very large dams to smaller reservoirs, impoundments and small weirs [Nilsson *et al.*, 2005a; Döll *et al.*, 2009]. Mediterranean fluvial networks are no exception, having mainly been modified by small man-made flow discontinuities such as impoundments or weirs [García-Ruiz *et al.*, 2011]. Such anthropogenic changes combined with the naturally marked seasonality of river flow in Mediterranean regions [Gasith and Resh, 1999; Bernal *et al.*, 2013], modulate the fluvial network hydrological dynamics (i.e., flow conditions) that, in turn, govern the overall physicochemical [Friedl and Wüest, 2002; Poff and Hart, 2002], structural [Clavero *et al.*, 2004; Buffagni *et al.*, 2009] and functional [Ward and Stanford, 1983; Acuña and Tockner, 2010; Elosegi and Sabater, 2013; Abril *et al.*, 2015] attributes of these fluvial networks. As a consequence, strong changes in the magnitude and sources of CO₂ emissions in response to flow modification are expected for fluvial networks in this region.

Here we evaluated and compared the magnitude and sources of CO₂ emissions between lotic and lentic waterbodies within a Mediterranean fluvial network and investigated their response to different hydrological conditions. To test the overarching objectives, we measured CO₂ emissions and the underlying fluxes that drive variation in CO₂ concentration within studied segments. We then computed the relative contribution of the CO₂ production by internal metabolism, the hydrological flux of CO₂ and the CO₂ flux of other non-measured processes to the emitted CO₂ by solving segment-scale mass balances over one hydrological year. We hypothesized that the magnitude and the relative contribution of the different sources to CO₂ emissions in our fluvial network would strongly depend on the waterbody type (i.e., lotic or lentic) as well as on the hydrological conditions (i.e., high or low water flow). During high flows, we expected that higher gas exchange as well as greater hydrological connectivity would homogenize gas dynamics along the lotic and lentic waterbodies of the fluvial network. Thus, we predicted generally higher fluvial network CO₂ emissions and similar rates of CO₂ emissions in lentic and lotic waterbodies, with dominant support of sources other than CO₂ produced by internal metabolism. In contrast, during low flows, we expected a general decrease in the gas exchange and hydrological connectivity, with an associated increased spatial heterogeneity in gas concentration and flux. Thus, we predicted generally lower fluvial network CO₂ emissions, and lower CO₂ emissions from lentic than from lotic segments, as well as a greater contribution of aquatic metabolic sources in lentic than in lotic waterbodies.

2. Methods

2.1. Site description

The Fluvià River (NE Iberian Peninsula) is a 97-km long river that drains a 990-km² catchment covered with mixed forests (78%), agricultural (19%) and urban (3%) areas (Land Cover Map of Catalonia, Centre of Ecology and Forestry Research of Catalonia, 2009, <http://www.creaf.uab.es/mcsc/>). The catchment is mostly calcareous, with some areas (<15%) of siliceous materials (Cartographic and Geological Institute of Catalonia, 2006, <http://www.icc.cat/>). The climate in the area is typically Mediterranean; the mean monthly air temperature ranges from 6 °C in January to 26 °C in July and the mean annual precipitation is 660 mm, with rainfall primarily occurring in autumn and spring, with occasional storms in summer (Data from 2004 to 2014, Catalan Water Agency, <http://aca-web.gencat.cat>). The water flow of Fluvià River has been deeply modified due to the high human demand for energy and water [García-Ruiz *et al.*, 2011]. Its fluvial network presents up to 61 small-size structures (i.e., weirs and small impoundments) that cause flow interruptions from its headwaters to the river mouth [Pavón, 2010].

In order to cover the wide spectrum of hydrological conditions occurring in the Fluvià River fluvial network, we performed monthly samplings (December 2012 to November 2013) in a set of 12 segments situated throughout the fluvial network, from headwaters to lowlands (Figure 1). The segments included 8 lotic (i.e., running water reaches) and 4 lentic (i.e., stagnant waters associated to a dam or weir) segments. The selected study segments were chosen as to avoid point source pollution, and their length was defined as a compromise between sufficient to detect changes in the variables of interest, while maintaining relative homogeneity of environmental conditions (i.e., canopy cover, morphology, and subcatchment land use). A detailed hydromorphological description of the selected segments along the sampling period is shown in Table S1 in the Supporting Information.

2.2. Hydromorphology

On each sampling date, we measured the cross-sectional water velocity (m s^{-1}) at the inlet and outlet of each segment with an acoustic-Doppler velocity meter (Sontek, YSI, USA), and we combined this with the cross-sectional depth (m) and width (m) to derive the water flow ($\text{m}^3 \text{s}^{-1}$). We used then the hydraulic modelling software HecRas 2.2 (US Army Corps of Engineers, USA) to estimate the mean cross-sectional water velocity, the wet segment area and the water volume every ca. 100 m along the segments. The model was fed with the measured water flow and segment geometrical data provided by the Catalan Water Agency (<http://aca-web.gencat.cat>). We calculated the slope of each lotic segment as the elevation difference over the length of the segment with the geospatial-processing software (ArcMap v10, ESRI, USA) using a 2-meter digital elevation model (Cartographic and Geological Institute of Catalonia, 2006, <http://www.icc.cat/>).

In lentic segments, we obtained the surface area, volume and mean and maximum depth from digitized bathymetric maps constructed with a geospatial-processing software (ArcMap v10, ESRI, USA) using in-situ morphological data obtained from different field surveys performed during 2013. The water residence time (WRT; h) in both lotic and lentic segments was calculated by dividing the segment volume by the segment average water flow.

2.3. Water-air flux of CO₂

In lotic segments we determined the CO₂ flux across the water-air interface ($F_{\text{CO}_2 \text{ emission}}$; mmol m⁻² d⁻¹) using Fick First Law of gas diffusion:

$$F_{\text{CO}_2 \text{ emission}} = k_{\text{CO}_2} K_h (p_{\text{CO}_2,w} - p_{\text{CO}_2,a}) \quad (1)$$

where K_h (mmol μatm^{-1} m⁻³) is the Henry's constant for CO₂ adjusted for salinity and temperature [Weiss, 1974; Millero, 1995], $p_{\text{CO}_2,w}$ (μatm) and $p_{\text{CO}_2,a}$ (μatm) are the mean partial pressures of CO₂ in surface water and air, respectively, and the k_{CO_2} (m d⁻¹) is the specific gas transfer velocity for CO₂. Positive values of $F_{\text{CO}_2 \text{ emission}}$ represent gas efflux from the water to the atmosphere, and negative values indicate gas influx from the atmosphere to the water.

At the inlet and the outlet of each segment, we measured the $p_{\text{CO}_2,w}$ and $p_{\text{CO}_2,a}$ with an infrared gas analyzer (EGM-4, PP-Systems, USA). Measurement accuracy of the EGM-4 is estimated to be within 1% over the calibrated CO₂ range. For $p_{\text{CO}_2,w}$ measurements, the water samples were circulated through a membrane contactor (MiniModule, Liqui-Cel, USA) coupled to the gas analyzer [Teodoru *et al.*, 2010] at 300 mL min⁻¹. For $p_{\text{CO}_2,a}$, the atmospheric air was taken approximately one meter above the water surface layer and circulated through the gas analyzer. We then averaged the $p_{\text{CO}_2,w}$ and $p_{\text{CO}_2,a}$ measured at the inlet and the outlet of each segment to obtain a mean segment $p_{\text{CO}_2,w}$ and $p_{\text{CO}_2,a}$.

We estimated a mean segment gas transfer velocity from the segment slope (s ; m m⁻¹) and the mean segment water velocity (v ; m s⁻¹) with equation (2) in Raymond *et al.* [2012]:

$$k_{600} = 1162 s^{0.77} v^{0.85} \quad (2)$$

where k_{600} (m d⁻¹) is the standardized gas transfer velocity at 20°C. The k_{600} was transformed to the k_{CO_2} following:

$$k_{CO_2} = k_{600} \left(\frac{Sc}{600} \right)^{-0.5} \quad (3)$$

where Sc (dimensionless) is the Schmidt number of CO_2 at the measured water temperature [Wanninkhof, 1992]. In addition, we compared our k_{CO_2} derived from equation (2) with the k_{CO_2} calculated from night-time oxygen dynamics (NTR method; [Hornberger and Kelly, 1972]; detailed description of the method in the Supporting Information) and direct chamber measurements to ensure their applicability throughout the study (Figure S1 in the Supporting information). This validation exercise showed that the range where 95% of the y-observations (i.e., k_{CO_2} from equation (2)) fall (95th percentile) showed a clear linear relationship with the x-observations (i.e., k_{CO_2} from the NTR method and from chamber measurement made in lotic segments), with almost all the observations falling very close to the 1:1 reference line.

In lentic segments, we determined $F_{CO_2 \text{ emission}}$ by the enclosed chamber method [Frankignoulle 1988]. Briefly, we monitored the CO_2 gas concentration in an opaque floating chamber every 4.8 s with an infrared gas analyser (EGM-4, PP-Systems, USA). In all the cases, flux measurements lasted until a change in CO_2 of at least 10 μatm was reached, with a maximum duration of 600 s and a minimum of 300 s. We calculated the $F_{CO_2 \text{ emission}}$ from the rate of change of CO_2 inside the chamber as follows:

$$F_{CO_2 \text{ emission}} = \left(\frac{dp_{CO_2}}{dt} \right) \left(\frac{V}{RTS} \right) \quad (4)$$

where $\frac{dp_{CO_2}}{dt}$ is the change in CO_2 concentration in the chamber along time in $\mu\text{atm s}^{-1}$, V and S are the volume and surface area of the chamber (27.1 dm^3 and 19.4 dm^2 , respectively), T is the air temperature in Kelvin and R is the ideal gas constant ($\text{L atm K}^{-1} \text{ mol}^{-1}$). We performed and averaged a minimum of 3 measurements in the central part of the lentic segment after flushing the chamber with ambient air between consecutive measurements.

At each lentic segment, we determined the $p_{\text{CO}_2,w}$ and the $p_{\text{CO}_2,a}$ at the same location where flux was measured using the methodology described for lotic segments and we then derived the k_{CO_2} from equation (1).

2.4. Internal metabolic flux of CO₂

We estimated the internal metabolic flux of CO₂ ($F_{\text{CO}_2 \text{ metabolism}}$; mmol m² d⁻¹) at each of the 12 segments from diel open-water dissolved oxygen (DO) variations [Odum 1956]. The diel DO data was obtained from automatic monitoring stations equipped with optical probes (YSI 600OMS V2, YSI 600XLM V2, Yellow Springs, USA, and MiniDOT, PME, USA). The YSI 600OMS V2, YSI 600XLM V2 and MiniDOT sensors have an accuracy of 0.1, 0.1 and 0.3 mg O₂ L⁻¹, respectively. All the probes were intercalibrated before deployment.

The metabolic rates were determined for those days coincident with the $F_{\text{CO}_2 \text{ emission}}$ samplings. Specifically, in those segments where permanent monitoring stations were available (#8, #3 and #11, Figure 1) the metabolic rates were determined for all the monthly $F_{\text{CO}_2 \text{ emission}}$ samplings (n=12). In the other segments, we used temporarily installed monitoring stations, and the metabolism was determined in two contrasted hydrological situations (high flow period, end of May 2013, and low flow period, end of August 2013; Figure 2a).

We obtained the solar irradiance reaching the surface (E ; W m⁻²) from a nearby meteorological station (<50 km away from the study segments) and converted it to photosynthetically active radiation (PAR; mmol m⁻² d⁻¹) following Kirk [1994].

We calculated the gross primary production (GPP) and ecosystem respiration (ER) using a linear photosynthesis–irradiance relationship [Van der Bogert *et al.*, 2007; Hanson *et al.*, 2008; Holtgrieve *et al.*, 2010]:

$$DO_t = DO_{t-1} + \left(\frac{GPP}{z} \cdot \frac{PAR_{t-1}}{PAR_{24}} \right) - \left(\frac{ER}{z} \Delta t \right) + F_{O_2} \Delta t \quad (6)$$

where GPP is the rate of O_2 production by photosynthesis ($\text{mmol } O_2 \text{ m}^{-2} \text{ d}^{-1}$), ER is the respiratory rate of O_2 consumption ($\text{mmol } O_2 \text{ m}^{-2} \text{ d}^{-1}$), PAR_{t-1} is the instantaneous photosynthetically active radiation ($\text{mmol m}^{-2} \text{ d}^{-1}$), PAR_{24} is the daily accumulated photosynthetically active radiation ($\text{mmol m}^{-2} \text{ d}^{-1}$), z is mean water column depth (m), F_{O_2} is the exchange of O_2 between the water and the atmosphere ($\text{mmol } O_2 \text{ m}^2 \text{ d}^{-1}$) and Δt is the time between measurements. F_{O_2} was calculated as $F_{O_2} = k_{O_2} (O_{2,w(t-1)} - O_{2,sat(t-1)})$, where k_{O_2} is the specific gas transfer velocity for O_2 (m d^{-1}), $O_{2,w}$ is the measured DO concentration in water, and $O_{2,sat}$ is the DO concentration in atmospheric equilibrium, calculated at each time step from temperature and corrected for barometric pressure from [Benson and Krause, 1984]. We obtained k_{O_2} from k_{CO_2} by applying equation (3).

We estimated GPP and ER by fitting Eq. 6 to the diel DO data for each day using a numerical minimization algorithm (the negative log likelihood function of a normal distribution), using the function `nlm` in R (R Core Team 2013). Model performance (i.e., how well the model fitted observed diel changes in DO) was assessed both visually, and numerically through the coefficient of determination ($r^2 > 0.75$, see examples in Figure S2 in the Supporting Information). Model fitting was generally good, and metabolic rates agreed with reported ranges for streams, rivers, lakes and reservoirs ([Hoellein et al., 2013], Table S2 and Figure S3 in the Supporting Information).

We then calculated the net ecosystem production (NEP; $\text{mmol } O_2 \text{ m}^2 \text{ d}^{-1}$) as:

$$NEP = GPP - ER \quad (7)$$

and we converted oxygen-based rates to carbon metabolic rates (expressed as $\text{mmol C m}^{-2} \text{ d}^{-1}$) using a $CO_2:O_2$ ratio of 138:106 [Torgersen and Branco, 2007]. For $NEP > 0$ (i.e., net autotrophy) there is more CO_2 being removed from the water column by photosynthesis than

added by respiration, leading to negative $F_{\text{CO}_2 \text{ metabolism}}$. In contrast, $\text{NEP} < 0$ (i.e., net heterotrophy) implies higher respiration than photosynthesis, and therefore a positive $F_{\text{CO}_2 \text{ metabolism}}$.

2.5. Source apportionment of CO_2 emissions

In addition to the upstream inputs and internal metabolism, other processes (i.e., groundwater fluxes, lateral surface water fluxes and internal fluxes derived from geochemical reactions of calcite precipitation and photochemical mineralization of organic solutes), can contribute to CO_2 supersaturation in each segment. We derived the flux of CO_2 associated to these unmeasured sources ($F_{\text{CO}_2 \text{ others}}$; $\text{mmol m}^{-2} \text{ d}^{-1}$) by applying a mass balance approach of CO_2 assuming steady state in each individual segment:

$$\frac{d\text{CO}_2}{dx} = F_{\text{CO}_2 \text{ inflow}} - F_{\text{CO}_2 \text{ outflow}} \pm F_{\text{CO}_2 \text{ emission}} \pm F_{\text{CO}_2 \text{ metabolism}} \pm F_{\text{CO}_2 \text{ others}} \quad (8)$$

where $F_{\text{CO}_2 \text{ inflow}}$ ($\text{mmol m}^{-2} \text{ d}^{-1}$) is the measured flux of CO_2 imported from upstream surface waters, $F_{\text{CO}_2 \text{ outflow}}$ ($\text{mmol m}^{-2} \text{ d}^{-1}$) is the measured flux of CO_2 exported to downstream surface waters, $F_{\text{CO}_2 \text{ emission}}$ ($\text{mmol m}^{-2} \text{ d}^{-1}$) is the measured flux of CO_2 across the water-air interface and $F_{\text{CO}_2 \text{ metabolism}}$ is the measured flux of CO_2 derived from aerobic metabolic processes occurring in the segment. Not all the CO_2 derived from internal metabolism will remain in the water as CO_2 because a portion will be converted to carbonate or bicarbonate depending on water alkalinity and pH. Thus, we calculated $F_{\text{CO}_2 \text{ metabolism}}$ by considering the geochemical speciation of inorganic carbon once CO_2 from internal metabolism is added to the water. Concentrations of different DIC species were calculated from DIC, pH and temperature using the speciation software CO2SYS [Lewis and Wallace, 1998].

To assess the relative contribution (%) of each source to the total CO₂ inputs into the segment, we divided each of the contributing fluxes (i.e., $F_{\text{CO}_2 \text{ inflow}}$, $F_{\text{CO}_2 \text{ metabolism}}$ and $F_{\text{CO}_2 \text{ others}}$) by their sum.

2.6. Statistical analyses

We tested the effect of the segment type (i.e., lotic segments, n=96; lentic segments, n=48) on the mean WRT, $F_{\text{CO}_2 \text{ emission}}$, $p_{\text{CO}_2, w}$ and k_{CO_2} using one-way analysis of variance (ANOVA). We assessed the effect of the WRT on the $F_{\text{CO}_2 \text{ emission}}$, $p_{\text{CO}_2, w}$ and k_{CO_2} in both lotic and lentic segments using linear and non-linear regressions. To determine the importance of the two main parameters directly involved in the CO₂ emission (i.e., $p_{\text{CO}_2, w}$ and k_{CO_2}) we applied simple and multiple linear regression models.

We tested the effect of the segment type (i.e., lotic segments, n=32; lentic segments, n=10) on the CO₂ fluxes that determined CO₂ variations within segments (i.e., $F_{\text{CO}_2 \text{ emission}}$, $F_{\text{CO}_2 \text{ metabolism}}$, $F_{\text{CO}_2 \text{ inflow}}$, $F_{\text{CO}_2 \text{ outflow}}$ and $F_{\text{CO}_2 \text{ others}}$) using one-way ANOVA. We investigated the dependency of $F_{\text{CO}_2 \text{ metabolism}}$ on $F_{\text{CO}_2 \text{ emission}}$ and $p_{\text{CO}_2, w}$ in both lotic and lentic segments with linear and non-linear regression models. A similar approach was used to assess the effect of the WRT on the $F_{\text{CO}_2 \text{ metabolism}}$ and of the WRT on the relative contribution of $F_{\text{CO}_2 \text{ metabolism}}$, $F_{\text{CO}_2 \text{ inflow}}$ and $F_{\text{CO}_2 \text{ others}}$.

When the statistical tests required it, we transformed the variables by their natural logarithm to meet the conditions of homogeneity of variance, normality of residuals and to avoid the deleterious effect of extreme large values. All statistical analyses were conducted in the R statistical environment (R Core Team 2013) using the Vegan package [Oksanen *et al.* 2013]. Statistical tests were considered significant at $p < 0.05$.

3. Results

3.1. Hydrologic regime

The WRT of lotic and especially that of lentic segments showed a wide annual variation, driven by changes in water flow (Figure 2a; Table S1 in the Supporting Information). Specifically, the first part of the monitored period (from December 2012 to March 2013) was characterized by low water flows. During this period, the average WRT in lotic segments was 10 h. In contrast, the presence of dams and weirs extended the WRT in lentic segments up to an average of 51 h. Subsequently, surface water flow in the fluvial network increased swiftly as a consequence of heavy rainfalls, leading to a minimum difference in WRT between segment types (mean WRT of lotic and lentic segments from April to May 2013 was 0.8 and 3.7 h, respectively). Following this hydrological peak (April 2013) the surface water flow gradually decreased until the end of the studied period (November 2013). Consequently, the mean fluvial network WRT increased progressively, and the difference in WRT between lotic and lentic segments increased again (mean WRT of lotic and lentic segments in November 2013 was 6.6 and 30.6 h, respectively).

3.2. CO₂ emissions

The $F_{\text{CO}_2 \text{ emission}}$ ranged from 627.2 to -11.2 mmol m⁻² d⁻¹ (mean = 131.9, n = 144) and showed a clear difference in magnitude and seasonal variation between lotic and lentic segments (Figure 2b). The lotic $F_{\text{CO}_2 \text{ emission}}$ was negatively related to WRT ($F_{\text{CO}_2 \text{ emission}} = -63.9 \ln(\text{WRT}) + 205.3$; $r^2 = 0.94$, $p < 0.001$, $n = 12$), indicating a strong dependency on hydrological dynamics. In contrast, a non-significant relationship between $F_{\text{CO}_2 \text{ emission}}$ and WRT was detected in lentic segments ($r^2 = 0.14$, $p = 0.29$, $n = 12$).

The $F_{\text{CO}_2 \text{ emission}}$ also showed a different spatial pattern in lotic and lentic segments (Figure S4 in the Supporting Information). In lotic segments, both the magnitude and the temporal variability decreased from upstream segments (i.e., headwaters streams) to lowland segments (i.e., river mouth). In contrast, lentic segments showed the opposite pattern, and emitted more CO_2 and were more temporally variable when situated close to the river mouth, and emitted less CO_2 and were less variable when they were situated upstream on the fluvial network.

Most observations (142 out of 144) were supersaturated in dissolved CO_2 in relation to the atmosphere (Figure S5b in the Supporting Information). The $p_{\text{CO}_2, w}$ ranged from 201 to 7213 μatm (mean = 1670, $n = 144$). The $p_{\text{CO}_2, w}$ from lotic (range = 495 to 5274, mean = 1743, $n = 96$) and from lentic segments (range = 201 to 7313, mean = 1670, $n = 48$) did not differ significantly (ANOVA, $p = 0.216$; Figure 2c). The $p_{\text{CO}_2, w}$ from lotic segments showed a weak but statistically significant positive relationship with the WRT ($p_{\text{CO}_2, w} = 230.1 \ln(\text{WRT}) + 1446.5$; $r^2 = 0.26$, $p = 0.04$, $n = 12$), whereas such dependency was not observed for the lentic segments ($r^2 = 0.08$, $p = 0.39$, $n = 12$).

The k_{CO_2} ranged from 0.04 to 15.8 m d^{-1} (mean = 2.1, $n = 144$; Figure S5a in the Supporting Information), and although variable, it was significantly higher (ANOVA, $p < 0.001$; Figure 2d) in lotic segments (range = 0.36 to 15.8 m d^{-1} , mean = 2.71, $n = 96$) than in lentic segments (range = 0.04 to 12.38 m d^{-1} , mean = 0.51, $n = 48$). Likewise, the k_{CO_2} from lotic segments clearly responded to the temporal hydrological fluctuations and gradually decreased with increasing WRT ($k_{\text{CO}_2} = -2.1 \ln(\text{WRT}) + 5.4$; $r^2 = 0.80$, $p < 0.001$, $n = 12$). In contrast, k_{CO_2} from lentic segments remained relatively stable along the WRT gradient ($r^2 = 0.03$, $p = 0.66$, $n = 12$).

Among the two main parameters directly driving $F_{\text{CO}_2 \text{ emission}}$ (i.e., $p_{\text{CO}_2,w}$ and k_{CO_2} ; Equation 1), the k_{CO_2} exhibited a significant positive relationship with the $F_{\text{CO}_2 \text{ emission}}$ ($F_{\text{CO}_2 \text{ emission}} = 31.1 k_{\text{CO}_2} + 46.2$; $r^2 = 0.61$, $p < 0.001$, $n = 144$; Figure S5a in the Supporting Information), while no significant dependency between $p_{\text{CO}_2,w}$ and $F_{\text{CO}_2 \text{ emission}}$ was detected ($r^2 = 0.02$, $p = 0.080$, $n = 144$; Figure S5b in the Supporting Information). The multiple regression analysis also revealed that k_{CO_2} and $p_{\text{CO}_2,w}$ explained respectively 86% and 0% of the total variation in $F_{\text{CO}_2 \text{ emission}}$. However, $p_{\text{CO}_2,w}$ explained a higher proportion of the variance of $F_{\text{CO}_2 \text{ emission}}$ (13.9%) when only lentic segments were included in the model.

3.3. Internal metabolism

While all segments where we estimated $F_{\text{CO}_2 \text{ metabolism}}$ ($n = 42$) were supersaturated in CO_2 , only 71% of them showed positive $F_{\text{CO}_2 \text{ metabolism}}$ values (i.e., internal metabolic production of CO_2 ; Figure 3 and Table S2 in the Supporting Information). This discrepancy was more evident in lentic segments, of which only 40% showed positive $F_{\text{CO}_2 \text{ metabolism}}$, and even in most cases these were only slightly positive. $F_{\text{CO}_2 \text{ metabolism}}$ did not show any significant relationship with $F_{\text{CO}_2 \text{ emission}}$ or $p_{\text{CO}_2,w}$ (Figure 3), neither when pooling all the data nor when considering lotic and lentic segments separately.

$F_{\text{CO}_2 \text{ metabolism}}$ in both lotic segments ($r^2 = 0.62$, $p < 0.001$, $n=30$) and lentic segments ($r^2 = 0.59$, $p=0.008$, $n=12$) showed a significant positive linear relationship with WRT (Figure 4).. However, $F_{\text{CO}_2 \text{ metabolism}}$ increased more rapidly with increasing WRT in lotic (slope= 0.08 ± 0.01) than in lentic segments (slope= 0.02 ± 0.006).

3.4. Source apportionment of CO₂ emissions

The $F_{CO_2\ inflow}$ and the $F_{CO_2\ others}$, were the dominant sources of CO₂ that sustained the $F_{CO_2\ emission}$ in the fluvial network (50.2 and 31.9% on average, respectively; Figure 5). A similar influence of the $F_{CO_2\ inflow}$ and the $F_{CO_2\ others}$ on the $F_{CO_2\ emission}$ was detected in lotic segments (43.4 and 41.1%, respectively), whereas a stronger influence of upstream inputs on the $F_{CO_2\ emission}$ was detected in lentic segments (73.9%). We also detected differences in the contribution of $F_{CO_2\ internal\ metabolism}$ to the $F_{CO_2\ emission}$ between segment typologies. Whereas $F_{CO_2\ internal\ metabolism}$ contributed an average of 24% in lotic segments, the mean contribution of $F_{CO_2\ internal\ metabolism}$ to the $F_{CO_2\ emission}$ was negligible (~ 0%) in lentic segments (Figure 5).

The relative contribution of $F_{CO_2\ metabolism}$ to the $F_{CO_2\ emission}$ in lotic segments showed a positive relationship with WRT (contribution of $F_{CO_2\ metabolism} = 18.6 \ln(\text{WRT}) + 4.1$; $r^2 = 0.65$, $p < 0.001$, $n = 32$; Figure 6a), and contributed up to 40-70% of the emitted CO₂ in situations of high WRT. In contrast, no hydrological dependence of the contribution of $F_{CO_2\ metabolism}$ to the $F_{CO_2\ emission}$ was detected in the case of lentic segments. The contribution of $F_{CO_2\ inflow}$ to the $F_{CO_2\ emission}$ showed a negative relationship with the WRT (contribution of $F_{CO_2\ inflow} = 52.009 e^{-0.602 \ln(\text{WRT})}$; $r^2 = 0.44$, $p < 0.001$, $n = 32$; Figure 6b) in lotic segments, while no hydrological dependence of the contribution of $F_{CO_2\ inflow}$ to the $F_{CO_2\ emission}$ was detected in the case of lentic segments. Finally, the contribution of $F_{CO_2\ others}$ to the $F_{CO_2\ emission}$, which was highly variable along the fluvial network and during the studied period, was not related to the WRT, neither in lotic nor in lentic segments (Figure 6c).

4. Discussion

Here, we showed that the CO₂ emitted from the interconnected lotic and lentic waterbodies found along a Mediterranean fluvial network mostly derives from sources other than internal metabolism. Such sources may include surface and subsurface hydrological inputs of CO₂ derived from soil respiration and mineral weathering within the catchment, internal geochemical reactions of calcite precipitation and internal photochemical mineralization of organic solutes (see below). Furthermore, both the magnitude of CO₂ emissions and the relative contribution of the different sources strongly depended on the hydrological dynamics of the fluvial network, being particularly dependent on them in the lotic segments.

Our results highlight the importance of CO₂ emissions from running waters compared to slow-moving waterbodies associated to weirs and small impoundments. In general, low-order streams deserve special attention since they cover a large surface area [*Butman and Raymond, 2011; Downing et al., 2012; Raymond et al., 2013*]. Several studies have shown that stream emissions dominate total aquatic CO₂ emissions [*Kokic et al., 2015*] at regional [*Lundin et al., 2013; Wallin et al., 2013*] and global scales [*Raymond et al., 2013*]. Our study adds to current knowledge by accounting for the pronounced spatial and temporal variability in streams and impounded waterbodies within fluvial networks. Specifically, we show that CO₂ emissions from headwater streams dominate aquatic CO₂ loss, especially during periods of high flows, when most of the stream network is hydrologically connected [*Benstead and Leigh, 2012; Downing, 2012; Bernal et al., 2013*].

Our results also agree with previous findings on the importance of k_{CO_2} as the major driver of the spatial and temporal variability in fluvial network CO_2 emissions [Wallin *et al.*, 2011; Gómez-Gener *et al.*, 2015; Kokic *et al.*, 2015; Long *et al.*, 2015]. However, the complexity of the hydrological regime of Mediterranean fluvial networks leads to particular situations (in space and time) where the $p_{\text{CO}_2,w}$ can exert a significant control on CO_2 emissions. These situations mainly occurred in lentic segments during low flows, when dams and weirs create discontinuities that decreased k_{CO_2} and led to higher supersaturation of CO_2 . Extended periods of low flows as a consequence of intensive use of the water resources or drought [Gasith and Resh, 1999; Gibson *et al.*, 2005] may lead to a higher increase of lentic habitats at the expenses of lotic environments in many fluvial networks [Sabater, 2008]. Consequently, the dominance of $p_{\text{CO}_2,w}$ on controlling the CO_2 emissions under situations of physical limitation induced by low flows [Demars and Manson, 2013; Gómez-Gener *et al.*, 2015] will probably be more common in the future.

Internal biomineralization of aquatic and terrestrial organic matter (here referred to as internal metabolism), has commonly been considered to be the main factor driving CO_2 supersaturation in lakes and rivers [Cole *et al.*, 2000; Duarte and Prairie, 2005]. Therefore, if no other processes are adding or removing CO_2 besides internal metabolism, the CO_2 present in the system and emitted to the atmosphere should be in line with the degree of net heterotrophy in the corresponding aquatic ecosystems. Our results showed a strong disagreement with this perspective, since the CO_2 produced by internal metabolism and both the CO_2 present in the segment and the CO_2 emitted to the atmosphere did not match (Figure 3). In fact, some of the supersaturated segments were actually net autotrophic, showing negative $F_{\text{CO}_2 \text{ metabolism}}$ values (overall, 60% of supersaturated lentic and 20% of lotic segments were found to have $F_{\text{CO}_2 \text{ metabolism}} < 0$; Figure 3b). In those situations, internal metabolism was acting as a net sink for inorganic carbon, but the magnitude of this sink was

not sufficient to maintain dissolved CO₂ concentrations below atmospheric levels. These results support previous findings that already indicated that sources other than internal metabolism can sustain CO₂ supersaturation in freshwaters [Stets *et al.*, 2009; McDonald *et al.*, 2013; Borges *et al.*, 2015; Hotchkiss *et al.*, 2015; Marcé *et al.*, 2015].

Our mass balance of CO₂ (Table 1; Figure 7) highlights a crucial role of hydrological inputs and other sources on sustaining the CO₂ emissions along the fluvial network. Several studies in lentic systems point towards the same direction. For example, Stets *et al.* [2009] showed that the sum of surface and subsurface hydrological inputs of DIC accounted for 41% to 100% of the observed CO₂ release from two lakes situated in north-central Minnesota, USA. Likewise, McDonald *et al.* [2013] and Weyhenmeyer *et al.* [2015] showed that the surface and subsurface hydrological inputs of DIC accounted for a significant fraction of the total CO₂ emitted from a large number of lakes and reservoirs in the contiguous United States and Scandinavia, respectively. Similarly, Marcé *et al.* [2015] showed that in up to 57% of the lakes and reservoirs worldwide, CO₂ supersaturation could be related to alkalinity inputs from the catchment, suggesting mineral weathering as a fundamental regulator of the DIC coming from terrestrial ecosystems. Also, Wilkinson *et al.* [2016] using high-frequency time series of O₂ and CO₂ confirmed the large influence of hydrological inputs on the CO₂ emissions, even in lakes where internal CO₂ uptake had been experimentally increased with nutrients. In the same direction, a recent study in lotic systems [Hotchkiss *et al.* 2015] showed that CO₂ produced by aquatic metabolism contributes on average to only 28% of CO₂ evasion from streams and rivers with flows ranging between 0.0001 and 19,000 m³ s⁻¹ in the contiguous United States. Our study adds to current knowledge by integrating the CO₂ fluxes determining CO₂ variation within lotic and lentic waterbodies that are interconnected in complex fluvial networks.

Despite the dominance of hydrological inputs and other sources to the net CO₂ emission, the contribution of internal metabolism was not negligible in lotic segments (Table 1; Figure 7), where we detected a predominance of net heterotrophy for most of the year. In contrast, lentic segments had much lower and balanced fluxes that varied between net autotrophy and heterotrophy, thus leading to a generally much smaller contribution of internal metabolism to the lentic CO₂ emissions (Table 1; Figure 7).

The relationships of the contribution of upstream inflow and internal metabolism to the CO₂ emissions with WRT in lotic segments reveals a clear coupling between the hydrological dynamics and the origin of CO₂ emissions (Figure 6a and 6b). During high flow periods, both the hydrological connectivity within the fluvial network and between the fluvial network and the catchment is maximized [Bernal *et al.*, 2013]. This favors longitudinal and lateral pathways of CO₂ supply along the fluvial network [Wallin *et al.*, 2010; Campeau and del Giorgio, 2013; Kokic *et al.*, 2015] and an efficient exchange between the adjacent terrestrial ecosystems and the stream channels [Stets *et al.*, 2009; Davidson *et al.*, 2010; McDonald *et al.*, 2013; Hotchkiss *et al.*, 2015]. At the same time, reduced WRT during high flows limits the capacity of the biota to interact with organic substrates [Battin *et al.*, 2009b], thereby constraining the internal metabolic pathway of CO₂ supply [Hotchkiss *et al.*, 2015]. Therefore, situations of high flows and short WRT lead to a higher contribution of externally derived CO₂ and a lower contribution of internal metabolically derived CO₂ to the finally emitted CO₂ (Figure 6). In contrast, during periods of low flows and long WRT, the reduced hydrological connectivity hampers the supply of CO₂ from upstream to downstream waters as well as from adjacent terrestrial ecosystems to the fluvial network. Additionally, organic matter processing is favored through increased interaction with biological actors [Battin *et al.*, 2009b]. Altogether, this leads to a higher contribution of internal metabolic CO₂ and a

lower contribution of externally derived CO₂ to the finally emitted CO₂ during low flows and long WRT.

Interestingly, the above hydro-biogeochemical model does not apply to lentic waterbodies. Our results indicate that the contribution of the upstream inflow and internal metabolism to the CO₂ efflux from lentic waters was independent of hydrological variation (Figures 6a and 6b). The contribution of the upstream inflow was very variable and did not follow any trend along the WRT axis, while the contribution of the internal metabolism remained fairly constant and close to the 0% line. A balanced metabolism (i.e., NEP ~0) is expected in aquatic systems over longer durations and for larger spatial scales, if burial is minimal [Staeher *et al.*, 2012; Hotchkiss *et al.*, 2015]. Theoretically, this balance arises because, given sufficient time, any increase in primary production yields organic matter, which in a relatively closed system, will be proportionally respired. Alternatively, any increases in respiration will release inorganic nutrients that proportionally stimulate primary production [Staeher *et al.*, 2012]. The higher WRT in lentic segments combined with their higher resistance to hydrological perturbations will therefore favor a balanced metabolism that leads to a low contribution of internal metabolism to CO₂ emissions.

The variance around the contribution of other non-measured sources to the CO₂ emissions with WRT in both lotic and lentic waterbodies (Figure 6c) reveals a rather hydrological independence of this third component. The flux of CO₂ coming from these other non-estimated sources includes a set of diverse processes, apart from internal metabolism and upstream inputs, that can add or remove CO₂ to the studied segments (i.e., groundwater fluxes, lateral surface water fluxes and internal fluxes derived from geochemical reactions of calcite precipitation and photochemical mineralization of organic solutes). Therefore, being not surprising that such diverse set of CO₂ sources and sinks in origin and magnitude) may respond differently to hydrological variations.

Groundwater inputs, typically composed by high CO₂ and low O₂, can alter the chemistry of surface waters, especially of those small lotic [Öquist *et al.*, 2009; Hotchkiss *et al.*, 2015] and lentic [Hanson *et al.*, 2006; López *et al.*, 2011] waterbodies situated along the fluvial network. Similarly, surface water lateral inputs (i.e., small low-order streams that flow into the segments) draining adjacent terrestrial ecosystems (i.e., riparian and upland) may also affect the CO₂ dynamics in the receiving waterbodies.

Precipitation and dissolution of carbonate minerals may, respectively, produce or consume CO₂ in fluvial networks. Considering the high alkalinity of our fluvial network (mean=4.1 meq L⁻¹, n=144), we suggest that calcite precipitation may be a relevant process contributing to the CO₂ supersaturation and emission [Otsuki and Wetzel, 1974; Stets *et al.*, 2009; Nöges *et al.*, 2016]. However, further investigation is needed in order to understand how and to what extent carbonate precipitation and dissolution reactions may potentially affect the CO₂ dynamics and further regulate the CO₂ emissions from fluvial network.

The photo-chemical mineralization of dissolved organic matter can contribute to a great extent of the C processing [Cory *et al.*, 2014] and CO₂ emissions from inland waters [Koehler *et al.*, 2014]. This reaction also influence the O₂ dynamics of our fluvial network [Amon and Benner, 1996], and thus may contribute to the metabolism estimates calculated using diel changes in dissolved oxygen (O₂).

In conclusion, this work represents a novel attempt to integrate a mass balance of CO₂ fluxes into the complex temporal and spatial dynamism of an anthropogenically altered fluvial network. Using a steady-state approach we were able to integrate most sources affecting CO₂ fluxes along the fluvial network. Still, uncertainty existed related to the substantial contribution of CO₂ from other non-measured sources, and this would require further efforts to describe the drivers of the other sources (apart from internal metabolism and external surface hydrological) under non-steady state conditions. This will enable a better

understanding of the conditions regulating the seasonal dynamics of CO₂ emissions at the fluvial network scale. But, because of the high human demand for energy and water, few fluvial networks worldwide remain free from impoundment over the entire course, and contrarily, they typically result in an alternating series of lentic and lotic [*Ward and Stanford, 1983; Nilsson et al., 2005b; Döll et al., 2009*]. Therefore, we suggest that our findings should not be restricted to Mediterranean fluvial networks, but also useful for predicting the integrated responses of fluvial networks that share similar spatial configurations.

Acknowledgements

This research was funded by the Spanish Ministry of Economy and Competitiveness through the project FUNSTREAM (CGL2014-58760-C3-1-R). Ll. Gómez-Gener and J. P. Casas-Ruiz were additionally supported by FPI predoctoral grants (BES-2012-059743 and BES-2012-059655). We thank Meritxell Abril, Carmen Gutiérrez and Lorenzo Proia for field and laboratory assistance. We are grateful to R.A. Sponseller for his constructive comments on this manuscript. All the data used for the results of this paper is available upon request to the corresponding author.

References

- Abril, M., I. Muñoz, J. P. Casas-Ruiz, L. Gómez-Gener, M. Barceló, F. Oliva, and M. Menéndez (2015), Effects of water flow regulation on ecosystem functioning in a Mediterranean river network assessed by wood decomposition, *Sci. Total Environ.*, 517(1), 57–65, doi:10.1016/j.scitotenv.2015.02.015.
- Acuña, V., and K. Tockner (2010), The effects of alterations in temperature and flow regime on organic carbon dynamics in Mediterranean river networks, *Glob. Chang. Biol.*, 16(9), 2638-2650, doi:10.1111/j.1365-2486.2010.02170.x.
- Amon, R. M. W., and R. Benner (1996), Photochemical and microbial consumption of dissolved organic carbon and dissolved oxygen in the Amazon River system, *Geochim. Cosmochim. Acta*, 60(10), 1783–1792, doi:10.1016/0016-7037(96)00055-5.
- Aufdenkampe, A. K., E. Mayorga, P. a Raymond, J. M. Melack, S. C. Doney, S. R. Alin, R. E. Aalto, and K. Yoo (2011), Riverine coupling of biogeochemical cycles between land, oceans, and atmosphere, *Front. Ecol. Environ.*, 9(1), 53–60, doi:10.1890/100014.
- Bade, D. L. (2009), Gas exchange across the air-water interface, in *Encyclopedia of Inland Waters*, Academic Press: Oxford, 2009, pp 70–78.
- Battin, T. J., S. Luysaert, L. A. Kaplan, A. K. Aufdenkampe, A. Richter, and L. J. Tranvik (2009a), The boundless carbon cycle, *Nat. Geosci.*, 2(9), 598–600, doi:10.1038/ngeo618.
- Battin, T. J., L. A. Kaplan, S. Findlay, C. S. Hopkinson, E. Marti, A. I. Packman, J. D. Newbold, and F. Sabater (2009b), Biophysical controls on organic carbon fluxes in fluvial networks, *Nat. Geosci.*, 2(8), 595–595, doi:10.1038/ngeo602.
- Benson, B. B., and D. Krause (1984), The concentration and isotopic fractionation of oxygen dissolved in freshwater and seawater in equilibrium with the atmosphere, *Limnol. Oceanogr.*, 29(3), 620–632, doi:10.4319/lo.1984.29.3.0620.
- Benstead, J. P., and D. S. Leigh (2012), An expanded role for river networks, *Nat. Geosci.*, 5, 678–679, doi:10.1038/ngeo1593.
- Bernal, S., D. Schiller, F. Sabater, and E. Martí (2013), Hydrological extremes modulate nutrient dynamics in mediterranean climate streams across different spatial scales, *Hydrobiologia*, 719(1), 31–42, doi:10.1007/s10750-012-1246-2.

- Borges, A. V. et al. (2015a), Globally significant greenhouse-gas emissions from African inland waters, *Nat. Geosci.*, 8, 637–642, doi:10.1038/ngeo2486.
- Buffagni, A., D. G. Armanini, and S. Erba (2009), Does the lentic-lotic character of rivers affect invertebrate metrics used in the assessment of ecological quality?, *J. Limnol.*, 68(1), 92–105, doi:10.4081/jlimnol.2009.92.
- Butman, D., and P. a. Raymond (2011), Significant efflux of carbon dioxide from streams and rivers in the United States, *Nat. Geosci.*, 4(12), 839–842, doi:10.1038/ngeo1294.
- Campeau, A., and P. del Giorgio (2013), Patterns in CH₄ and CO₂ concentrations across boreal rivers: Major drivers and implications for fluvial greenhouse emissions under climate change scenarios, *Glob. Chang. Biol.*, 20(4), 1–14, doi:10.1111/gcb.12479.
- Clavero, M., F. Blanco-Garrido, and J. Prenda (2004), Fish fauna in Iberian Mediterranean river basins: Biodiversity, introduced species and damming impacts, *Aquat. Conserv. Mar. Freshw. Ecosyst.*, 14(6), 575–585, doi:10.1002/aqc.636.
- Cole, J. J., M. L. Pace, S. R. Carpenter, and J. F. Kitchell (2000), Persistence of net heterotrophy in lakes during nutrient addition and food web manipulations, *Limnol. Oceanogr.*, 45(8), 1718–1730, doi:10.4319/lo.2000.45.8.1718.
- Cole, J. J. et al. (2007), Plumbing the Global Carbon Cycle: Integrating Inland Waters into the Terrestrial Carbon Budget, *Ecosystems*, 10(1), 172–185, doi:10.1007/s10021-006-9013-8.
- Cory, R. M., C. P. Ward, B. C. Crump, and G. W. Kling (2014), Sunlight controls water column processing of carbon in arctic fresh waters, *Science*, 345, 925–928, doi:10.1126/science.1253119.
- Davidson, E. a., R. O. Figueiredo, D. Markewitz, and A. K. Aufdenkampe (2010), Dissolved CO₂ in small catchment streams of eastern Amazonia: A minor pathway of terrestrial carbon loss, *J. Geophys. Res. Biogeosciences*, 115(4), 1–6, doi:10.1029/2009JG001202.
- Demars, B. O. L., and J. R. Manson (2013), Temperature dependence of stream aeration coefficients and the effect of water turbulence: a critical review, *Water Res.*, 47(1), 1–15, doi:10.1016/j.watres.2012.09.054.
- Döll, P., K. Fiedler, and J. Zhang (2009), Global-scale analysis of river flow alterations due to water withdrawals and reservoirs, *Hydrol. Earth Syst. Sci. Discuss.*, 6(4), 4773–4812, doi:10.5194/hessd-6-4773-2009.

- Downing, J. A., J. J. Cole, C. M. Duarte, J. J. Middelburg, J. M. Melack, Y. T. Prairie, P. Kortelainen, R. G. Striegl, W. H. McDowell, and L. J. Tranvik (2012), Global abundance and size distribution of streams and rivers, *Inl. Waters*, 2(4), 229–236, doi:10.5268/IW-2.4.502.
- Duarte, C. M., and Y. T. Prairie (2005), Prevalence of Heterotrophy and Atmospheric CO₂ Emissions from Aquatic Ecosystems, *Ecosystems*, 8(7), 862–870, doi:10.1007/s10021-005-0177-4.
- Elosegi, A., and S. Sabater (2013), Effects of hydromorphological impacts on river ecosystem functioning: A review and suggestions for assessing ecological impacts, *Hydrobiologia*, 712(1), 129–143, doi:10.1007/s10750-012-1226-6.
- Frankignoulle, M. (1988), Field measurements of air-sea CO₂ exchange, *Limnol. Ocean.*, 33(3), 313–322.
- Friedl, G., and A. Wüest (2002), Disrupting biogeochemical cycles - Consequences of damming, *Aquat. Sci.*, 64(1), 55–65, doi:10.1007/s00027-002-8054-0.
- García-Ruiz, J. M., J. I. López-Moreno, S. M. Vicente-Serrano, T. Lasanta-Martínez, and S. Beguería (2011), Mediterranean water resources in a global change scenario, *Earth-Science Rev.*, 105(3-4), 121–139, doi:10.1016/j.earscirev.2011.01.006.
- Gasith, A., and V. H. Resh (1999), Streams in Mediterranean climate regions: Abiotic influences and biotic responses to predictable seasonal events, *Annu. Rev. Ecol. Syst.*, 30, 51–81, doi:http://dx.doi.org/10.1146/annurev.ecolsys.30.1.51.
- Gibson, C. A., J. L. Meyer, N. L. Poff, L. E. Hay, and A. Georgakakos (2005), Flow regime alterations under changing climate in two river basins: Implications for freshwater ecosystems, *River Res. Appl.*, 21(8), 849–864, doi:10.1002/rra.855.
- Gómez-Gener, L., B. Obrador, D. von Schiller, R. Marcé, J. P. Casas-Ruiz, L. Proia, V. Acuña, N. Catalán, I. Muñoz, and M. Koschorreck (2015), Hot spots for carbon emissions from Mediterranean fluvial networks during summer drought, *Biogeochemistry*, 125(3), 409–426, doi:10.1007/s10533-015-0139-7.
- Hanson, P. C., S. R. Carpenter, D. E. Armstrong, E. H. Stanley, and T. K. Kratz (2006), Lake dissolved inorganic carbon and dissolved oxygen: Changing drivers from days to decades, *Ecol. Monogr.*, 76(3), 343–363, doi:10.1177/0888325406287176.
- Hanson, P. C., S. R. Carpenter, N. Kimura, C. W. S. P. Cornelius, and T. K. Kratz (2008),

- Evaluation of metabolism models for free-water dissolved oxygen methods in lakes, *Limnol. Oceanogr. Methods*, 6(3), 454–465, doi:10.4319/lom.2008.6.454.
- Hoellein, T. J., D. A. Bruesewitz, and D. C. Richardson (2013), Revisiting Odum (1956): A synthesis of aquatic ecosystem metabolism, *Limnol. Oceanogr.*, 58(6), 2089–2100, doi:10.4319/lo.2013.58.6.2089.
- Holtgrieve, G. W., D. E. Schindler, T. A. Branch, and Z. T. Amar (2010), Simultaneous quantification of aquatic ecosystem metabolism and reaeration using a Bayesian statistical model of oxygen dynamics, *Limnol. Oceanogr.*, 55(3), 1047–1062, doi:10.4319/lo.2010.55.3.1047.
- Hornberger G.M., Kelly M.G. (1972). The determination of primary production in a stream using an exact solution to the oxygen balance equation. *Water Resources Bulletin* 8, 795–801.
- Hotchkiss, E. R., R. O. Hall Jr, R. A. Sponseller, D. Butman, J. Klaminder, H. Laudon, M. Rosvall, and J. Karlsson (2015), Sources of and processes controlling CO₂ emissions change with the size of streams and rivers, *Nat. Geosci.* 8, 696–699, doi:10.1038/ngeo2507.
- Humborg, C., C.-M. Mörth, M. Sundbom, H. Borg, T. Blenckner, R. Giesler, and V. Ittekkot (2010), CO₂ supersaturation along the aquatic conduit in Swedish watersheds as constrained by terrestrial respiration, aquatic respiration and weathering, *Glob. Chang. Biol.*, 16(7), 1966–1978, doi:10.1111/j.1365-2486.2009.02092.x.
- Koehler, B., T. Landelius, G. A. Weyhenmeyer, N. Machida, and L. J. Tranvik (2014), Sunlight-induced carbon dioxide emissions from inland waters, *Glob. Biogeochem. Cycles*, 28, 696–711, doi:10.1002/2014GB004850.
- Kokic, J., M. B. Wallin, H. E. Chmiel, B. A. Denfeld, and S. Sobek (2015), Carbon dioxide evasion from headwater systems strongly contributes to the total export of carbon from a small boreal lake catchment, *Geophys. Res. Biogeosciences*, 120, 13–28, doi:10.1002/2014JG002706.
- Kirk JTO (1994), *Light and photosynthesis in aquatic ecosystems*, Cambridge University Press, Cambridge.

- Lewis, E., and D. W. R. Wallace (1998), Program Developed for CO₂ System Calculations. ORNL/CDIAC-105, Carbon dioxide Information Analysis Center, Oak Ridge Natl. Lab. Oak Ridge, Tenn.
- Long, H., L. Vihermaa, S. Waldron, T. Hoey, S. Quemin, and J. Newton (2015), Hydraulics are a first-order control on CO₂ efflux from fluvial systems, *J. Geophys. Res. Biogeosciences*, 120, 1912–1922, doi:10.1002/2015JG002955.
- López, P., R. Marcé, and J. Armengol (2011), Net heterotrophy and CO₂ evasion from a productive calcareous reservoir: Adding complexity to the metabolism-CO₂ evasion issue, *J. Geophys. Res.*, 116(G2), G02021, doi:10.1029/2010JG001614.
- Lundin, E. J., R. Giesler, A. Persson, M. S. Thompson, and J. Karlsson (2013), Integrating carbon emissions from lakes and streams in a subarctic catchment, *J. Geophys. Res. Biogeosciences*, 118(3), 1200–1207, doi:10.1002/jgrg.20092.
- Marcé, R., B. Obrador, J. Morguá, J. L. Riera, P. López, and J. Armengol (2015), Carbonate weathering as a driver of CO₂ supersaturation in lakes, *Nat. Geosci.*, 8, 107–111, doi:10.1038/NGEO2341.
- McDonald, C. P., E. G. Stets, R. G. Striegl, and D. Butman (2013), Inorganic carbon loading as a primary driver of dissolved carbon dioxide concentrations in the lakes and reservoirs of the contiguous United States, *Global Biogeochem. Cycles*, 27(2), 285–295, doi:10.1002/gbc.20032.
- Millero, F. (1995), Thermodynamics of the carbon dioxide system in the oceans, *Geochim. Cosmochim. Acta*, 59(4), 661–677, doi:10.1016/0016-7037(94)00354-O.
- Nilsson, C., C. Reidy, M. Dynesius, and C. Revenga (2005), Fragmentation and flow regulation of the world's large river systems, *Science*, 308(5720), 405–408, doi:10.1126/science.1107887.
- Nõges, P., F. Cremona, A. Laas, T. Martma, E. I. Rõõm, K. Toming, M. Viik, S. Vilbaste, and T. Nõges (2016), Role of a productive lake in carbon sequestration within a calcareous catchment, *Sci. Total Environ.*, 550, 225–230, doi:10.1016/j.scitotenv.2016.01.088.
- Odum, T. H. (1955), Primary Production in Flowing Waters, *Limnol. Ocean.*, 1(2), 102–117.
- Oksanen, J, Blanchet F.G., Kindt R. et al. (2013). Vegan: community ecology package. R package version 2.0-10. <http://CRAN.R-project.org/package=vegan>

- Öquist, M. G., M. Wallin, J. Seibert, K. Bishop, and H. Laudon (2009), Dissolved Inorganic Carbon Export Across the Soil / Stream Interface and Its Fate in a Boreal Headwater Stream, *Environ. Sci. Technol.*, 43(19), 7364–7369.
- Otsuki, A., and R. G. Wetzel (1974), Calcium and total alkalinity budgets and calcium carbonate precipitation of a small hard-water lake, *Arch. Hydrobiol.*, 73, 14–30.
- Pavón, D. (2010), Desarrollo y decadencia hidroeléctrica en los pequeños ríos del litoral mediterráneo catalán. El caso de las cuencas del Fluvià y de la Muga, *Rev. Hist. Ind.*, 42(1), 43–87.
- Poff, N. L., and D. D. Hart (2002), How Dams Vary and Why It Matters for the Emerging Science of Dam Removal, *Bioscience*, 52(8), 659–668, doi:10.1641/0006-3568(2002)052[0659:HDVAWI]2.0.CO;2.
- Raymond, P. A., C. J. Zappa, D. Butman, T. L. Bott, J. Potter, P. Mulholland, a. E. Laursen, W. H. McDowell, and D. Newbold (2012), Scaling the gas transfer velocity and hydraulic geometry in streams and small rivers, *Limnol. Oceanogr. Fluids Environ.*, 2, 41–53, doi:10.1215/21573689-1597669.
- Raymond, P. A. et al. (2013), Global carbon dioxide emissions from inland water, *Nature*, 503, 355–359, doi:10.1038/nature12760.
- R Development Core Team (2008). R: A language and environment for statistical computing. R Foundation for Statistical Computing, Vienna, Austria. ISBN 3-900051-07-0, URL <http://www.R-project.org>.
- Sabater, S. (2008), Alterations of the global water cycle and their effects on river structure, function and services, *Freshw. Rev.*, 1(1), 75–88, doi:10.1608/FRJ-1.1.5.
- Staeher, P. a., J. M. Testa, W. M. Kemp, J. J. Cole, K. Sand-Jensen, and S. V. Smith (2012), The metabolism of aquatic ecosystems: History, applications, and future challenges, *Aquat. Sci.*, 74(1), 15–29, doi:10.1007/s00027-011-0199-2.
- Stets, E. G., R. G. Striegl, G. R. Aiken, D. O. Rosenberry, and T. C. Winter (2009), Hydrologic support of carbon dioxide flux revealed by whole-lake carbon budgets, *J. Geophys. Res. Biogeosciences*, 114(1), 1–14, doi:10.1029/2008JG000783.
- Teodoru, C. R., Y. T. Prairie, and P. a. del Giorgio (2010), Spatial Heterogeneity of Surface CO₂ Fluxes in a Newly Created Eastmain-1 Reservoir in Northern Quebec, Canada, *Ecosystems*, 14(1), 28–46, doi:10.1007/s10021-010-9393-7.

- Torgersen, T., and B. Branco (2007), Carbon and oxygen dynamics of shallow aquatic systems: Process vectors and bacterial productivity, *J. Geophys. Res.*, 112, G03016, doi:10.1029/2007JG000401.
- Tranvik, L., J. Downing, and J. Cotner (2009), Lakes and reservoirs as regulators of carbon cycling and climate, *Limnol. Ocean.*, 54(1), 2298–2314, doi:10.4319/lo.2009.54.6_part_2.2298.
- Van de Bogert, M. C., S. R. Carpenter, J. J. Cole, and M. L. Pace (2007), Assessing pelagic and benthic metabolism using free water measurements, *Limnol. Oceanogr.*, 5, 145–155, doi:10.4319/lom.2007.5.145.
- Von Schiller, D., R. Marcé, B. Obrador, L. Gómez-Gener, J. P. Casas-Ruiz, V. Acuña, and M. Koschorreck (2014), Carbon dioxide emissions from dry watercourses, *Inland Waters* 4, 377–382, doi:10.5268/IW-4.4.746.
- Wallin, M., I. Buffam, M. Öquist, H. Laudon, and K. Bishop (2010), Temporal and spatial variability of dissolved inorganic carbon in a boreal stream network: Concentrations and downstream fluxes, *J. Geophys. Res.*, 115, 1–12, doi:10.1029/2009JG001100.
- Wallin, M. B., M. G. Öquist, I. Buffam, M. F. Billett, J. Nisell, and K. H. Bishop (2011), Spatiotemporal variability of the gas transfer coefficient (K_{CO_2}) in boreal streams: Implications for large scale estimates of CO_2 evasion, *Global Biogeochem. Cycles*, 25, GB3025, doi:10.1029/2010GB003975.
- Wallin, M. B., T. Grabs, I. Buffam, H. Laudon, A. Ågren, M. G. Öquist, and K. Bishop (2013), Evasion of CO_2 from streams - The dominant component of the carbon export through the aquatic conduit in a boreal landscape, *Glob. Chang. Biol.*, 19, 785–797, doi:10.1111/gcb.12083.
- Wanninkhof, R. (1992), Relationship between wind speed and gas exchange over the ocean, *J. Geophys. Res. Ocean.*, 97(92), 7373–7382, doi:10.1029/92JC00188.
- Ward, J. V., and J. a Stanford (1983), Serial Discontinuity Concept of Lotic Ecosystems, *Dyn. Lotic Syst. Ann Arbor Sci. Ann Arbor*, 29–42.
- Wehrli, B. (2013), Conduits of the carbon cycle, *Nature*, 503(21), 9–10, doi:10.1038/503346a.
- Weiss, R. (1974), Carbon dioxide in water and seawater: the solubility of a non-ideal gas, *Mar. Chem.*, 2(3), 203–215, doi:10.1016/0304-4203(74)90015-2.

Weyhenmeyer, G. A., S. Kosten, M. B. Wallin, L. J. Tranvik, E. Jeppesen, and F. Roland (2015), Significant fraction of CO₂ emissions from boreal lakes derived from hydrologic inorganic carbon inputs, 8, 933-936, doi:10.1038/NGEO2582.

Wilkinson, G. M., C. D. Buelo, J. J. Cole, and M. L. Pace (2016), Exogenously produced CO₂ doubles the CO₂ efflux from three north temperate lakes, *Geophys. Res. Lett.*, doi:10.1002/2016GL067732.

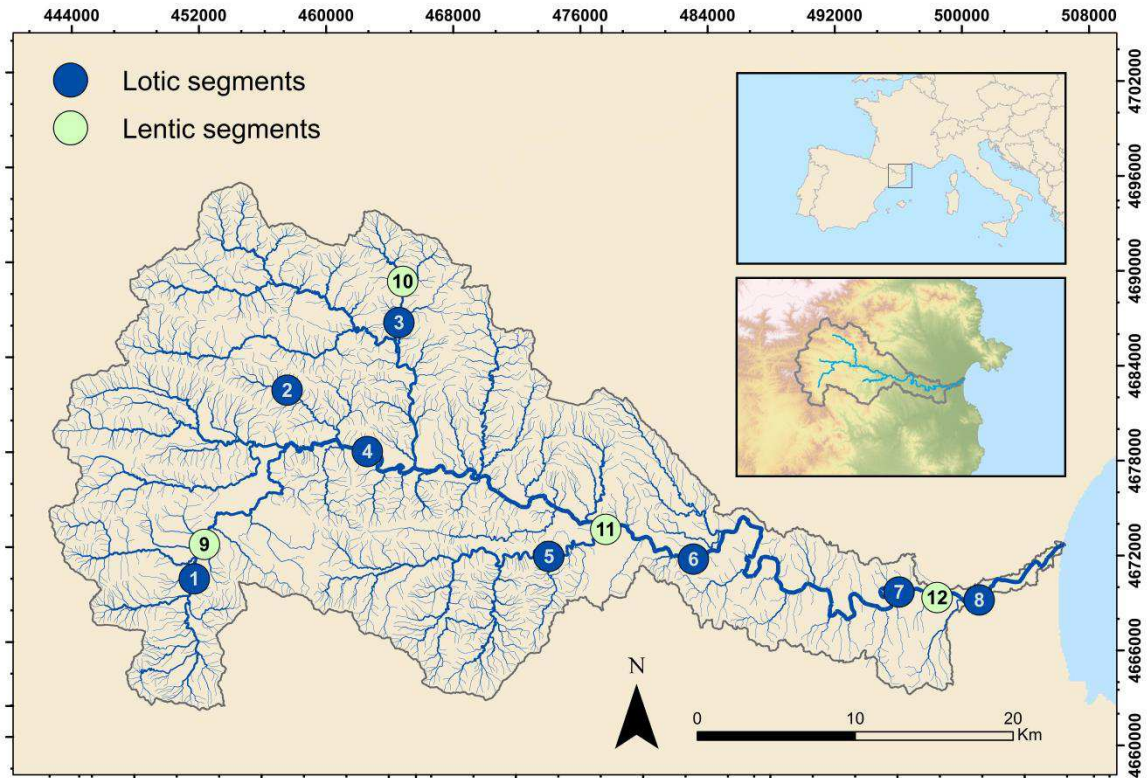


Figure 1. Location of the Fluvià River catchment in Catalonia (NE Iberian Peninsula), with the corresponding position of the study segments. Dark blue circles indicate lotic segments (n=8) and light green circles lentic segments (n=4). See Table S1 in the supporting information for a detailed description of the hydromorphological characteristics of the segments.

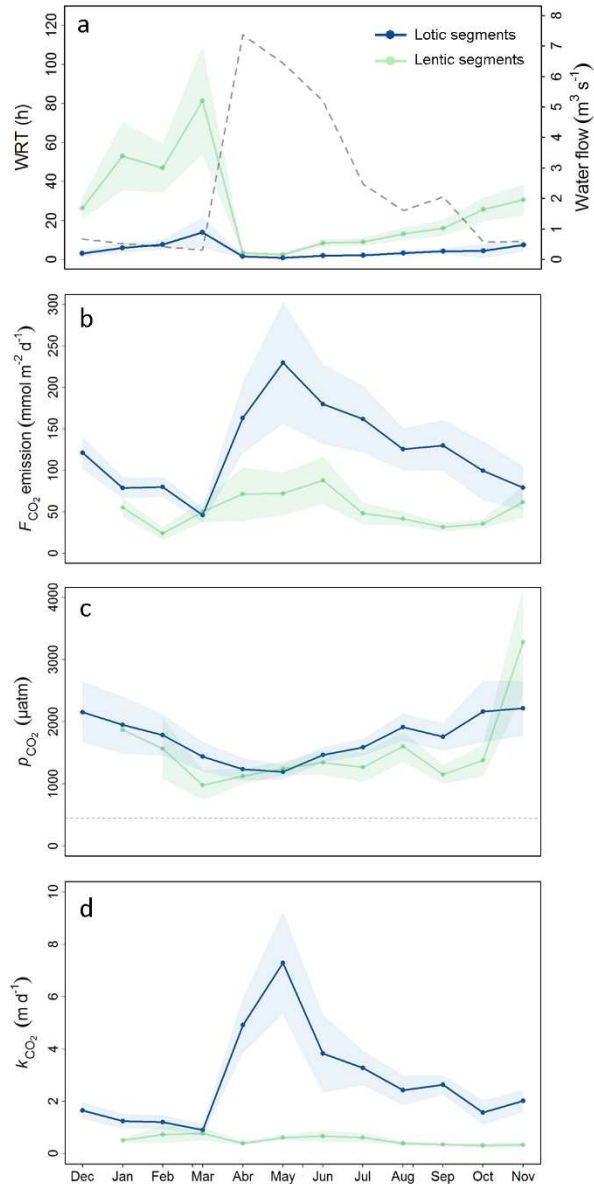


Figure 2. Temporal variation (from December 2012 to November 2013) of (a) water residence time (WRT), (b) CO_2 emissions ($F_{\text{CO}_2 \text{ emission}}$), (c) partial pressure of CO_2 in water ($p_{\text{CO}_2,w}$) and (d) specific gas transfer velocity for CO_2 (k_{CO_2}). Solid lines represent monthly averages for the lotic (blue, $n=8$) and lentic (green, $n=4$) segments. Shaded regions are monthly standard errors (SE) that represent spatial variations. The dashed grey line in panel (a) represents the water flow at the outlet of the catchment. The horizontal dashed line in panel (c) represents the average partial pressure of CO_2 in air ($p_{\text{CO}_2,a}$) for all the segments (418 μatm).

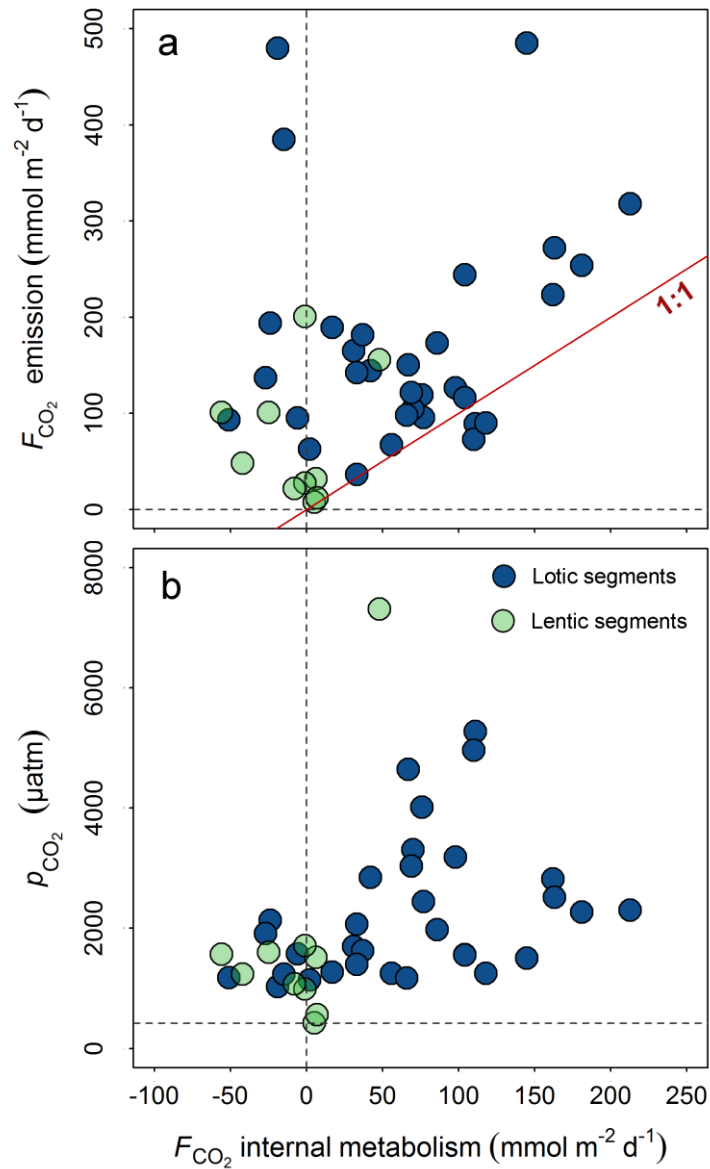


Figure 3. Relationship between the internal metabolic flux of CO_2 (F_{CO_2} metabolism) and (a) the CO_2 emissions (F_{CO_2} emission) and (b) the partial pressure of CO_2 in water ($p_{\text{CO}_2,w}$) for both lotic (dark blue circles; $n=32$) and lentic segments (light green circles; $n=10$). The vertical dashed lines represent F_{CO_2} metabolism = 0. The horizontal dashed line in panel (a) represents F_{CO_2} emission = 0. The horizontal dashed line in panel (b) represents the average partial pressure of CO_2 in air ($p_{\text{CO}_2,a}$) for all the segments (418 μatm). The 1:1 reference line is shown in panel (a).

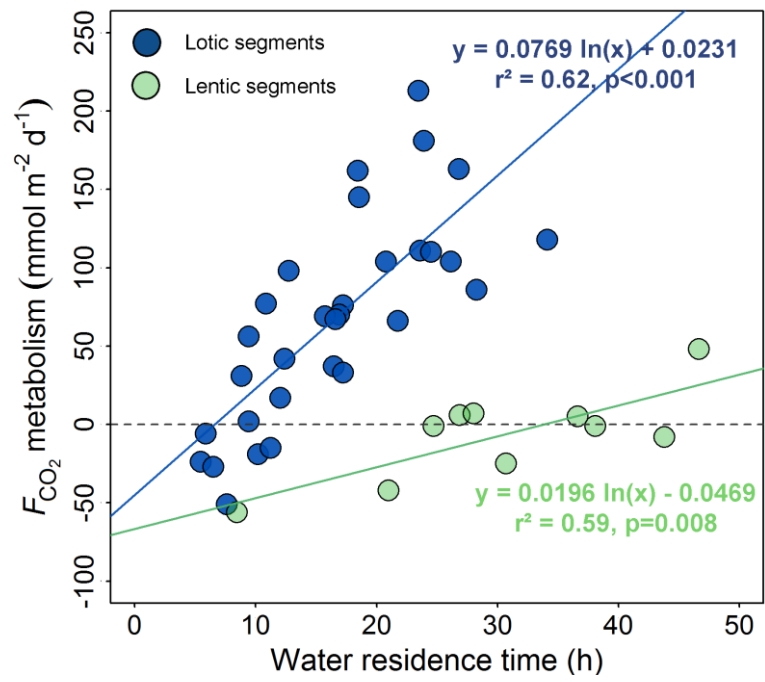


Figure 4. Internal metabolic flux of CO_2 (F_{CO_2} metabolism) as a function of water residence time for both lotic (dark blue circles) and lentic segments (light green circles). The horizontal dashed line represent F_{CO_2} metabolism = 0. The solid lines correspond to the regression model lines best fitting the data. Model equations are also shown close to model lines.

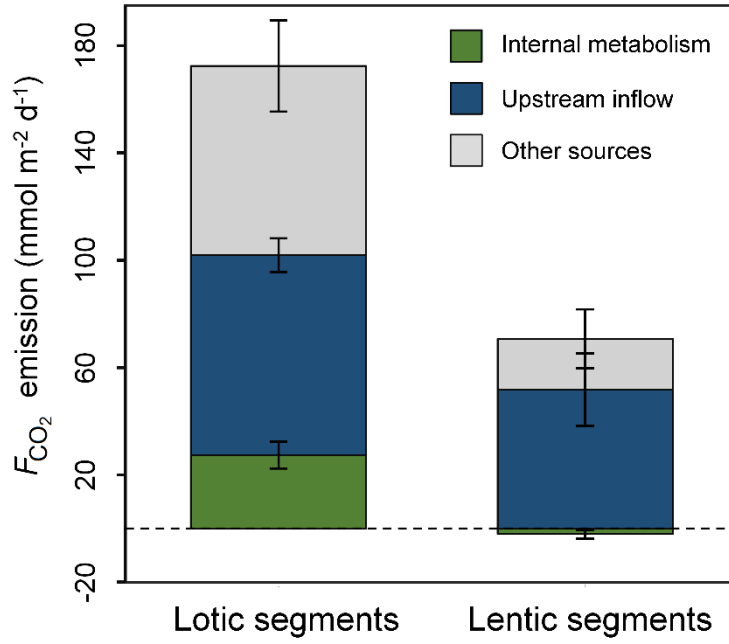


Figure 5. Source apportionment of CO_2 emissions (F_{CO_2} emission) for lotic (left) and lentic (right) segments. Columns represent averages and error bars standard errors for the different studied segments. The horizontal dashed line represent F_{CO_2} emission = 0.

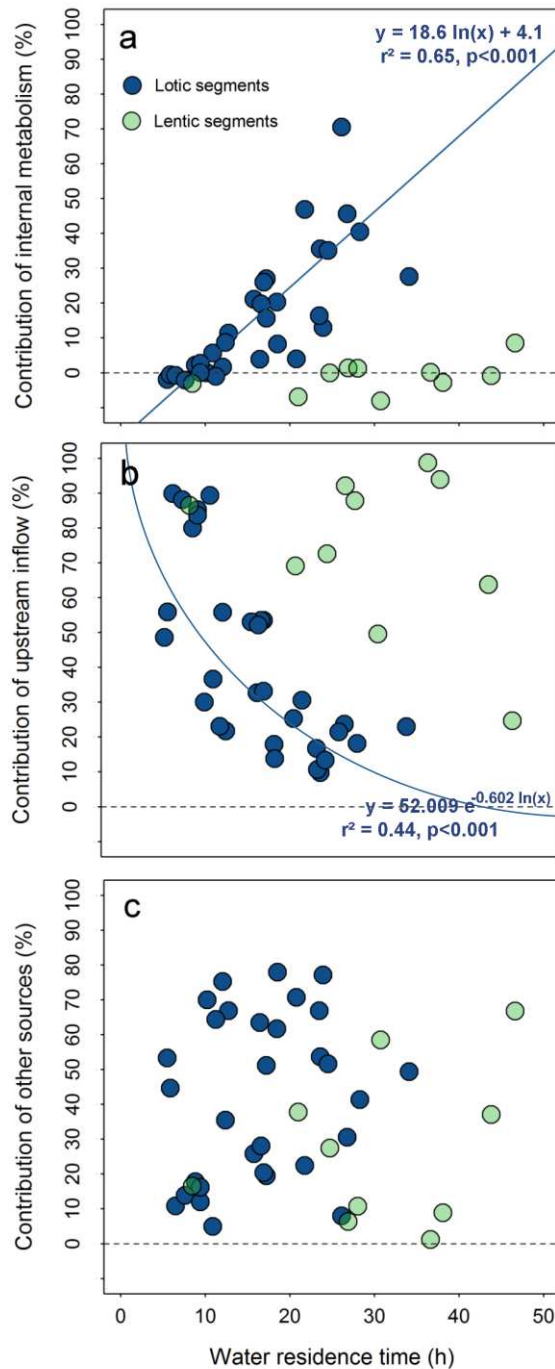


Figure 6. Relative contribution of (a) internal metabolism, (b) upstream inflow and (c) other non-measured sources to CO₂ emissions as a function of the water residence time for lotic (dark blue circles) and lentic segments (light green circles). The horizontal dashed lines represent reference lines for 0% contribution. The solid lines in panels (a) and (b) correspond to the regression lines best fitting the data (included when statistical significant). Model equations are also shown close to model lines.

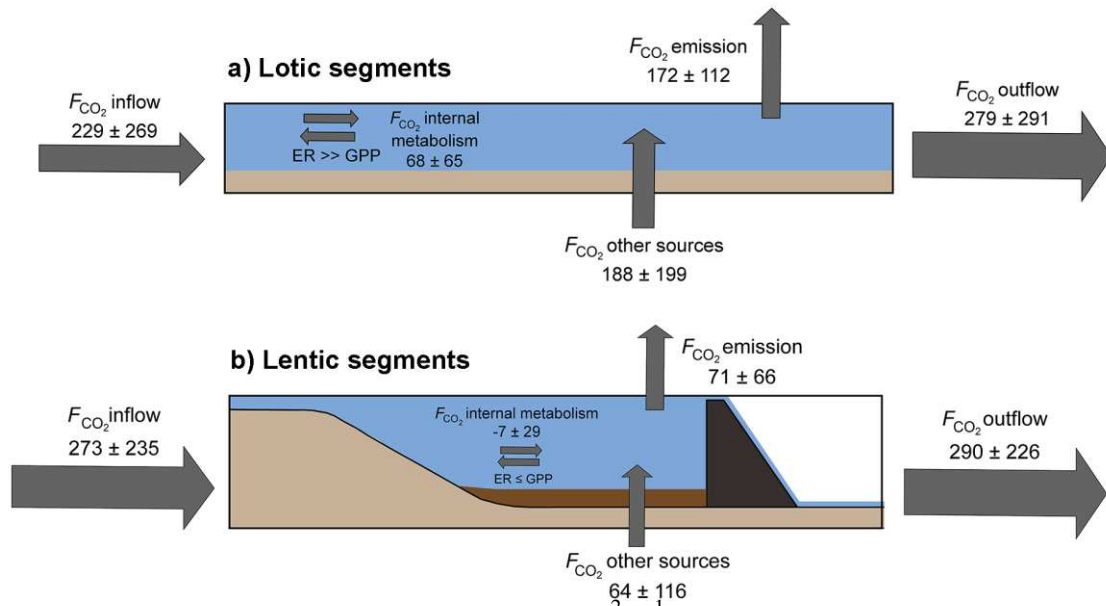


Figure 7. Summary of the CO₂ fluxes ($\text{mmol m}^{-2} \text{d}^{-1}$) determining CO₂ variations within the studied (a) lotic and (b) lentic segments. Values are averages \pm standard deviations among studied segments. Note that the arrow direction indicate direction of the CO₂ within the segment (i.e., a gain when pointing to the segment and a loss when pointing out from the segment) and the arrow size matches with the magnitude of the flux.

Table 1. Summary of the CO₂ fluxes determining CO₂ variations within the studied lotic (n=32) and lentic segments (n=10)

F_{CO_2} (mmol m ⁻² d ⁻¹)	Lotic segments				Lentic segments				ANOVA test
	Mean	Min	Max	n	Mean	Min	Max	n	<i>p</i> value
Emission	-172	-490	-40	32	-71	-203	-8	10	<0.001
Inflow	229	20	1230	32	273	37	630	10	0.65
Outflow	-279	-1280	-60	32	-290	-650	-40	10	0.91
Internal metabolism	68	-51	213	32	-7	-52	46	10	0.015
Other sources	188	30	1070	32	64	-160	250	10	0.07

Positive CO₂ fluxes indicate a gain of CO₂ within the segment (i.e. invasion from the atmosphere, upstream import, internal metabolic production or production from other sources) while negative CO₂ fluxes indicate a loss of CO₂ within the segment (i.e. emission to the atmosphere, downstream export, internal metabolic consumption or consumption by other sources)